2001

Synthetic Peptides: Design, Structure and Biological Function.

Lars Gustav johan Hammarstrom
Louisiana State University and Agricultural & Mechanical College

INFORMATION TO USERS

This manuscript has been reproduced from the microfilm master. UMI films the text directly from the original or copy submitted. Thus, some thesis and dissertation copies are in typewriter face, while others may be from any type of computer printer.

The quality of this reproduction is dependent upon the quality of the copy submitted. Broken or indistinct print, colored or poor quality illustrations and photographs, print bleedthrough, substandard margins, and improper alignment can adversely affect reproduction.

In the unlikely event that the author did not send UMI a complete manuscript and there are missing pages, these will be noted. Also, if unauthorized copyright material had to be removed, a note will indicate the deletion.

Oversize materials (e.g., maps, drawings, charts) are reproduced by sectioning the original, beginning at the upper left-hand corner and continuing from left to right in equal sections with small overlaps.

Photographs included in the original manuscript have been reproduced xerographically in this copy. Higher quality 6" x 9" black and white photographic prints are available for any photographs or illustrations appearing in this copy for an additional charge. Contact UMI directly to order.

ProQuest Information and Learning
300 North Zeeb Road, Ann Arbor, MI 48106-1346 USA
800-521-0600

SYNTHETIC PEPTIDES: DESIGN, STRUCTURE AND BIOLOGICAL FUNCTION

A Dissertation

Submitted to the Graduate Faculty of the
Louisiana State University and
Agricultural and Mechanical College
in partial fulfillment of the
requirements for the degree of
Doctor of Philosophy

in

The Department of Chemistry

by
Lars Gustav Johan Hammarström
B.S., University of Tampa, 1996
May, 2001

DEDICATION

I wish to dedicate this dissertation to my wonderful family.

ACKNOWLEDGEMENTS

I would like to thank Dr. Mark McLaughlin, for his invaluable insight, wisdom and dedication to this work. Thanks for the 400 cases of Coca Cola I must have taken from your fridge and all the laughs we've had together. I am also in debt to Dr. Robert P. Hammer, Yanwen Fu, and Dr. Tod Miller, for helpful discussions.

I am deeply grateful to Martha Juban of the Louisiana State University Department of Chemistry Protein Facility. Were it not for her, I would surely have destroyed every HPLC in the building. I would also like to thank Dr. Phil Elzer, Dr. Fred Enright and Natha Booth for all the work done on the biological testing of the antimicrobial peptides, Dr. Tracy McCarley for the mass spectra, and Dr. Frank Fronczek for the crystal structure determinations.

I am in debt to the wonderful graduate students of the McLaughlin group, past and present, which I have been fortunate to know and work with. Many thanks to Dr. Scott Yokum, Dr. Alfonso Davila, Umut Oguz and José Giraldes for their support and hard work in the lab. I wish to extend a special thank you to Dr. Ted Gauthier, with whom I spent endless hours in front of the CD, HPLC and NMR. It would have been impossible for me to reach this point were it not for your guidance and friendship. Many thanks to the Blanceflor Boncompagni-Ludovisi Foundation, the Helge Axelsson Jonson Foundation, and the Anna Whitlocks Memorial Fund for financial support.

Finally, I wish to express my thanks and love to my friends and family all over the world who have stayed with me and supported me through this challenging task.

TABLE OF CONTENTS

LIST OF TABLES

LIST OF FIGURES

LIST OF ABBREVIATIONS

ααAA	C^{α},C^{α}-disubstituted amino acid
Ac_5c	1-Aminocyclopentane-1-carboxylic acid
Ac_6c	1-Aminocyclohexane-1-carboxylic acid
Ac_7c	1-Aminocycloheptane-1-carboxylic acid
Aib	2-Aminoisobutyric acid
AIDS	Acquired Immune Deficiency Syndrome
Alloc	Allyloxycarbonyl
Api	4-Aminopiperidine-4-carboxylic acid
ATP	Adenosine triphosphate
ATCC	American type culture collection
b	Pathlength
Ba	*Brucella abortus*
Bglu	2,2-Bis(carboxyethyl) glycine
Bae	2,2-Bis(aminoethyl) glycine
Bap	2,2-Bis(aminopropyl) glycine
Basp	2,2-Bis(carboxymethyl) glycine
Boc	*tert*-Butyloxycarbonyl
BTC	Bis(trichloromethyl) carbonate
Bts	Benzothiazole-2-sulfonyl

c	Concentration
ECD	Electronic circular dichroism
cm	Centimeter
d	Doublet
DAG	Diacylglycerol
DBU	1,8-Diazobicyclo[4.5.0]undec-7-ene
DCC	Dicyclohexylcarbodiimide
DCE	1,2-Dichloroethane
DCM	Dichloromethane
DEC	Diethylcarbodiimide
DIEA	Diisopropylethylamine
DIPCDI	Diisopropylcarbodiimide
DMAP	4-Dimehtylaminopyridine
DMF	*N,N*-dimethylformamide
DMSO	Dimethylsulfoxide
Dmt	Dimethoxytrityl
Deg	Diethylglycine
Dpg	Dipropylglycine
DTH	Delayed-type hypersensitivity
ENA	Ethyl 2-nitroacetate
Et_2O	Diethyl Ether

EtOAc	Ethyl Acetate
Equiv.	Equivalents
FAB	Fast atom bombardment
FBS	Fetal Bovine Serum
FCS	Fetal Calf Serum
Fmoc	9-Fluorenylmethyloxycarbonyl
Fmoc-Cl	9-Fluorenylmethyl chloroformate
GFP	Green fluorescent protein
h	Hour
HATU	*N*-[[(dimethylamino)-1*H*-1,2,3-triazolo[4,5-b]pyrindin-1-yl]methylene]-*N*-methylmethanaminium hexafluorophosphate *N*-oxide
HBTU	*O*-benzotriazolyl-*N,N,N',N'*-tetramethyluronium hexafluorophosphate
HOAt	1-Hydroxy-7-azabenzotriazole
HOBt	1-Hydroxybenzotriazole
HPLC	High Performance Liquid Chromatography
LCP	Left circularly polarized
Lys	L-Lysine
m	Multiplet
M	Molar
MALDI	Matrix Assisted Laser Desorption Ionization
MHz	Megahertz

MIC	Minimum Inhibitory Concentration
mL	Milliliter
mM	Millimolar
mmol	Millimole
MS	Mass spectrometry
Mtb	*Mycobacterium tuberculosis*
µM	Micromolar
µg	Microgram
NCA	*N*-carboxyanhydride
nM	Nanomolar
NMR	Nuclear Magnetic Resonance
Nsc	2-(4-nitrophenylsulfonyl) ethoxycarbonyl
*o*NBS	*ortho*-Nitrobenzenesulfonyl
*o*NBS-Cl	*ortho*-Nitrobenzenesulfonyl chloride
PAL	Peptide Amide Linker
PBS	Phosphate Buffered Saline
PEG	Polyethylene glycol
PKC	Protein Kinase C
PMA	Phorbol 12-myristiol 13-acetate
PS	Polystyrene
Psi	Pounds per square inch

PyAOP	7-Azabenzotriazole-1-yloxytris(pyrrolindino)phosphonium hexafluorophosphate
R_E	Electrophile
s	Singlet
SDS	Sodium Dodecyl Sulfate
SPPS	Solid-Phase Peptide Synthesis
t	Triplet
Tb	Tuberculosis
*t*Bu	*tert*-Butyl
TBAI	Tetrabutylammonium iodide
TEAB	Tetraethylammonium bromide
TFA	Trifluoroacetic Acid
TFE	Trifluoroethanol
THF	Tetrahydrofuran
Ths	5-Methyl-1,3,4-thiadiazole-2-sulfonyl
TMS-Cl	Trimethylsilyl chloride
UV	Ultraviolet
Vis	Visible
Z	Benzyloxycarbonyl
ε	Molar absorptivity
λ	Wavelength

ABSTRACT

The synthesis of a series of polyfunctional C^{α},C^{α}-disubstituted glycines is described. The lysine-like amino acid analog, Api, was prepared by regioselective hydrolysis of a triBoced hydantoin intermediate, followed by N^{α}-protection to yield the first orthogonally protected ionizable C^{α},C^{α}-disubstituted amino acid which is alicyclic in nature.

The synthesis of three orthogonally protected tetrafunctional amino acids, Bap, Bglu, and Basp was envisioned by the mild alkylation of the common organic synthon ethyl nitroacetate. Subsequent regioselective modification should allow for the isolation of the first synthesized tetrafunctional amino acid derivatives suitable for solid-phase synthesis. These amino acids are designed to induce peptide secondary structure by salt-bridge stabilization.

A series of peptides, incorporating 80% C^{α},C^{α}-disubstituted glycines were synthesized to establish the helix stabilizing effect of amphipathicity in short helices. The peptides were prepared as the following permutation isomer pairs, Pi-10 & Ipi-10; Ach-10α & Ach-10; and Cyh-10 & Ich-10. The peptides within each pair contains the same amino acid content, but with different sequences, each designed to preferentially adopt a 3_{10}- or α-helix. Circular dichroism studies confirm that amphipathicity is a significant factor in shifting the 3_{10}-/α-helix equilibrium, notably so in micellar environments which mimic biological membranes.

The bioactivity of the aforementioned peptides was established by minimum inhibitory concentrations (MICs) against representative Gram-positive and Gram-

negative bacteria. The more hydrophobic peptides showed higher levels of cytotoxicity than the less hydrophobic peptides. In addition, *in vitro* studies using a strain of *Brucella abortus* expressing Green Fluorescent Protein (GFP) show that all of the peptides exhibit moderate to high selectivity towards the destruction of murine macrophages infected with the intracellular pathogen.

The spectroscopic properties of the *o*-nitrobenzenesulfonyl (*o*NBS) group have been established to confirm the practical use of this protecting group in solid-phase synthesis. Synthesis of the deprotection product, resulting from treatment of the oNBS-protected amino acid with mercaptoacetic acid / DBU, shows a linear correlation between concentration and absorption at 390nm. The molar absorptivity, ε_{390} was determined to be 2950 $cm^{-1}M^{-1}$. This number was verified by solution-phase cleavage of several *o*NBS-protected C^{α},C^{α}-disubstituted amino acids, which were synthesized by a modified Bolin procedure to allow for synthesis under non-aqueous conditions.

CHAPTER 1
AN INTRODUCTION TO PEPTIDE CHEMISTRY

1.1. INTRODUCTION

Proteins, along with carbohydrates, lipids and nucleic acids, make up the cornerstones upon which life is based. Yet the structural, functional and catalytic mechanisms, by which proteins function, are just beginning to be understood. This is presumably due to the incredible ubiquity and complexity of proteins in nature. As structural molecules they provide much of the cytoskeletal framework of cells, as enzymes they act as biocatalysts for innumerable physiological functions, and as motile structures, they provide movement to cells and cell structures. They stabilize and control the activity of nucleic acids, forming active parts of ribosomal processes, and play a key role in membrane transport and recognition. The ability of these molecules to adopt such a broad spectrum of functional and structural properties is due to the ingenious design scheme by which these molecules are structured. Proteins are composed of as many as 50,000 individual amino acid residues (Figure 1.1). The

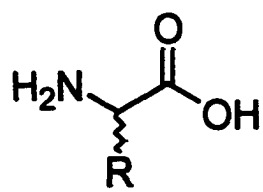

Figure 1.1. Basic structure of the amino acid. Stereochemistry about the C^{α}-carbon is not specified, but exists overwhelmingly as the L-isomer in nature. All common amino acids vary only by the R-group side chain, which distinguishes the amino acids from one another.

presence of the 20 commonly occurring amino acids, and the more than 300 less common variants which have been found to exist in nature, make an almost endless variety of proteins possible. A relatively small protein of only 50 amino acid residues in length, in which any of the naturally occurring amino acids may occupy any position along the sequence, allows for 20^{50} permutation isomers, without modifying any individual amino acid. This number is roughly equivalent to the number of grams of matter in the known universe.[1.1] Considering the huge spectrum of protein size, the large number of modified amino acids, the recent rise in the number of synthetic amino acids, and the conformational and quaternary structural interactions which are possible, the numbers of possible proteins and protein conformations are essentially infinite. However, every change in sequence and/or composition can result in distinctly different functions and properties. It is the ability to understand the structure and function of protein fragments, or peptides, as a result of primary amino acid sequence which is the very dogma of peptide chemistry. This introduction will present an overview of the basic principles of peptide chemistry and introduce some of the vital contributions made to this field in recent years.

1.2. THE AMINO ACID

Amino acids are the building blocks of all proteins. There are 20 commonly occurring amino acids in nature that are encoded by the genome, and hundreds of post-translationally modified amino acid derivatives which are used to synthesize the countless proteins which provide structure and function to the biological world. The first natural amino acid to be discovered in proteins was asparagine, in 1806, the last of the common 20 was threonine, which was not identified until 1938.[1.2] Since then, a

multitude of synthetic amino acids have emerged to complement the naturally occurring 20. A list of the commonly occurring amino acids is presented in Table 1.1. Once released from the ribosome, proteinogenic amino acids can be post-translationally modified by processes such as acetylation, amidation, glycosylation, methylation, hydroxylation, halogenation and phosphorylation.[1,3] These alterations provide endless possibilities in terms of final form and function of the resulting peptide.

In addition to the 20 naturally occurring amino acids and their post-translationally modified analogs, several synthetic amino acids and amino acid analogs have been reported within the past twenty years. A particularly interesting group of these synthetic amino acids are the C^{α},C^{α}-disubstituted amino acids ($\alpha\alpha$AAs), whose most common member, 2-aminoisobutyric acid (Aib) or C^{α}-methylalanine, is illustrated in Figure 1.2. C^{α},C^{α}-disubstituted amino acids are characterized by substituting the hydrogen at the C^{α}-carbon with an alkyl group. Most $\alpha\alpha$AAs are achiral, although synthesis and application of chiral $\alpha\alpha$AAs, where the amino acid side-chains are different, has become more common in recent years.

2-Aminoisobutyric acid was first discovered as a strongly helix promoting residue in the channel-forming peptide alamethicin. Alamethicin was found to be more helical than would have been predicted by the helix forming propensities of the proteinogenic amino acids which encompass the peptide.[1,4] Since, it has been shown that Aib, and several other disubstituted amino acids, are strongly helix promoting.[1,5,6] The additional R group at the C^{α}-carbon sterically restricts the possible conformations of the peptide, and in the case of Aib and alicyclic C^{α},C^{α}-disubstituted amino acids, favors the formation of a helix. It has also been shown that amino acids with extended

Table 1.1. The twenty commonly occurring amino acids.

Amino Acid	Code	R	Amino Acid	Code	R
Alanine	Ala (A)	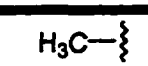	Leucine	Leu (L)	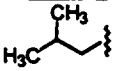
Arginine	Arg (R)	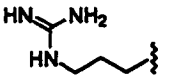	Lysine	Lys (K)	
Asparagine	Asn (N)	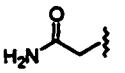	Methionine	Met (M)	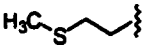
Aspartic Acid	Asp (D)	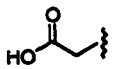	Phenylalanine	Phe (F)	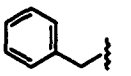
Cysteine	Cys (C)		Proline	Pro (P)	
Glutamic Acid	Glu (E)	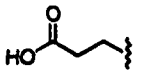	Serine	Ser (S)	
Glutamine	Gln (Q)	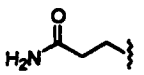	Threonine	Thr (T)	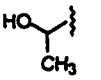
Glycine	Gly (G)		Tryptophan	Trp (W)	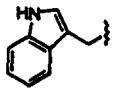
Histidine	His (H)	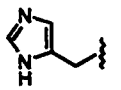	Tyrosine	Tyr (Y)	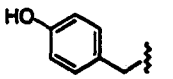
Isoleucine	Ile (I)	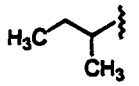	Valine	Val (V)	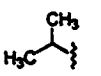

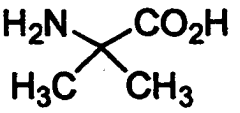

Figure 1.2. 2-aminoisobutyric acid

n-alkyl side chains larger than a methyl group, i.e. diethylglycine and dipropylglycine, favor extended conformations.[1.7] ααAA influences on peptide structure is discussed in more detail in chapter 3 of this document.

Since most C^{α},C^{α}-disubstituted amino acids are hydrophobic in nature, peptides rich in these derivatives are generally restricted to study in organic solvents due to their low solubility in aqueous media. There have been very few examples of side-chain functionalized C^{α},C^{α}-disubstituted amino acids which would allow for the synthesis of highly water-soluble peptide rich in C^{α},C^{α}-disubstituted amino acid content.[1.8] This is primarily due to difficulty of synthesis. Since poly-functionalized C^{α},C^{α}-disubstituted amino acids have the ability to induce branching and side-reaction at their side-chain functionality, they must be orthogonally protected to allow for incorporation into solid-phase peptide synthesis. Thus, we present the syntheses of new orthogonally protected polyfunctional amino acids in Chapter 2 of this text. These synthetic schemes include two C^{α},C^{α}-disubstituted amino acid analogs of lysine, the alicyclic 4-aminopiperidine-4-carboxylic acid (Api) and 2,2-bis(3-aminopropyl)glycine (Bap), and two C^{α},C^{α}-disubstituted amino acid analog of glutamic/aspartic acid, 2,2-bis(3-carboxyethyl)glycine (Bglu) and 2,2-bis(3-carboxymethyl)glycine (Basp). The structures of these amino acid targets are shown in Figure 1.3. The incorporation of these new residues should allow for the development of short peptides, with highly stabilized secondary structures.

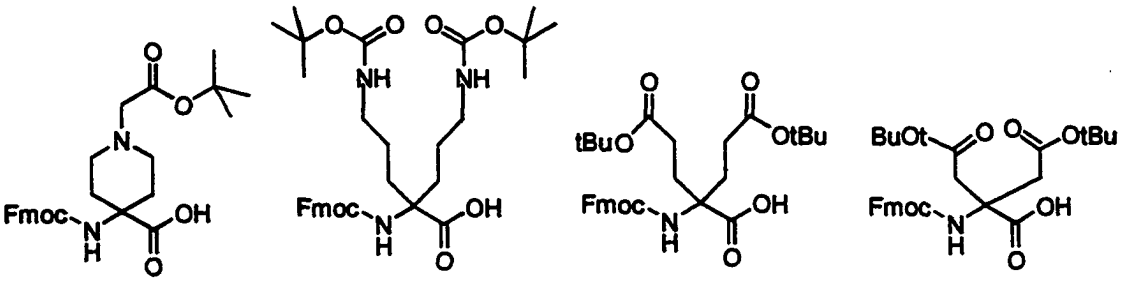

Fmoc-Api(Boc)-OH **Fmoc-Bap(Boc)$_2$-OH** **Fmoc-Bglu(*t*Bu)$_2$-OH** **Fmoc-Basp(*t*Bu)$_2$-OH**

Figure 1.3. Target C^{α},C^{α}-disubstituted amino acids Api, Bap, and Bglu and Basp in their fully protected forms.

1.3. PRIMARY STRUCTURE AND SOLID-PHASE PEPTIDE SYNTHESIS.

Amino acids are joined to produce peptide segments by linking them together via a condensation reaction to make a chain of intramolecular amides known as "peptide bonds", as is illustrated in Figure 1.4. All peptides have this fundamental substructure and vary only in the composition of amino acids and the sequence in the polypeptide backbone, which is referred to as the *primary structure* of the peptide. The process by which peptide bonds are formed synthetically are very different from those performed by biological processes. There have been numerous methods developed to synthesize peptides chemically. However, none of them have been as revolutionary for the field of peptide chemistry as solid-phase peptide synthesis (SPPS), introduced by Merrifield in the 1960s.[1,9] Merrifield's method is founded on anchoring an amino acid to an insoluble polymeric support and "growing" the peptide off of the polymer until it has reached it's final sequence. The peptide is then cleaved from the resin and purified. The advantage of using solid-phase methods is the ability to utilize large excesses of reagent without encountering difficulties in purification. These excesses drive the equilibrium

towards completion and thus provide greater yield and purity of the targeted product. SPPS has grown into a prominent application in chemistry since the first seminal publications, and is now a major driving force behind discovery sciences such as combinatorial chemistry,[1.10] the incorporation of synthetic amino acid derivatives and the synthesis of other biomolecules.[1.11-19] SPPS has, in turn, enabled peptide structure-function studies, such as those presented in chapters 3 and 4 of this dissertation.[1.20-28] The theory and practice of solid-phase peptide synthesis, coupling methods for peptide linkage formation and protection schemes are reviewed in further detail in chapter 5.

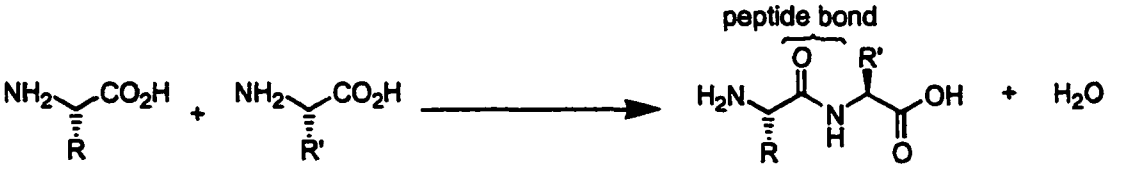

Figure 1.4. Condensation of two amino acids to generate a peptide bond.

As with *N*-alkylated amino acids, C^{α},C^{α}-disubstituted amino acids offer a significant challenge in their ability to couple under solid phase peptide synthesis conditions.[1.30-31] The difficulty in coupling C^{α},C^{α}-disubstituted amino acids stems primarily from the steric repulsion that arises between residues being coupled.[1.31] Although some C^{α},C^{α}-disubstituted amino acids, such as 2-aminoisobutyric acid, are found extensively in nature and are easily coupled under solid-phase peptide conditions, couplings of larger and more sterically hindered residues are tedious and require long coupling times under harsh reaction conditions.[1.47] The need for a newer, more efficient coupling method for the incorporation of C^{α},C^{α}-disubstituted amino acids and other

sterically hindered residues into synthetic peptides led to the development of the *o*-nitrobenzenesulfonyl (*o*NBS)/acid chloride coupling scheme which is presented in chapter 5. This method is designed to utilize the higher reactivity of protected amino acid chloride derivatives[1,29-31] as activated coupling agents, which has so far been impossible with the use of Fmoc chemistry due to high levels of competing oxazolone formation by intramolecular cyclization. Use of the less nucleophilic *o*-nitrobenzenesulfonyl protecting group should allow for the synthesis of this highly active species without competing side-reactions. Successful application of these derivatives should dramatically increase coupling yields and lower reaction times required for the coupling of C^{α},C^{α}-disubstituted amino acids. We have shown that the protecting group is easily incorporated into proteinogenic amino acids and ααAAs under non-aqueous conditions (Figure 1.5) and is quantitatively cleaved under nucleophilic conditions to yield a chromophore that can be detected by UV-spectroscopy, allowing for on-resin monitoring of coupling efficiency.

1.4. PEPTIDE SECONDARY STRUCTURE

Biological function of peptides and/or proteins is dependent on two factors: 1) bonding interactions with the substrate (usually hydrogen bonding or coulombic effects), and 2) overall peptide structure. Protein structure is divided into four levels of complexity, *primary, secondary, tertiary* and *quaternary* (see chapter 3), where *primary structure* is the description of amino acid sequence and composition. The chemical characteristics of the primary sequence allow the peptide to establish internal hydrogen bonding patterns along the amino acid backbone. This bonding pattern, in turn, induces the next level of structure in the peptide, *secondary structure*. Factors that determine

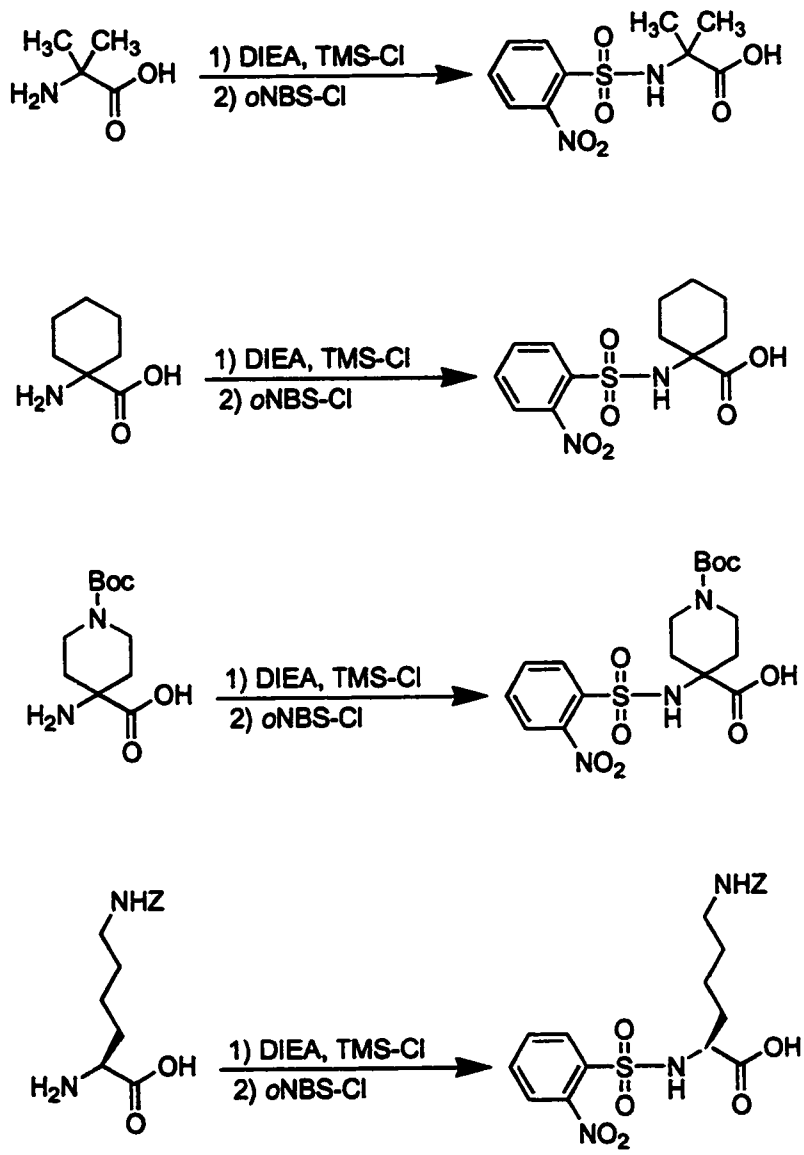

Figure 1.5. Synthesized *o*NBS-C^{α},C^{α}-disubstituted amino acid adducts.

which secondary structure will be adopted and the characteristics of secondary structure are discussed further in the introduction of chapter 3. The secondary structure of peptides can be divided into four general categories: 1) the extended conformation, 2) helices, 3) β-sheets and 4) β-turns. Of these four, the helical configurations are of most interest for the work presented in this dissertation. Figure 1.6 illustrates several helical secondary structures of peptides. Using fundamental chemical principles and a few experimental observations, Linus Pauling and Robert Corey elucidated the two most prominent secondary structures, the α-helix and β-sheet, as early as 1951, years before

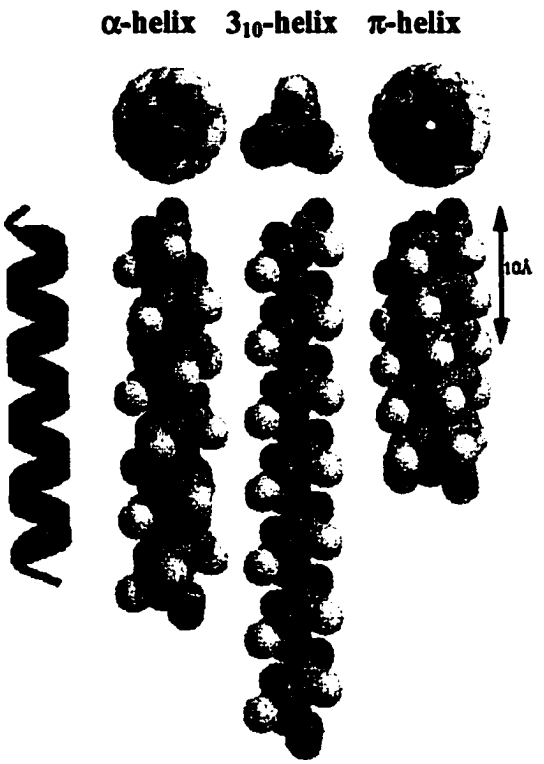

Figure 1.6. Helical secondary structure conformations. Of these structures, the α-helix is by far the most common. The 3_{10}-helix makes up less than 10% of all peptide structure. The π-helix is not found in nature.

the first crystal structure of a protein was ever defined.[1.32] Of the known helical secondary structures, the α-helix is the most thermodynamically stable and is the most common secondary structure in nature.

Recently, the 3_{10}-helix has gained attention as a significant helical motif in peptides, making up nearly 10% of all peptide helices.[1.33] The delicate equilibrium between the 3_{10}- and α-helix, which is thought to be significant in protein folding processes, has not been fully explored. In addition, it is not known what factors stabilize one helix over the other. To gain understanding of this process, we prepared a series of short peptides rich in C^{α},C^{α}-disubstituted amino acids. The peptides were designed to be perfectly amphipathic as a result of adopting either an α- or 3_{10}-helical conformation. Since the peptides are paired as permutation sequence isomers, the adopted conformation is based purely on the peptides' preference to adopt an amphipathic cross-section, not induced by their amino acid composition. The structures of the peptides were deduced by electronic circular dichroism spectroscopy (ECD)[1.32-35]. ECD, along with crystallographic methods and NMR, are the primary methods of obtaining information of peptide secondary structure. The results of these structural studies are presented in chapter 3 of this dissertation.

1.5. AMPHIPATHIC PEPTIDES

Amphipathic peptides are predominantly hydrophilic along one side of the helix axis and predominantly hydrophobic in character on the other side (Figure 1.7). The tendency of these structures to self-associate and interact with bi-lipid membranes result in high levels of bioactivity. They play an important part in membrane-dependent processes[1.41] and are found extensively in lipoproteins[1.42], hormones[1.43], lung surfactant

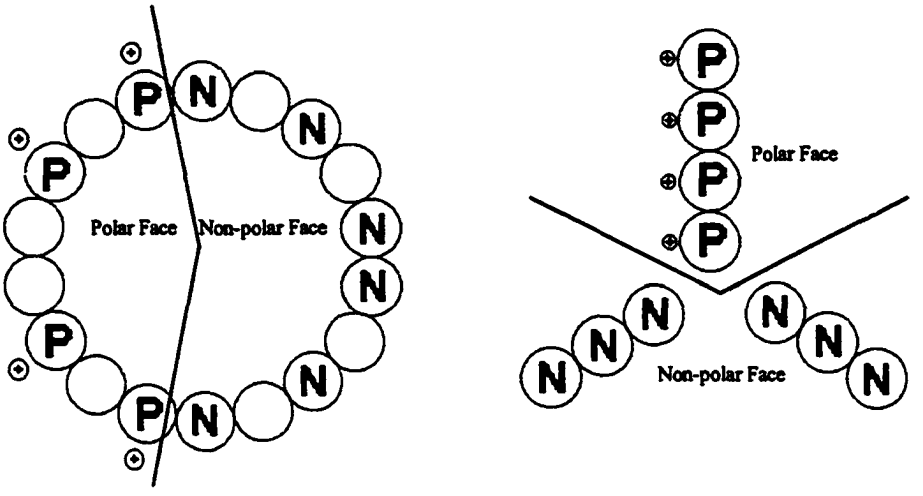

Figure 1.7. Representative amphipathic α-helix and 3_{10}-helix wheel diagrams. **N** represents non-polar, hydrophobic residues. **P** represents polar, cationic residues. Empty circles represent non-occupied positions on the helical wheel cross-section.

proteins[1.44], cytotoxic immunodefense proteins[1.45] and antimicrobial agents.[1.46] By generating sequence permutation isomers of several peptides, we have attempted to selectively induce α- or 3_{10}-helices, based purely on amphipathic sequence design. Incorporation of the ionizable C^{α},C^{α}-disubstituted amino acid, 4-aminopiperidine-4-carboxylic acid (Api) (see chapter 2) along with other common C^{α},C^{α}-disubstituted amino acids such as 2-aminoisobutyric acid (Aib) and 1-aminocyclohexane-1-carboxylic acid (Ac_6c) allows for the production of short, amphipathic peptides with up to 80% C^{α},C^{α}-disubstituted amino acids which are highly water soluble, but retain helical character in organic and aqueous/organic media (Table 1.2). Each peptide is designed to have maximum amphipathic character either as an α-helix or a 3_{10}-helix, and were found to preferentially adopt their respectively designed structures (see Chapter 3).

Table 1.2. List of prepared *de novo* peptides designed for study of structural influences of amphipathic design and antimicrobial activity against *Brucella abortus*.

Peptide	Sequence	Design
Pi-10	H-Aib-Aib-Api-*Lys*-Aib-Aib-Api-*Lys*-Aib-Aib-NH_2	α
Ipi-10	H-Api-Aib-Aib-*Lys*-Aib-Aib-*Lys*-Aib-Aib-Api-NH_2	3_{10}
Ach-10α	H-Ac_6c-Aib-*Lys*-Api-Aib-Ac_6c-Api-*Lys*-Ac_6c-Aib-NH_2	α
Ach-10	H-Api-Aib-Ac_6c-*Lys*-Ac_6c-Aib-*Lys*-Aib-Ac_6c-Api-NH_2	3_{10}
Cyh-10	H-Ac_6c-Ac_6c-Api-*Lys*-Ac_6c-Ac_6c-Api-*Lys*-Ac_6c-Ac_6c-NH_2	α
Ich-10	H-Api-Ac_6c-Ac_6c-*Lys*-Ac_6c-Ac_6c-*Lys*-Ac_6c-Ac_6c-Api-NH_2	3_{10}

Amphipathic peptide structures are gaining considerable recent attention due to growing interest in utilizing these compounds as antimicrobial agents.[1,36,37] Antibiotic resistance is a growing problem, which is developing in a number of pathogenic bacteria. To combat this problem, new sources of antibiotic therapy are required. Some of the most promising candidates for this purpose are antimicrobial peptides. Naturally occurring antimicrobial peptides are generally linear, amphipathic α-helices, and are relatively short in length (<40 residues). Although this number is relatively small in the realm of protein science, it is far too large to allow these compounds to be used effectively in a therapeutic fashion. However, sequences of this length are generally required to produce significant helical character in proteinogenic helices. The

incorporation of high levels of C^{α},C^{α}-disubstituted amino acids into the peptide structure allows for the production of relatively short sequences (~10 amino acids) which display high levels of helicity in amphipathic environments. Besides showing moderate to high levels of antimicrobial activity against representative Gram-positive and Gram-negative bacteria, the designed peptides show a significant selectivity towards the destruction of macrophages infected with intracellular pathogens (see chapter 4). An added benefit of using ααAAs in the design of therapeutic peptides is their resistance towards enzymatic degradation and increased thermal stability.

1.6. INTRACELLULAR PATHOGENS

Infection with intracellular pathogens, such as *Brucella abortus* (*Ba*) and *Mycobacterium tuberculosis* (*Mtb*), are very difficult to treat by classical antibiotics due to the lack of any significant extracellular component to the infection.[1.38] The bacteria reside within the white blood cells of the host, where no significant concentrations of antibiotic accumulate. Current recommended treatments for *Mtb* infection include the administration of four first-line antibiotics over periods of six to eight months.[1.39] *In vitro* studies of the cytolytic activity of our designed peptides show that infected macrophages are killed selectively over non-infected macrophages with high selectivity.[1.40] In addition, *in vivo* studies of the peptide Pi-10 have shown that administration of oxytetracycline together with peptide in BALB/c mice infected with *Ba* results in a dramatic reduction of intracellular infection over 24 hours.[1.40] This promising result prompted us to investigate the selective cytolytic activity of the rest of the peptides in the Pi-10 family (Table 1.2). These results are presented in chapter 4 of this manuscript.

The mechanism by which antibiotic peptides function is still under considerable debate. It is generally accepted, however, that the peptides induce cell membrane disruption by one of several proposed mechanisms (see chapter 4). In contrast to classical antibiotics, the interaction is not enzyme or receptor mediated, which lowers the possibility of resistance development towards this kind of therapy. Peptide selectivity towards bacterial cells in mammalian environments is due to cellular membrane composition differences between eukaryotic and prokaryotic cells.[1,37] Bacterial cell walls are unique in that they contain lipopolysaccharides (Gram-negative) or teichoic and teichuronic acids (Gram-positive), giving their cell wall a predominantly *negative* charge, which attracts the *positive* charge of cationic peptides. Mammalian cells are composed predominantly of zwitterionic sphingomyelin phospholipids, which have been shown to show low affinity for natural antimicrobial peptides.[1,37] This theory is further supported by the significantly lower activity of linear amphipathic peptides which are anionic in character, suggesting a coulombic interaction between peptide and target cell. Subsequent incorporation of the peptide into the cellular membrane of the target causes membrane disruption and cell death.

A question that remains unanswered is why these peptides are selective towards macrophages that are infected with intracellular pathogens. Since it has been established that coulombic attraction is the prime method of peptide incorporation into pathogenic membranes, is there a change of potential in the infected macrophage which promotes incorporation of the peptide, or are peptides evenly distributed between healthy macrophages and infected ones? In the latter case, are the infected macrophages more susceptible towards membrane disruption than the healthy ones?

These questions are addressed further in chapter 4. The first step towards answering these questions is addressed by a study in which macrophages are activated by PMA and show the same susceptibility towards Pi-10 as macrophages infected with intracellular pathogens. In turn, inhibition of PKC production in the cell results in reduced sensitivity, rendering Pi-10 inactive. This suggests that intracellular pathways "signal" the presence of an infection to the exterior cellular matrix (chapter 4).

1.7. CONCLUSIONS

Clearly there is more to be discovered within this field of peptide chemistry. New amino acids, new solid-phase coupling techniques, and new methods for the determination of peptide structure will provide the tools with which we can accomplish these goals. The ultimate goal is, of course, to deduce protein function directly from primary sequence. A greater understanding of peptide structure-function relationships will allow us to apply synthetic peptides more effectively as therapeutic agents. Future studies stemming from the material presented in this dissertation are summarized in chapter 6. These future studies include fluorescently labeling peptides so as to more carefully monitor the mechanism by which macrophages infected with intracellular pathogens are destroyed, and designing new, highly active peptides with shorter length. Increased awareness of the cellular response to these types of infections is crucial for the ongoing war against disease.

1.8. REFERENCES

1.1 Wolfe, S. L., *Molecular and Cellular Biology*, Wadsworth, Belmont, CA, **1993.**

1.2 Lehninger, A. L., Nelson, D. L., Cox, M. M., *Principles of Biochemistry*. 2nd ed. Worth Publishers, New York, NY. **1993.**

1.3 Creighton, T.E., *Proteins: Structure and Molecular Properties.* 2nd ed., New York: W.H. Freeman and Co. **1993.**

1.4 Nagaraj, R., Balaram, P. *Acc. Chem. Res.* **1981,** *14,* 356-362.

1.5 Karle, I. L., Balaram, P. *Biochemistry* **1990,** *29,* 6747-6756.

1.6 Benedetti, E. *Biopolymers (Peptide Sci.),* **1996,** *40,* 3-44.

1.7 Paul, P. K. C., Sukumar, M., Bardi, R., Piazzesi, A. M., Valle, G., Toniolo, C., Balaram, P. *J. Am. Chem. Soc.,* **1986,** *108,* 6363-6370.

1.8 Yokum, T. S., Bursavich, M. G., Piha-Paul, S. A., Hall, D. A., McLaughlin, M. L. *Tetrahedron Lett.* **1997,** *38,* 4013-4016.

1.9 Merrifield, R. B. *J. Am. Chem. Soc.* **1963,** *85,* 2149-2154.

1.10 Thompson, L. A., Ellman, J. A. *Chem. Rev.* **1996,** *96,* 555-600.

1.11 Yokum, S. T., Barany, G. B. In *Solid-Phase Synthesis: A Practical Guide.,* Kates, S. A., Albericio, F., Eds., Marcel Dekker, Inc.: New York, **2000,** pp 79-102.

1.12 Gisin, B., F., Merrifield, R. B., Tosteson, D. C. *J. Am. Chem. Soc.* **1969,** *91,* 2691-2695.

1.13 Rothe, M., Dunkel, W. *J. Polym. Sci., Part B,* **1967,** *5,* 589-593.

1.14 Burgess, K., Linthicum, D. S., Shin, H. *Angew. Chem., Int. Ed. Engl.* **1995,** *34,* 907-909.

1.15 Cho, C. Y., Moran, E. J., Cherry, S. R., Stephans, J. C., Fodor, S. P. A., Adams, C. L., Sundaram, A., Jacobs, J. W., Schultz, P. G. *Science* **1993,** *261,* 1303-1305.

1.16 Simon, R. J., Kania, R. S., Zuckermann, R. N., Huebner, V. D., Jewell, D. A., Banville, S., Ng, S., Wang, L., Rosenberg, S., Marlowe, C. K., Spellmeyer, D. C., Tan, R., Frankel, A. D., Santi, D. V., Cohen, F. E., Bartlett, P. A. *Proc. Natl. Acad. Sci. U.S.A.* **1992,** *89,* 9367-9371.

1.17 Caruthers, M. H. *Science* **1985,** *230,* 281-285.

1.18 Osborne, S. E., Ellington, A. D. *Chem. Rev.* **1997,** *97,* 349-370.

1.19 Randolph, J. T., McClure, K. F., Danishefsky, S. J. *J. Am. Chem. Soc.* **1995,** *117,* 5712-5719.

1.20 Toniolo, C. & Benedetti, E. *Trends Biochem. Sci.* **1991**, *16*, 350-3.

1.21 Smythe, M. L., Nakaie, C. R. & Marshall, G. R. *J. Am. Chem. Soc.* **1995**, *117*, 10555-62.

1.22 Basu, G., Kitao, A., Hirata, F. & Go, N. *J. Am. Chem. Soc.* **1994**, *116*, 6307-6316.

1.23 Otoda, K., Kitagawa, Y., Kimura, S. & Imanishi, Y. *Biopolymers* **1993**, *33*, 1337-45.

1.24 Tirado-Rives, J., Maxwell, D. S. & Jorgensen, W. L. *J. Am. Chem. Soc.* **1993**, *115*, 11590-11593.

1.25 Smythe, M. L., Huston, S. E. & Marshall, G. R. *J. Am. Chem. Soc.* **1993**, *115*, 11594-5.

1.26 Barlow, D. J. & Thornton, J. M. *J. Mol. Biol.* **1998**, *201*, 601-19.

1.27 Millhauser, G. L. *Biochemistry* **1995**, *34*, 3873-7.

1.28 Miick, S. M., Martinez, G. V., Fiori, W. R., Todd, A. P. & Millhauser, G. L. *Nature (London)* **1992**, *359*, 653-5.

1.29 Falb, E., Yechezkel, T., Salitra, Y., Gilon, C. *J. Peptide Res.* **1999**, *53*, 507-517.

1.30 Carpino, L. A., Chao, H. G., Beyermann, M., Bienert, M. *J. Org. Chem.* **1991**, *56*, 2635-2642.

1.31 Carpino, L. A., Ionescu, D., El-Faham, A., Henklein, P., Wenschuh, H., Bienert, M., Beyermann, M. *Tetrahedron Lett.* **1998**, *39*, 241-244.

1.32 Toniolo, C., Polese, A., Formaggio, F., Crisma, M. & Kamphuis, J. *J. Am. Chem. Soc.* **1996**, *118*, 2744-5.

1.33 Iqbal, M. & Balaram, P. *Biopolymers* **1982**, *21*, 1427-33.

1.34 Gratias, R., Konat, R., Kessler, H., Crisma, M., Valle, G., Polese, A., Formaggio, F., Toniolo, C., Broxterman, Q. B. & Kamphuis, J. *J. Am. Chem. Soc.* **1998**, *120*, 4763-4770.

1.35 Long, H. W. & Tycko, R. *J. Am. Chem. Soc.* **1998**, *120*, 7039-7048.

1.36 Andreu, D., Rivas, L. *Biopolymers, Pept. Sci.* **1998**, *47*, 415-433.

1.37 Tossi, A., Sandri, L., Giangspero, A. *Biopolymers, Pept. Sci.* **2000**, *55*, 4-30.

1.38 Bloom, B.R., *Tuberculosis: Pathogenesis, Protection and Control.* **1994,** Washington, DC: ASM Press.

1.39 Murray, C. J. L., Salomon, J. A. *Proc. Natl. Acad. Sci. U.S.A.* **1998,** *95,* 13881-13886.

1.40 Yokum, T. S., Elzer, P. H., McLaughlin, M. L. *J. Med. Chem.* **1996,** *39,* 3603-3605.

1.41 Tomich, J. M. In *The Amphipathic Helix,* **1993,** CRC Press, Boca Raton, pp. 222-249.

1.42 Anantharanaiah, G. M., Jones, M. K., Segrest, J. P. In *The Amphipathic Helix,* **1993,** CRC Press, Boca Raton, pp. 109-140.

1.43 Taylor, J. W. In *The Amphipathic Helix,* **1993,** CRC Press, Boca Raton, pp. 286-308.

1.44 Waring, A. J., Gordon, L. M., Taeusch, W., Bruni, R. In *The Amphipathic Helix,* **1993,** CRC Press, Boca Raton, pp. 143-167.

1.45 Cornut, I., Thiaudiére, E., Dufourcq, J. In *The Amphipathic Helix,* **1993,** CRC Press, Boca Raton, pp. 173-210.

1.46 Chopra, I. *Journal of Antimicrobial Chemotherapy* **1993,** *32,* 351-353.

CHAPTER 2
SYNTHESIS OF A SERIES OF IONIZABLE C^{α},C^{α}-DISUBSTITUTED AMINO ACIDS

2.1. INTRODUCTION

The use of C^{α},C^{α}-disubstituted amino acids ($\alpha\alpha$AAs, Figure 2.1) in the design of novel peptides has taken a sharp rise within the past few years. There are several reasons why these derivatives are desirable in the synthesis of *de novo* peptides with bioactive applications. 1) It has been shown that peptides containing high levels of C^{α},C^{α}-disubstituted amino acids are resistant to enzymatic degradation under physiological conditions.[2.1,61] 2) The presence of the common C^{α},C^{α}-disubstituted amino acid Aib (2-aminoisobutyric acid) in naturally occurring, membrane active peptides.[2.2,3] 3) The high secondary structure promoting ability of C^{α},C^{α}-disubstituted amino acids by peptide torsion angle restriction.[2.4-13]

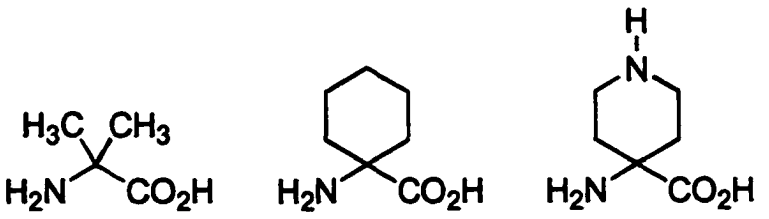

Aib **Ac_6c** **Api**

Figure 2.1. C^{α},C^{α}-Disubstituted amino acids aminoisobutyric acid (Aib), 1-aminocyclohexyl-1-carboxylic acid (Ac_6c), and 1-aminopiperidine-1-carboxylic acid (Api).

2-Aminoisobutyric acid (Aib) is the most commonly used C^{α},C^{α}-disubstituted amino acid and is found extensively in nature. The antibiotic alamethicin,[2.14-15] and related antimicrobial peptides suzukacillin,[2.16] emmerimicins,[2.17] and antiamoebins[2.18] all contain high levels of this amino acid. Most of the pioneering work on the structural influences of Aib in short, synthetic peptides is accredited to Balaram, [2.8,10,11,19,20] and more recently by Toniolo, Benedetti and coworkers.[2.2,12,21,22] Aib, and other ααAAs like it, promote secondary structure formation by severely restricting possible rotation about the N-C^{α} (ϕ) and C^{α}-C' (ψ) bonds.[2.8] Theoretical calculations have deduced that allowable torsion angles of these bonds in ααAA-rich peptides fall in a very narrow region near -57°, -47°, and +57°, +47°, respectively.[2.23] In Ramachandran space, this corresponds to the formation of a right or left handed α-helix or 3_{10}-helix (see chapter 3). Since symmetrical ααAAs do not have a chiral center, they may give rise to either right or left handed screw sense, if no other chiral amino acids are present in the peptide to induce enantiomeric preference. In contrast to Aib, C^{α},C^{α}--di-*n*-ethylglycine and C^{α},C^{α}-di-*n*-propylglycine have been shown to induce extended conformations of resulting peptides (Figure 2.2).[2.10]

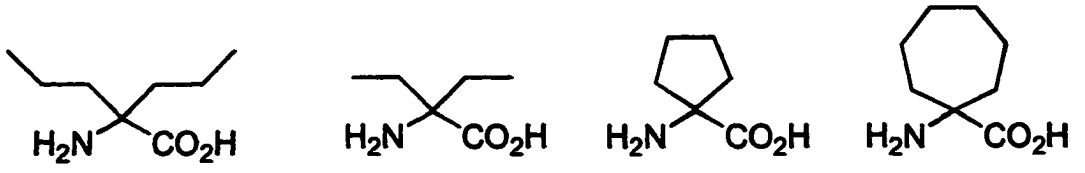

Dpg **Deg** **Ac_5c** **Ac_7c**

Figure 2.2. Other common C^{α},C^{α}-disubstituted amino acids: C^{α},C^{α}-Dipropylglycine (Dpg), C^{α},C^{α}-Diethylglycine (Deg), 1-amino-1-cyclopentanoic acid (Ac_5c), and 1-amino-1-cycloheptanoic acid (Ac_7c).

The effect of alicyclic C^{α},C^{α}-disubstituted amino acids on secondary structure has been extensively researched.[2.10,12,24,25] While longer chain C^{α},C^{α}-di-*n*-alkyl amino acids promote extended conformations,[2.10] alicyclic C^{α},C^{α}-disubstituted amino acids, in which the C^{α} carbon forms a cyclic bridge with itself, such as 1-aminocyclopentane-1-carboxylic acid (Ac_5c) and 1-aminocyclohexane-1-carboxylic acid (Ac_6c), have helix forming characteristics similar to those of Aib.[2.10,24] This theory was recently extended to include the seven membered ring variant, 1-amino-cycloheptane-1-carboxylic acid (Ac_7c) (Figure 2.2).[2.24]

Due to the presence of symmetry at the C^{α}-position, achiral ααAAs due not induce selective screw sense and are equally prone towards the formation of right and left handed helices. Synthetic peptides, incorporating high levels of C^{α},C^{α}-disubstituted amino acids, often include proteinogenic amino acids to induce preferred helical sense. It has been shown that synthetic peptides increase their helical character by substituting Aib residues with chiral ααAAs such as C^{α}-methyl valine or C^{α}-ethyl alanine.[2.26,27] Some chiral C^{α}-alkylated phenylglycines have also recently found use as selective antagonists of metabotropic glutamate receptor.[2.28,29] Chiral ααAAs are generally synthesized by the enantioselective alkylation of chiral enolates.[2.30-32] However, these reaction conditions are limited due to multiple reaction steps and difficult separations of racemic products.

Since most C^{α},C^{α}-disubstituted amino acids are hydrophobic in nature, peptides rich in ααAAs are generally restricted to study in organic solvents due to their low solubility in aqueous media. There have been very few examples of side-chain functionalized ααAAs that would allow for the synthesis of highly water soluble

peptide rich in C^{α},C^{α}-disubstituted amino acid content.[6.62] This is primarily due to difficulty of synthesis. Since side-chain functionalized ααAAs have the ability to induce branching and side-reaction at their side-chain functionality, they must be orthogonally protected to allow for incorporation into solid-phase peptide synthesis. The harsh conditions, under which standard methods of C^{α},C^{α}-disubstituted amino acid synthesis are performed, make this a difficult task (Figure 2.3).

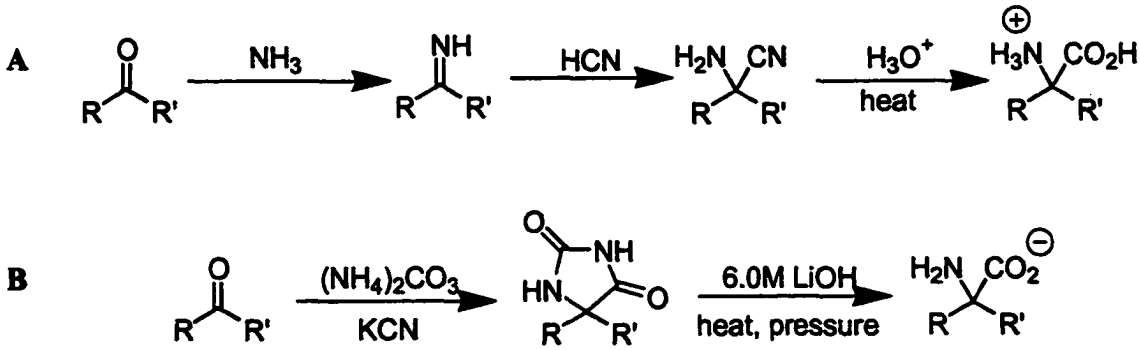

Figure 2.3. The Strecker Method **A**, and the Bucherer-Berg Method **B**, for the synthesis of C^{α},C^{α}-disubstituted amino acids.

Two traditional methods exist for the synthesis of ααAAs. The Strecker method is characterized by the addition of cyanide to an imine synthesized from the corresponding symmetrical ketone, followed by acid catalyzed hydrolysis of the resulting α-aminonitrile (Figure 2.3).[2.33] This method is experimentally simple, but limited to the use of simple ketones as starting materials as the hydrolysis requires strongly acidic conditions, high temperatures and pressure. Recently, Ma and coworkers presented an asymmetrical Strecker synthesis to generate chiral ααAAs from α-aryl ketones.[2.34] The Bucherer-Berg method of hydantoin formation by the reaction

of ketones with sodium cyanide and ammonium carbonate is still the most prevalent method to generate ααAAs in good yields.[2.35,36] However, hydantoins also suffer from the limitation of requiring harsh conditions for hydrolysis, thus minimizing the ability to generate side-chain functionalized amino acids (Figure 2.3). This problem was partially overcome by Rebek and coworkers, whom discovered that N,N'-Bis-(*t*-butyloxycarbonyl) hydantoins can be hydrolyzed under much milder conditions.[2.37] The ease of hydrolysis of the functionalized hydantoin is presumably due to a number of reasons: 1) Induced ring strain in the hydantoin moiety, 2) greater electrophilicity of the hydantoin carbonyls, making it more susceptible towards nucleophilic attack by hydroxide and, 3) The nitrogen of the hydantoin becomes a better leaving group as a carbamate. The progress made in C^{α},C^{α}-disubstituted amino acid synthesis by hydantoin hydrolysis allowed us to develop the synthesis of the orthogonally protected C^{α},C^{α}-disubstituted amino acid Fmoc-Api(Boc)-OH **2.1** (Figure 2.4).[2.38] This alicyclic C^{α},C^{α}-disubstituted amino acid analog of lysine allows for the preparation of peptides rich in ααAAs, while retaining water-solubility.[2.6] As with other alicyclic ααAAs, Api has been found to strongly favor helical conformations of resulting peptides.

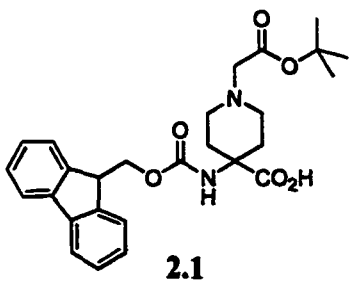

2.1

Figure 2.4. Orthogonally protected C^{α},C^{α}-disubstituted amino acid 9-1-*tert*-butyloxycarbonyl-4-((9-fluorenylmethyloxycarbonyl)amino)-piperidine-4-carboxylic acid (Fmoc-Api(Boc)-OH).

Nitroacetic esters are common starting materials for a number of synthetic transformations.[2.39] The high reactivity of the α-methylene group of these compounds allows for unique carbon-carbon bond forming ability. Alkylations of these activated starting materials has been useful in the synthesis of 2-nitroalkanoic acids, nitro alcohols, nitro amines, halonitro compounds, nitroacrylates, oxazolidines, oxazoles and carbohydrates.[2.39] Although there have been reports of the use of benzyl- and *t*-butyl-nitroacetate,[2.40-43] most of the work on nitroacetates have been restricted to the use of the methyl and ethyl esters[2.44-47] due to the difficulty of synthesizing other derivatives. The ability to efficiently alkylate nitroacetic esters has lead to the successful synthesis of amino acids and amino acid esters.[2.48-53] These reactions are usually monoalkylations with an appropriate electrophile using weakly basic conditions, followed by reduction of the nitro group to the corresponding amine. Alkylations have been performed by the use of sodium or potassium hydroxide, benzyltrimethyl ammonium hydroxide, trimethylanilinium benzenesulfonate and diethylamine as bases.[2.39] In addition, metal catalysis by copper (II) acetate and palladium catalysts has been employed for a number of Michael additions.[2.45,54] Electrochemically generated anions have been used on a small scale to perform mono- and di-alkylations of nitroacetic esters.[2.47] However, since monoalkylation of nitro acetates is non-stereospecific, these reactions result exclusively in racemic mixtures of α-nitro esters, which have limited application for peptide synthesis.

Dialkylation of nitroacetic esters yields symmetrical dialkylated nitroacetates which are suitable precursors for the synthesis of C^{α},C^{α}-disubstituted amino acids (Figure 2.5). The high acidity of the α-methylene protons of ethyl nitro acetate allow

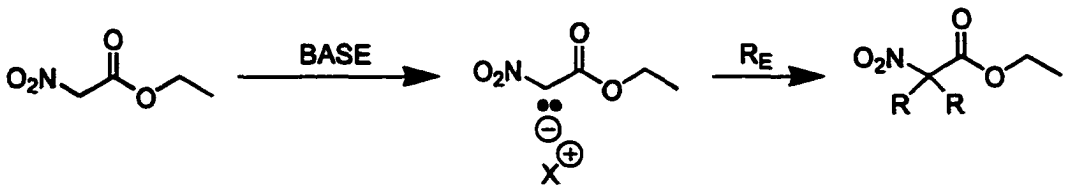

Figure 2.5. Base catalyzed alkylation of ethyl nitroacetate. BASE= potassium hydroxide, sodium hydroxide, sodium ethoxide, trialkylamine. R_E= alkyl halide, Michael acceptor.

for alkylations under very mild conditions. This, in turn, allows for the incorporation of chemically labile groups, which would be too unstable to incorporate via the Strecker, Bucherer-Bergs, malonic ester alkylation or glycine template alkylation methods. A synthetic scheme was envisioned for the preparation of three orthogonally protected tetrafunctional C^{α},C^{α}-disubstituted amino acid analogs of glutamic acid, aspartic acid and lysine / ornathine using ethyl nitroacetate as a synthetic precursor: N^{α}-(9-fluorenylmethyloxycarbonyl)-2,2-bis(*tert*-butylcarboxyethyl) glycine (Fmoc-Bglu(*t*-Bu)$_2$-OH, **2.2**), N^{α}-(9-fluorenylmethyloxycarbonyl)-2,2-bis(*tert*-butylcarboxymethyl) glycine (Fmoc-Basp(*t*-Bu)$_2$-OH, **2.3**) and N^{α}-(9-fluorenylmethyloxycarbonyl)-2,2-bis(N^{γ}-*tert*-butyloxycarbonyl-3-aminopropyl) glycine (Fmoc-Bap(Boc)$_2$-OH, **2.4**) (Figure 2.6). These targets were chosen for three reasons: 1) There does not, as of date, exist any recorded results on the synthesis of orthogonally protected tetrafunctional amino acids capable of incorporation into peptides by solid-phase peptide synthesis (see chapter 6). 2) The use of a polyfunctional amino acid may allow for the synthesis of peptides that retain high levels of amphipathicity with very short length (see chapter 3). 3) Polyanionic and polycationic amino acids have interesting possibilities for application as salt bridge inducers towards stabilization of peptide secondary structure.

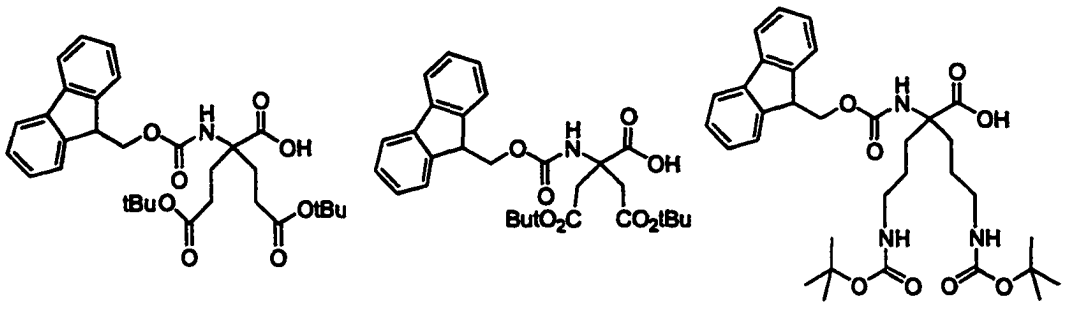

2.2 2.3 2.4

Figure 2.6. Fmoc-Bglu(*t*-Bu)$_2$-OH **2.2**, Fmoc-Basp(*t*Bu)$_2$-OH **2.3** and Fmoc-Bap(Boc)$_2$-OH **2.4**.

2.2. RESULTS AND DISCUSSION

Synthesis of 1-*tert*-butyloxycarbonyl-4-((9-fluorenylmethyloxycarbonyl) amino)-piperidine-4-carboxylic acid (Fmoc-Api(Boc)-OH) **2.1** was realized according to the synthetic scheme in Figure 2.7. The reaction of 4-piperidone hydrate **2.1a** with potassium cyanide and ammonium carbonate in ethanol/water gives the resulting hydantoin **2.1b** in good yields. The piperidone hydantoin is then tri-Boced using excess *t*-butyldicarbonate in DME with triethylamine and a catalytic amount of DMAP as deduced by Wysong et. al.[2.55] Attempts to tri-Boc the piperidone hydantoin without the use of DMAP or triethylamine results in incomplete reaction. Hydrolysis of the resulting triBoc piperidine hydantoin **2.1c** under alkaline conditions results in the formation of the amino acid **2.1d** in good yield. This hydrolysis was initially achieved by aqueous NaOH. However, isolation of the resulting zwitterion **2.1d** is difficult, as the product is highly contaminated with the hydrolysis side-product, bis(*t*-butyl)carbamate. Isolation of this side product verifies that the mechanism of hydrolysis occurs by one of two pathways as shown in Figure 2.8. In the first

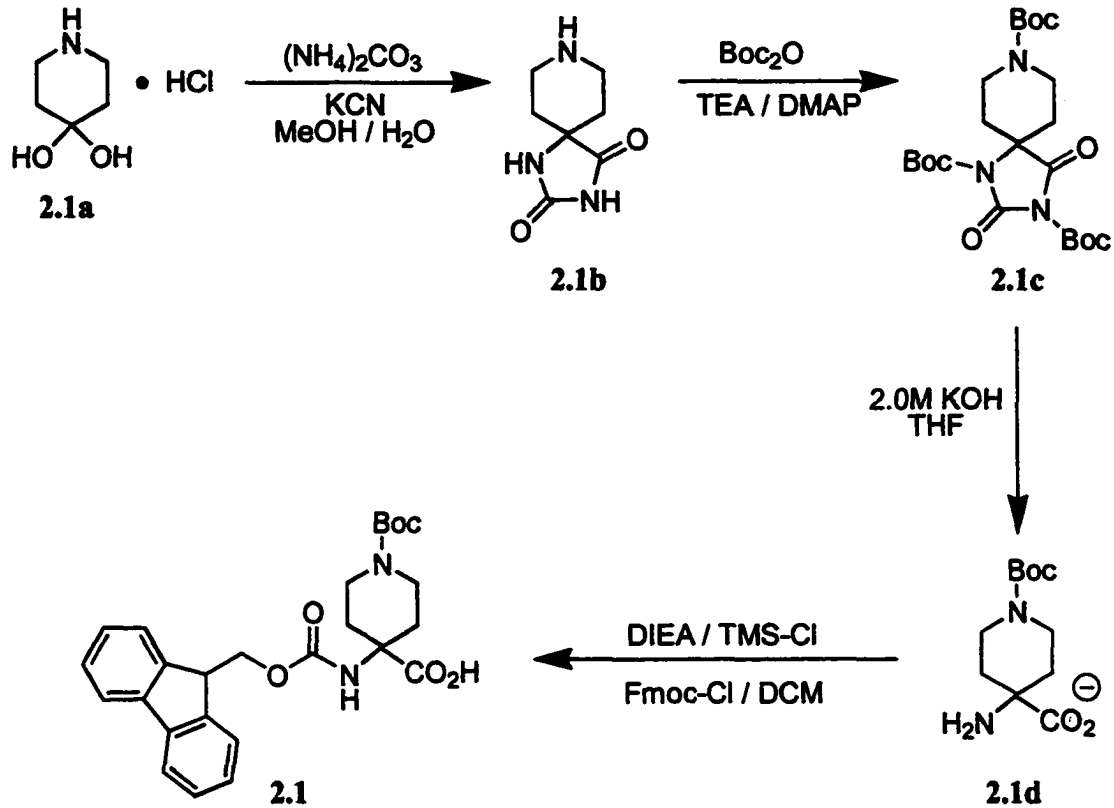

Figure 2.7. Synthesis of Fmoc-Api(Boc)-OH **2.1**.

mechanism, **A**, nucleophilic attack of hydroxide on the amide carbonyl of the hydantoin ring substitutes the carbamate-type moiety. Intramolecular *t*-butyloxycarbonyl transfer, followed by base catalyzed hydrolysis and subsequent decarboxylation of the resulting carbamic acid give the observed products. The other hydrolysis mechanism, **B**, is initiated by nucleophilic hydroxide attack on the urea-carbonyl of the hydantoin. Decarboxylation of the carbamic acid and intramolecular *t*-butyloxycarbonyl transfer yields the free amine. Base hydrolysis of the resulting amide releases bis-(*t*-butyl)-carbamate and results in the free carboxylate (Figure 2.8).

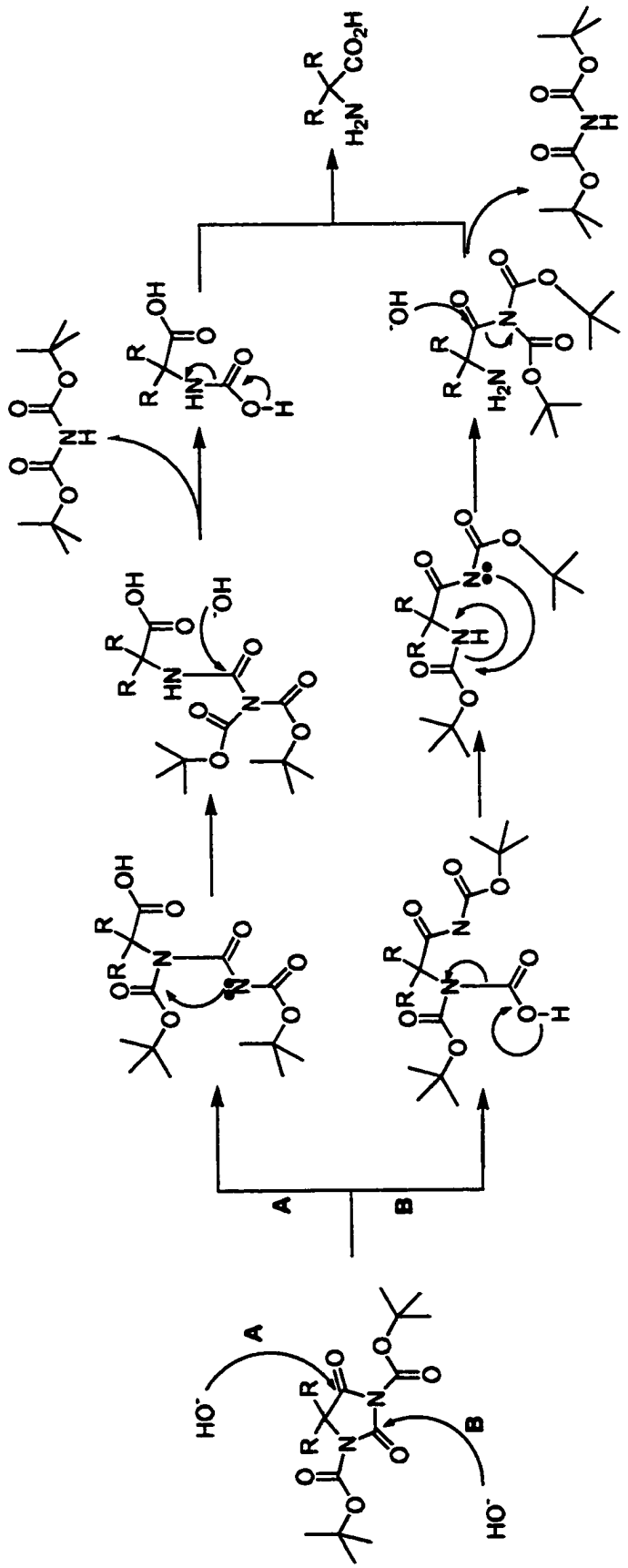

Figure 2.8. Possible mechanisms of di-Boc hydantoin hydrolysis.

Although both mechanisms are theoretically feasible, mechanism **A** is more likely to occur for two reasons: 1) The greater electrophilicity of the amide-type carbonyl versus the urea-type carbonyl promotes initial nucleophilic attack according to mechanism A. 2) Intramolecular *t*-butyloxycarbonyl transfer in mechanism **A** involves an amide leaving group, mechanism **B** requires that a deprotonated amine act as a leaving group. The greater kinetic activity of the amide-type leaving group would promote mechanism **A**. It was attempted to probe the mechanism of the hydrolysis by ^{13}C-NMR. However, the results were inconclusive.

Although the hydrolysis of the tri-Boc hydantoin give the desired amino acid in high yield, the reaction has difficulties associated with bis-(*t*-butyl)-carbamate contamination of the isolated amino acid. Bis-(*t*-butyl)-carbamate has a pKa and solubility similar to that of the Api(Boc) zwitterion making separation difficult even by chromatographic means. Presence of this contamination causes difficulty in isolation and residual bis-(*t*-butyl)-carbamate results in severe side reaction if present in the preparation of Fmoc-Api(Boc)-OH.

Contamination with bis-(*t*-butyl)-carbamate is avoided by performing the hydrolysis of **2.1c** in a biphasic mixture of THF and 2.0M KOH. Under basic conditions, bis-(*t*-butyl)-carbamate has a higher solubility in THF, while the deprotonated zwitterion stays in the aqueous solution. Under high ionic contents THF and water are not miscible and are easily separated in a separatory funnel (Figure 2.9). Evaporation of the separated THF yields a nearly quantitative recovery of bis-(*t*-butyl)-carbamate. Neutralization of the aqueous layer yields the precipitated zwitterion **2.1d** in very good yield. To introduce the Fmoc group for N^{α}- protection, Fmoc-Cl is used, as

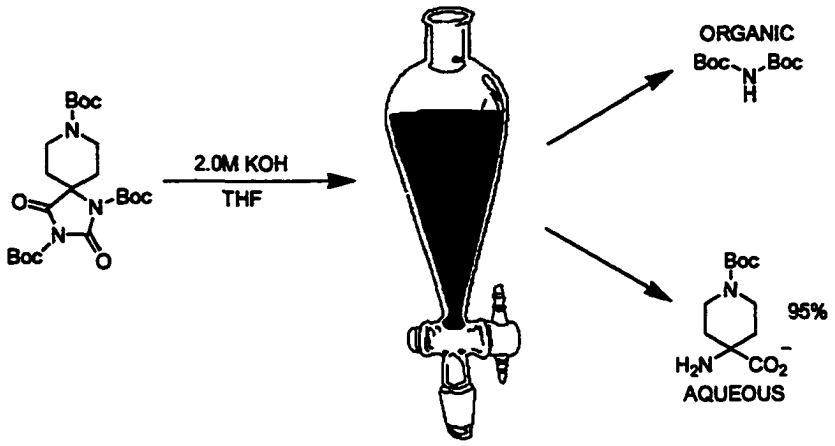

Figure 2.9. Biphasic hydrolysis of triBoc Api hydantoin.

reported by Bolin.[2.63] The N^{ε}-*t*-butyloxycarbonyl group was found to be stable under these conditions and the reaction yields the orthogonally protected amino acid **2.1** in good overall yield. Unfortunately, the tri-Boc-hydantoin route can not be extended to non-cyclic multi-functional amino acid derivatives. The required α-, β-, or γ-difunctionalized ketones do not form hydantoins to an appreciable extent (Figure 2.10). Thus, the tri-Boc-hydantoin route was not utilized for the synthesis of Fmoc-Bglu(*t*-Bu)$_2$-OH and Fmoc-Bap(Boc)$_2$-OH.

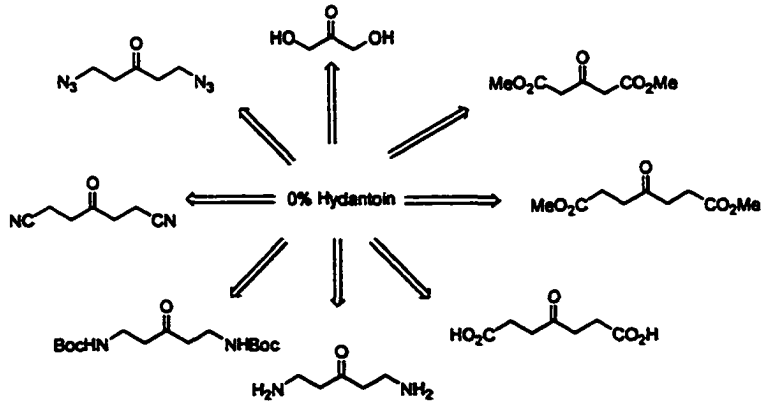

Figure 2.10. Failed attempts at difunctionalized hydantoin synthesis.

The scheme devised for the synthesis of Fmoc-Bglu(t-Bu)$_2$-OH and Fmoc-Bap(Boc)$_2$-OH is shown in Figure 2.11 and 2.12. Based on evidence that the ethyl nitroacetate anion is a more potent nucleophile when the counter ion is a highly dissociated quaternary ammonium salt, initial dealkylation was achieved using N,N'-diisopropyl ethylamine.[2.47] The reactivity of the anion is increased when a catalytic amount of tetraethylammonium bromide is added to the reaction to act as an activated counter ion. Michael addition was performed with a number of electrophilic acceptors. Reaction of the nucleophile with acrolein is facile but gives a diastereomeric mixture of products due to the very rapid intramolecular Aldol cyclization of the resulting enolate (Figure 2.13). Michael addition with *tert*-butyl acrylate and acrylonitrile, respectively, gave the C^{α}-disubstituted ethyl nitroesters in excellent yields. Interestingly, alkylation with benzyl acrylate gave only a small portion of dialkylated product after 24 hours at room temperature. Most of the recovered product was monoalkylated. The ethyl ester of the dialkylated nitroacetate cannot be hydrolyzed without risking carbon dioxide elimination. Thus, the next logical step in the synthesis of an amino acid derivative is to reduce the α-nitro group to the corresponding amine. However, reduction of the nitro group did not prove trivial. Nitro compounds are known to be reduced by a variety of methods, the most prevalent being catalytic hydrogenation over Pd[2.49-50] or Raney Ni.[2.48,52,53] There are, however, several other techniques, such as Zn/acetic acid reduction and tin catalyzed hydrochloric acid reduction. Ammonium formate has recently found application as a suitable catalytic hydrogen transfer agent for the reduction of nitro compounds.[2.56-58] To our surprise, only catalytic hydrogenation at 50 psi over T-1 Raney Nickel in ethanol resulted in the desired amine: ethyl-2,2-bis(t-

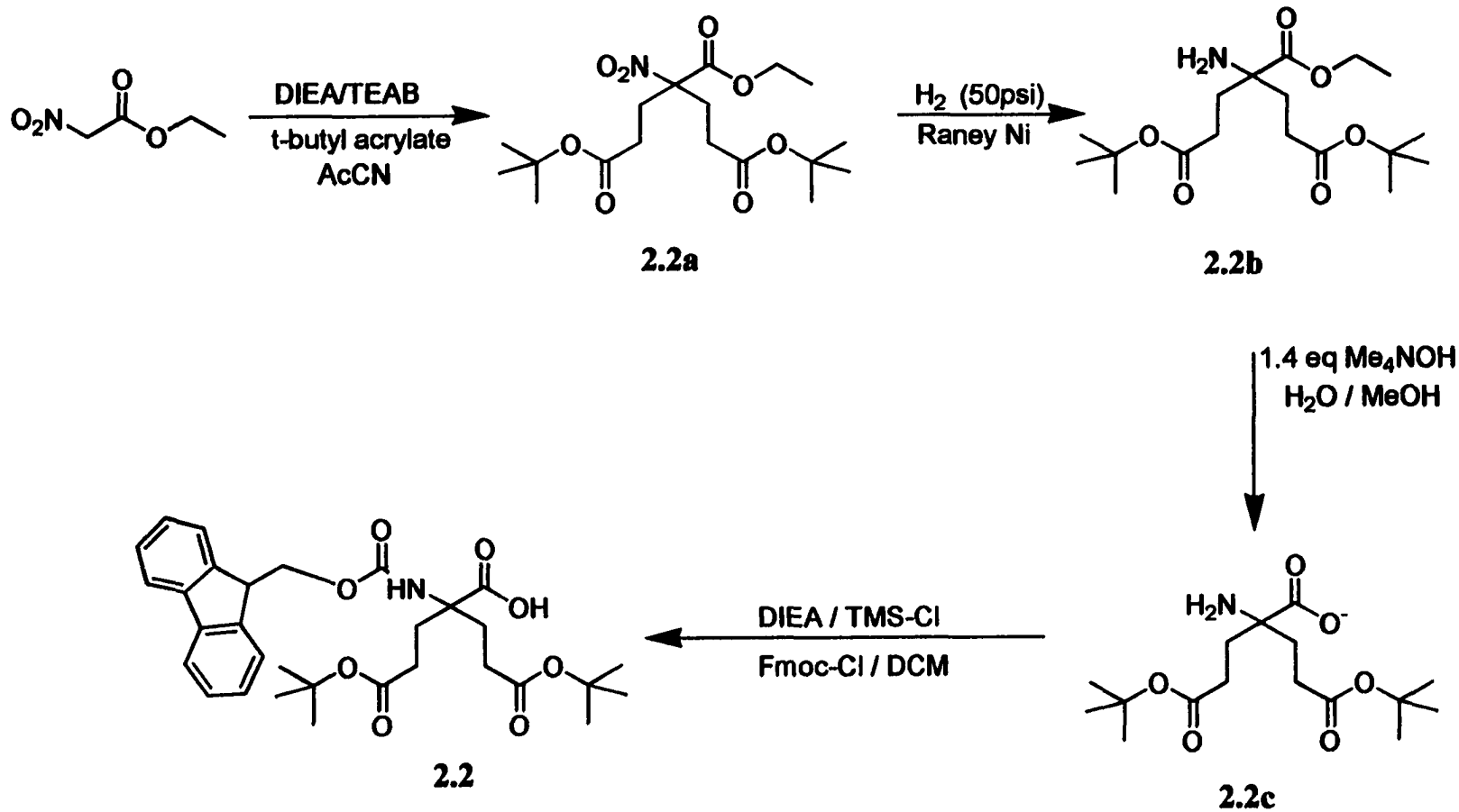

Figure 2.11. Synthetic soheme of the synthesis of Fmoc-Bglu(tBu)$_2$-OH **2.2**.

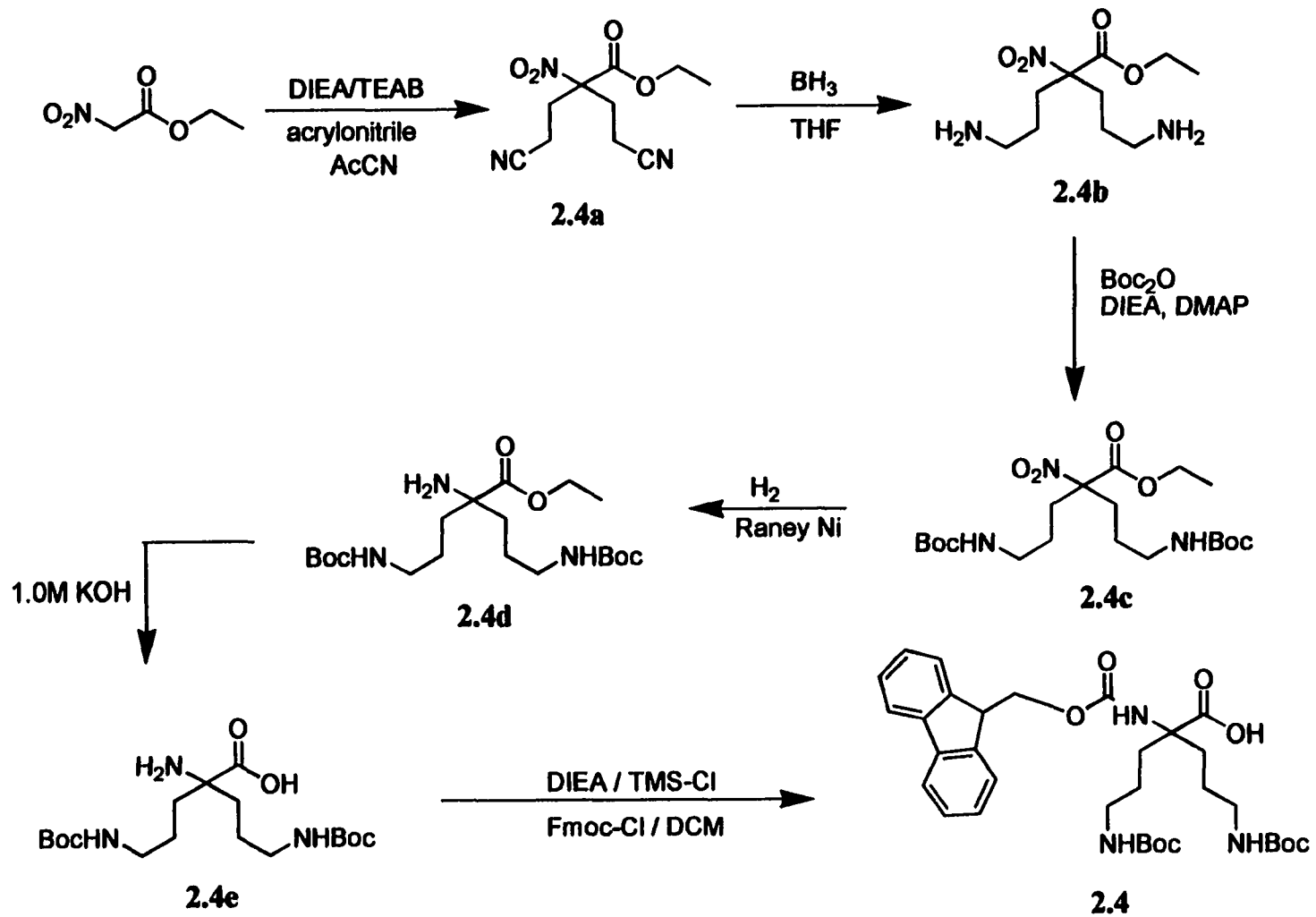

Figure 2.12. Synthetic scheme of the synthesis of Fmoc-Bap(Boc)$_2$-OH **2.4**.

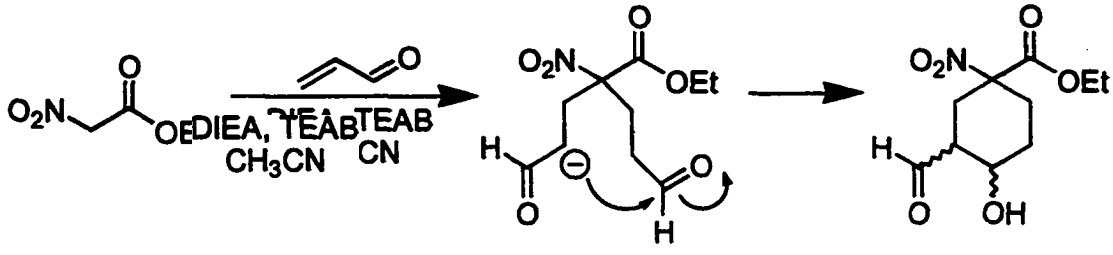

Figure 2.13. Addition of acrolein to ethyl nitroacetate, followed by base catalyzed intramolecular Aldol cyclization to yield diastereomeric mixture.

butylcarboxyethyl)glycine **2.2b**. Hydrogenation over Pd/C (5 or 10%) at 50 psi in ethanol or with ammonium formate results in almost quantitative conversion to the corresponding hydroxylamine, which was apparent by NMR and MS analysis (Figure 2.14-16). While suitable for the reduction of ethyl-2,2-bis(*t*-butylcarboxyethyl)-2-nitroacetate **2.2a**, catalytic hydrogenation can not be utilized in the reduction of the corresponding nitro group of ethyl-2,2-bis(3-cyanoethyl)-2-nitroacetate **2.4a**, as nitriles are readily reduced under these conditions.

Acid catalyzed hydrolysis of the ethyl ester of **2.2b** results in immediate *t*-butyl deprotection and saponification using KOH, NaOH, or LiOH in various aqueous and/or aqueous/organic mixtures failed to selectively hydrolyze the ethyl ester. Recovered material from several hydrolyses showed evidence that the *t*-butyl groups of the δ-carboxylates were also lost to an appreciative extent. Selective hydrolysis of ethyl versus *t*-butyl esters has been well documented. [2.59, 60] However, hydrolysis of this ethyl / *t*-butyl ester compound is very difficult. Difficulty in isolation of the complex mixtures of partially hydrolyzed derivatives makes definitive evidence impossible, but a

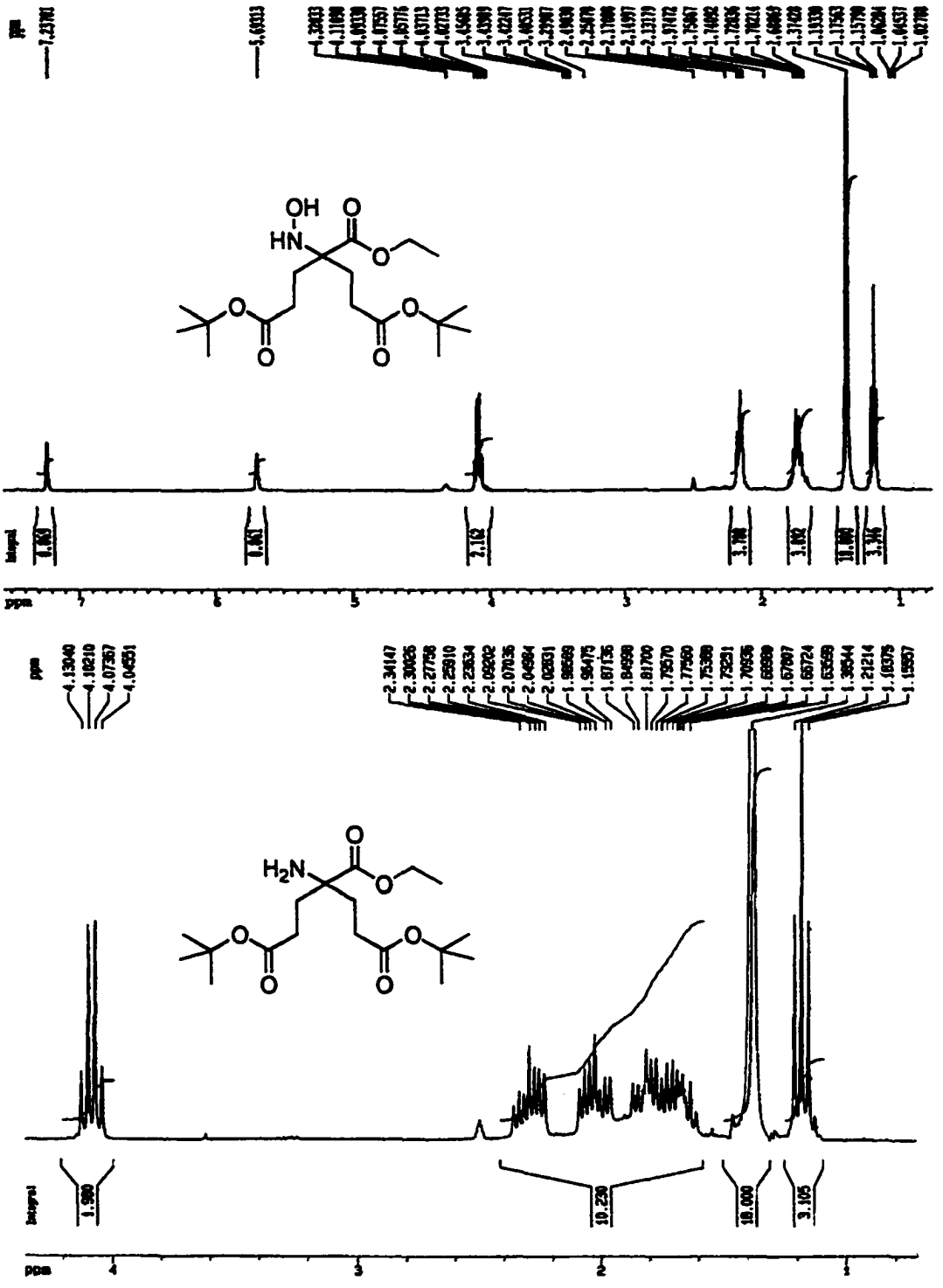

Figure 2.14. ^{1}H-NMR analysis of Pd catalyzed reduction of nitro group to yield hydroxylamine (top) versus Raney nickel catalysis to yield amine **2.2b** (bottom).

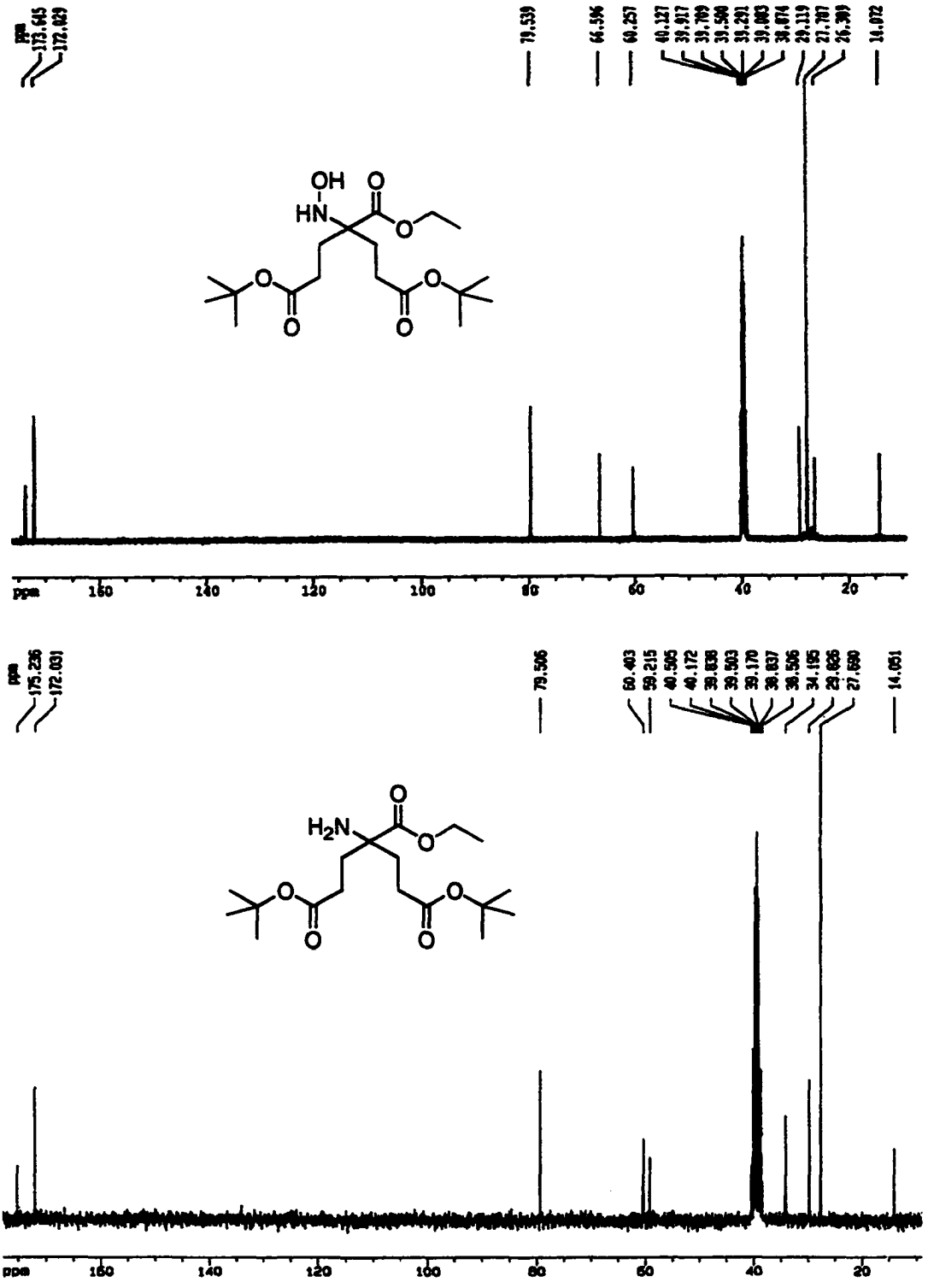

Figure 2.15. ^{13}C-NMR analysis of Pd catalyzed reduction of nitro group to yield hydroxylamine (top) versus Raney nickel catalysis to yield amine **2.2b** (bottom).

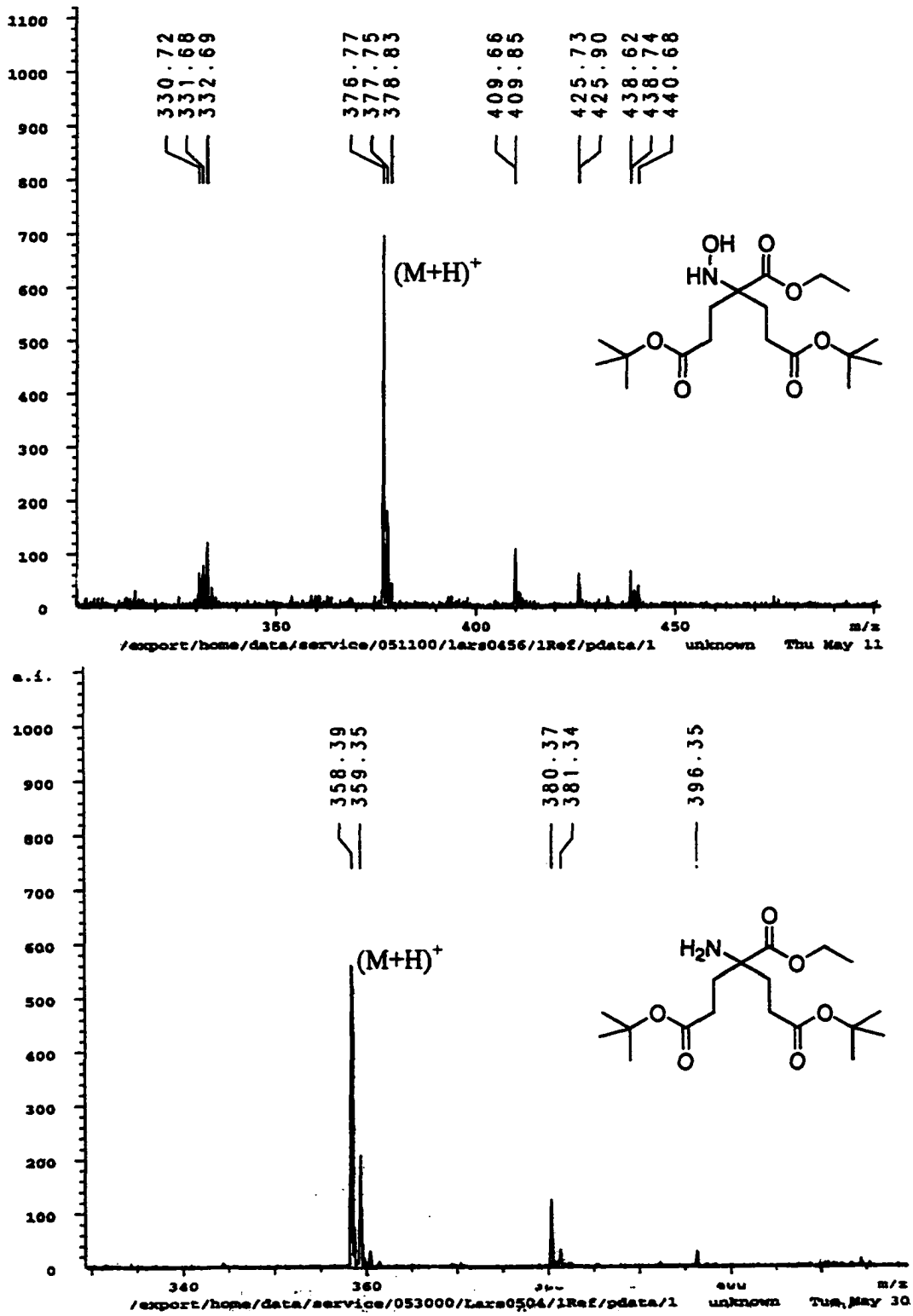

Figure 2.16. MALDI-MS analysis of Pd catalyzed reduction of nitro group to yield hydroxylamine (top) versus Raney nickel catalysis to yield amine **2.2b** (bottom).

theoretical lack of selectivity in hydrolysis arises from the presence of a tertiary carbon center α to the ester carboxylate. This ester, thus, becomes essentially neopentyl in character and is highly sterically inaccessible. The lowered kinetics of the ethyl ester hydrolysis may compete with the already very low rates of t-butyl ester hydrolysis and result in lower selectivity. In turn, side-chain α-deprotonation and/or intramolecular cyclization by Dieckmann-type reactions may be a prominent factor. In addition to acid and base catalyzed ester hydrolysis, nucleophilic dealkylations of the ethyl ester with NaCN, NaI, NaSePh and $KOSi(Me)_3$ were attempted with no success.[2.60] The best hydrolysis results were realized by the use of 1.4 equivalents tetramethyl ammonium hydroxide in a 1:2 water and methanol mixture which was cooled to zero degrees and slowly allowed to rise to room temperature over 24 hours. Evaporation of the solvent and acidic precipitation of the zwitterion from a saturated sodium chloride solution gives the amino acid in 20-30% yield. Isolation of side-products from this hydrolysis showed that ester-hydrolysis selectivity was not the primary cause of the problems associated with the synthesis. Selective ethyl ester hydrolysis occurs slowly under weakly basic conditions. However, the α-amino carboxylate that results rapidly cyclizes with the δ-*t*-butyl ester to form a racemic mixture of 3-carboxy-3-(*t*-butylcarboxyethyl)-2-pyrrolidinone (Figure 2.17). The structure of this intermediate, which was isolated in ~70% yield, was verified by X-ray crystallography and NMR (Figure 2.18). The N^{α}-Alloc protected ethyl amino ester was also prepared (see experimental 2.3.15) to attempt to avoid cyclization. However, hydrolysis of this compound resulted in a complex mixture of side-products, most likely arising from incomplete hydrolysis, over-hydrolysis of the *t*-butyl esters, and/or cyclization.

To overcome the problem of intermediate cyclization during ethyl ester hydrolysis, ethyl-2-nitroacetate was alkylated with *t*-butyl-2-bromoacetate in DMF and tetrabutyl ammonium iodide at 50 °C. The shorter chain length of this alkylating agent

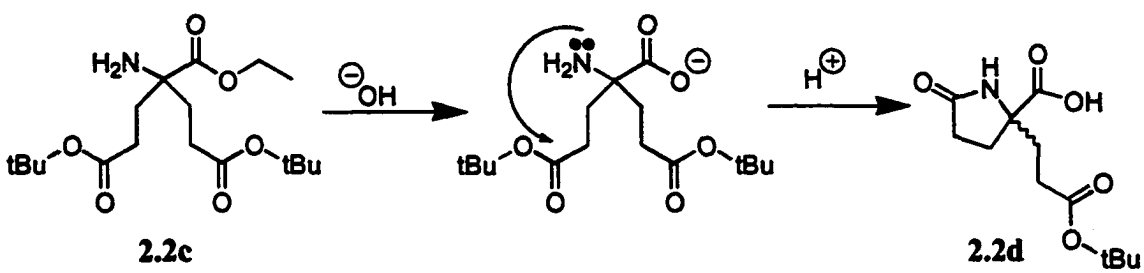

2.2c 2.2d

Figure 2.17. Base catalyzed intramolecular cyclization of 2,2-Bis(*t*-butylcarboxyethyl) glycine to yield racemic mixture of 3-carboxy-3-(*t*-butylcarboxyethyl)-2-pyrrolidinone **2.2d**.

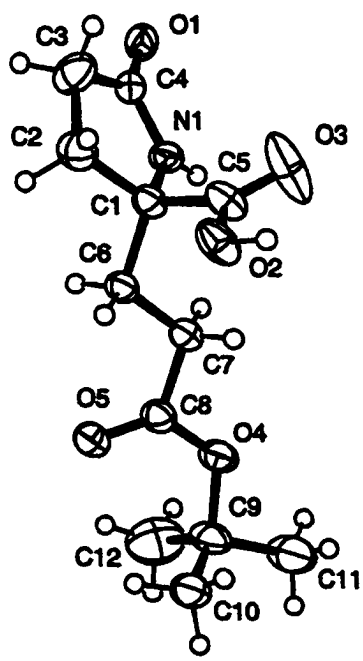

Figure 2.18. ORTEP of 3-carboxy-3-(*t*-butylcarboxyethyl)-2-pyrrolidinone.

assures that base catalyzed cyclization does not occur. Subsequent catalytic hydrogenation over Raney nickel in EtOH/AcOH at 60 psi yields the desired ethyl-2,2-bis(*t*-butylcarboxymethyl)glycine in quantitative yield (Figure 2.19). Lithium hydroxide induced hydrolysis yields the desired zwitterion of 2,2-bis(*t*-butyl carboxymethyl)glycine in high yield. The zwitterion of this derivative can now be N^{α}-protected to allow for SPPS incorporation (Figure 2.20).

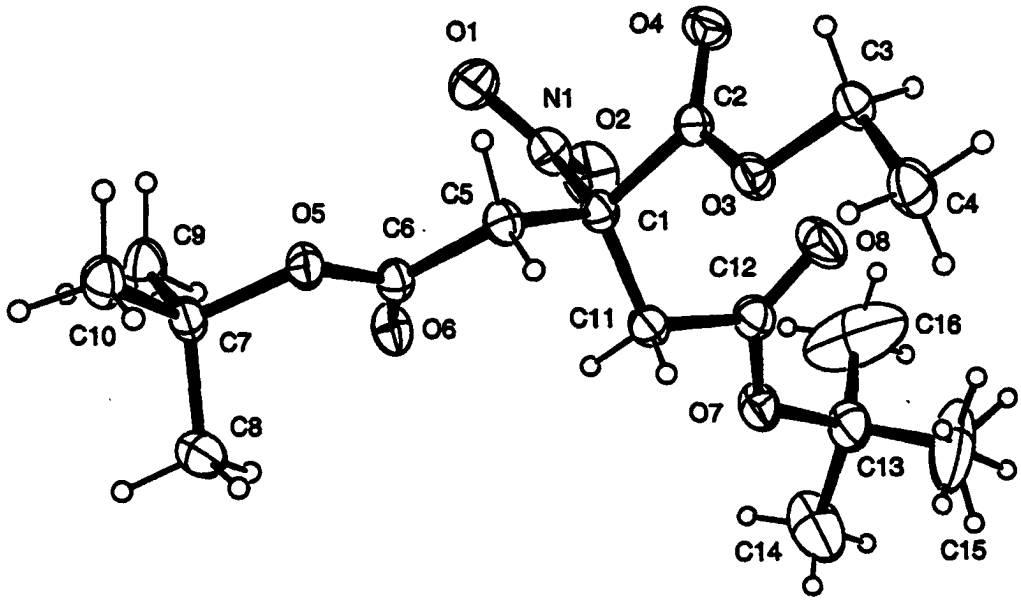

Figure 2.19. ORTEP of 2,2-Bis(*t*-butylcarboxymethyl)-2-nitroacetate.

A selectivity problem is encountered when attempting selective reduction of the nitro versus nitrile groups in the synthesis of Fmoc-Bap(Boc)$_2$-OH. Catalytic hydrogenation over Raney nickel shows complete reduction of all three functional groups. However, isolation of the triamine derivative has been found to be difficult and selective Fmoc/Boc protection of the resulting triamine resulted in low yields and

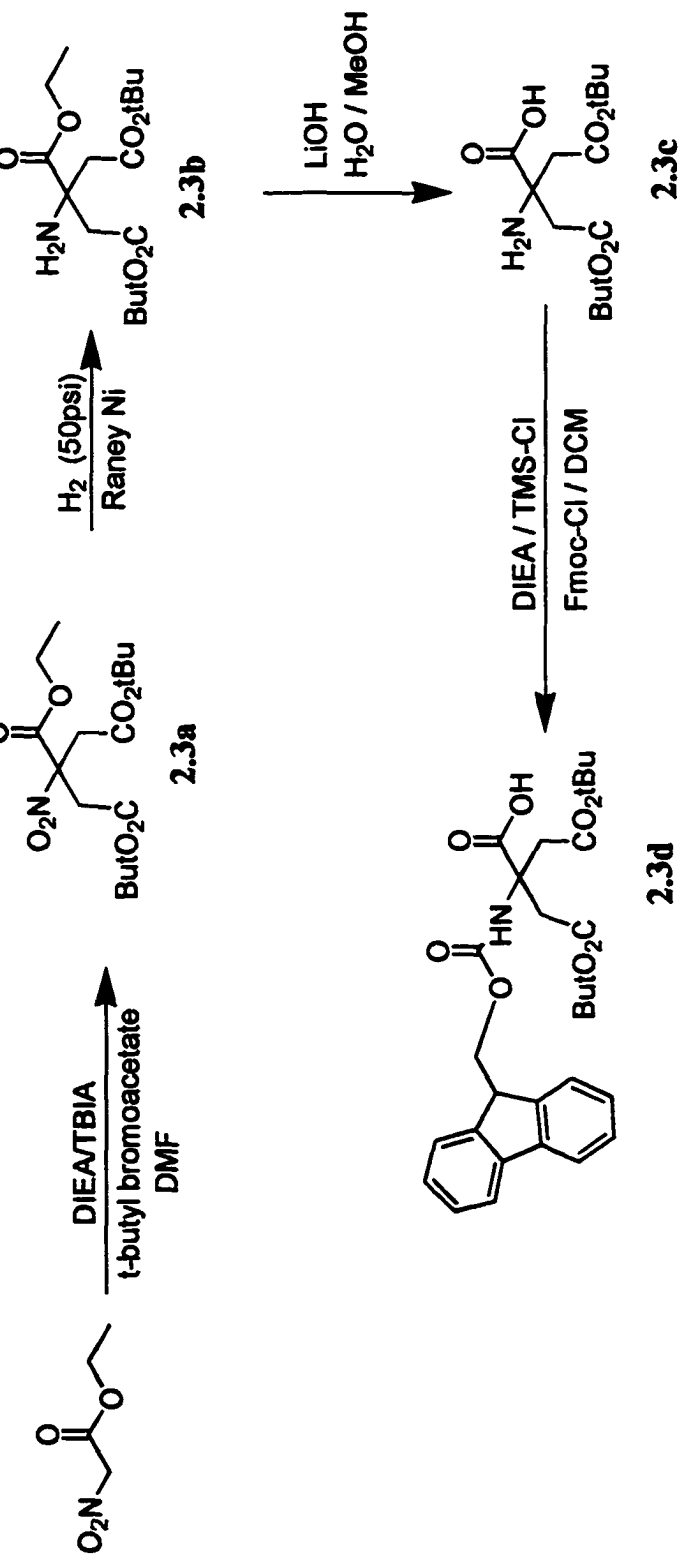

Figure 2.20. Synthetic scheme of the synthesis of Fmoc-Basp(Boc)$_2$-OH **2.3**.

complex mixtures. Borane is known to selectively reduce nitriles in the presence of nitro groups. Reduction with this reagent, however, yielded primarily starting material. Additional attempts at selective reduction of the nitro or nitriles have been unsuccessful. Thus, further attempts at the synthesis of Fmoc-Bap(Boc)$_2$-OH from this starting material were abandoned. Alternative routes, which may lead to the successful synthesis of this fascinating amino acid, are presented in chapter 6 of this dissertation.

2.3. EXPERIMENTAL

2.3.1. Piperidine-4-spiro-5′-hydantoin (2.1b)

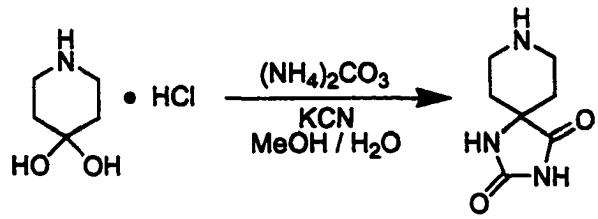

2.1a **2.1b**

A 1000 mL round-bottom flask was fitted with a stirbar and charged with 4-piperidone monohydrate hydrochloride **2.1a** (30.0 g, 195 mmol), ammonium carbonate (41.29 g, 420 mmol), methanol (250 mL) and deionized water (150 mL). The mixture was allowed to stir at room temperature until all solids were dissolved and potassium cyanide (26.71 g, 410 mmol) dissolved in deionized water (100 mL) was added dropwise to the reaction mixture over a period of 10 minutes. The reaction was sealed with a rubber stopper and allowed to stir at room temperature for 48 hours. The resulting suspension was concentrated to a volume of 300 mL using rotary evaporation at 40 °C and the solution was cooled to 10 °C. The precipitated white solid was collected in a Buchner funnel using suction filtration. Additional concentration of the filtrate to a volume of 200 mL gave some additional product that was filtered and added

to the first crop. The combined light yellow solid was washed with portions of deionized water (4 x 25 mL) until pure white. The product was allowed to air dry for 2 hours and then dried in a vacuum oven (85 °C, 0.5 torr) overnight to yield 28.10 g (85% yield) of pure hydantoin **2.1b**. ^{1}H NMR (200 MHz, d_6-DMSO) δ 10.75 (bs, 1H), 8.35 (s, 1H), 2.84 (dt, 2H), 2.66 (td, 2H), 1.67 (td, 2H), 1.38-1.24 (m 2H). ^{13}C NMR (50 MHz, d_6-DMSO) 177.46, 156.30, 61.09, 41.14, 37.79.

2.3.2. 1-*tert*-butyloxycarbonylpiperidine-4-spiro-5'-(1',3'-bis(*t*-butyloxycarbonyl)) hydantoin (2.1c)

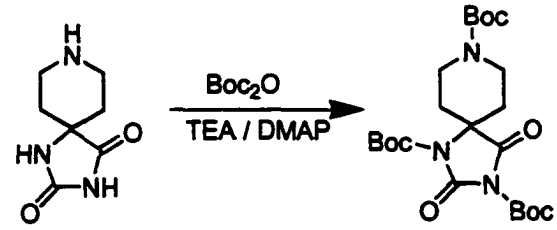

2.1b **2.1c**

Hydantoin **2.1b**, (26.0 g, 154 mmol), was suspended in 1000 mL of dry 1,2-dimethoxyethane in a 2000 mL three-necked round bottom flask, which was equipped with an argon inlet valve, an oil bubbler, and an overhead mechanical stirrer. To this suspension, triethylamine (15.7 g, 154 mmol) was added in one portion and the suspension was allowed to stir for 30 minutes. While stirring, di-*tert*-butyl dicarbonate (168.0 g, 770 mmol) was transferred by pipette into the reaction mixture, followed by 4-dimethylaminopyridine (DMAP) (0.19 g, 1.54 mmol). A catalytic amount (0.20 g) of DMAP was added every 12 hours during the course of the reaction. The reaction vessel was flushed briefly with argon and allowed to stir vigorously for 72 hours. The solvent was removed by rotary evaporation and the crude product was dissolved in chloroform (500 mL). The solution was washed with 1.0 N HCl (3 x 200 mL) and the combined

acid washes were backwashed with chloroform (100 mL). The organic layer was washed with saturated $NaHCO_3$ (100 mL) and brine (100 mL). The organic layer was dried over $MgSO_4$ and the solvent removed by rotary evaporation. The resulting crude product was dried under vacuum at 0.01 torr for 24 hrs. The resulting light yellow solid was triturated by suspending the finely ground product in diethyl ether (400 mL), stirring for two hours, and vacuum filtering the solid in a Buchner funnel followed by washings with portions of diethyl ether (4 x 50 mL). The product was dried under vacuum (85 °C, 0.5 torr) for 24 hours to give 57.9 g (80% yield) of **2.1c**. ^{1}H NMR (200 MHz, $CDCl_3$) δ 4.29-4.01 (m, 2H), 3.42-3.57 (app dt, 2H), 2.67 (dt, 2H), 1.76 (m, 2H), 1.58 (s, 9H), 1.54 (s, 9H), 1.47 (s, 9H). ^{13}C NMR (50 MHz, $CDCl_3$) 169.98, 154.71, 148.24, 147.50, 145.35, 87.51, 85.36, 80.13, 62.53, 39.96, 29.87, 28.62, 28.21, 27.91.

2.3.3. 1-*tert*-butyloxycarbonylpiperidine-4-amino-4-carboxylic acid (2.1d)

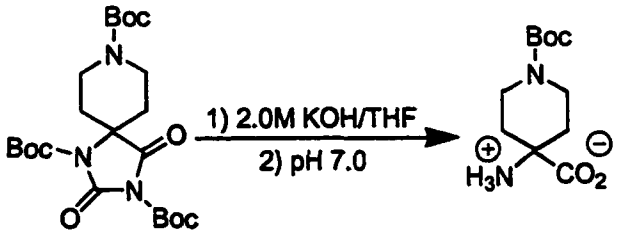

2.1c **2.1d**

1-*tert*-butyloxycarbonylpiperidine-4-spiro-5'-(1',3'-bis(*tert*butyloxycarbonyl)) hydantoin **2.1c** (40.0 g, 0.083 mole), was suspended in THF (340 mL) in a 2000 mL Erlenmeyer flask. While stirring vigorously with a stirbar, 2.0 M aqueous potassium hydroxide solution (340 mL) was added in one portion. The flask was stoppered and the mixture was allowed to stir for 4 hours. The clear solutions were poured into a separatory funnel and the bottom layer was drained into a 1000 mL round bottom flask. Residual dissolved THF was removed by rotary evaporation and the aqueous solution

was chilled in an ice bath. While stirring at 4 °C, the pH of the aqueous solution was adjusted to 7.0 by slow addition of a 2.0 N HCl solution. The resulting white precipitate is filtered and dried *in vacuo* (85 °C, 0.5 torr) to yield 19.7 g (95% yield) of the amino acid. ^{1}H NMR (200 MHz, d_6-DMSO) δ 3.61-3.35 (m, 4H), 1.95-1.79 (m, 4H), 1.39 (s, 9H).

2.3.4. 1-*tert*-butyloxycarbonyl-4-(9-fluorenylmethyloxycarbonylamino)-piperidine 4-carboxylic acid (2.1)[4]

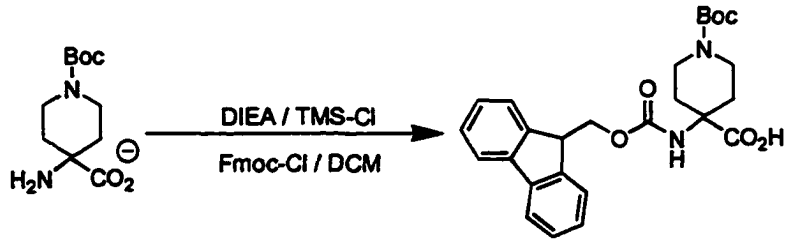

2.1d **2.1**

Finely ground tri-Boc hydantoin **2.1d** (17.0 g, 69.6 mmol) was placed, together with a stirring bar, in a 1000 mL three-necked round bottom flask, which was stoppered and evacuated for three hours prior to use. While flushing with argon, the flask was equipped with an argon inlet/outlet valve, a septum, and a bubbler submerged into a 6.0 M KOH bath. Anhydrous DCM (500 mL) was cannulated into the reaction vessel and DIEA (22.5 g, 174 mmol, 30.3 mL) was added via syringe. The reaction was stirred for thirty minutes and chlorotrimethylsilane (17.6 mL, 15.1 g, 140 mmol) was added dropwise while stirring. The reaction was allowed to stir for an additional thirty minutes and the septum was replaced with a reflux condenser. The solution was refluxed for three hours during which the reaction became homogeneous. At thirty-minute intervals, the reaction vessel was flushed for thirty seconds with argon to remove HCl formed in the reaction. The solution was cooled to –10 °C and 9-

fluorenylmethyl chloroformate (Fmoc-Cl) (18.0 g, 70.0 mmol) was added in one portion. The solution was allowed to stir for 3 hours, under a constant slow stream of argon. The solvent was removed by rotary evaporation and the product distributed between diethyl ether (200 mL) and aqueous 2.5% Na_2CO_3 (1000 mL). The aqueous layer was separated and washed with additional portions of diethyl ether (2 x 100 mL). The aqueous layer was placed on a rotary evaporator at room temperature to remove any dissolved ether and acidified to pH 2.0 in an ice bath using 2.0 N HCl. The precipitated free acid was extracted with ethyl acetate (300 mL) and additional portions of ethyl acetate (2 x 150 mL). The ethyl acetate extracts were combined, dried over $MgSO_4$, filtered, and the solvent was removed by rotary evaporation to yield 29.56 g (91 % yield) of pure product **2.1e**. ^{1}H NMR (200 MHz, $CDCl_3$) δ 8.30 (bs, 1H), 7.70 (d, 2H), 7.53 (d, 2H), 7.30 (t, 2H), 7.25 (t, 2H), 4.37 (m, 3H), 3.76 (m, 2H), 3.04 (m, 2H), 1.96 (m, 2H), 1.51 (m, 2H), 1.44 (s, 9H). ^{13}C NMR (50 MHz, d_6-DMSO) 175.01, 155.41, 153.89, 143.81, 140.76, 127.63, 127.06, 125.28, 120.07, 78.71, 65.39, 59.74, 56.69, 46.78, 31.28, 28.05.

2.3.5. Ethyl-2,2-Bis(*t*-butylcarboxyethyl)-2-nitroacetate (2.2a)

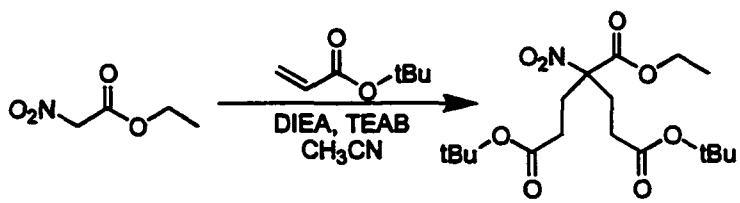

2.2a

Ethyl nitroacetate (8.0 g, 60.1 mmol) was dissolved in acetonitrile (100 mL) in a 250 mL roundbottom flask together with a magnetic stirrer. N,N'-diisopropylethylamine (15.54 g, 120.0 mmol) was slowly added to the solution while

stirring at 0 °C. A catalytic amount of tetraethylammonium bromide (TEAB) (0.63g, 0.3 mmol) was added, the reaction was sealed with a rubber septum and allowed to stir at 0 °C for 10 minutes. *t*-Butylacrylate (15.41g, 17.6 mL, 120.0 mmol) was added dropwise over a period of 15 minutes. The reaction was allowed to slowly rise to room temperature and stirred for 48 hours. The reaction was monitored by TLC (100% dichloromethane) until all starting material was consumed. The acetonitrile was removed *in vacuo* and the resulting crude was dissolved in diethyl ether (100 mL). The organic layer was washed with 1N HCl (2 x 100 mL) and saturated sodium carbonate solution (2 x 100 mL). The organic layer was separated and filtered over a thin pad of silica in a Buchner funnel. The silica was washed with diethyl ether (2 x 30 mL) and all organic fractions combined. The ether was dried over anhydrous sodium sulfate and removed by rotary evaporation. The desired dialkylated α-nitro ester **2.2a** was obtained in good purity with no further need for purification (21.95 g, 94.1%). ^{1}H NMR (250 MHz, d_6-DMSO) δ 4.24 (q, 2H), 2.38 (m, 4H), 2.24 (m, 4H), 1.40 (s, 18H), 1.21 (t, 3H). ^{13}C NMR (60 MHz, d_6-DMSO) 170.39, 165.81, 94.58, 80.33, 62.94, 29.04, 28.33, 27.63, 13.53. HRFAB-MS m/z 390.2119 $(M+H)^+$, EA: $C_{18}H_{31}NO_8$, calc: 55.51% C, 8.02% H, 3.60% N, found: 55.31%C, 7.83% H, 3.87% N.

2.3.6. Ethyl-2,2-bis(*t*-butylcarboxyethyl) glycine (2.2b)

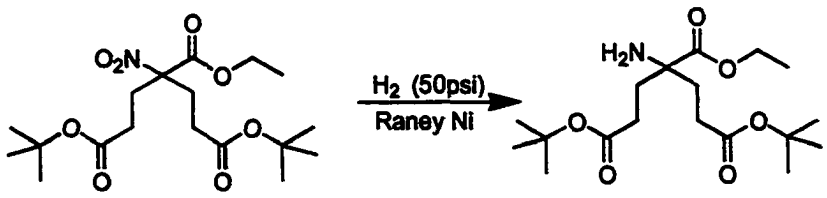

2.2a **2.2b**

Nitroester **2.2a** (8.0 g, 24.63 mmol) was dissolved in absolute ethanol (30 mL) and 3.0 g of a 50% (w/w) slurry of Raney Nickel in water was added. The reaction was

hydrogenated over hydrogen gas (60 psi) for 72 hours. The reaction was monitored by TLC (100% DCM). The reaction was filtered carefully over Celite and the Celite cake washed with DCM (100 mL). Organic solvents were removed *in vacuo* to yield **2.2b** in excellent purity (7.4 g, 93%). ^{1}H NMR (250 MHz, d_6-DMSO) δ 4.09 (q, 2H), 2.34-1.64 (m, 8H), 1.81 (s, 2H), 1.39 (s, 18H), 1.84 (t, 3H). ^{13}C NMR (60 MHz, d_6-DMSO) 175.24, 172.03, 79.51, 60.40, 59.22, 34.20, 29.83, 27.69, 14.05.

2.3.7. Ethyl-2,2-bis(*t*-butylcarboxyethyl)-2-hydroxylaminoacetate

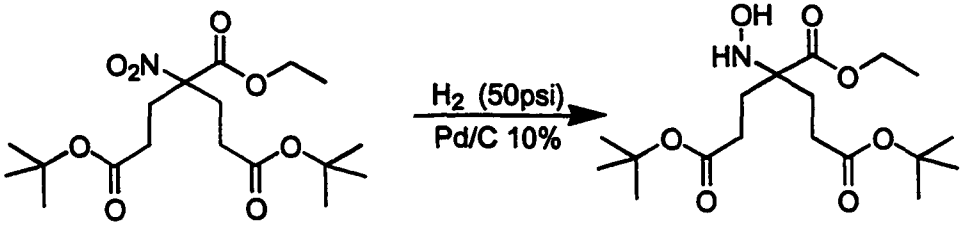

2.2a

Nitro ester **2.2a** (1.0 g, 2.57 mmol) was dissolved in absolute ethanol (20 mL) and 10% (w/w) palladium on carbon (0.1g) was added carefully to the solution. The dark black suspension was placed in a hydrogenation flask and hydrogenated at 50 psi for 24 hours. The reaction was monitored by TLC (100% DCM) and continued until all starting material was consumed. The Pd / C was removed by vacuum filtration through a Celite cake which was washed with several portions of ethyl acetate. Additional filtrations through Celite may be required to remove all traces of catalyst. The organic filtrate was dried over anhydrous sodium sulfate and the crude isolated by rotary evaporation. Drying under high vacuum overnight yields the hydroxylamine in quantitative yield (0.97 g, 100%). ^{1}H NMR (250 MHz, d_6-DMSO) δ 7.23 (s, 1H), 5.69

(s, 1H), 4.06 (q, 2H), 2.15 (m, 4H), 1.72 (m, 4H), 1.37 (s, 18H), 1.17 (t, 3H).). ^{13}C NMR (60 MHz, d_6-DMSO) 173.65, 172.03, 79.54, 66.60, 29.12, 27.71, 26.31, 14.07. FAB-MS m/z 376.77 $(M+H)^+$.

2.3.8. 2,2-bis(*t*-butylcarboxyethyl) glycine (Bglu(*t*Bu)$_2$-OH, 2.2c)

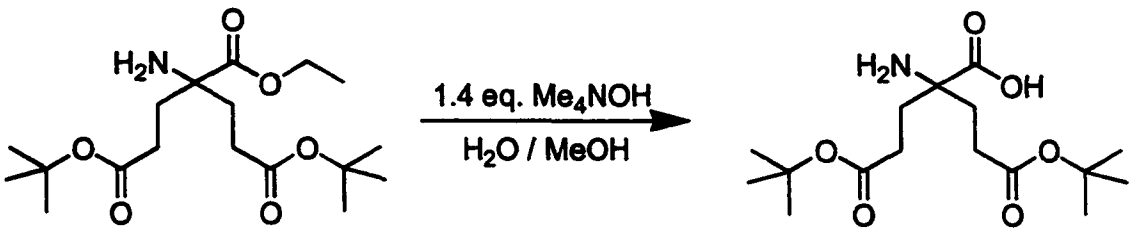

2.2b **2.2c**

Amino ethyl ester **2.2b** (3.0 g, 8.34 mmol) was dissolved in methanol (20 mL) in a 100 mL round-bottom flask and 10 mL water was added to the solution. The solution was cooled to 0 °C and Me_4NOH solution (4.26 g, 25% w/w in methanol) was added dropwise through a pressure equalizing addition funnel. The flask was sealed with a rubber septum and was slowly allowed to rise to room temperature and stirred for 24 hours. The reaction is monitored by TLC (100% EtOAc) until complete. After the reaction was determined to be complete, it was diluted with saturated NaCl (50 mL) solution and the pH adjusted to 5.0 with 1.0 N HCl. The methanol was removed *in vacuo* by rotary evaporation and the resulting suspension cooled in the refrigerator at 6 °C for 24 hours until of the zwitterion precipitated from solution. The precipitated zwitterion was removed by suction filtration and dried overnight under high vaccum to yield the pure product **2.2c** (0.72 g, 26%). ^1H NMR (250 MHz, d_6-DMSO) δ 4.92 (s, 3H), 2.42-1.91 (m, 8H), 1.43 (s, 18H) ^{13}C NMR (60 MHz, d_6-DMSO) 180.22, 173.78, 81.87, 66.60, 34.44, 31.41, 28.31.

2.3.9. 3-Carboxy-3-(*t*-butylcarboxyethyl)-2-pyrrolidinone (2.2d)

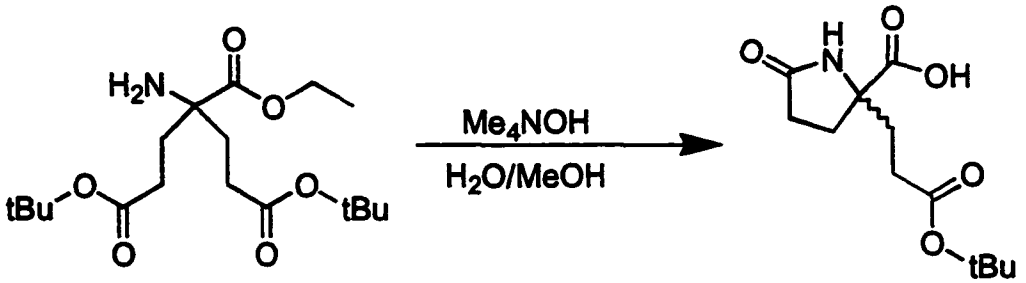

2.2b **2.2d**

Amino ethyl ester **2.2b** (3.0 g, 8.34 mmol) was dissolved in methanol (20 mL) in a 100 mL round-bottom flask and water (10 mL) added to the solution. The solution was cooled to 0 °C and Me_4NOH solution (4.26 g, 25% w/w in methanol) was added dropwise through a pressure equalizing addition funnel. The flask was sealed with a rubber septum and slowly allowed to rise to room temperature while stirring for 24 hours. The reaction was monitored by TLC (100% EtOAc) until complete. After the reaction was determined to be complete, it was diluted with saturated NaCl (50 mL) solution and the pH adjusted to 5.0 with 1.0 N HCl. The methanol was removed *in vacuo* by rotary evaporation and the resulting suspension cooled in the refrigerator at 6 °C for 24 hours until the zwitterion precipitated from solution. The precipitated zwitterion was removed by suction filtration and the aqueous filtrate further acidified to pH 2.0 with 1.0N HCl. The precipitated product was extracted with diethyl ether (2 x 50 mL) and recrystallized from hot carbon tetrachloride to yield pyrrolidinone **2.2d** in good yield (2.07 g, 78%) ^{1}H NMR (250 MHz, d_6-DMSO) δ 8.10 (s, 1H), 2.46-1.63 (m, 8H), 1.39 (s, 9H).

2.3.10. Ethyl-2,2-bis(*t*-butylcarboxymethyl)-2-nitroacetate (2.3a)

2.3a

Ethyl nitroacetate (5.0 g, 37.5 mmol) was dissolved in 20 mL DMF in a 250 mL round-bottom flask and 2-bromo-*t*-butylacetate (15.4 g, 78.9 mmol) was added. While stirring, tetrabutylammonium bromide (1.39 g, 3.75 mmol) was added in one portion and the solution allowed to stir for 15 minutes. In a pressure equalizing addition funnel, DIEA (10.7 g, 82,6 mmol) was added dropwise. The rate of addition was controlled to keep the temperature of the reaction at under 50 °C. After addition, the reaction was sealed tightly and kept at 50 °C for an additional 24 hours while stirring. The consumption of 2-bromo-*t*-butylacetate can be monitored by gas chromatography. After 24 hours, the reaction was allowed to cool to room temperature, diluted with diethyl ether (500 mL) and washed successively with 1N HCl (2 x 100 mL), saturated aqueous sodium carbonate solution (2 x 100 mL), water (4 x 100 mL) and brine (100 mL). The organic phase was dried over anhydrous sodium sulfate and the solvent removed *in vacuo* by rotary evaporation. Residual DMF was removed under high vacuum over 24 hours. The resulting dark red crude was recrystallized from boiling hexane to yield 9.8 g (79%) of analytically pure ethyl-2,2-bis(*t*-butylcarboxymethyl)-2-nitroacetate (**2.3a**) as pale yellow crystals. ^{1}H NMR (250 MHz, $CDCl_3$) δ 4.25 (q, 2H), 3.35 (dd, 4H), 1.42 (s, 18H), 1.27 (t, 3H). ^{13}C NMR (60 MHz, $CDCl_3$) 167.43, 165.07, 90.09, 82.64, 63.58, 39.90, 28.15, 13.91. FAB-MS m/z 362.40 $(M+H)^+$

2.3.11. Ethyl-2,2-bis(*t*-butylcarboxymethyl) glycine (2.3b)

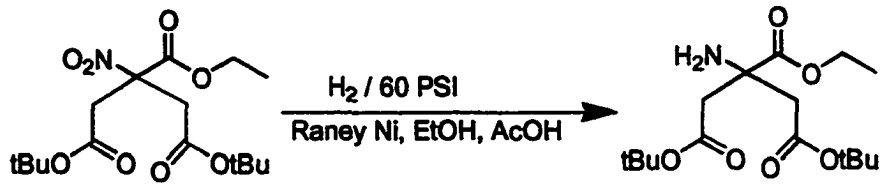

2.3a **2.3b**

Ethyl-2,2-bis(*t*-butylcarboxymethyl)-2-nitroacetate **2.3a** (1.3 g, 3.92 mmol) was dissolved in absolute ethanol (10 mL) together with glacial acetic acid (1 mL). A 50% (w/w) slurry of Raney nickel in water (1.0 g) was added. The reaction was hydrogenated over hydrogen gas (60 psi) for 24 hours. The reaction was monitored by TLC (silica gel, 100% DCM). The resulting solution was filtered carefully over Celite and the Celite cake washed with EtOH (30 mL). Volatile solvents were removed *in vacuo* and the resulting crude dissolved in diethyl ether (30 mL). The ether was washed with saturated sodium carbonate (30 mL) and brine (50 mL). The organic fraction was separated, dried over anhydrous sodium sulfate and rotary evaporated to yield **2.3b** in excellent yield (1.1 g, 92%) and purity ^{1}H NMR (250 MHz, $CDCl_3$) δ 4.12 (q, 2H), 2.58 (dd, 4H), 2.26 (s, 2H), 1.37 (s, 18H), 1.20 (t, 3H). ^{13}C NMR (60 MHz, $CDCl_3$) 174.98, 169.74, 81.50, 61.53, 57.79, 45.05, 28.19, 14.28. FAB-MS m/z 331.8 $(M+H)^+$

2.3.12. 2,2-bis(*t*-butylcarboxymethyl) glycine (Basp(*t*Bu)$_2$-OH, 2.3c)

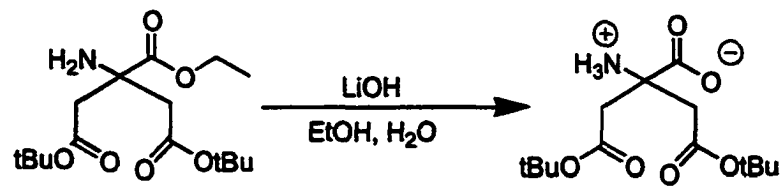

2.3b **2.3c**

Ethyl-2,2-bis(*t*-butylcarboxymethyl) glycine (2.0g, 6.03 mmol) was dissolved in absolute ethanol (20 mL). LiOH (0.4g, 18.1 mmol) in water (10 mL) was added and the reaction stirred at 50 °C until all starting material was consumed by thin layer chromatography (silica gel, 100% ethyl acetate, ca. 3 hours). The resulting solution was cooled to room temperature, diluted with brine (40 mL) and the ethanol removed *in vacuo*. The aqueous solution was neutralized with 1N HCl to pH 6.0 and the resulting precipitate was filtered. The white powder was allowed to dry under vacuum for 24 hours to yield the analytically pure zwitterion **2.3c** in quatitative yield (1.81.g, 100%). ^{1}H NMR (250 MHz, d_6-DMSO) δ 2.69 (dd, 4H), 1.40 (s, 18H). ^{13}C NMR (60 MHz, d_6-DMSO) 171.80, 171.23, 82.40, 71.23, 59.59, 29.51.

2.3.13. N'-(9-fluorenylmethyloxycarbonyl)-2,2-bis(*t*-butylcarboxymethyl) glycine (Fmoc-Basp(*t*Bu)$_2$-OH, 2.3)

2.3c **2.3**

2.3c (0.25 g, 0.81 mmol) was dissolved in wet DMF (10 mL) along with DIEA (0.22 g, 1.61 mmol). Enough water was added to allow for the amino acid to go into solution, and Fmoc-Cl (0.20 g, 0.78g) was added in one portion. The reaction was kept at 50 °C for 24 hours. 1N HCl (30 mL) was added and the reaction extracted with diethyl ether (30 mL). The ether was washed with 1N HCl (3 x 20 mL) and the organic layer dried over Na_2SO_4. Rotary evaporation gives the crude Fmoc-Basp(*t*Bu)$_2$-OH in fair yield (0.30g, 71%). ^{1}H NMR (400 MHz, $CDCl_3$) δ 7.68-7.19 (m, 8H), 6.22 (t, 1H), 4.26 (d, 2H), 3.36-2.61 (dd, 4H), 1.31 (s, 18H).

2.3.14. Ethyl-2,2-Bis(2-cyanoethyl)-2-nitroacetate (2.4a)

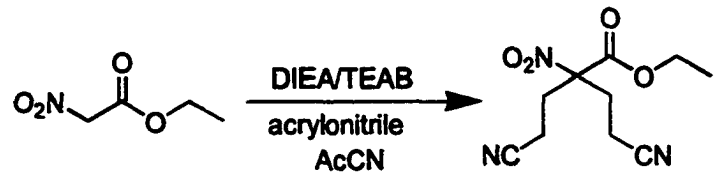

2.4a

Ethyl nitroacetate (8.0 g, 60.1 mmol) was dissolved in acetonitrile (100 mL) in a 250 mL roundbottom flask together with a magnetic stirrer. N,N'-diisopropylethylamine (15.54 g, 120.0 mmol) was slowly added to the solution while stirring at 0 °C. A catalytic amount tetraethylammonium bromide (TEAB) (0.63g, 0.3 mmol) was added, the reaction was sealed with a rubber septum and allowed to stir at 0 °C for 10 min. Acrylonitrile (6.37 g, 120.0 mmol) was added dropwise over a period of 15 min. The reaction was allowed to slowly rise to room temperature and stirred for 48 h. The reaction was monitored by TLC (100% dichloromethane) until all starting material was consumed. The acetonitrile was then removed *in vacuo* and dissolved in diethyl ether (100 mL). The organic layer was washed with 1N HCl (2 x 100 mL) and saturated sodium carbonate solution (2 x 100 mL). The organic layer was separated and filtered over a thin pad of silica in a Buchner funnel. The silica was washed with diethyl ether (2 x 30 mL) and all organic fractions combined. The ether was dried over anhydrous sodium sulfate and removed by rotary evaporation. The desired dialkylated α-nitro ester was obtained in good purity with no further need for purification (16.47 g, 84.1%). ^{1}H NMR (250 MHz, d_6-DMSO) δ 4.27 (q, 2H), 2.63 (m, 8H), 1.24 (t, 3H) ^{13}C NMR (60 MHz, d_6-DMSO) 164.71, 118.99, 93.27, 63.58, 28.55, 13.44, 11.79 HRFAB-

MS m/z 262.0809 $(M+H)^+$, EA: $C_{10}H_{13}N_3O_4$, calc: 50.20% C, 5.48% H, 17.56% N, found: 50.07% C, 5.36% H, 17.61% N.

2.3.15. O-Ethyl-N$^{\alpha}$-Allyloxycarbonyl-2,2-Bis(*t*-butylcarboxyethyl) glycine

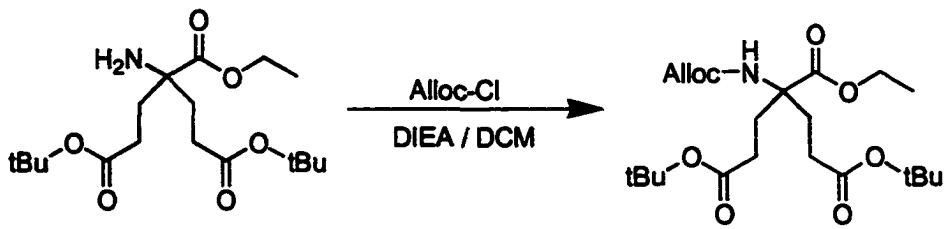

2.2b

The α-amino ethyl ester **2.2b** (4.0g, 11.1mmol) was dissolved in anhydrous DCM (40 mL) in a round-bottom flask. DIEA (1.72g, 13.4 mmol, 2.33 mL) was added in one portion and the reaction cooled to 0 °C in an ice-bath. Allyl chloroformate (1.48g, 12.24 mmol, 1.30 mL) was added dropwise through an addition funnel and the reaction was allowed to rise to room temperature over 20 h. The reaction was then diluted with DCM (50 mL) and washed with 1.0 N HCl (2 x 100 mL). The organic layer was dried over anhydrous sodium sulfate and all volatiles removed *in vacuo* to yield the crude Alloc-Bglu(*t*Bu)$_2$-OEt as a pale yellow oil (4.82 g, 97%), which was used without further purification. ^{1}H NMR (250 MHz, d_6-DMSO) δ 7.53 (s, 1H), 5.73 (m, 1H), 5.27 (dd, 1H), 5.15 (dd, 1H), 4.42 (d, 2H), 4.03 (q, 2H), 2.13-1.81 (m, 8H), 1.37 (s, 18H), 1.13 (t, 3H). ^{13}C NMR (60 MHz, d_6-DMSO) 172.18, 171.57, 154.40, 133.71, 116.74, 79.69, 64.23, 60.45, 32.30, 29.16, 28.32, 27.66, 13.93.

2.4. CONCLUSIONS

C$^{\alpha}$,C$^{\alpha}$-disubstituted amino acids (ααAAs) are highly useful tools for inducing desired secondary structure in short peptide segments. The synthesis of highly water-soluble amphipathic peptides with high levels of ααAAs is hindered by the intrinsically

low solubilities of these residues. The synthesis of a series of polyfuctional ααAAs have been presented to overcome these difficulties. The incorporation of the C^{α},C^{α}-disubstituted lysine analog, Api, into short peptides has been shown to successfully induce helical secondary structures while retaining high water solubility. Api has been synthesized through the application of the Bucherer-Berg hydantoin hydrolysis to yield an orthogonally protected derivative suitable for solid-phase peptide synthesis. Problems associated with contamination by bis(*t*-butyl)carbamate can be overcome by utilizing a selective aqueous / organic hydrolysis mixture composed of 2.0 M KOH and THF.

The successful application of Bglu/Basp and Bap, will allow for new peptides with interesting salt-bridging possibilities and increased amphipathic character in short sequences. These derivatives are synthesized by the rapid dialkylation of ethyl nitroacetate under weakly basic conditions. Tetraethylammonium bromide (TEAB) facilitates Michael-type alkylations by acting as a highly dissociated counterion. S_N2 alkylation with *t*-butylbromoacetate was achieved with DMF/TBAI. The use of a tetraalkylammonium iodide in the reaction of alkyl bromides was found necessary to result in satisfactory yields. Catalytic hydrogenation of the bis(*t*-butylcarboxylate) derivatives yields the corresponding ethyl amino esters in excellent yield. Saponification of the ethyl ester of the Bglu derivative results in rapid intramoecular cyclization to yield a racemic mixture of lactams. This was not observed in the corresponding 2,2-bis(*t*-butylcarboxymethyl) derivative, as the cyclization would result in a four-membered ring. N^{α}-Fmoc protection yields the orthogonally protected amino acid.

The use of these synthetic pathways allows for the preparation of synthetically sensitive side-chain protecting groups to be incorporated into polyfunctional amino acid derivatives. Application of these derivatives in peptide synthesis will give new insight into sequence induced secondary structure formation and structure-function studies.

2.5. REFERENCES

2.1 Spatola, A. In *Chemistry and Biochemistry of Amino Acids, Peptides and Proteins, Vol. VII*, Weinstein, B., Ed., Dekker, New York, **1983**, pp. 267-357.

2.2 Benedetti, E., Bavoso, A., DiBlasio, B., Pavone, V., Pedone, C., Toniolo, C., Bonora, G. M., *Proc. Natl. Acad. Sci. U.S.A.* **1982**, *79*, 7951-7957.

2.3 Prasad, B. V. V., Balaram, P., *CRC Crit. Rev. Biochem.* **1984**, *16*, 307-348.

2.4 Hammarström, L. G. J., Gauthier, T. J., Yokum, T. S., Hammer, R. P., McLaughlin, M. L., *J. Pep. Res.* **2000**, submitted for publication.

2.5 Wysong, C. L., Yokum, T. S., McLaughlin, M. L., Hammer, R. P. *Chemtech* **1997**, *27*, 26-33.

2.6 Yokum, T. S., Gauthier, T. J., Hammer, R. P., McLaughlin, M. L., *J. Am. Chem. Soc.* **1997**, *119*, 1167-1168.

2.7 Peggion, C., Flammengo, R., Mossel, E., Broxterman, Q. B., Kaptein, B., Kamphius, J., Formaggio, F., Crisma, M., Toniolo, C. *Tetrahedron* **2000**, *56*, 35-3601.

2.8 Karle, I. L., Balaram, P., *Biochemistry* **1990**, *29*, 6747-6755.

2.9 Hodgkin, E. E., Clark, J. D., Miller, K. R., Marshall, G. R., *Biopolymers* **1990**, *30*, 533-546.

2.10 Paul, P. K. C., Sukumar, M., Bardi, R., Piazzesi, A. M., Valle, G., Toniolo, C., Balaram, P. *J. Am. Chem. Soc.* **1986**, *108*, 6363-6370.

2.11 Nagaraj, R., Shamala, N., Balaram, P. *J. Am. Chem. Soc.* **1979**, *101*, 16-20.

2.12 Toniolo, C., Benedetti, E. *Macromolecules* **1991**, *24*, 4004-4009.

2.13 Marshall, G. R., Hodgkin, E. E., Langs, D. A., Smith, D., Zabrocki, J., Leplawy, M. T. *Proc. Natl. Acad. Sci. U.S.A.* **1990**, *87*, 487-491.

2.14 Martin, D. R., Williams, R. J. P. *Biochem. J.* **1976**, *153*, 181-190.

2.15 Pandey, R. C., Carter Cook, Jr., J., Rinehart, Jr., K. L. *J. Am. Chem. Soc.* **1977**, *99*, 8469-8483.

2.16 Jung, G., Konig, W. A., Liebfritz, D., Ooka, T., Janko, K., Boheim, G. *Biochim. Biophys. Acta* **1976**, *433*, 164-181.

2.17 Pandey, R. C., Carter Cook, Jr., J., Rinehart, Jr., K. L. *J. Am. Chem. Soc.* **1977**, *99*, 5205-5206.

2.18 Pandey, R. C., Meng, H., Carter Cook, Jr., J., Rinehart, Jr., K. L. *J. Am. Chem. Soc.* **1977**, *99*, 5203-5205.

2.19 Gurunath, R., Balaram, P. *Biopolymers* **1995**, *35*, 21-29.

2.20 Karle, I. L., Flippen-Andersson, J. L., Uma, K., Balaram, H., Balaram, P. *Proc. Natl. Acad. Sci. U.S.A.* **1989**, *86*, 765-769.

2.21 Toniolo, C. *Brit. Polm. J.* **1986**, *18*, 221-225.

2.22 Benedetti, E., DiBlasio, B., Pavone, V., Pedone, C., Santini, A., Crisma, M., Valle, G., Toniolo, C. *Biopolymers* **1989**, *28*, 175-184.

2.23 Burgess, A. W., Leach, S. J. *Biopolymers* **1973**, *12*, 2599-2605.

2.24 Benedetti, E., DiBlasio, B., Iacovino, R., Menchise, V., Saviao, M., Pedone, C., Bonora, G. M., Ettorre, A., Graci, L., Formaggio, F., Crisma, M., Valle, G., Toniolo, C. *J. Chem. Soc., Perkin Trans. 2.* **1997**, 2023-2032.

2.25 Toniolo, C., Crisma, M., Formaggio, F., Benedetti, E., Santini, A., Iacovino, R., Saviano, M., Di Blasio, B., Pedone, C., Kamphius, J. *Biopolymers* **1996**, *40*, 519-522.

2.26 Formaggio, F., Crisma, M., Rossi, P., Scrimin, P., Kaptein, B., Broxterman, Q. B., Kamphius, J., Toniolo, C. **2000**, in print.

2.27 Lapeña, Y., Lopez, P., Cativiela, C., Kaptein, B., Broxterman, Q. B., Kamphius, J., Mossel, E., Peggion, C., Formaggio, F., Crisma, M., Toniolo, C. J. *Chem. Soc., Perkin Trans. 2*, **2000**, 631-636.

2.28 Hayashi, Y., Sekiyama, N., Nakanishi, S., Jane, D. E., Sunter, D. C., Bire, E. F., Udvarhelyi, P. M., Watkins, J. C. *J. Neurosci.* **1994**, *14*, 3370-3377.

2.29 Sekiyama, N., Hayashi, Y., Nakanishi, S., Jane, D. E., Tse, H.-W., Birse, E. F., Watkins, J. C. *Br. J. Pharmacol.* **1996**, *117*, 1493-1503.

2.30 Schoellkopf, U. *Pure Appl. Chem.* **1983**, *55*, 1799-1806.

2.31 Hsiao, Y., Hegedus, L. S. *J. Org. Chem.* **1997**, *62*, 3586-3591.

2.32 Smith, A. B., Benowitz, A. B., Favor, D. A., Sprengeler, P. A., Hirschmann, R. *Tetrahedron Lett.* **1997**, *38*, 3809-3812.

2.33 Wirth, T. *Angew. Chem. Int. Ed., Engl.* **1997**, *36*, 225-227.

2.34 Ma, D., Tian, H., Zou, G. *J. Org. Chem.* **1999**, *64*, 120-125.

2.35 Bucherer, H. T., Steiner, W. *J. Prakt. Chem.* **1934**, *140*, 291-316.

2.36 Edward, J. T., Jitrangsri, C. *Can. J. Chem.* **1975**, *53*, 3339-3350.

2.37 Kubik, S., Meissner, Rebek, Jr., J. *Tetrahedron Lett.* **1994**, *35*, 6635-6638.

2.38 Hammarström, L. G. J., McLaughlin, M. L. *Org. Syn.* **2000**, submitted for publication.

2.39 Shipchandler, M. T. *Synthesis*, **1979**, *9*, 666-686.

2.40 Feuer, H., Monter, R. P. *J. Org. Chem.* **1969**, *34*, 991-995.

2.41 Taylor, A. British Patent 835521 1960, *C.A.* **1960**, *54*, 24551.

2.42 Sylvain, C., Wagner, A., Mioskowski, C. *Tetrahedron Lett.* **1999**, *40*, 875-878.

2.43 Takeuchi, Y., Takagi, K., Nagata, K., Koizumi, T. *Chem. Pharm. Bull.* **1991**, *39*, 3120-3122.

2.44 Zen, S., Koyama, M., Koto, S. *Org. Synth.* **1976**, *55*, 77-80.

2.45 Coda, A. C., Desimoni, G., Invernizzi, A. G., Righetti, P., Seneci, P. F., Tacconi, G. *Gaz. Chim. Ital.* **1985**, *115*, 111-117.

2.46 Takeuchi, Y., Nagata, K., Koizumi, T. *J. Org. Chem.* **1989**, *54*, 5453-5459.

2.47 Niyazymbetov, M. E., Evans, D. H. *J. Org. Chem.* **1993**, *58*, 779-783.

2.48 Kaji, E., Zen, S. *Bull. Chem. Soc. Jap.* **1973**, *46*, 337-338.

2.49 Dauzonne, D., Royer, R. *Synthesis* **1987**, *4*, 399-401.

2.50 Horwell, D. C., Nichols, P. D., Ratcliffe, G. S., Roberts, E. *J. Org. Chem.* **1994**, *59*, 4418-4423.

2.51 Li, M., Johnson, M. E. *Tetrahedron Lett.* **1994**, *35*, 6255-6258.

2.52 Rodriguez, R., Viñets, I., Diez, A., Rubiralta, M. *Synth. Commun.* **1996**, *26*, 3029-3059.

2.53 Majchrak, M. W., Zobel, J N., Obradovich, D. J. *Synth. Commun.* **1997**, *27*, 3201-3211.

2.54 Genet, J. P., Juge, S., Besnier, I., Uziel, J., Ferroud, D., Kardos, N., Achi, S., Ruiz-Montes, J., Thorimbert, S. *Bull. Soc. Chim. Fr.* **1990**, *127*, 781-786.

2.55 Wysong, C. L., Yokum, T. S., Morales, G. A., Gundry, R. L. McLaughlin, M. L., Hammer, R. P. *J. Org. Chem.* **1996**, *61*, 7650-7651.

2.56 Ram, S., Spicer, L. D. *Tetrahedron Lett.* **1987**, *28*, 515-516.

2.57 Ram, S., Ehrenkaufer, R. E. *Synthesis* **1986**, *2*, 133-135.

2.58 Ram, S., Ehrenkaufer, R. E. *Synthesis* **1988**, *2*, 91-95.

2.59 Koerber-Plé, K., Massiot, G. *J. Heterocyclic Chem.* **1995**, *32*, 1309-1315.

2.60 Salomon, C. J., Mata, E. G., Mascaretti, O. A. *J. Org. Chem.* **1994**, *59*, 7259-7266.

2.61 Augspurger, J. D., Bindra, V. A., Scheraga, H. A., Kuki, A. *Biochemistry* **1995**, *34*, 2566-2576.

2.62 Yokum, T. S., Bursavich, M. G., Piha-Paul, S. A., Hall, D. A., McLaughlin, M. L. *Tetrahedron Lett.* **1997**, *38*, 4013-4016.

2.63 Bolin, D. R., Sytwu, I. –I., Humiec, F., Meienhofer, J., *Int. J. Pept. Protein Res.*, **1989**, 353-359.

CHAPTER 3
AMPHIPATHIC CONTROL OF PEPTIDE STRUCTURE

3.1. INTRODUCTION

The ability to design desired secondary peptide structure is a major goal in peptide studies. How proteins function, as a result of peptide structure, is the central dogma of many areas of pharmacology, immunology, cell biology and medicinal chemistry. Like learning a new written language, the process of understanding how a protein works, is dependant upon one's ability to first have a thorough concept of the letters (or amino acids) which make up the alphabet of protein science. Once this is achieved, and the basis of the language is established, one moves on to piece the letters together to form words, which would represent structural domains within the protein. Next, the words are connected to make sentences, paragraphs, chapters and so on, until the entire quaternary structure of the protein is realized. However, to understand the meaning of what is in the text, one must be able to decipher the code of the words. What effect does rearranging the words in a sentence have on the overall expression of the sentence? In turn, what effect does rearranging the amino acid sequence of a peptide ultimately have on peptide structure and function? To answer this question, one must strive towards the ability to determine peptide structure and function *a priori* from specific amino acid sequence.

Protein structure is composed of four levels of complexity: 1) *Primary structure*: the description of which amino acids are present in the peptide and in what sequence they are found. 2) *Secondary structure*: the local folding pattern that arises, as a direct result of hydrogen bonding in the primary sequence. These patterns include primarily sheet-type folding or helix-type folding. 3) *Tertiary structure*: long-distance

interactions between residues (hydrogen bonding or covalent (disulfide bridging)), which induce a globular three-dimensional shape to the protein. 4) *Quaternary structure*: two or more proteins may converge to form a macromolecular cluster, which in turn encompass the functional protein.

The determination of peptide secondary structure depends on the intrinsic ability of covalent bonds within the peptide backbone to adopt preferred torsion angles. The torsion angle about the N-C^{α} bond of a peptide is denoted by ϕ; the torsion angle about the C^{α}-C' bond is denoted by ψ; and the torsion angle about the amide C'-N bond by ω, as is shown in Figure 3.1. In the *cis* configuration, these angles are all given the value of 0. Rotation from this point about the bonds, so that the atoms viewed behind the bond move clockwise are given *positive* values up to 180°. Rotation in the counterclockwise direction gives a negative torsion angle, to the extent of -180°.[3.1] The torsion angles of conformations such as β-sheets, α-helices and 3_{10}-helices are well established (Table 3.1).

Table 3.1. Parameters for peptide secondary structure.[3.1]

Conformation	Bond Angle (degrees)			Residues /turn	Translation /residue (Å)
	ϕ	ψ	ω		
Antiparallel β-sheet	-139	+135	-178	2.0	3.4
Parallel β-sheet	-119	+113	180	2.0	3.2
α-helix	-57	-47	180	3.6	1.5
3_{10}-helix	-49	-26	180	3.0	2.0
π-helix	-57	-70	180	4.4	1.15

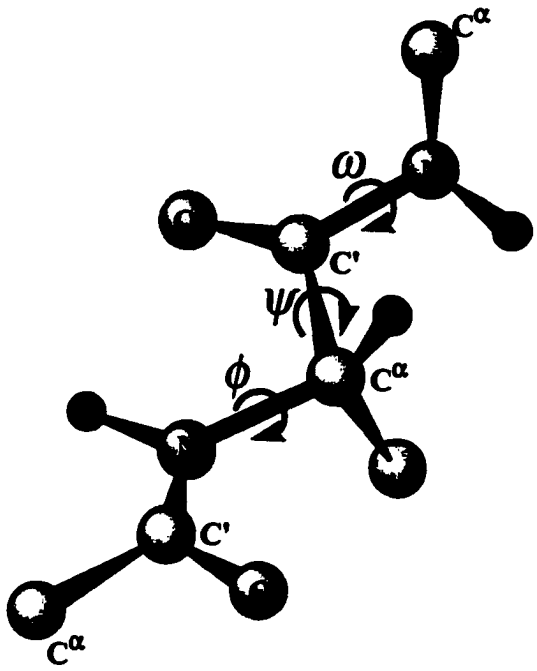

Figure 3.1. Perspective drawing of polypeptide backbone showing two peptide units. The peptide is shown in the fully extended *trans* conformation where $\phi=\psi=\omega=180^{\circ}$.

More than any other secondary structure, the helix motif is found throughout nature in proteins. Helices are often found in, or near, active sites and constitute a large portion of the functional aspect of proteins. Of these helical motifs, the α-helix is by far the most prevalent, constituting nearly 80% of all protein structure. The α-helix has 3.6 residues per turn and a translation per residue of 1.5Å, or 5.41Å per turn. The torsional angles for the α-helix are very favorable for most amino acids. The structure is characterized by the *i*th carbonyl oxygen of each residue hydrogen bonding to the backbone amide N-H bond of the *i*+4th residue along the chain. These hydrogen bonds are nearly parallel to the helix axis (Figure 3.2). This allows most proteinogenic amino acids to adopt the conformation without side chain interaction. Only proline is not found in the α-helical motif.[3.1]

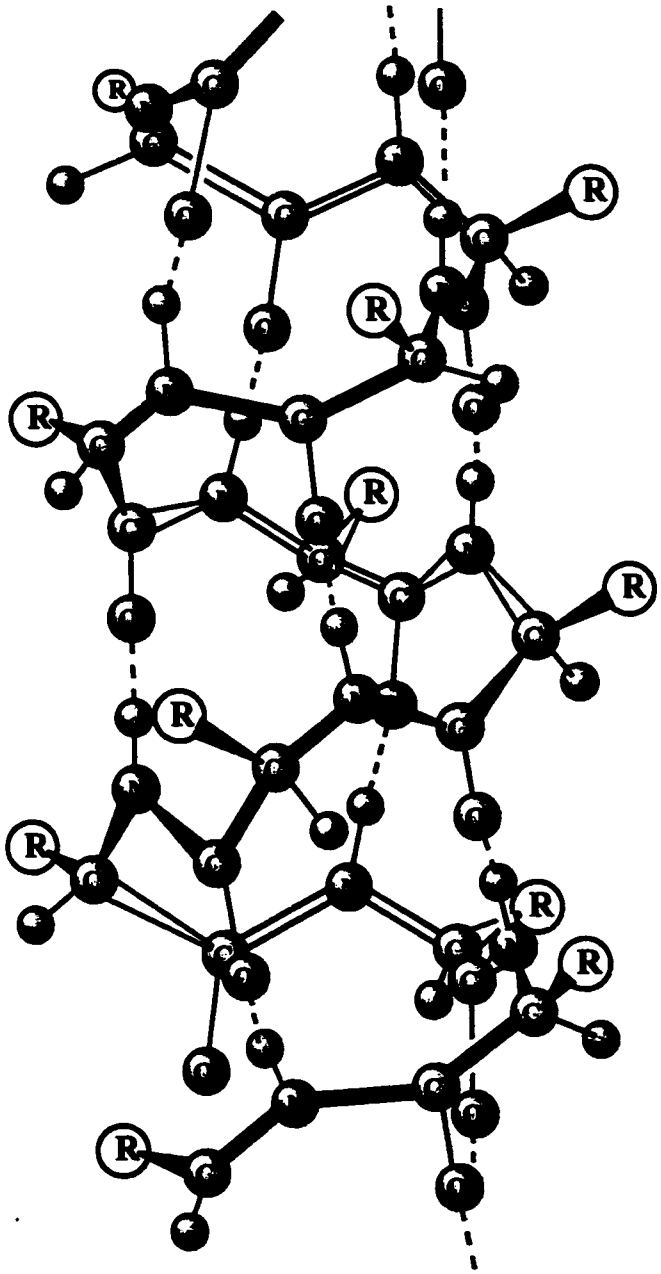

Figure 3.2. Hydrogen bonding pattern of the right handed α-helix.

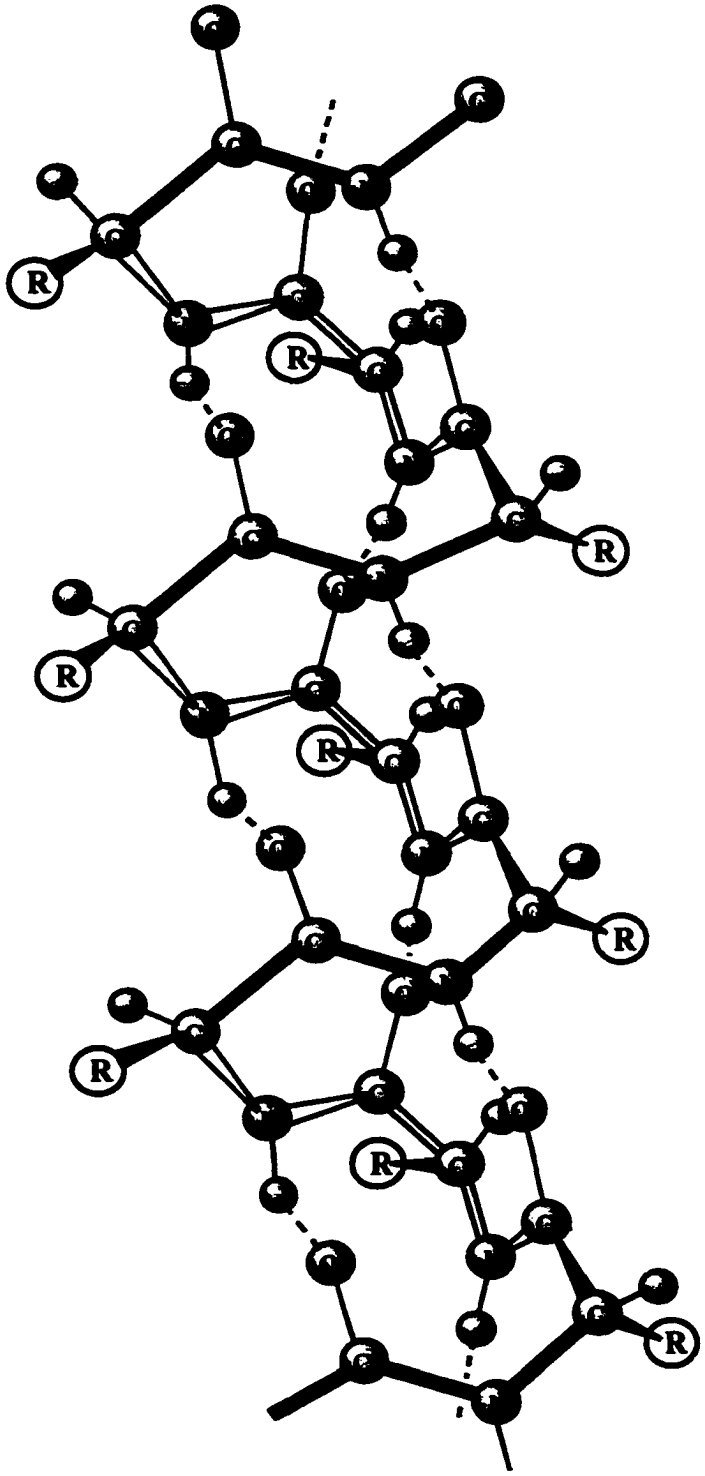

Figure 3.3. Hydrogen bonding pattern of the right handed 3_{10}-helix.

Although similar in structure, the α-helix is much more stable and occurs more frequently than it's relatively unexplored cousin, the 3_{10}-helix; which comprises <10% of all helix structure and is often found at the ends of α-helices (Figure 3.3). While the factors favoring α-helical (*i*←*i*+*4*) structures have been well documented, the secrets of the 3_{10}-helical conformation (*i*← *i* + *3* hydrogen bonding) have only recently begun to be understood. This helix is, however, gaining interest, as it is believed to be a folding intermediate to the α-helical configuration.[3.2-7] In addition, short stretches of 3_{10}-helix frequently occur in globular proteins and protein recognition steps may involve facile transitions between the α-helix and 3_{10}-helix.[3.2-10] Thus, the ability to understand and control the delicate equilibrium between these two closely related structures is desirable in the development of peptide design research.

Most studies exploring the equilibrium between the α- and 3_{10}-helix have been concentrated on short, hydrophobic peptides containing several C^{α},C^{α}-disubstituted amino acids (ααAA's).[3.11-14] Natural α-helical sequences commonly require more than 20-30 amino acid residues to obtain a significant helical character at room temperature.[3.15-17] However, the incorporation of high levels of C^{α},C^{α}-disubstituted amino acids (e.g. aminoisobutyric acid) into the sequence allows for the preparation of much shorter peptides with significant helical character (Figure 3.4).[3.12,14,18-22] These peptides, however, exhibit higher hydrophobic character than their proteinogenic counterparts. As a result, spectroscopic studies of these peptides have often been limited to organic solvents such as dimethylsulfoxide (DMSO), methanol, trifluoroethanol (TFE) and acetonitrile. Structures of these peptides have also been obtained by X-ray analysis of crystals grown from organic solvents.[3.19,23,24] Recently,

Toniolo and co-workers have reported spectroscopic studies of a peptide exhibiting 3_{10}-helical structure in water by the incorporation of the novel, aza-crown amino acid ATANP.[3.25,26] Due to the interest of these helical configurations as they relate to physiological conditions and membrane interactions, it is important to study the helix equilibrium in aqueous/organic environments.

The first characterization of the amphipathic helix was performed by Kendrew and Perutz on the heme proteins.[3.27] These structures are defined by the presence of a hydrophilic face and a hydrophobic face along the axis of the peptide. The tendency of these types of structures to self-associate and interact with bi-lipid membranes results in high levels of bioactivity and they play an important part in membrane-dependent processes[3.28] as well as lipoproteins[3.29], hormones[3.30], lung surfactant proteins[3.31], cytotoxic immunodefense proteins[3.32] and antimicrobial agents.[3.33]

The use of C^{α},C^{α}-disubstituted amino acids in synthetic helix design has been shown to induce high levels of helicity into short peptide sequences by introducing steric constraints on the peptide backbone. This has been exhaustively investigated with the use of α-aminoisobutyric acid, Aib (**1**, Figure 3.4)[3.11-14], but also with the use of alicyclic amino acids, such 1-cyclohexane-1-carboxylic acid, Ac_6c (**2**, Figure 3.4).[3.12,34] Recently, the availability of the ionizable C^{α},C^{α}-disubstituted amino acid 4-aminopiperidine-4-carboxylic acid, Api (**3**, Figure 3.4) allows us to investigate the helix-forming ability of highly polar cyclic residues towards peptide secondary structure.[3.35] In addition to introducing high levels of helicity to the peptide, ααAAs stabilize the peptide towards enzymatic degradation *in vivo*, which is important in the development of bioactive agents.

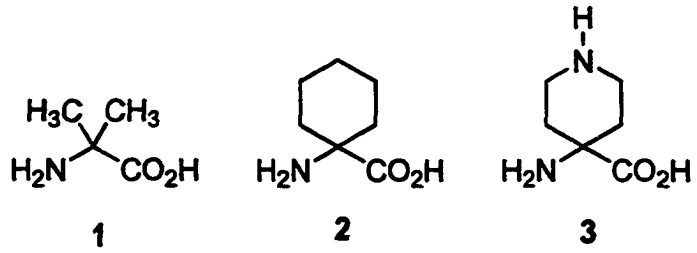

Figure 3.4. C^{α},C^{α}-Disubstituted amino acids aminoisobutyric acid (Aib) **1**, 1-aminocyclohexyl-1-carboxylic acid (Ac_6c) **2** and 1-aminopiperidine-1-carboxylic acid (Api) **3**.

Amphipathicity is a characteristic found in most naturally occurring antimicrobial peptides such as magainins, cercropins and dermaseptin.[3.36] Due to the high levels of bioactivity of amphipathic peptides, it is not surprising that 50% of all α-helices in soluble globular proteins are amphipathic.[3.37] The amphipathic character of these peptides is thought to play a dominant role in the peptide-membrane interactions, which are responsible for antimicrobial activity. These amphipathic membrane interactions prompted us to investigate peptide helicity in micellar and aqueous/organic environments. Researchers have demonstrated that amphipathicity and hydrophobic interactions have a large influence on helix stability in aqueous solution.[3.37] By generating sequence permutation isomers of several peptides, we have attempted to selectively induce α- or 3_{10}-helices, based purely on primary sequence design. Incorporation of ionizable and alicyclic C^{α},C^{α}-disubstituted amino acids allow for the production of short, amphipathic peptides with up to 80% C^{α},C^{α}-disubstituted amino acids which are highly water soluble, but retain helical character in organic and aqueous/organic media (Table 3.2). Each peptide is designed to have maximum amphipathic character either as an α-helix or a 3_{10}-helix.

Table 3.2. List of prepared *de novo* peptides. The incorporation of 20% L-lysine (*Lys*) allows for CD spectroscopic determination of peptide secondary structure by inducing right-handed helix formation. Pi-10, ACh-10α and Cyh-10 were designed to be perfectly amphipathic as an α-helix while Ipi-10, ACh-10 and Ich-10 were designed to be perfectly amphipathic as a 3_{10}-helix.

Peptide	Sequence	Design
Pi-10	H-Aib-Aib-Api-*Lys*-Aib-Aib-Api-*Lys*-Aib-Aib-NH_2	α
Ipi-10	H-Api-Aib-Aib-*Lys*-Aib-Aib-*Lys*-Aib-Aib-Api-NH_2	3_{10}
Ach-10α	H-Ac_6c-Aib-*Lys*-Api-Aib-Ac_6c-Api-*Lys*-Ac_6c-Aib-NH_2	α
Ach-10	H-Api-Aib-Ac_6c-*Lys*-Ac_6c-Aib-*Lys*-Aib-Ac_6c-Api-NH_2	3_{10}
Cyh-10	H-Ac_6c-Ac_6c-Api-*Lys*-Ac_6c-Ac_6c-Api-*Lys*-Ac_6c-Ac_6c-NH_2	α
Ich-10	H-Api-Ac_6c-Ac_6c-*Lys*-Ac_6c-Ac_6c-*Lys*-Ac_6c-Ac_6c-Api-NH_2	3_{10}

The ability of the peptides to selectively adopt their preferred helical motifs can be illustrated by studying the helical wheel conformations of the peptides in their α- and their 3_{10}-helical configurations. Amphipathicity is maximized when the peptides have a continuous hydrophobic and a continuous hydrophilic face. Otherwise hydrophilic residues are distributed throughout the cross-section of the helix. The work presented in this chapter tests this premise as a design principle. The general sequence of our α-helical peptides is: H-N-N-P-P-N-N-P-P-N-N-NH_2; (N=non-polar residues; P=polar residues) and our 3_{10}-helical peptides have the sequence: H-P-N-N-P-N-N-P-N-N-P-NH_2. Peptides designed to adopt the α-helical amphipathic conformation are less amphipathic in the 3_{10}-helical form and vice versa, (Figure 3.5-11).

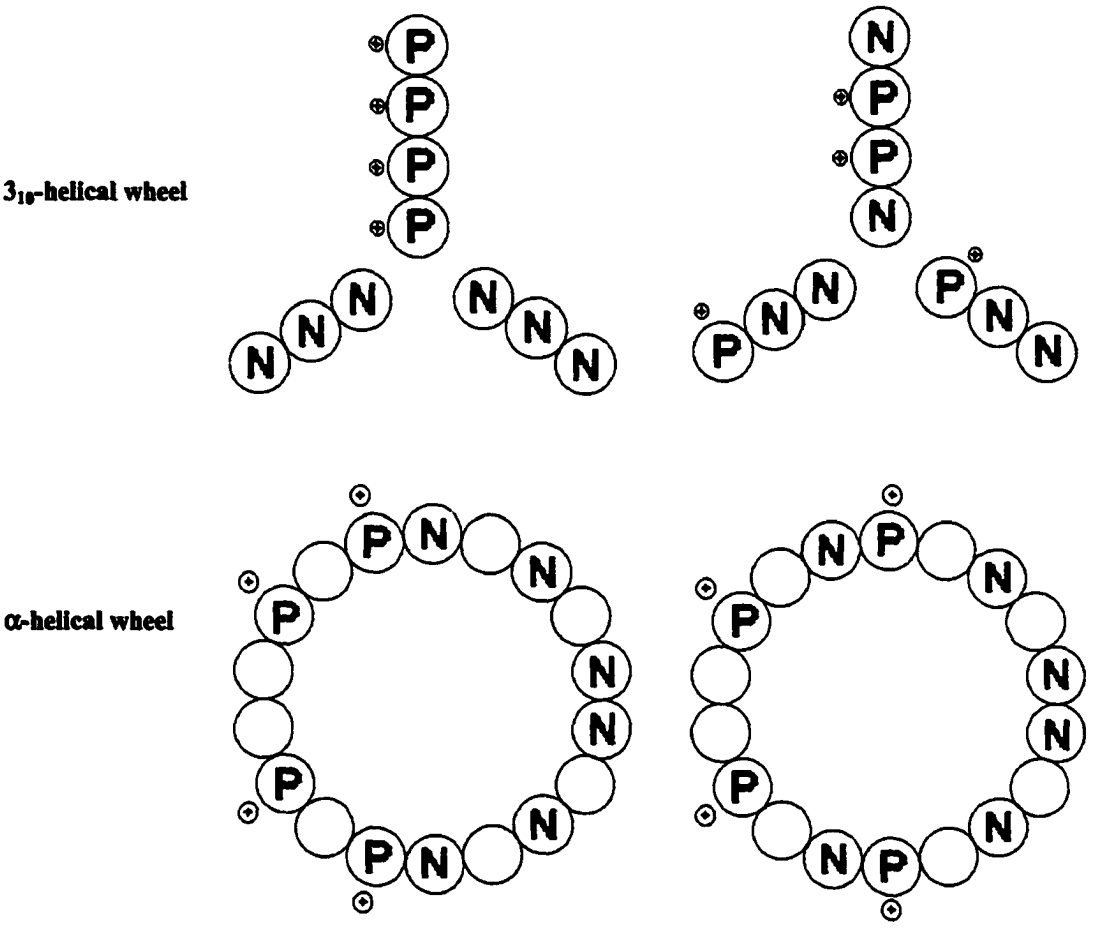

Figure 3.5. Helical wheel cross-sections of empirical peptide sequences in their preferred conformation and non-preferred conformations. **P** designates ionizable polar amino acid residues (Lys or Api); **N** designates non-polar residues (Aib or Ac_6c). Empty circles represent non-occupied locations in the alpha helical wheel.

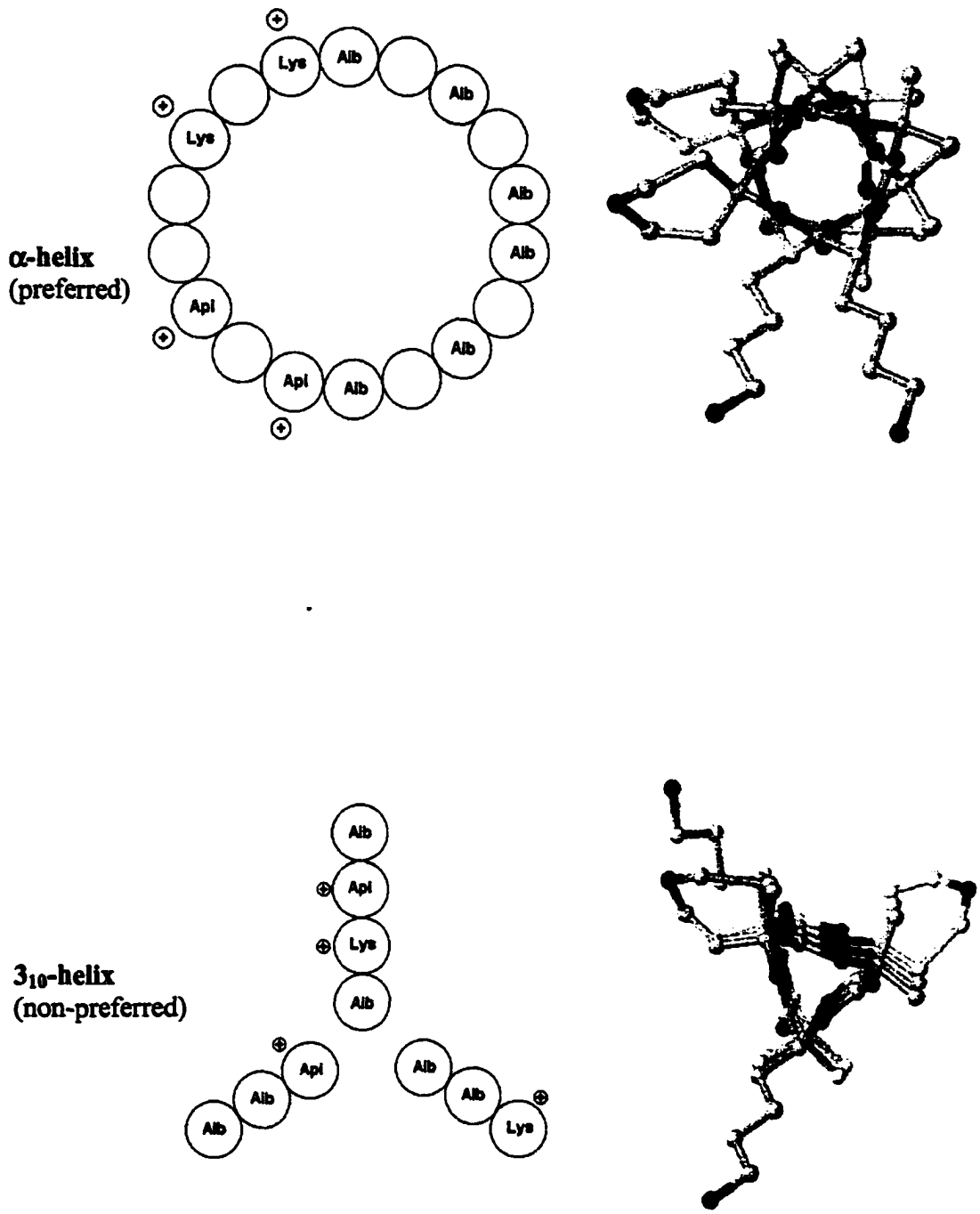

Figure 3.6. Helical wheel motifs showing α-helical and 3_{10}-helical conformations of Pi-10 (designed to be α-helical).

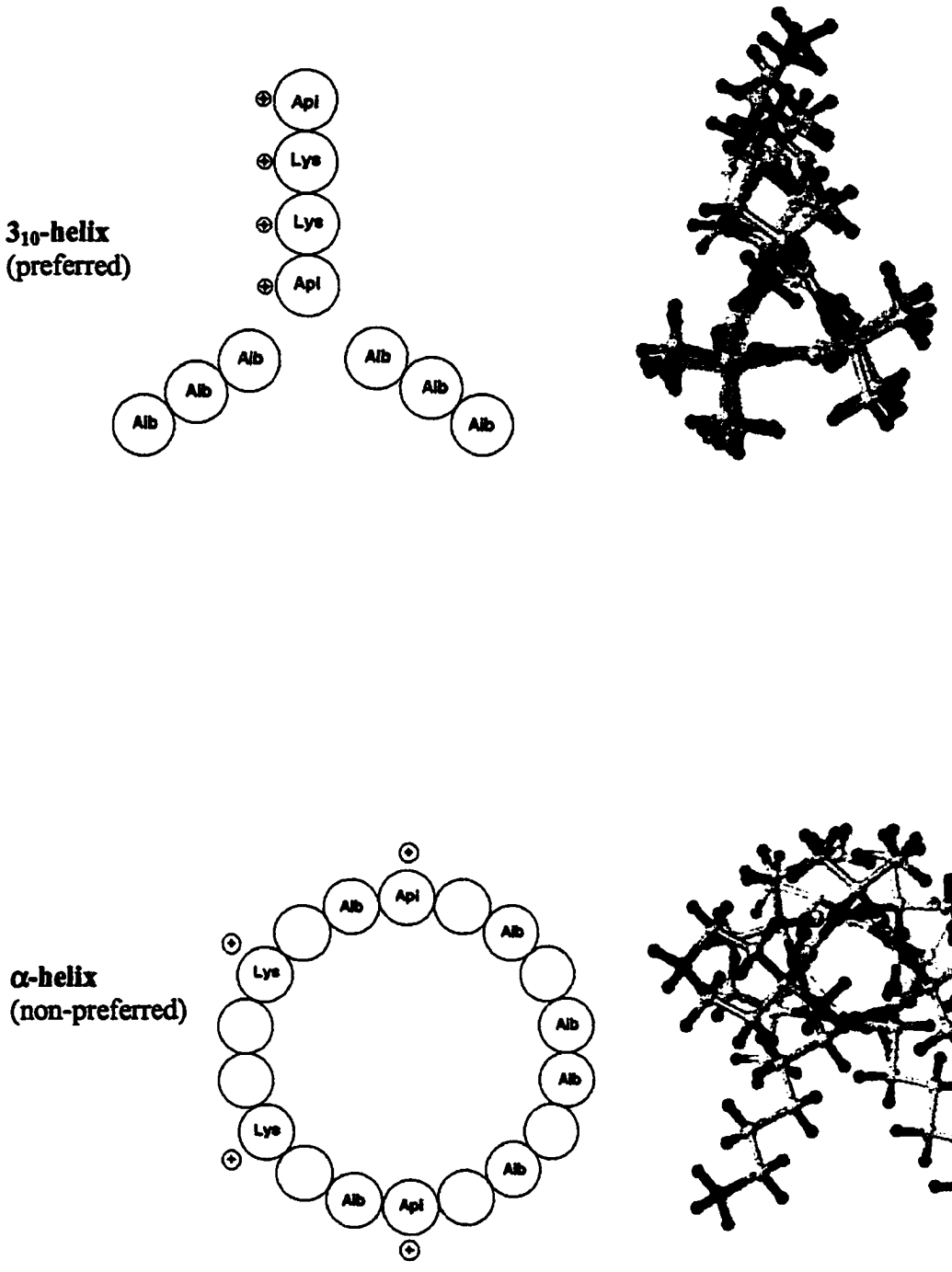

Figure 3.7. Helical wheel motifs showing α-helical and 3_{10}-helical conformations of Ipi-10 (designed to be 3_{10}-helical).

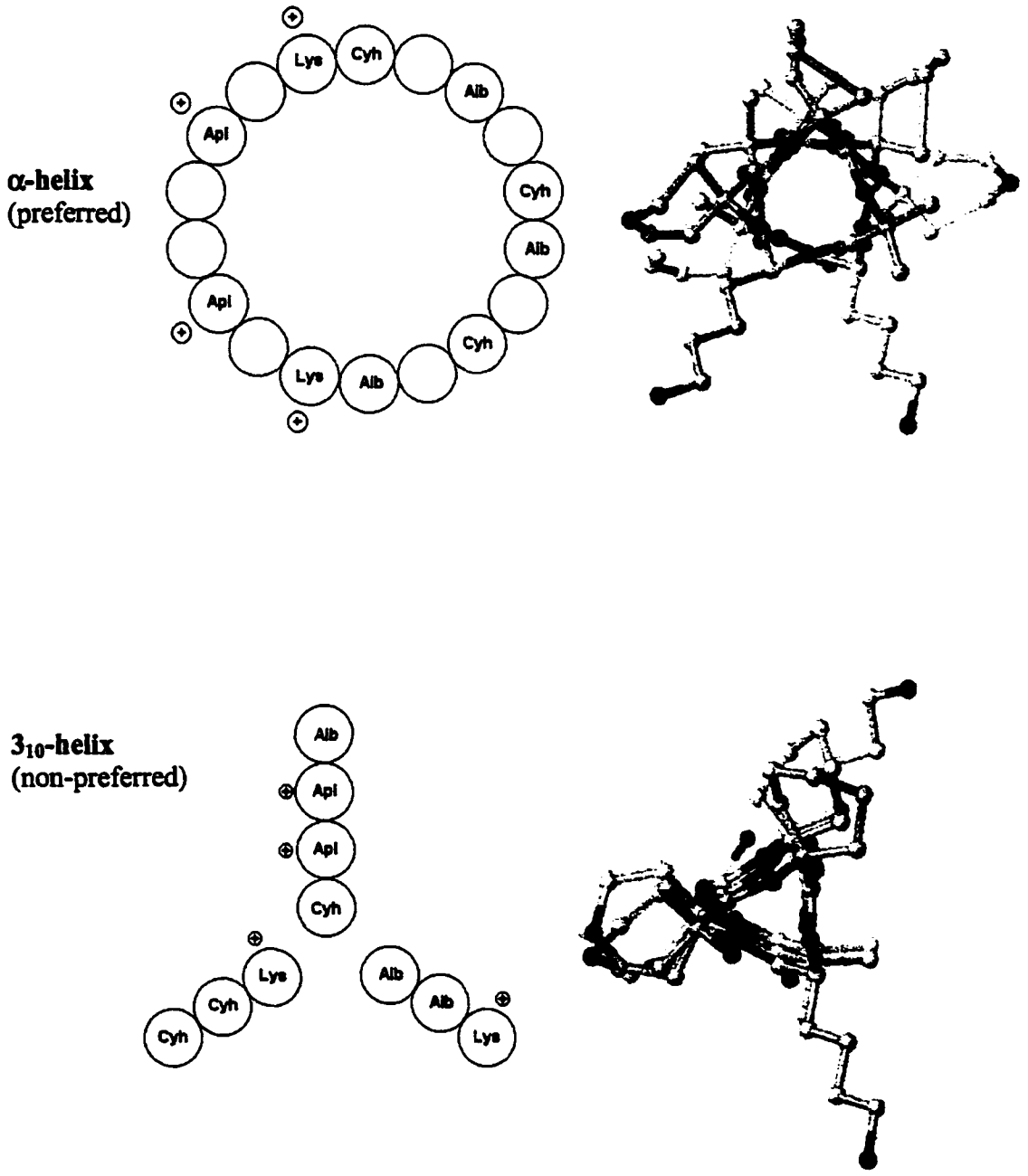

Figure 3.8. Helical wheel motifs showing α-helical and 3_{10}-helical conformations of ACh-10α (designed to be α-helical; Cyh=Ac_6c).

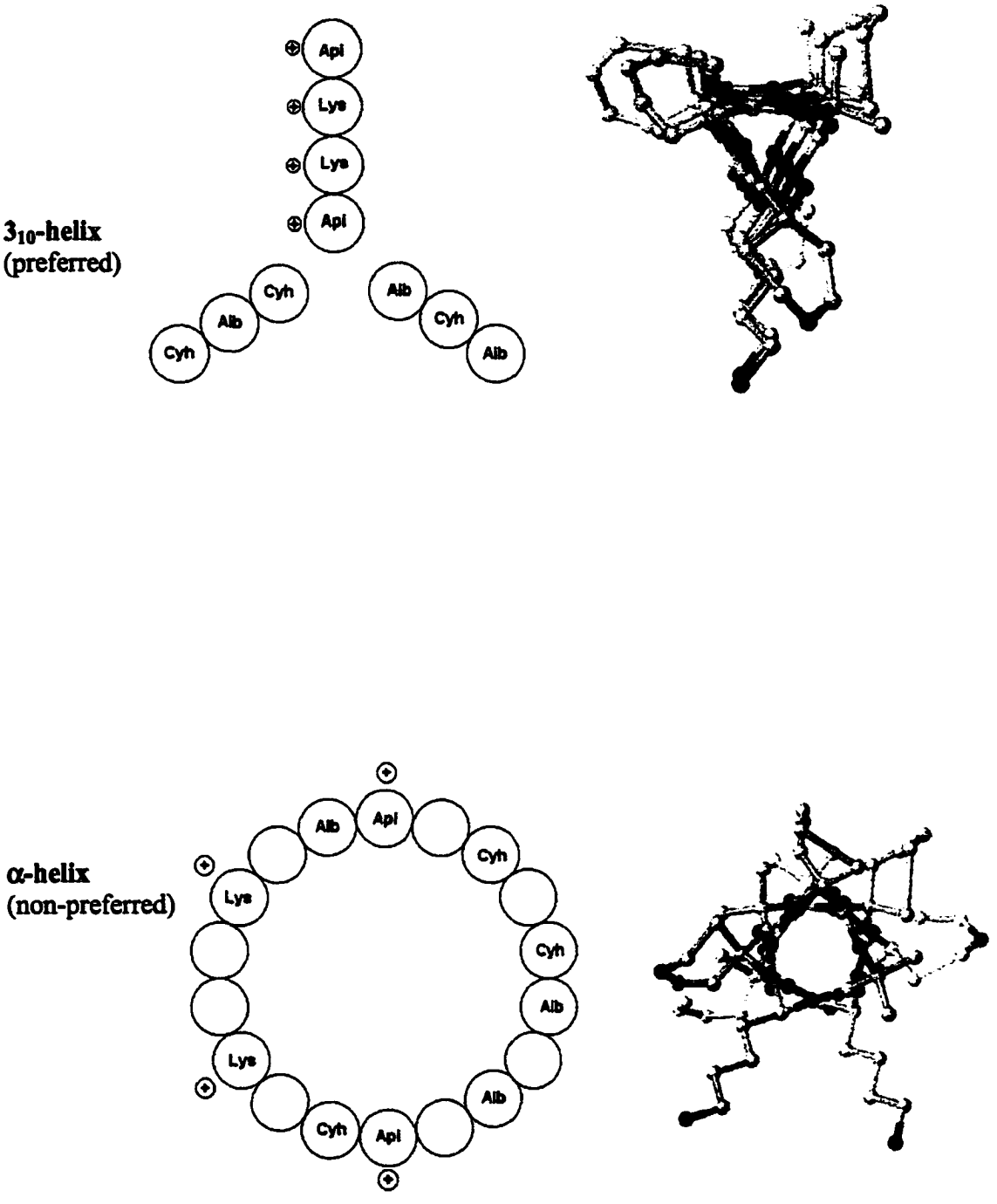

Figure 3.9. Helical wheel motifs showing α-helical and 3_{10}-helical conformations of ACh-10 (designed to be 3_{10}-helical; Cyh=Ac_6c).

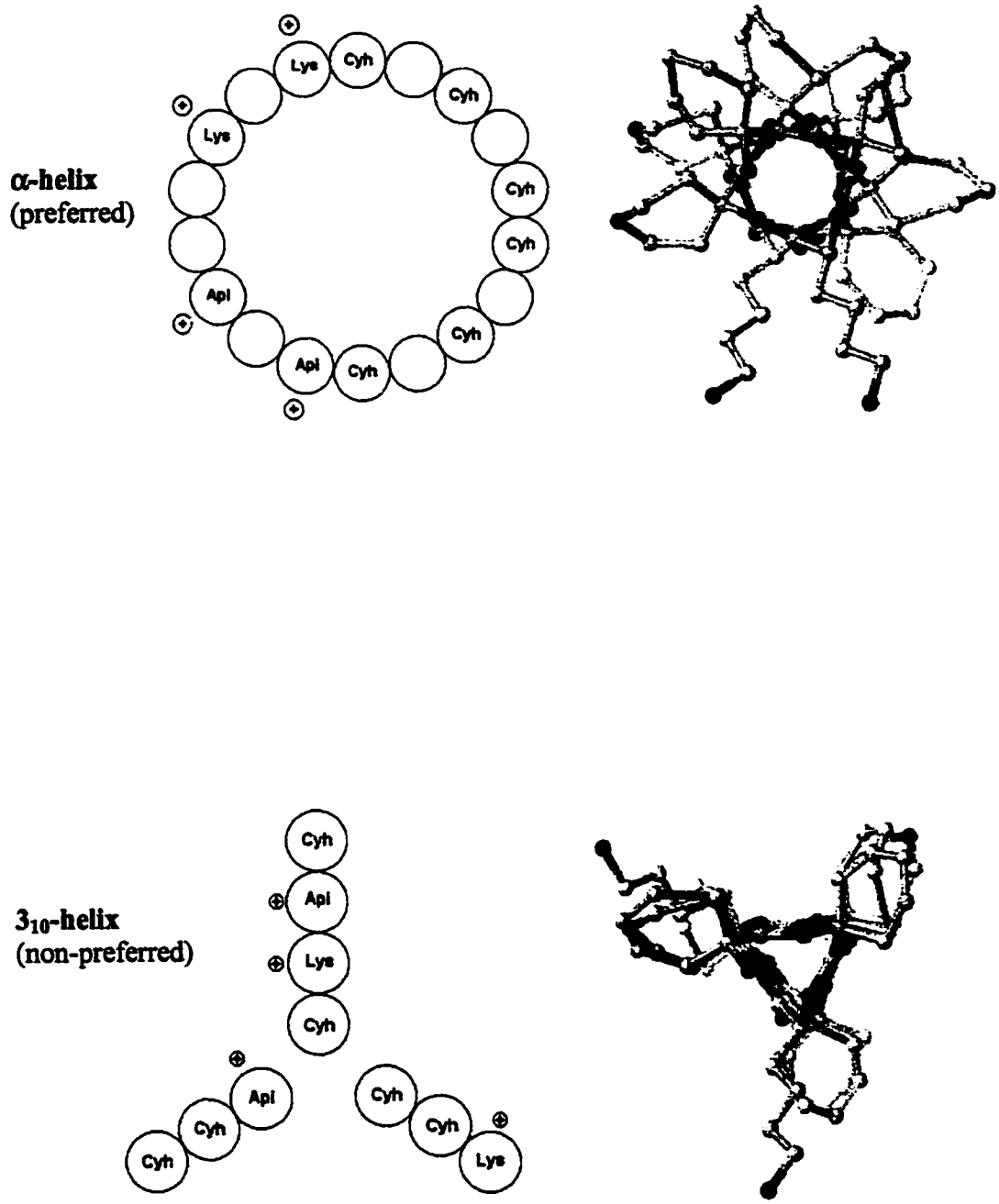

Figure 3.10. Helical wheel motifs showing α-helical and 3_{10}-helical conformations of Cyh-10 (designed to be α-helical; Cyh=Ac_6c).

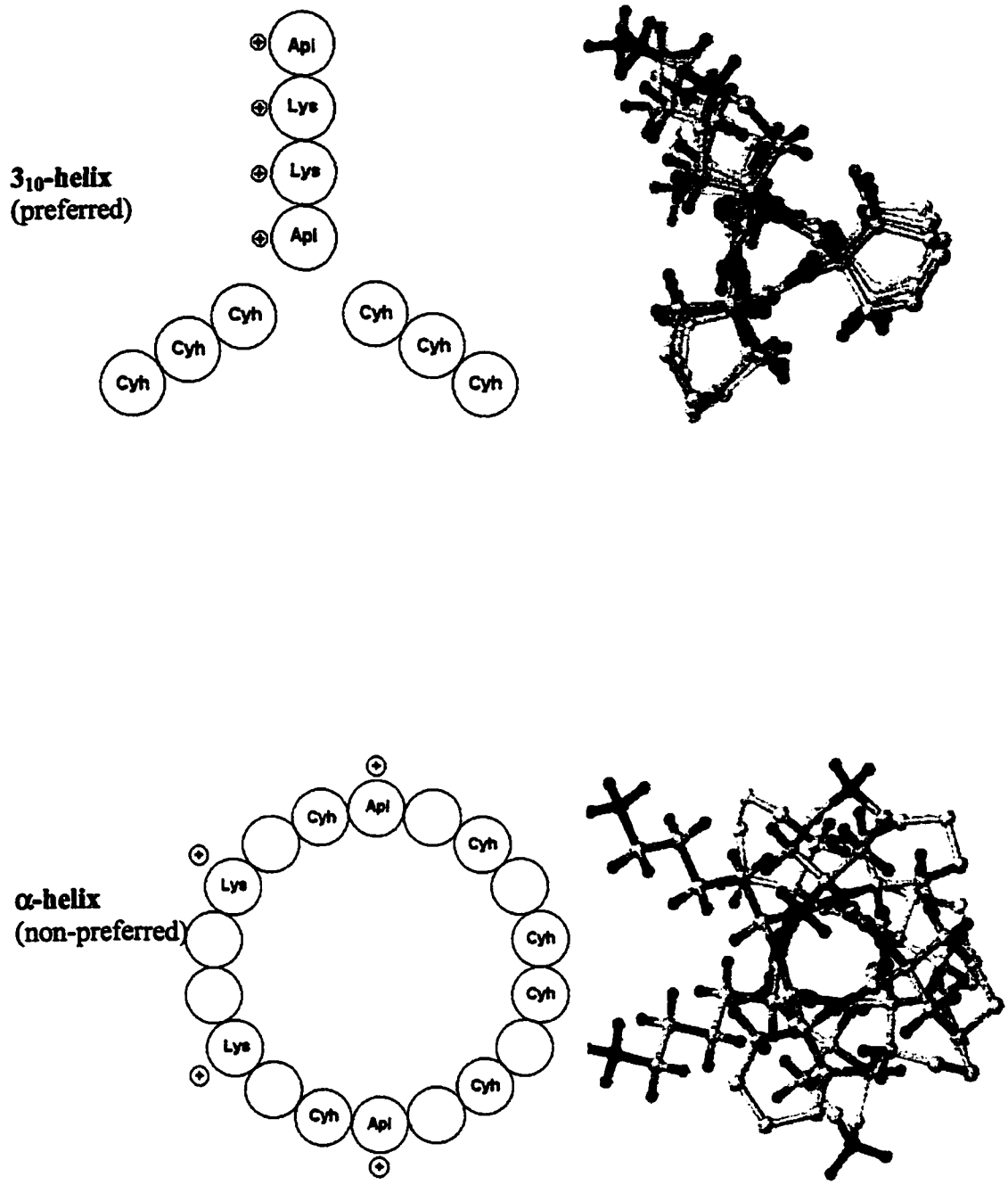

Figure 3.11. Helical wheel motifs showing α-helical and 3_{10}-helical conformations of Ich-10 (designed to be 3_{10}-helical; Cyh=Ac_6c).

In order to study the relative formation of 3_{10}- and α-helices in the aforementioned peptides, one needs to distinguish between the two. For this purpose, electronic circular dichroism (ECD) spectroscopy has been established as a powerful tool. In ECD spectroscopy, helical peptides are characterized by two minima. The $n\rightarrow\pi^*$ transition is centered around 222 nm and one of the two the $\pi\rightarrow\pi^*$ transitions is centered near 207 nm. Since both the 3_{10}- and α-helices exhibit these minima, the relative intensities of the minima are used to distinguish between α-helical and 3_{10}-helical structures. The ratio, R, where $R = [\theta]_{n\rightarrow\pi^*}/[\theta]_{n\rightarrow\pi^*}$, has been proposed as the factor to distinguish a 3_{10}-helix from an α-helix. In 3_{10}-helices $R \leq 0.4$, while for α-helices $R \cong 1$.[3.38] An additional distinguishing feature is the positive CD band near 195 nm. This band is much weaker in the 3_{10}-helix than in the α-helix. Other techniques such as electron spin resonance and NMR are complicated by peptide dynamics and have met with mixed results, especially with peptides containing ααAA's.[3.39-41]

As stated previously, a sufficient database of 3_{10}-helix structures does not yet exist. As a result, exact estimation of % 3_{10}-helicity in a specific peptide is very difficult. It has been suggested that the CD bands of a 3_{10}-helix will be highly dependent on the ϕ- and ψ-torsion angles in the peptide backbone. 3_{10}-Helical peptides comprised of ααAA's have different ϕ- and ψ-angles than 3_{10}-helical peptides comprised only of natural amino acids. Toniolo and co-workers synthesized Ac-(αMeVal)$_8$-OtBu which exhibited significant 3_{10}-helical structure, and recently reported a short peptide exhibiting significant 3_{10}-helical structure in water.[3.38,42] The peptide contains the novel azacrown functionalized amino acid, 2-amino-3-[1-(1,4,7-triazacyclononane)] propanoic acid.[3.26]

3.2. RESULTS AND DISCUSSION

It was hypothesized that the peptides would adopt the helical structure that allowed them to be most amphipathic. As expected, Pi-10 (Figure 3.12), ACh-10α (Figure 3.14) and Cyh-10 (Figure 3.16) shows CD spectra characteristic of an α-helix in all solvent systems. Ipi-10 (Figure 3.13) and ACh-10 (Figure 3.15) display a transition from an α-helix to a 3_{10}-helix as the solvent system increases in organic content. The most prominent 3_{10}-helical character for both Ipi-10 and ACh-10 was observed in SDS micelles, which indicates that an amphipathic environment strongly favors the amphipathic structure in the peptide. It was expected that Ich-10 would display this same transition; however, this does not occur. Ich-10 displays an nearly perfect α-helical CD-spectrum in all of the solvent systems tested (Figure 3.17). This effect may be due to steric interactions between adjacent cyclohexano moieties in the tightly wound 3_{10}-helix (see modeling in figure 3.11). A transition to an α-helix would relieve this stress by increasing the diameter of the helix, as well as staggering adjacent alicyclic groups to avoid interference. It is interesting to note the prominent minimum present at 185 nm for both of these 3_{10}-helices in SDS micelles. These minima are not found in any of the α-helical peptides, nor are they apparent in the constitutional isomers of Ipi-10 and Ach-10. Thus, one must assume that this transition is structure based and not an effect of solvent or residue absorption. This minimum has seldom been studied due to solvent interferences in the <190 nm region. It may, however, be an important factor in the interpretation of 3_{10}- vs. α-helical segments. Further investigation into the significance of these minima in 3_{10}-helical peptides is currently underway.

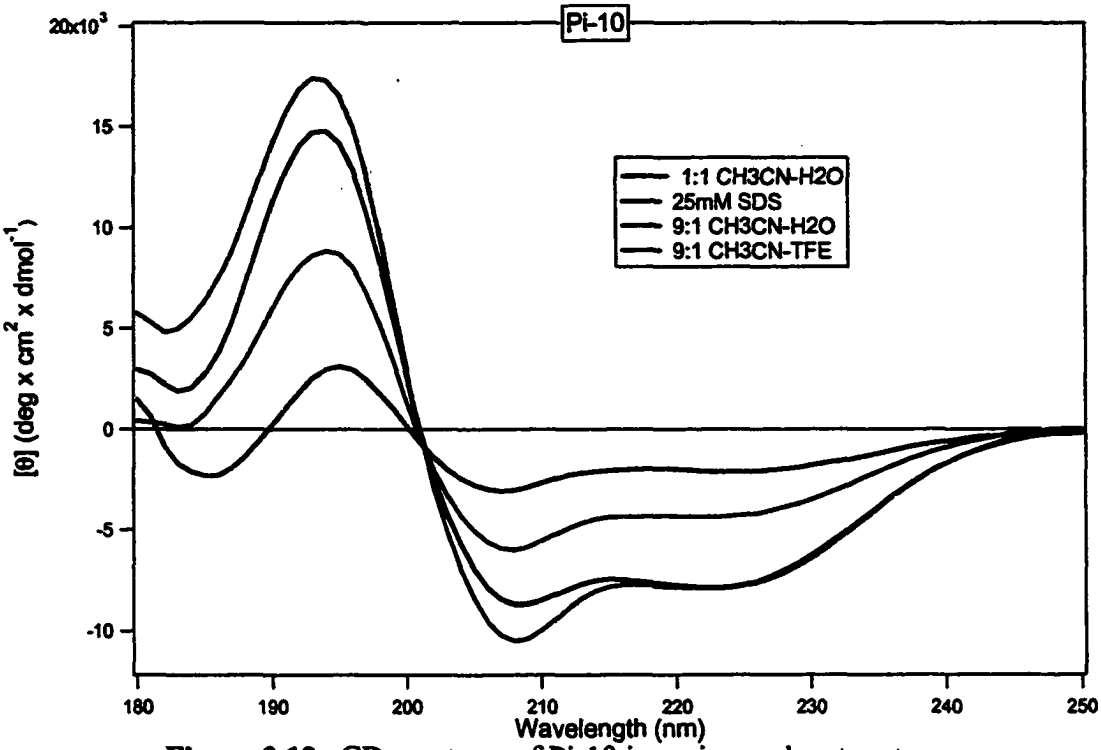

Figure 3.12. CD spectrum of Pi-10 in various solvent systems.

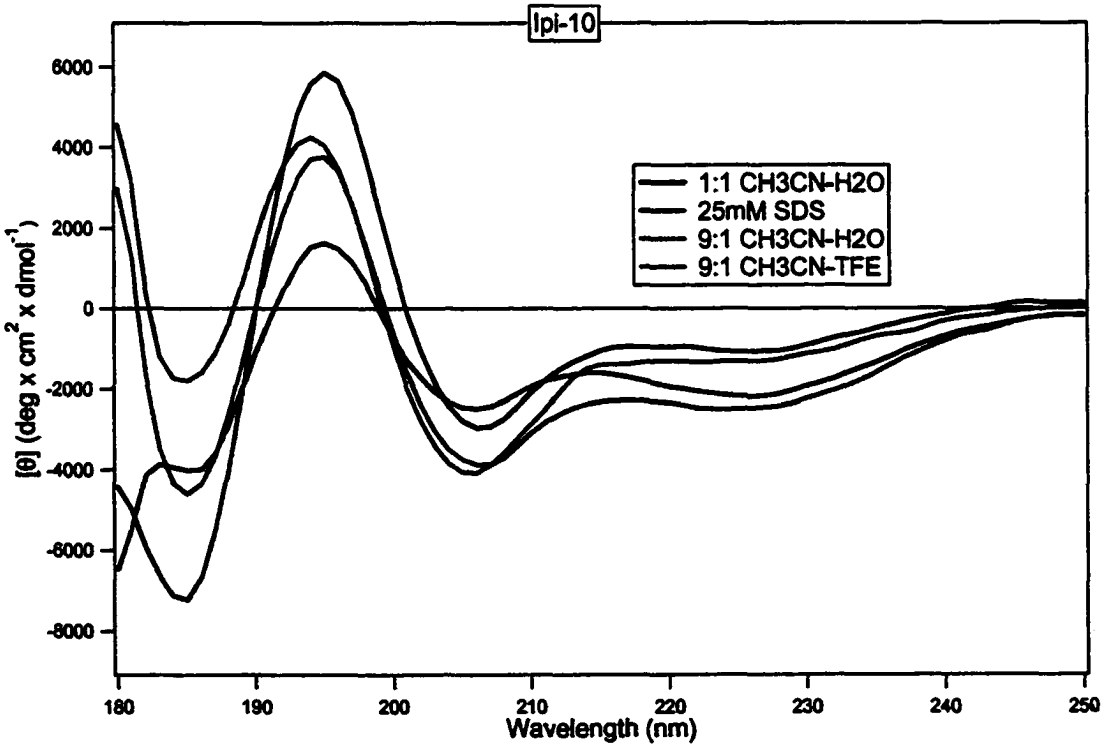

Figure 3.13. CD Spectrum of Ipi-10 in various solvent systems.

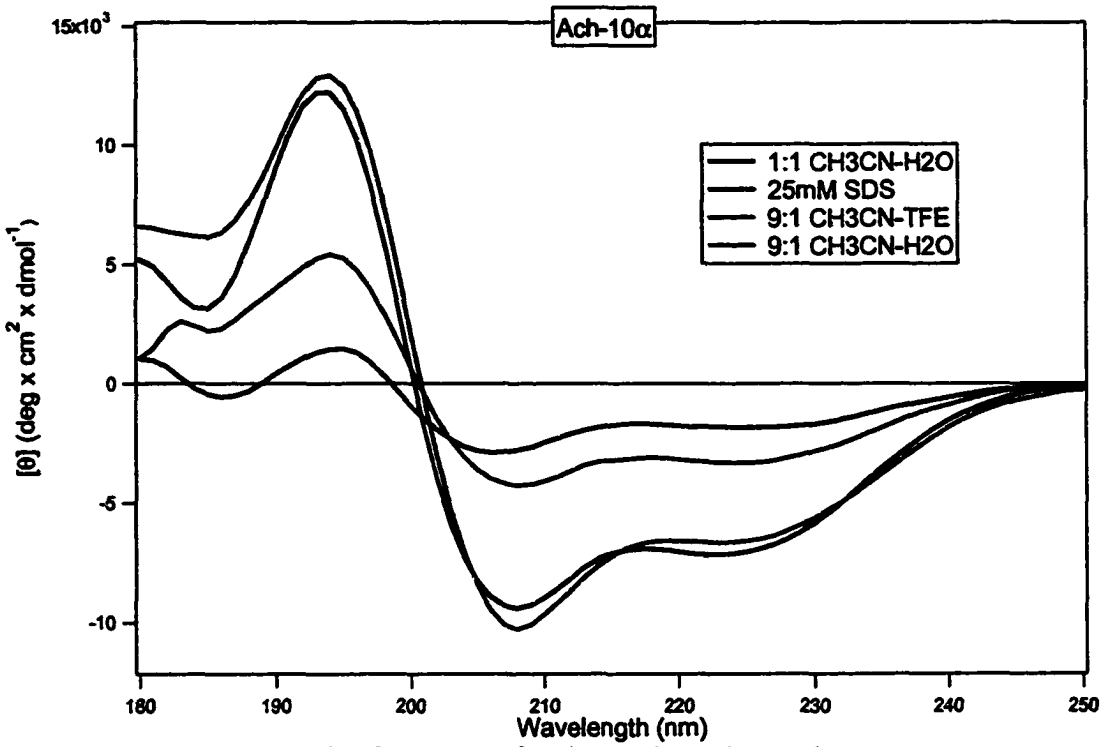

Figure 3.14. CD Spectrum of Ach-10α in various solvent systems.

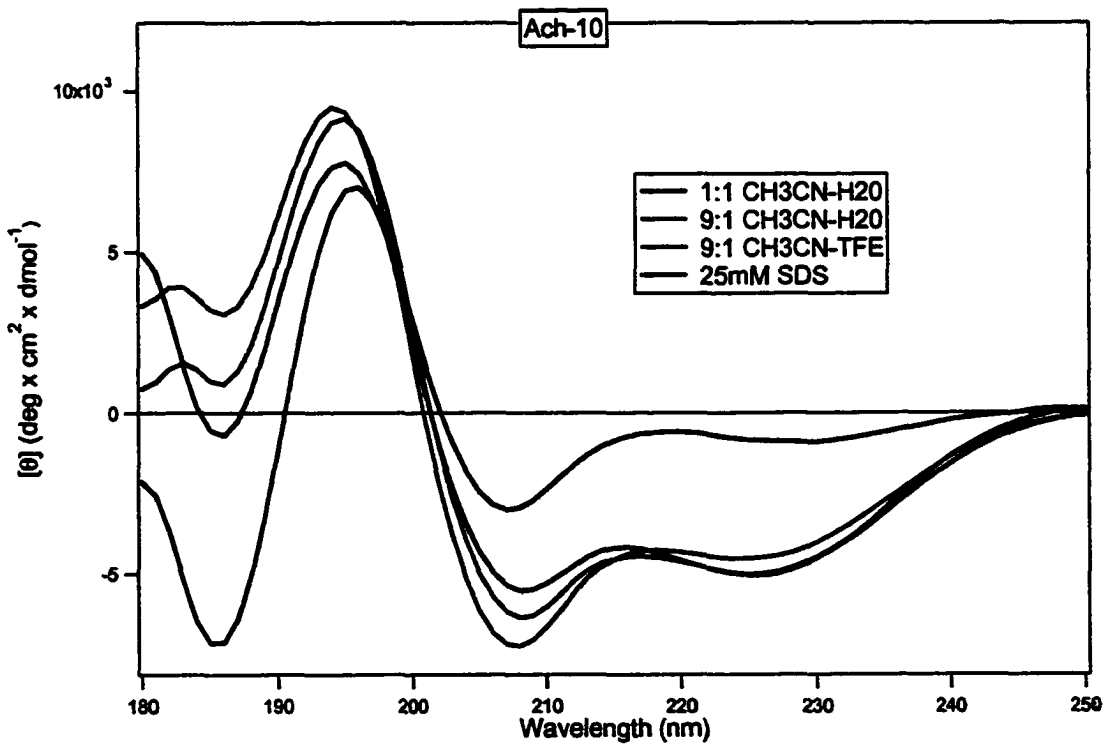

Figure 3.15. CD Spectrum of Ach-10 in various solvent systems.

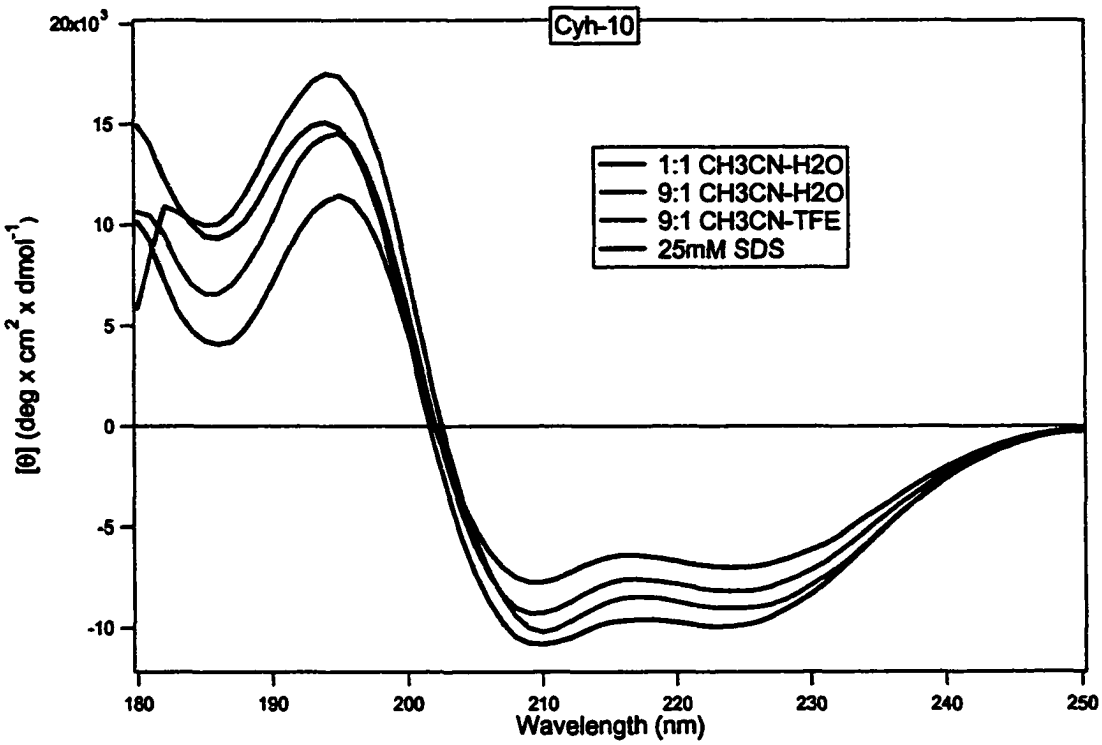

Figure 3.16. CD Spectrum of Cyh-10 in various solvent systems.

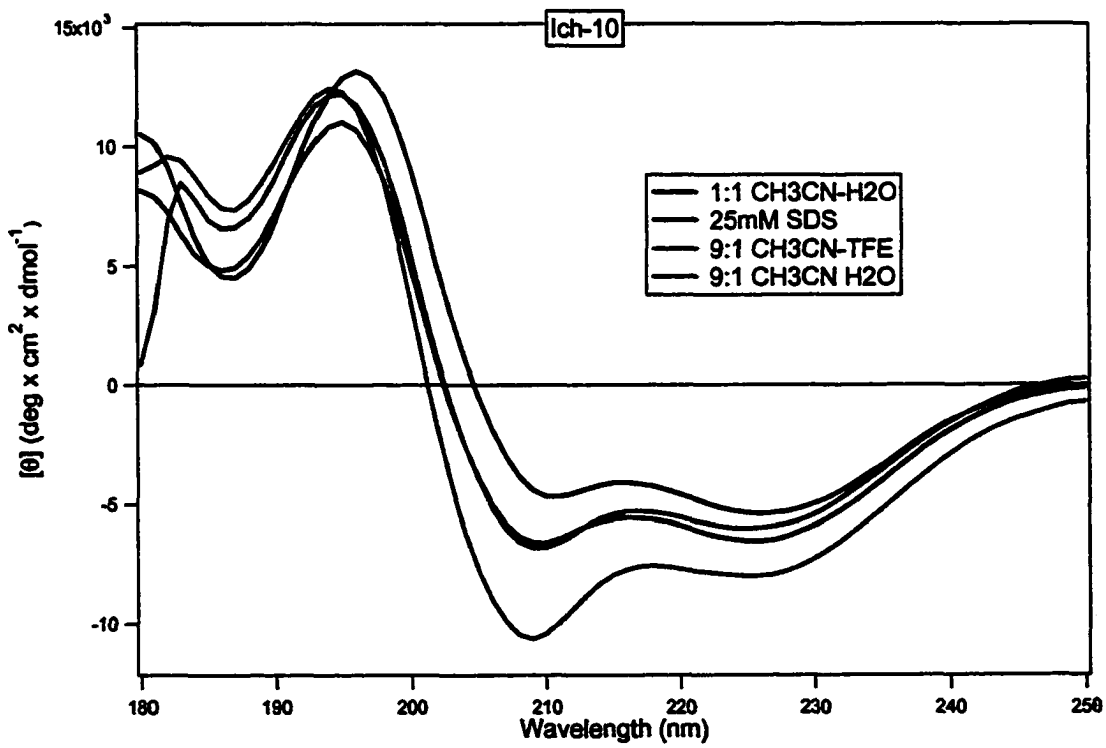

Figure 3.17. CD Spectrum of Ich-10 in various solvent systems.

The percent α-helix was estimated according to the following: percent α-helix = $-100([\theta]_{n\rightarrow\pi^*} + 3000)/33000$, where the minimum for the $[\theta]_{n\rightarrow\pi^*}$ transition is observed in the range 222-225 nm. Little work has been done to quantify the percent 3_{10}-character in a helix; therefore, we have used the CD spectrum of H-(Leu-Arg-Leu)$_8$-OH in diphosphatidyl-choline liposomes as the model 3_{10}-helix.[3.42] In this peptide, $[\theta]_{\pi\rightarrow\pi^*} = -21{,}500$ deg cm^2 dmol^{-1} is defined as 100% 3_{10}-helix. Using this model, the above equation is modified to estimate percent 3_{10}-helicity: percent 3_{10}-helix = $-100([\theta]_{\pi\rightarrow\pi^*}/-21500)$. It should, however, be noted that the issue of determining relative amounts of 3_{10}-helical character is still under review and a widely accepted determination of % 3_{10}-helicity is still not available. The results of CD-spectra 3.12-17 are summarized in Tables 3.3,4 and 5. The peptides showed minimal structure in water or pH 7.1-7.4, 2.5 mM phosphate buffer. This is not surprising since solvation of the ionizable residues, which account for 40% of the peptide composition would inhibit intramolecular hydrogen bonding patterns necessary for secondary structure formation. Interestingly, Pi-10, ACh-10α and Cyh-10 all exhibit an isodichroic point near 201, 203 and 205 nm, respectively. This suggests a cooperative helix/coil transition. An additional observation is the reduction of helicity as organic solvent composition declines. The increase in helicity as the solvent system becomes rich in organic composition has been observed in other monomeric α-helices.[3.37] Others have predicted that peptides with high percentages of ααAA's (≥ 50%), such as Pi-10 and Cyh-10, would be 3_{10}-helical.[3.19,43] In addition, theoretical calculations suggest these peptides would exhibit a shift to a 3_{10}-helix as organic content increases.[3.3] This is not observed in our studies, suggesting that amphipathy is a significant factor in determining helix

Table 3.3. CD data and calculated structural information for Pi-10 and Ipi-10. [a] Peptide concentration was 200 μM. [b] Units for [θ] are deg cm^2 $dmol^{-1}$. [c] The minimum for the $[\theta]_{\pi\rightarrow\pi^*}$ band is taken in the range from 205-209 nm. [d] The minimum for the $[\theta]_{n\rightarrow\pi^*}$ band is taken in the range from 222-225 nm. [e] In this solvent, Ipi-10 is probably mixtures of coil structures. The % α-helix is estimated to be ~20% and the % 3_{10}-helix is estimated to be ~30%.

Peptide[a]	Solvent	$[\theta]_{\pi\rightarrow\pi^*}$[b,c]	$[\theta]_{n\rightarrow\pi^*}$[b,d]	R	% Helicity	Helix
Pi-10	25 mM SDS	-8748	-7933	0.90	33	α
	9:1 CH_3CN-TFE	-10709	-7930	0.74	33	α
	9:1 CH_3CN-H_2O	-6184	-4287	0.71	22	α
	1:1 CH_3CN-H_2O	-3181	-2128	0.66	15	α
Ipi-10	25 mM SDS	-5516	-1750	0.32	25	3_{10}
	9:1 CH_3CN-TFE	-9916	-3145	0.33	33	3_{10}
	9:1 CH_3CN-H_2O	-6740	-3605	0.54	e	e
	1:1 CH_3CN-H_2O	-4204	-3118	0.74	19	α

Table 3.4. CD data and calculated structural information for ACh-10α and ACh-10. [a] Peptide concentration was 200 μM. [b] Units for [θ] are deg cm^2 $dmol^{-1}$. [c] The minimum for the $[\theta]_{\pi\rightarrow\pi^*}$ band is taken in the range from 205-209 nm. [d] The minimum for the $[\theta]_{n\rightarrow\pi^*}$ band is taken in the range from 222-225 nm. [e] In this solvent, ACh-10 is probably mixtures of coil structures. The % α-helix is estimated to be ~20% and the % 3_{10}-helix is estimated to be ~30%.

Peptide[a]	Solvent	$[\theta]_{\pi\rightarrow\pi^*}$[b,c]	$[\theta]_{n\rightarrow\pi^*}$[b,d]	R	% Helicity	Helix
ACh-10α	25 mM SDS	-9542	-7218	0.76	31	α
	9:1 CH_3CN-TFE	-10580	-6714	0.63	29	α
	9:1 CH_3CN-H_2O	-4334	-3358	0.77	19	α
	1:1 CH_3CN-H_2O	-2943	-1886	0.64	15	α
ACh-10	25 mM SDS	-3288	-893	0.27	15	3_{10}
	9:1 CH_3CN-TFE	-7480	-4622	0.62	e	e
	9:1 CH_3CN-H_2O	-6898	-5785	0.84	27	α
	1:1 CH_3CN-H_2O	-6869	-6494	0.95	29	α

Table 3.5. CD data and calculated structural information for Cyh-10 and Ich-10. [a] Peptide concentration was 200 μM. [b] Units for [θ] are deg cm^2 $dmol^{-1}$. [c] The minimum for the $[\theta]_{\pi\rightarrow\pi^*}$ band is taken in the range from 205-209 nm. [d] The minimum for the $[\theta]_{n\rightarrow\pi^*}$ band is taken in the range from 222-225 nm.

Peptide[a]	Solvent	$[\theta]_{\pi\rightarrow\pi^*}$[b,c]	$[\theta]_{n\rightarrow\pi^*}$[b,d]	R	% Helicity	Helix
Cyh-10	25 mM SDS	-10874	-9978	0.92	39	α
	9:1 CH_3CN-TFE	-10285	-9014	0.88	37	α
	9:1 CH_3CN-H_2O	-9339	-8185	0.88	34	α
	1:1 CH_3CN-H_2O	-7846	-7027	0.88	30	α
Ich-10	25 mM SDS	-4792	-5461	1.14	26	α
	9:1 CH_3CN-TFE	-10959	-8063	0.73	33	α
	9:1 CH_3CN-H_2O	-6974	-6094	0.87	28	α
	1:1 CH_3CN-H_2O	-6766	-6579	0.97	29	α

structure. The transition of Ipi-10 from an α-helix to a 3_{10}-helix and the lower R-value for Ich-10 in 100% organic solvent agrees with predictions of solvent effects on the 3_{10}-/α-helix equilibrium. It has been shown that peptides rich in Aib favor a 3_{10}-helix in less polar media and an α-helix in water.[3.3] The increased stability of the 3_{10}-helix in non-polar solvents is attributed to the extra hydrogen bond formed relative to the α-helix. α-Helices are favored in water because the "extra" carbonyl and amide are able to interact with the solvent. For Pi-10, Ich-10, Cyh-10 and Ach-10α, a maximum number of 7 hydrogen bonds are possible in the α-helix conformation. For Ipi-10 and ACh-10, in 3_{10}-helical structure, 8 hydrogen bonds are possible. Helix end effects and incomplete micelle binding tend to reduce the absolute helicity of peptides. In the case of Pi-10, ACh-10α, Cyh-10 and Ich-10, three N-terminal amides and the two C-terminal carbonyls do not have any internal hydrogen bonding partners. For Ipi-10 and ACh-10, the two N-terminal amides and the two C-terminal carbonyls are without internal hydrogen bonding partners. As a result, the peptides may adopt non-ideal structures at the ends to interact with solvent.

Temperature studies of a number of the peptides show a surprisingly high stability towards helix melting in the range 5-50 °C. This further confirms the theory that α,α-disubstituted amino acids stabilize helix stability towards temperature denaturation, as well as enzymatic hydrolysis.[3.13] Representative CD spectra of ACh-10 in SDS micelles and Cyh-10 in 9:1 acetonitrile/TFE are shown in Figure 3.18 and 3.19. This relatively small deviation in peptide helicity as a result of increasing temperature in the range between 5-50 °C was, however, observed in all of the peptides. Helicity was not determined at 0°C due to the insolubility of SDS micelles at that temperature.

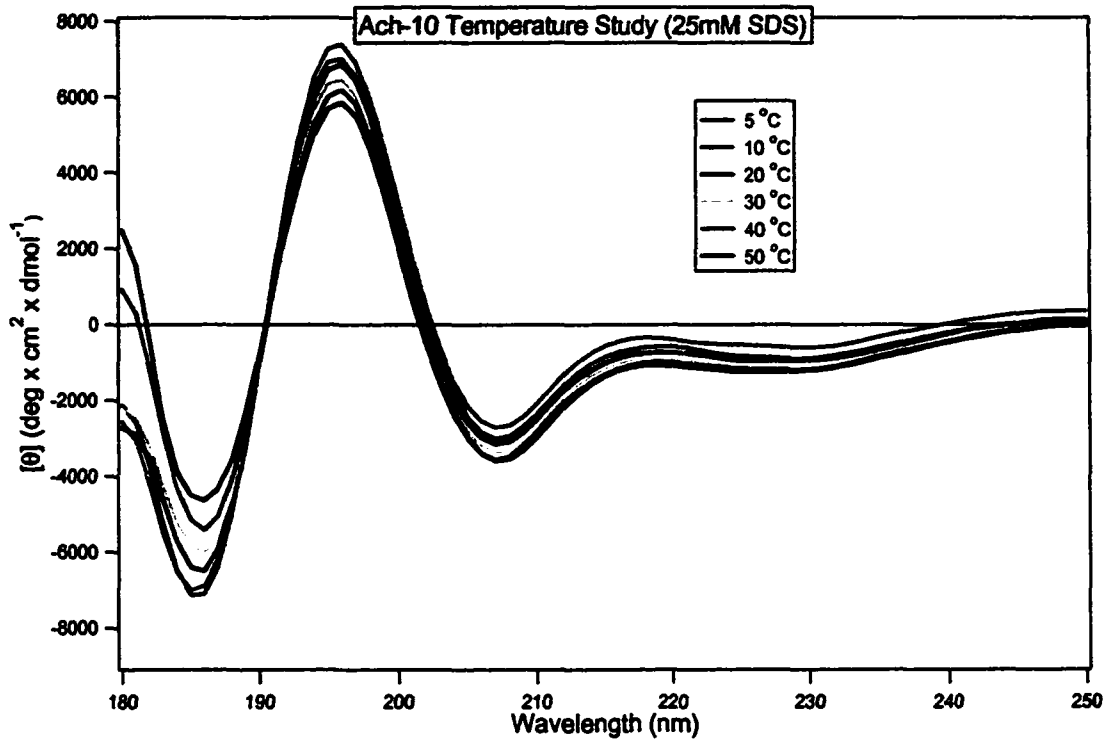

Figure 3.18. Helix stability temperature studies of ACh-10 in 25mM SDS micelles. Note the strong minimum at 186 nm.

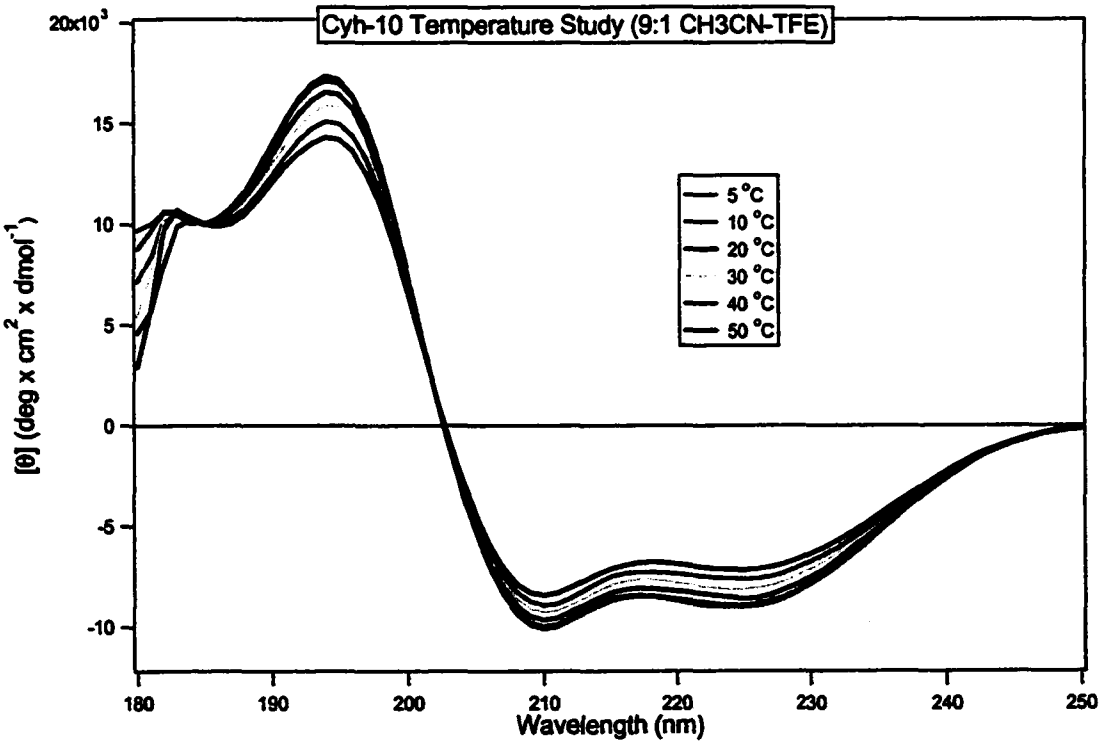

Figure 3.19. Helix stability temperature studies of Cyh-10 in 9:1 CH_3CN-TFE .

3.3. EXPERIMENTAL

3.3.1. Peptide synthesis

Peptides were synthesized using standard Fmoc-amino acid fluoride coupling conditions. The first 3 or 4 residues were manually coupled onto PAL-PEG-PS solid support by gently stirring 8 equivalents of the Fmoc-acid fluoride, 3 equivalents of DIEA and the resin in methylene chloride, until an acceptable yield was determined by quantitative Fmoc test. Sometimes gentle reflux was required to obtain successful coupling. After the first residues were coupled to the resin, the remainder of the peptide was synthesized using a Milligen 9050 peptide synthesizer on the PAL-PEG-PS solid support using 8 equivalents of preformed Fmoc-amino acid fluorides, 3 equivalents of DIEA and a 1.5 h recycling time. Residues were double coupled when they are third in a series of C^{α},C^{α}-disubstituted amino acids and the coupling times were extended to 2.5 hrs. A solution of 20% piperidine / 2% 1,8-diazabicyclo[4.5.0]undec-7-ene (DBU) in DMF was used for Fmoc removal. The peptides were simultaneously cleaved from the resin and side-chain deprotected using reagent B (8.8 : 0.2 : 0.5 : 0.5, trifluoroacetic acid (TFA) : triisopropylsilane : water : phenol). The resulting acidic solution was diluted with cold 30% acetic acid, washed with diethyl ether (4 x 50 mL), and lyophilized.

3.3.2. Peptide Purification

The crude peptides were purified by preparative reverse-phase HPLC on a Waters 15 μM Deltapak C_4 column using a water (0.05% TFA) and acetonitrile (0.05% TFA) gradient system. The gradient was run from 10% to 50% organic and the absorption monitored at 222 nm. Purity of the peptides was then checked on a Vydac 5

μM C_{18} column using the same conditions. Matrix assisted laser desorption ionization (MALDI) mass spectrometry was used to verify the peptide masses. All peptides were analyzed in positive ion mode using a glycerol matrix. Pi-10, 1037.1 $(M+H)^+$; Ipi-10, 1037.1 $(M+H)^+$; ACh-10α, 1157.6 $(M+H)^+$; ACh-10, 1157.6 $(M+H)^+$; Cyh-10, 1277.8 $(M+H)^+$; Ich-10, 1277.8 $(M+H)^+$.

3.3.3. Circular Dichroism

Circular dichroism measurements were taken on a (+)-camphor sulfonic acid calibrated Aviv 60DS spectrophotometer at 5°C. The measurements were recorded over 250-180 nm using a 0.1 cm path length quartz cell, 1 nm bandwidth, 10 nm/min scan speed and a 5 second time constant. Background spectra were acquired prior to each sample spectrum and the two subtracted. Three repetitive scans were recorded and averaged to improve signal to noise. The reported mean residue ellipticity [θ] (deg cm^2 $dmol^{-1}$) was derived from the observed ellipticity, $[\theta]_{obs}$ (millidegrees), using the formula $[\theta] = [\theta]_{obs}(MRW/10lc)$, where MRW is the mean residue molecular weight of the peptide (molecular weight of the peptide divided by the number of peptide bonds), l is the pathlength (cm) and c is the peptide concentration (mg/mL). CD spectra of all peptides in this study were taken in solvent systems ranging from 100% organic to 1:1 organic/water. Final peptide concentrations of 0.2 mM were used for all CD experiments. The peptides were dissolved in trifluoroethanol for spectra taken in 9:1 CH_3CN:TFE, pH 7.1-7.4, 2.5 mM phosphate buffer for spectra taken in SDS, and doubly distilled water for the aqueous/organic spectra. For representative aqueous/organic experiments, pH 7.1, 2.5 mM buffer was also used as the aqueous component and resulting spectra were nearly identical to the pure H_2O/CH_3CN spectra.

3.4. CONCLUSIONS

C^{α},C^{α}-Disubstituted amino acids have long been recognized as powerful tools for inducing helicity into relatively short peptide sequences. With this work, we have shown that amphipathicity, too, is a significant driving force in the secondary structure adopted by short peptides rich in C^{α},C^{α}-disubstituted amino acids. Increasing helicity, and a transition from α-helix to 3_{10}-helices as a result of increasing organic environments may suggest that there is a cooperative aggregation by the hydrophilic side of the amphipathic helices in organic solvents. In addition, it is shown that micellar environments, similar to those found under physiological conditions, have a significant effect upon the ability of peptides to adopt an amphipathic configuration. It is interesting to hypothesize as to the nature of Ich-10 and why it does not, in fact, adopt the 3_{10}-helical formation. Previous studies have supported the fact that cyclic ααAAs form stable 3_{10}-helices. This does not, however, occur in the case of Ich-10. It is possible that steric repulsion, due to the eclipsed *i* and *i*+3rd residues in 3_{10}-helical segments, is a determining factor.

The study of the bioactivity of these types of peptides may lead to the development of new therapeutic agents that act by selective interactions with cellular membranes of macrophages that are infected with pathogenic bacteria such as *Brucella abortus* and *Mycobacterium tuberculosis*. The bioactivity assays and selectivity of the peptides included in this study are described in chapter 4 of this manuscript.

3.5. REFERENCES

3.1 Creighton, T. E., *Proteins: Structure and Molecular Properties*, **1983**, W. H. Freeman, New York, pp. 2-60.

3.2 Toniolo, C. & Benedetti, E. *Trends Biochem. Sci.* **1991**, *16*, 350-3.

3.3 Smythe, M. L., Nakaie, C. R. & Marshall, G. R. *J. Am. Chem. Soc.* **1995**, *117*, 10555-62.

3.4 Basu, G., Kitao, A., Hirata, F. & Go, N. *J. Am. Chem. Soc.* **1994**, *116*, 6307-6316.

3.5 Otoda, K., Kitagawa, Y., Kimura, S. & Imanishi, Y. *Biopolymers* **1993**, *33*, 1337-45.

3.6 Tirado-Rives, J., Maxwell, D. S. & Jorgensen, W. L. *J. Am. Chem. Soc.* **1993**, *115*, 11590-11593.

3.7 Smythe, M. L., Huston, S. E. & Marshall, G. R. *J. Am. Chem. Soc.* **1993**, *115*, 11594-5.

3.8 Barlow, D. J. & Thornton, J. M. *J. Mol. Biol.* **1998**, *201*, 601-19.

3.9 Millhauser, G. L. *Biochemistry* **1995**, *34*, 3873-7.

3.10 Miick, S. M., Martinez, G. V., Fiori, W. R., Todd, A. P. & Millhauser, G. L. *Nature (London)* **1992**, *359*, 653-5.

3.11 Prasad, B. V. V. & Balaram, P. *CRC Crit. Rev. Biochem.* **1984**, *16*, 307-348.

3.12 Marshall, G. R., Hodgkin, E. E., Langs, D. A., Smith, G. D., Zabrocki, J. & Leplawy, M. T. *Proc. Natl. Acad. Sci. U. S. A.* **1990**, *87*, 487-91.

3.13 Augspurger, J. D., Bindra, V. A., Scheraga, H. A. & Kuki, A. *Biochemistry* **1995**, *34*, 2566-76.

3.14 Nagaraj, R., Shamala, N. & Balaram, P. *J. Am. Chem. Soc.* **1979**, *101*, 16-20.

3.15 Steiner, H., Hultmark, D., Engstrom, A., Bennich, H. & Boman, H. G. *Nature* **1981**, *292*, 246-248.

3.16 Zasloff, M. *Proceedings of the National Academy of Sciences, U.S.A.* **1987**, *84*, 5449-5453.

3.17 Mor, A., Nguyen, V. H., Delfour, A., Migliore-Samour, D. & Nicolas, P. *Biochemistry* **1991**, *30*, 8824-8830.

3.18 Paul, P. K. C., Sukumar, M., Bardi, R., Piazzesi, A. M., Valle, G., Toniolo, C. & Balaram, P. *J. Am. Chem. Soc.* **1986**, *108*, 6363-70.

3.19 Karle, I. L. & Balaram, P. *Biochemistry* **1990**, *29*, 6747-56.

3.20 Toniolo, C. & Benedetti, E. *Macromolecules* **1991**, *24*, 4004-9.

3.21 Hodgkin, E. E., Clark, J. D., Miller, K. R. & Marshall, G. R. *Biopolymers* **1990**, *30*, 533-46.

3.22 Lapena, Y., Lopez, P., Cativiela, C., Kaptein, B., Broxterman, Q. B., Kamphuis, J., Mossel, E., Peggion, C., Formaggio, F., Crisma, M. & Toniolo, C. *J. Chem. Soc., Perkin Trans. 2* **2000**, 631-636

3.23 Karle, I. L. *Acta Crystallogr. B.* **1992**, *48*, 341-356.

3.24 Karle, I. L., Flippen-Anderson, J. L., Gurunath, R. & Balaram, P. *Biopolymers (Protein Sci.)* **1994**, *4*, 1547-1555.

3.25 Rossi, P., Felluga, F. & Scrimin, P. *Tetrahedron Letters* **1998**, *39*, 7159-7162.

3.26 Rossi, P., Felluga, F., Tecilla, P., Formaggio, F., Crisma, M., Toniolo, C. & Scrimin, P. *J. Am. Chem. Soc.* **1999**, *121*, 6948-6949.

3.27 Perutz, M. F., Kendrew, J. C., Watson, H. C. *J. Mol. Biol.* **1965**, *13*, 669-677.

3.28 Tomich, J. M. In *The Amphipathic Helix*, **1993**, CRC Press, Boca Raton, pp. 222-249.

3.29 Anantharanaiah, G. M., Jones, M. K., Segrest, J. P. In *The Amphipathic Helix*, **1993**, CRC Press, Boca Raton, pp. 109-140.

3.30 Taylor, J. W. In *The Amphipathic Helix*, **1993**, CRC Press, Boca Raton, pp. 286-308.

3.31 Waring, A. J., Gordon, L. M., Taeusch, W., Bruni, R. In *The Amphipathic Helix*, **1993**, CRC Press, Boca Raton, pp. 143-167.

3.32 Cornut, I., Thiaudiére, E., Dufourcq, J. In *The Amphipathic Helix*, **1993**, CRC Press, Boca Raton, pp. 173-210.

3.33 Chopra, I. *Journal of Antimicrobial Chemotherapy* **1993**, *32*, 351-353.

3.34 Toniolo, C., Benedetti, E. *Macromolecules* **1991**, *24*, 4004-4009.

3.35 Hammarström, L. G. J. & McLaughlin, M. L. *Organic Synthesis* **2001** (Submitted for publication).

3.36 Oren, Z. & Shai, Y. *Biopolymers (Peptide Science)* **1998**, *47*, 451-463.

3.37 Mant, C. T., Zhou, N. E., Hodges, R. S.. In *The Amphipathic Helix*, **1993**, CRC Press, Boca Raton, pp. 39-66.

3.38 Toniolo, C., Polese, A., Formaggio, F., Crisma, M. & Kamphuis, J. *J. Am. Chem. Soc.* **1996**, *118*, 2744-5.

3.39 Iqbal, M. & Balaram, P. *Biopolymers* **1982**, *21*, 1427-33.

3.40 Gratias, R., Konat, R., Kessler, H., Crisma, M., Valle, G., Polese, A., Formaggio, F., Toniolo, C., Broxterman, Q. B. & Kamphuis, J. *J. Am. Chem. Soc.* **1998**, *120*, 4763-4770.

3.41 Long, H. W. & Tycko, R. *J. Am. Chem. Soc.* **1998**, *120*, 7039-7048.

3.42 Iwata, T., Lee, S., Oishi, O., Aoyagi, H., Ohno, M., Anzai, K., Kirino, Y. & Sugihara, G. *J. Biol. Chem.* **1994**, *269*, 4928-33.

3.43 Basu, G., Bagchi, K. & Kuki, A. *Biopolymers* **1991**, *31*, 1763-74

CHAPTER 4
SELECTIVE BIOACTIVITY OF SYNTHETIC AMPHIPATHIC PEPTIDES AGAINST AN INTRACELLULAR PATHOGEN

4.1. INTRODUCTION

Brucella abortus (*Ba*) and *Mycobacterium tuberculosis* (*Mtb*) are intracellular pathogens that live and replicate within the macrophages of their hosts.[4.1] *Ba* are rod-shaped gram-negative bacteria which are the primary cause of brucellosis, or undulant fever in humans.[4.2] The fever is characterized by fever, anorexia, muscular weakness, arthritis and dementia, as well as cardiac and neurological disorders, and may be fatal if untreated.[4.3] In animals, *Ba* localizes in the reproductive organs, resulting in abortion and infertility.[4.4,5] Human infection often results from exposure to infected animals or infected animal products, thus brucellosis is a prominent occupational hazard for humans whom are involved with animal handling.[4.6] Since the bacteria live and replicate within the white blood cells of the host, treatment is difficult. The multiple membrane barrier which seperates the pathogen from the extracellular environment reduces the antibiotic concentration within the macrophage and reduces the effectiveness of the antibiotic.[4.7,8] In addition, the mechanism by which these organisms survive and replicate within host macrophages is poorly understood.[4.15,16]

Mycobacterium species are intracellular pathogens that cause diseases with etiologies similar to *Brucella*. *Mycobacterium tuberculosis* (*Mtb*), the causative agent of tuberculosis, and is one of the more worrisome elements of the developing antibiotic-resistance problem since *Mtb* patients that fail treatment have a high risk of death. The pathogen infects about a third of the world's population and kills more people, about two million each year, than any other infectious agent besides HIV/AIDS.[4.9,12] Unlike

many lethal pathogens, *Mtb* has been found on all continents and is especially prevalent in countries of the former Soviet Union.[4.13]

Mtb is a rod-shaped, acid-fast Gram-positive bacterium that localizes mainly in the respiratory system. The symptoms of tuberculosis include low-grade fever, night sweats, fatigue, weight loss and persistent cough. Like *Ba*, *Mtb* can live and replicate within a host's macrophages, making it difficult to treat. Current treatment consists of short-course chemotherapy based on a regiment of four first-line drugs taken for 6-8 months.[4.9,10,12] In addition, there are currently no vaccines to prevent *Ba* or *Mtb* in humans.[4.14] Many strains of *Mycobacterium* now resist antibiotics, making the development of alternative treatments critical.

Due to exponential growth in the use of classical antibiotic therapy, bacterial resistance towards antibiotics is becoming an ever growing problem. This problem is exacerbated in the case of intracellular pathogens since they reside within the cellular environment of the very immune system which is used to target it and infection is not associated with a significant extracellular component of the pathogen. Because of this resistance problem, several new approaches towards antimicrobial defense have been explored within the past twenty years. One of the most promising routes toward developing a new weapon to battle bacterial agents have been the growing interest in linear amphipathic peptides as antimicrobial agents. Amphipathic peptides are highly ubiquitous in nature and make up an important part of the natural defenses of several species of invertebrates,[4.17-22,36,37] fish,[4.23-26] amphibians,[4.27-30,39,40] and mammals.[4.31,32,42] The peptides are characterized by the presence of a definable cationic amphipathic helical structure and are usually relatively short (<40 residues), thus suggesting that

considerable biological activity can be exhibited by relatively short sequences.[4.33] These peptides have been found to be active against a wide array of pathogens, including gram-positive and gram-negative bacteria, protozoa, and fungi.[4.34] Although currently not prevalent as therapeutic agents, some peptides are currently under review for use as drugs. Recently, Hancock reviewed two antimicrobial peptides that are currently being clinically studied as topical treatments for oral mucositis and the sterilisation of central venous catheters.[4.35] Some examples of naturally occuring, linear antimicrobial peptides are listed in Table 4.1.

Table 4.1. Naturally occurring antimicrobial peptides.

Peptide	Source	Ref.
Andropin	Fruit Fly (*Drosophila melangaster*)	4.36
Bombolitin	Bumblebee (*Megabombus pennsylvanicus*)	4.37
Cercropin A	Silk Moth (*Hyalophora cercropia*)	4.18
Clavanin A	Tunicate (*Styela clava*)	4.38
Dermaseptin 1	Arboreal frog (*Phyllomedusa sauvageii*)	4.39
Magainin 1	South African clawed frog (*Xenopus laevis*)	4.40
Melittin	Honeybee (*Apis mellifera*)	4.41
Pleurocidin	Winter flounder (*Pleuronectes americanus*)	4.23
Seminalplasmin	Ox (*Bos taurus*)	4.42

There has been overwhelming evidence to suggest that these peptides function by a non-receptor mediated response, thus making them less susceptible towards the development of resistance.[4.43-47] This has been established by the fact that most antimicrobial peptides are equally active in their D- and L-isoforms. Peptides are, apparently, initially attracted to cellular membranes by coulombic interactions. The charge on the polar face of the peptide cross-section is almost exclusively positive, which accounts for the peptides' selectivity and bioactivity towards bacterial cells. Bacterial cell membranes are unique in that they contain lipopolysaccharides (gram-negative) or teichoic and teichuronic acids (gram-positive), giving their cell membrane a predominantly negative charge, which attracts the positive charge of the peptides.[4.34] Mammalian cells are composed predominantly of zwitterionic sphingomyelin phospholipids, which have been shown to show low affinity for natural antimicrobial peptides.[4.33,34] Although there have been several theories on the mode of action of antimicrobial peptides, it is generally accepted that they function by cellular membrane permeation after a threshold concentration has been established on the cell surface. Most antimicrobial peptides are non-helical in solution, which makes pre-surface aggregation to form rod-like pores, that insert into the membrane, an unlikely scenario. Hydrophobic partitioning of the surface peptides into the amphipathic environment of the cellular membrane induces helix formation and disrupts the membrane integrity by one of two proposed mechanisms: the "carpet model"[4.48] or the "barrel-stave model".[4.49] Each of these models involves the aggregation of peptides on the cell surface and disruption of the cellular membrane. However, the process by which the membrane is permeabilized varies between the two mechanisms. The carpet

mechanism is characterized by massive peptide aggregation on the cell surface with the non-polar face of the peptides incorporated into the hydrophobic interior of the lipid bi-layer and the polar face facing the exterior of the cell (A). This aggregation is most likely electrostatically driven between the negative phospholipid headgroups and the positive charge of the amphipathic peptide. When a threshold concentration of peptide has been reached, the membrane can fold in on itself (B), exocytizing a portion of the membrane as a solubilized micelle (C), resulting in membrane disruption. (Figure 4.1).

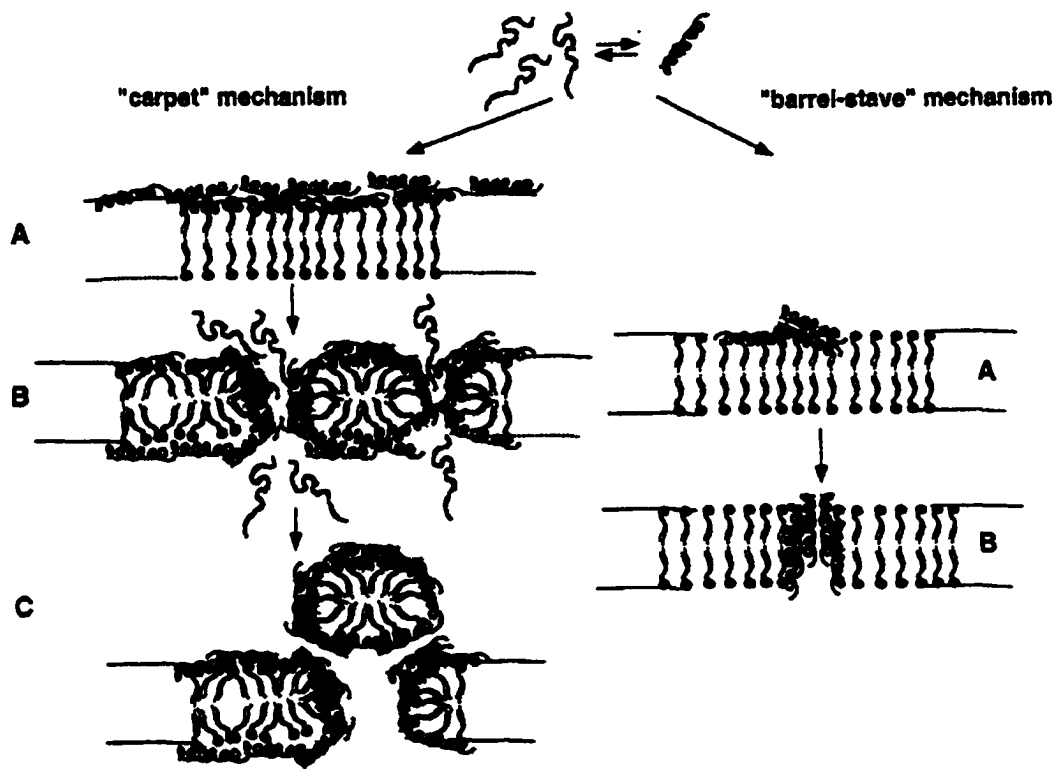

Figure 4.1. "Carpet" vs. "Barrel-Stave" mechanism of amphipathic peptide-cell membrane insertion (reproduced from: Oren, Z., Shai, Y. *Biopolymers, Pept. Sci.* **1999**, 451-463).

The "barrel-stave" model follows a different pathway. It assumes that peptides aggregate into a pore-like superstructure on the surface prior to membrane interaction (A). The pre-formation of a peptide-aggregate pore allows a relatively small number of peptides to acquire great potency as membrane disruptors. After the intial pore formation, the pore inserts itself into the membrane causing cell lysis (B). This model holds less credence for explaining the activity of shorter peptides (<20 residues), which in theory do not have the physical size to transverse the cell membrane bilayer (~35 Å).[4.34] Because the peptide-host interaction is not receptor mediated, the issue of selectivity has always been a key factor to consider in anti-microbial peptide design. This question of selectivity may be overcome by the presence of hyper-susceptibility of target cells towards the attacking peptide.

Due to the promising outlook of amphipathic peptides as potential antimicrobial agents, six helical amphipathic peptides were designed to act as natural antimicrobial peptide analogs. Incorporation of high levels of C^{α},C^{α}-disubstituted amino acids allowed for the preparation of amphipathic helices which were helical in amphipathic environments despite very short sequences (10 residues, see chapter 3). In addition, the presence of C^{α},C^{α}-disubstituted amino acids prevents enzymatic degradation of the peptides *in vitro* and *in vivo*. The designed peptides are shown in Table 4.2.

These peptides were designed to be either 3_{10}- or α-helical based on amphipathic distribution of the residues (see chapter 3). Although preliminary testing of the direct bacteriacidal activity of these peptides showed low to moderate direct effect towards bacteria, the selectivity of Pi-10 towards killing macrophages infected with intracellular pathogens such as *Ba* and *Mtb*[4.50] prompted us to further investigate the selectivity of

the rest of this family of peptides. Studies on the effect of these peptides on intracellular pathogens, such as *Ba*, may provide insight in to the development of therapeutics to battle infections of higher current interest, such as *Mtb*.

Table 4.2. List of prepared *de novo* peptides. The incorporation of 20% L-lysine (*Lys*) allows for CD spectroscopic determination of peptide secondary structure by inducing right-handed helix formation. Pi-10, Ach-10α and Cyh-10 were designed to be perfectly amphipathic as an α-helix while Ipi-10, Ach-10 and Ich-10 were designed to be perfectly amphipathic as a 3_{10}-helix.

Peptide	Sequence	Helix Design
Pi-10	H-Aib-Aib-Api-*Lys*-Aib-Aib-Api-*Lys*-Aib-Aib-NH_2	α
Ipi-10	H-Api-Aib-Aib-*Lys*-Aib-Aib-*Lys*-Aib-Aib-Api-NH_2	3_{10}
Ach-10α	H-Ac_6c-Aib-*Lys*-Api-Aib-Ac_6c-Api-*Lys*-Ac_6c-Aib-NH_2	α
Ach-10	H-Api-Aib-Ac_6c-*Lys*-Ac_6c-Aib-*Lys*-Aib-Ac_6c-Api-NH_2	3_{10}
Cyh-10	H-Ac_6c-Ac_6c-Api-*Lys*-Ac_6c-Ac_6c-Api-*Lys*-Ac_6c-Ac_6c-NH_2	α
Ich-10	H-Api-Ac_6c-Ac_6c-*Lys*-Ac_6c-Ac_6c-*Lys*-Ac_6c-Ac_6c-Api-NH_2	3_{10}

To test the hypothesis, that the selective cytocidal character of the peptides are dependent on the activation of the macrophage membrane, *in vitro* activation of protein kinase C (PKC) was performed with the application of PMA.[4,53,54] PMA (Phorbol 12-myristiol 13-acetate) is a polycyclic alcohol derived from croton oil, and is persistent in physiological conditions as it is not readily degraded. PMA is a known activator of

PKC when applied in a short-term manner, and mediates the response to a number of hormones and growth factors, which stimulate phospholipid hydrolysis (via phospholipase *C*, *D*, and A_2).[4.55] The activation includes the translocation of PKC to cellular membranes as a result of increased levels of *n*-1,2-diacylglycerol (DAG) of fatty acids.[4.56] 12 PKC isoforms are described: conventional PKC (cPKC) α, βI, βII and γ; novel PKC (nPKC) as δ, ε, o, μ, η, and θ; and atypical PKC (aPKC) ζ, λ, ι.[4.57] The different types of PKC show different activation patterns: cPKC isoforms are activated by calcium and DAG fatty acids in presence of phosphatidyl serine. nPKC isoforms are activated by PMA and DAG, but are insensitive to Ca. aPKC ζ and members of nPKC class can be activated by the phospholipid phosphatidylinositol-3,4,5-trisphosphate, produced in response to growth factors and G protein linked receptors. The unique activation of PKC δ and PKC ξ link the PKC system to actions of growth factors which stimulate tyrosine kinase activity. Long term incubation (>12 h) depleted PKC, probably through proteolytic degradation of the activated enzyme.[4.58]

A number of PKC inhibitors have been described. A novel PKC inhibitor: *GF109203X* is a bisindolylmaleimide (Bis). Bis is highly specific as it inhibits only PKC as a competetive inhibitor of ATP.[4.59] In contrast to other PKC inhibitors, Bis is very specific for PKC without interaction with protein kinase A. Several studies were performed incorporating the administration of PMA, PKC inhibitor and peptide to determine whether peptide activity is dependent on cellular membrane activation and subsequent increased PKC activity. Observations clearly indicate that cellular membrane pathways are involved in the increased susceptibility of infected macrophages towards cell lysis by selective peptides.

To test the hypothesis that these peptides selectively destroy infected macrophages over non-infected macrophages, *in vitro* studies were performed using a strain of *Ba* containing a green fluorescent protein (GFP). *Ba* is too small to be seen at the magnification levels used to visualize the macrophages; therefore, the strain expressing the GFP allows the infected macrophages to be identified. Post-infection, the infected macrophages are plated out together with the non-infected macrophages and the infected cells can clearly be visualized by fluorescence photography (See Figure 4.2)

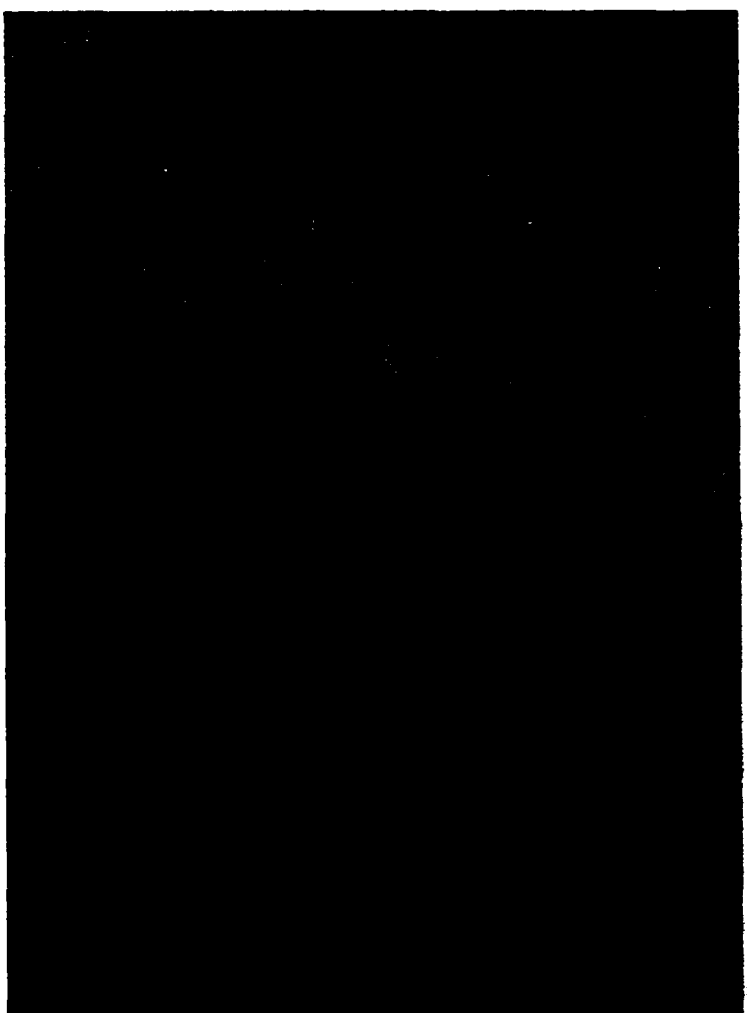

Figure 4.2. Visible photomicrograph of untreated macrophages infected with *Ba*- GFP (top). Fluorescence photomicrograph of untreated macrophages infected with *Ba*-GFP (bottom).

4.2. RESULTS AND DISCUSSION

It is not known why synthetic peptide of this family selectively destroy macrophages infected with intracellular pathogens, since macrophages, like most mammalian cells are known to be relatively resistant to amphipathic peptides of this length. Linear α-helical antimicrobial peptides containing high levels of hydrophobic residues with lengths over 20 residues are known to retain high levels of cytotoxicity.[4,51,52] Lowering the length to 10 amino acid residues reduces direct bacterial and mammalian cytotoxicity; however, the peptides still retain high levels of bioactivity against macrophages infected with intracellular pathogens. There are two plausible explanations for the phenomenon: 1) Infection of the macrophage causes a cellular membrane alteration, making the peptide more "attracted" towards its membrane, or, 2) peptide distribution is equal in infected and healthy macrophages and the infected cells display an increased sensitivity towards membrane disruption.

In order to establish direct antibacterial activity, minimum inhibitory concentration (MIC) studies were performed to determine relative cytolytic activity against representative Gram-positive (*S. aureus*) and Gram-negative (*E. coli*) bacteria. The MIC data of naturally occurring antimicrobial peptides mellitin, cercropin B amide and magainin 2 amide are included as reference. Table 4.3 summarizes the results. The synthesized peptides showed moderate to high levels of activity for both representative bacterial groups. Oddly, Pi-10 and Ipi-10 showed little to no effect on *S. aureus*. Direct cytolytic activity against *Ba* was also tested to verify that no significant cytotoxity was observed under conditions similar to those of the studies of selective macrophage destruction. 20 μL of a 1.4×10^9 suspension of *Brucella abortus* 2308/gfp was added to

Table 4.3. Peptide antimicrobial activity as determined by minimum inhibitory concentrations.

Peptide	MIC (μM) vs. *E. coli*	MIC (μM) vs. *S. aureus*
Pi-10	8	123
Ipi-10	4	Not active
Ach-10α	8	4
Ach-10	4	4
Cyh-10	6	6
Ich-10	13	3
Melittin	3	3
Cecropin B amide	1	12
Magainin 2 amide	10	19

200 μL of media in individual wells. Each well contained media with 200 μM of one of the peptides in Table 4.2. At 30 minutes post addition of bacterial cells, the wells were serially diluted and plated on blood agar. They were left to incubate for 72 hours and counted. The inoculation suspension was also serially diluted and plated to ascertain the precise number of bacteria added. A standard two-sample T-test and confidence interval was run to compare the final counts with the inoculation suspension count, and no significant differences were noted. There was no significant killing with any of the

peptides as was apparent by comparing post-treatment colony forming units as compared with the inoculation dose. This was not surprising since it has been thoroughly documented that *Ba* is considerably more resistant to bactericidal cationic peptides than most gram-negative bacteria (See Table 4.4).[4.60-62]

Table 4.4. Direct toxicity of peptides against *Brucella abortus* 2308/gfp.

Peptide Treatment (200 uM)	CFU/ml	Significance
Ipi-10	1.2×10^9	None
Ach-10	1.3×10^9	None
Pi-10	1.5×10^9	None
Ach-10α	1.4×10^9	None
Ich-10	1.4×10^9	None
Cyh-10	1.3×10^9	None
Control (no peptide)	1.4×10^9	

Table 4.5 summarizes the direct cytotoxic effect of the presented peptides against non-infected murine peritoneal macrophages. Peptides were dilutes in warm 0.9% Saline + Fetal Calf Serum (10%) and added to cells. Cells were allowed to incubate 1.5 hours and then stained for viability with Trypan Blue. As expected, the more hydrophobic Cyh-10 and Ich-10, incorporating four Ac_6c residues, had the highest direct cytolytic activity against non - infected macrophages. ACh-10α and ACh-10

Table 4.5. Normal macrophage survival versus peptide concentration.

Peptide	% Macrophage Survival							
	200 μM	100μM	50μM	10μM	8μM	6μM	3μM	1μM
Pi-10	>95 %	75%	100 %	100 %	100 %	100 %	100 %	100 %
Ipi-10	>95 %	>95 %	100 %	100 %	100 %	100 %	100 %	100 %
Ach-10α	20 %	30%	100 %	100 %	100 %	100 %	100 %	100 %
Ach-10	<5 %	70%	90 %	100 %	100 %	100 %	100 %	100 %
Cyh-10	0 %	0 %	<5 %	<5 %	25 %	50 %	90 %	100 %
Ich-10	0 %	0 %	<5 %	85 %	>95 %	>95 %	100 %	100 %

show slightly higher cytotoxic character due to the incorporation of two residues of Ac_6c; Pi-10 and Ipi-10 had the lowest cytotoxicity levels and are the least hydrophobic of this family of peptides. Cyh-10 and Ich-10 are highly active, but may be too toxic to pursue as selective agents for the destruction of infected macrophages. In contrast, the high activity and relatively low cytotoxicity of ACh-10α and ACh-10 make them promising candidates.

In vitro studies confirming the selective killing of infected vs. non-infected macrophages by the designed peptides were performed using a strain of *Ba* containing a green fluorescent protein (GFP). *Ba* is too small to be seen at the magnification levels used to visualize the macrophages; therefore, the strain expressing the GFP allows the infected macrophages to be identified. Trypan blue exclusion was used to visualize dead macrophages. The results of the peptide selectivity studies are illustrated in Figures 4.3-4.5. Cyh-10 was, by far, the most bioactive peptide, showing an optimum

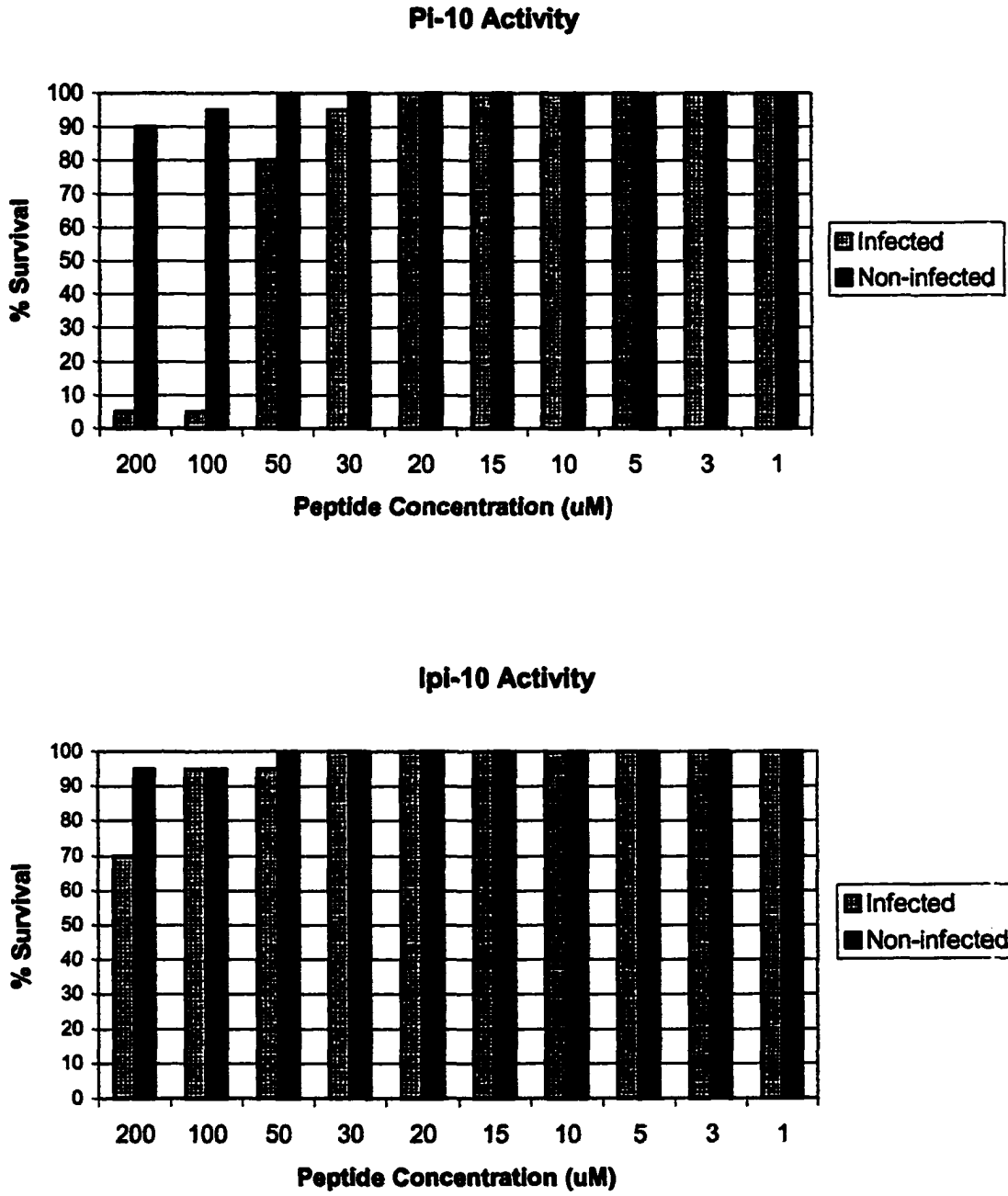

Figure 4.3. Selective bioactivity of Pi-10 (top) and Ipi-10 (bottom) towards healthy macrophages and macrophages infected with *Brucella abortus*-GFP.

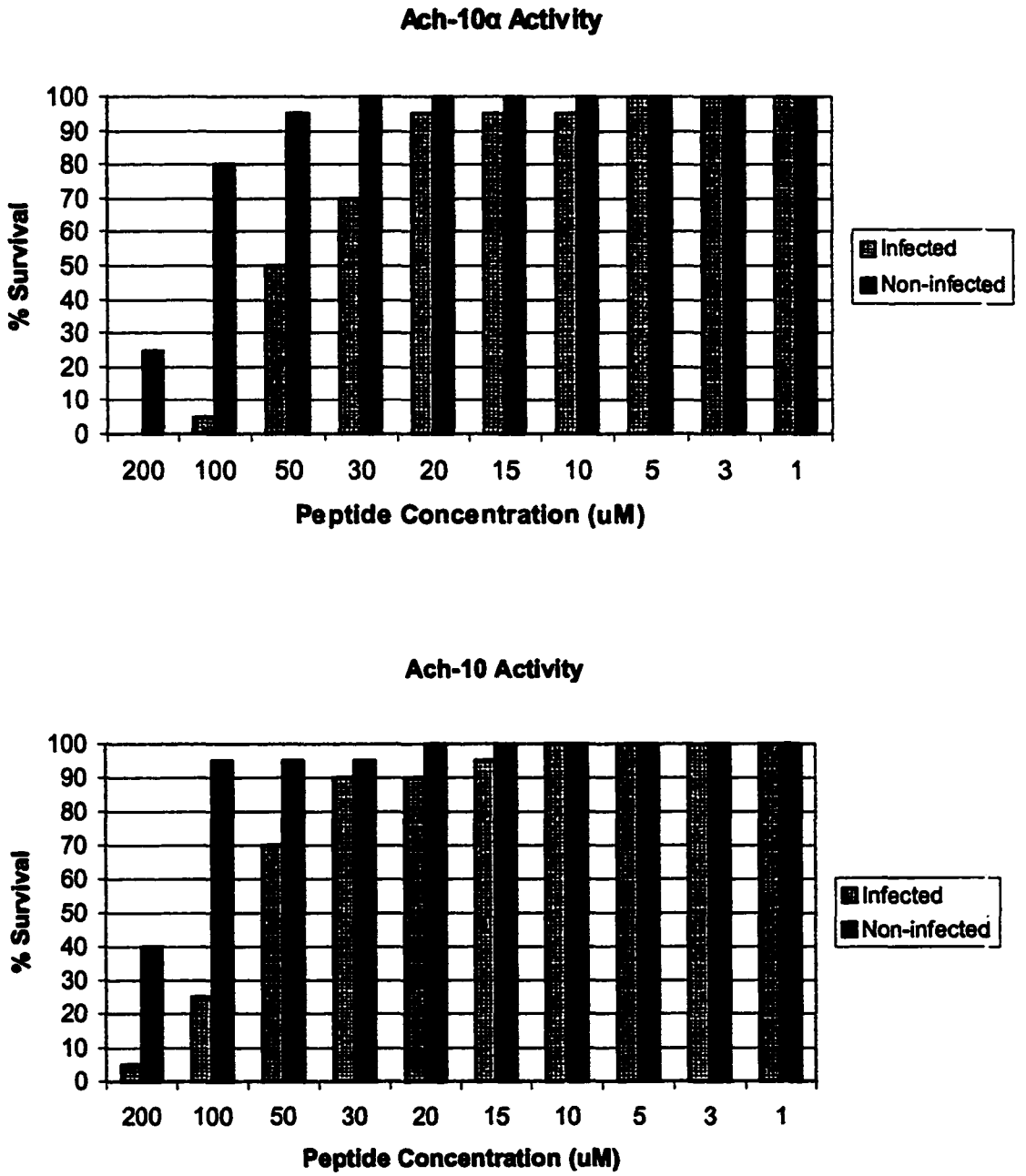

Figure 4.4. Selective bioactivity of Ach-10α (top) and Ach-10 (bottom) towards healthy macrophages and macrophages infected with *Brucella abortus*-GFP.

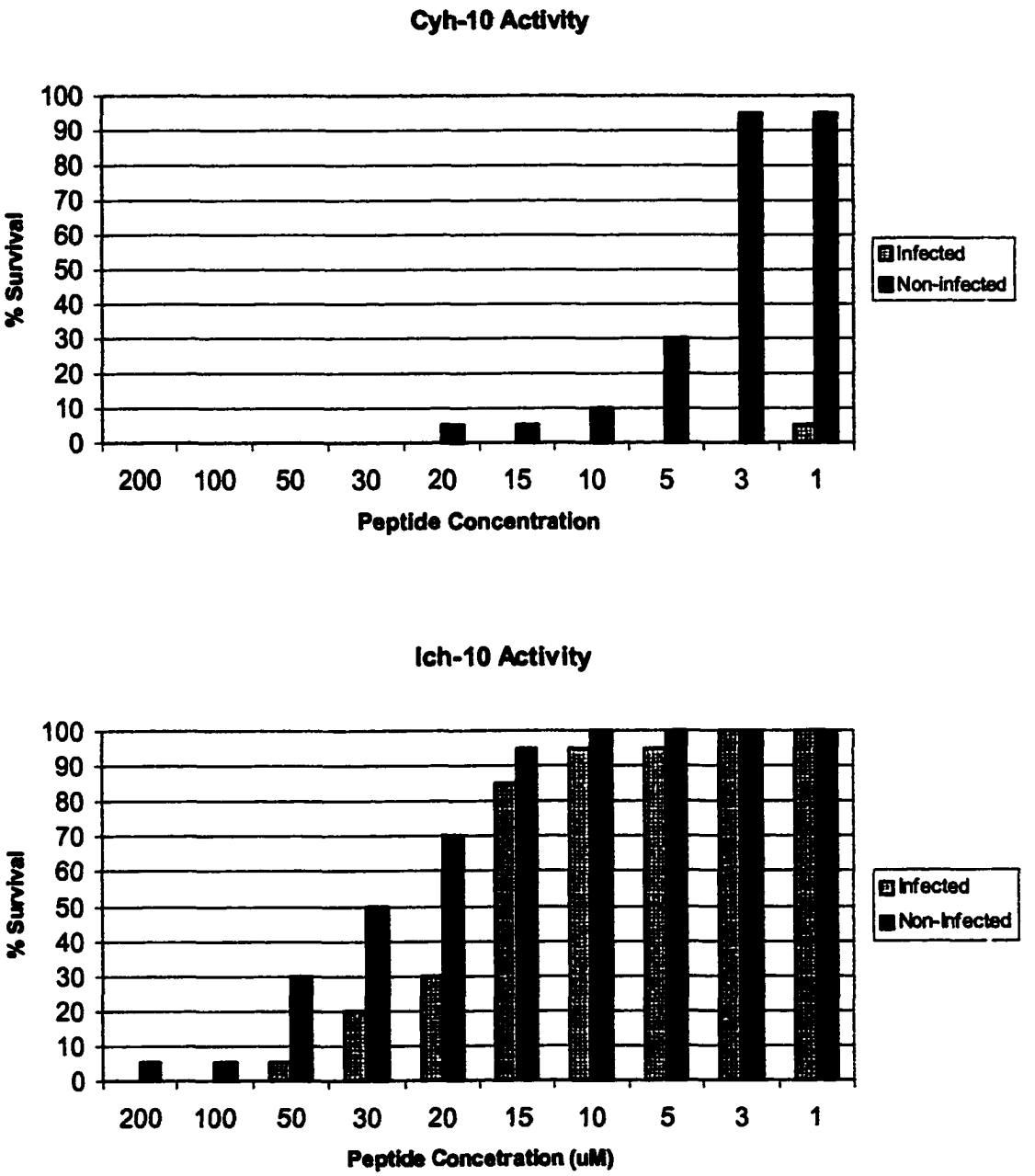

Figure 4.5. Selective bioactivity of Cyh-10 (top) and Ich-10 (bottom) towards healthy macrophages and macrophages infected with *Brucella abortus*-GFP.

concentration dose at 3 μM. Although the *in vitro* bioactivity and selectivity of this peptide is very high, *in vivo* toxicity studies may reveal this peptide to be too cytotoxic to be used effectively in therapeutic studies. Ich-10 also showed high activity at low dosage concentrations. However, cytolytic activity was much lower, as was selectivity at all concentrations. In general, all peptides designed with the 3_{10}-helix permutations showed significantly lower bioactivity and selectivity than their α-helical counterparts Table 4.6). The optimum concentration for each peptide was established as the dosage at which maximum differentiation between infected macrophage killing and non-infected macrophage killing was observed.

Table 4.6. Activity summary of designed peptides. [a] Optimum concentrations for each peptide were established at the dose which gave highest selectivity between infected macrophage killing and non-infected macrophage killing. [b] Activity = (% Infected killed - % Non-infected killed) at optimum concentration. [c] Efficacy = Activity / optimum concentration.

Peptide	Optimum Concentration (μM)[a]	Activity[b]	Efficacy[c]
Pi-10	100	90	0.9
Ipi-10	>200	25	0.13
Ach-10α	100	75	0.75
Ach-10	100	60	0.60
Cyh-10	3	95	31.67
Ich-10	20	40	2.0

Optimum concentrations decreased as the peptides increased in hydrophobicity, with the α-helical permutation isomer retaining higher activity than the 3_{10}-helical isomer. This may suggest that the α-helical conformation is a more active membrane-disruption agent than a 3_{10}-helical peptide of the same hydrophobicity. As expected, Pi-10 and Ipi-10 showed the lowest direct activity, as a result of their lower hydrophobicity. Ipi-10 showed significantly lower activity than Pi-10. Overall efficacy of the tested peptides was established by peptide activity (% difference in infected vs. non-infected killing at the optimum concentration) divided by the optimum concentration dosage. As can be seen in Table 4.6., Cyh-10 and Ich-10 showed the highest efficacy. However, as previously stated, these peptides may be too cytotoxic to be utilized effectively in *in vivo* studies. Ach-10α and Pi-10 are the most interesting candidates for further study, as they retain high activity and relatively low cytotoxicity.

It is not known what mechanism is responsible for peptide selectivity towards infected macrophages. However, it is hypothesized that cellular membrane activation is responsible for increased sensitivity towards the administered peptides. Studies were performed incorporating the administration of PMA, PKC inhibitor and peptide to determine whether peptide activity is dependent on cellular membrane activation and subsequent increased PKC production. Infected and non-infected macrophages in DMEM with 5% Fetal bovine serum (FBS) were treated with either 1.0 μM, 100 nM, or 50 nM concentrations of Phorbol-12-myristalate-13-acetate (PMA) at 1 hour prior to treatment with 5 μM Bisindoly maleimide 1 (PKC inhibitor). Separate groups of both infected and non-infected macrophages were treated with 5 μM PKC inhibitor 1 hour prior to treatment with the various concentrations of PMA. Following each treatment,

the macrophages were incubated for 1 hour at 37 °C with 5.0 % CO_2. 100 uM Pi-10 was added to PMA, PMA/PKC inhibitor, or PKC inhibitor/PMA treated infected and non-infected macrophages and allowed to incubate at 37 °C with 5.0 m% CO_2. Infected and uninfected macrophages, which had not been exposed to PMA or PKC inhibitor, were also treated with 100 µM Pi-10 for comparison. Macrophages were then washed 3 times with warm Phosphate buffered saline (PBS) with 5% FBS (PBS/FBS) after which warm PBS/FCS was added back and cells were examined microscopically. Trypan Blue exclusion was used to determine viability of cells (Table. 4.7).

Table 4.7. PMA / PKC inhibitor studies showing differential bioactivity of Pi-10 towards PMA infected macrophages. [a] PMA concentration: H=1.00µM, M=100nM, L=50nM. [b] PKC inhibitor concentration: H = 1.00µM , L = 50.0nM. [c] Peptide treatment: Pi-10 concentrations = 100µM. * Denotes significant killing of macrophages due to PMA activation.

Experiment #	PMA[a]	PKc Inhibitor[b]	Peptide[c]	% Survival
1	-	-	-	94.4
2	H, M, L	-	-	93.6
3	-	H, L	-	95.8
4	-	-	1 hr	97.1
5	H, M, L	H, L	-	96.7
6	H, M, L	-	1 hr	40.8 ($p<0.005$)*
7	L	H	1 hr	96.8
8	M	L	1 hr	95.3
9	H	L	1 hr	49.8 ($p<0.005$)*

Observations clearly indicate that cellular membrane pathways are involved in the increased susceptibility of infected macrophages towards cell lysis by selective peptides. Control populations of macrophages only (experiment 1), PMA and macrophages (experiment 2), PKC inhibitor and macrophages (experiment 3), Pi-10 and macrophages (experiment 4) and PMA with PKC inhibitor (experiment 5) all showed insignificant variation in viable macrophage populations. Macrophage activation with PMA at varying concentrations combined with Pi-10 treatment showed significant killing of infected macrophage populations (experiment 6). Incubation times for PMA activation over 2-24 hours showed no significant difference in activation levels of macrophages. PKC inhibitor was successful in inhibiting low to medium levels of PMA activation in the presence of peptide to show no significant levels of infected macrophage killing (experiment 7,8). However, high levels of PMA with low levels of PKC inhibitor still showed significant cytolytic activity of Pi-10. This suggests that there is a quenching of the PKC inhibitor by excess PMA and PKC production is not successfully repressed. Thus, cell membrane activation is still significant enough to induce cell lysis.

4.3. EXPERIMENTAL

4.3.1. Peptide Synthesis

Peptides were synthesized using standard Fmoc-amino acid fluoride coupling conditions. The first 3 or 4 residues were manually coupled onto PAL-PEG-PS solid support by gently stirring 8 equivalents of the Fmoc-acid fluoride, 3 equivalents of DIEA and resin in methylene chloride, until an acceptable yield was determined by quantitative Fmoc test. Sometimes gentle reflux was required to obtain successful

coupling. After the first residues were coupled to the resin, the remainder of the peptide was synthesized using a Milligen 9050 peptide synthesizer on the PAL-PEG-PS solid support using 8 equivalents of preformed Fmoc-amino acid fluorides, 3 equivalents of DIEA and a 1.5 h recycling time. Residues were double coupled when they are third in a series of C^{α},C^{α}-disubstituted amino acids and the coupling times were extended to 2.5 hrs. A solution of 20% piperidine / 2% 1,8-diazabicyclo[4.5.0]undec-7-ene (DBU) in DMF was used for Fmoc removal. The peptides were simultaneously cleaved from the resin and side-chain deprotected using reagent B (8.8 : 0.2 : 0.5 : 0.5, trifluoroacetic acid (TFA) : triisopropylsilane : water : phenol). The resulting solution was diluted with cold 30% acetic acid, washed with diethyl ether (4 x 50 mL), and lyophilized.

4.3.2. Peptide Purification

The crude peptides were purified by preparative reverse-phase HPLC on a Waters 15 μM Deltapak C_4 column using a water (0.05% TFA) and acetonitrile (0.05% TFA) gradient system. The gradient was run from 10% to 50% organic and the absorption monitored at 222 nm. Purity of the peptides was then checked on a Vydac 5 μM C_{18} column using the same conditions.

4.3.3. Peptide Analysis (MALDI-MS, AAA, CD)

Matrix assisted laser desorption ionization (MALDI) mass spectrometry was used to verify the peptide masses. Pi-10, 1037.1 $(M+H)^+$; Ipi-10, 1037.1 $(M+H)^+$; ACh-10α, 1157.6 $(M+H)^+$; ACh-10, 1157.6 $(M+H)^+$; Cyh-10, 1277.8 $(M+H)^+$; Ich-10, 1277.8 $(M+H)^+$.

Amino acid analyses were performed according to reference 2.21 using a Beckman 6300 Amino Acid Analyzer. In short, the peptides were hydrolyzed in 6N

HCl and 0.01% phenol for 24 h at 110°C. The samples were analyzed on a cation exchange column at 65°C with post-column ninhydrin derivitization at 130°C.

Circular dichroism measurements were taken on a (+)-camphor sulfonic acid calibrated Aviv 60DS spectrophotometer at 5°C. See chapter 3 for experimental details.

4.3.4. MIC Experiments

E. coli American type culture collection (ATCC) 25922 and *S. aureus* ATCC 25922 were used as representative Gram-positive and Gram-negative bacteria in minimum inhibitory concentration assays. The bacterial cultures were grown in nutrient broth to midlog phase and standardized using McFarland standard before dilution. A 512 μg/mL peptide stock solution was prepared and 1:2 serial dilutions were prepared and added to the culture media to give final peptide concentrations of 256 μg/mL.

50 μL of cells (5 X 10^4) and 50 μL of the peptide solution were added to a sterile well and the MIC was determined by the lowest concentration that inhibited cell growth. The inhibition of cell growth was indicated by the absence of turbidity after four hours. Turbidity in the wells was monitored visually. The MIC values are reported as the median value for at least three experiments.

4.3.5. Peptide Cytotoxicity Assays Against *Brucella abortus*

A suspension of 20 μL of a 1.4x10^9 of *Brucella abortus* 2308/GFP (green fluorescent protein) was added to 200 μl of media in individual wells. Each well contained media with 200 μM of a particular peptide. At 30 minutes post addition of bacterial cells, the wells were serially diluted and plated on blood agar. They were left to incubate for 72 hours and counted. The inoculation suspension was also serially diluted and plated to ascertain the precise number of bacteria added. A standard two-

sample T-test and confidence interval was run to compare the final counts with the inoculation suspension count, and no significant differences were noted.

4.3.6. Direct Peptide Toxicity Against Murine Peritoneal Macrophages

Briefly, harvested peritoneal macrophages were harvested from Balb/C mice, and $2x10^7$ cells were laid down in wells of a 96 well plate. Cells were allowed to adhere for 2 1/2 hours at 37 °C, 5.0% CO_2. Peptides were dilutes in warm 0.9 % Saline + Fetal Calf Serum (10 %) and added to the cells. Cells were allowed to incubate 1.5 hours and then stained for viability with Trypan Blue. The cells were then examined microscopically after viable staining with Trypan Blue for morphological changes and viability. Reported macrophage viability is determined by the total %-ratio of dead vs. healthy cells in three separate fields of three experimentally identical wells. The results are reported in the Table 4.5.

4.3.7. GFP-*Ba* Studies

Following euthanasia, cells were harvested by lavage from the peritoneal cavity of ten-week old BALB/c mice using 8 mL of DMEM (Dulbecco's Modified Eagle Medium) + 5% fetal calf serum (FCS). The cells were cultured in 96 well plates at a concentration of $1.5x10^5$ per well in 200 µL of DMEM + 5% FCS at 37°C in 5% CO_2. Cell cultures were enriched for macrophages by washing away non-adherent cells after overnight incubation with PBS + 5% FCS and 200 µL of fresh media was added to the cultures. Normal macrophage cultures were treated with 0 to 200 µM of the test peptide. The peptides were incubated with the cells for 1 hour at 37°C in 5% CO_2. The cells were washed 3 times with PBS + 5% FCS to remove any residual peptide. Peptide treated cells were stained with 0.04% trypan blue in DMEM + 5% FCS. One to two

hundred cells per well were counted using an inverted microscope and the number of stained cells was recorded. Three wells were examined per peptide concentration. Percent survival was calculated by subtracting the number of blue (dead) cells from the total cells and normalized. *B. abortus*-GFP opsonized with a sub-agglutinating dilution (1:2000) of hyperimmune BALB/c mouse sera in DMEM + 5% FCS was added to the macrophages at a ratio of approximately 100 bacteria per macrophage. Phagocytosis proceeded for 2 h at 37°C. Extracellular organisms were removed by washing 3 times with PBS + 5% FCS and fresh DMEM. Peptides were added to infected and non-infected cell cultures for 1 hour at 37°C, 5% CO_2. The cells were washed 3 times with PBS + 5% FCS to remove any residual peptide. Percent viability was determined as described above.

4.3.8. PMA Activation / PKC Inhibition of Macrophages.

Infected and non-infected macrophages in DMEM with 5% Fetal bovine serum (FBS) were treated with either 1.0 µM, 100 nM, or 50 nM concentrations of Phorbal 12-myristalate 13-acetate (PMA) at 1 hour prior to treatment with 5 uM Bisindoly maleimide 1 (PKC inhibitor). Separate groups of both infected and non-infected macrophages were treated with 5 µM PKC inhibitor 1 hour prior to treatment with the various concentrations of PMA. Following each treatment, the macrophages were incubated for 1 hour at 37 °C with 5.0 % CO_2. 100 uM Pi-10 was added to PMA, PMA/PKC inhibitor, or PKC inhibitor/PMA treated infected and non-infected macrophages and allowed to incubate at 37 °C with 5.0m% CO_2. Infected and uninfected macrophages that had not been exposed to PMA or PKC inhibitor were also treated with 100 µM **Pi-10** for comparison. Macrophages were then washed 3 times

with warm Phosphate buffered saline (PBS) with 5% FBS (PBS/FBS) after which warm PBS/FCS was added back and cells were examined microscopically. Trypan Blue exclusion was used to determine viability of cells (Table 4.7).

4.3.9. Pi-10 Peptide Treatment of PMA Activated Macrophages

100 uM Pi-10 was added to PMA, PMA/PKC inhibitor, or PKC inhibitor/PMA treated infected and non-infected macrophages and allowed to incubate at 37 °C with 5.0m% CO_2. Infected and uninfected macrophages which had not been exposed to PMA or PKC inhibitor were also treated with 100 μM **Pi-10** for comparison. Macrophages were then washed 3 times with warm Phosphate buffered saline (PBS) with 5% FBS (PBS/FBS) after which warm PBS/FCS was added back and cells were examined microscopically. Trypan Blue exclusion was used to determine viability of cells.

4.3.10. Biological Containment and Animal Use

All procedures involving live Brucellae and Mycobacteria were performed in a Biological Level 3 (BL-3) containment facility at the LSU-SVM following Centers for Disease Control/National Institutes of Health guidelines.[4.63] In conducting research using animals, the investigators adhered to the "Guide for the Care and Use of Laboratory Animals" prepared by the Committee on Care and Use of Laboratory Animals of the Institute of Laboratory Animal Resources, National Research Council.[4.64]

4.4. CONCLUSIONS

A series of novel linear amphipathic peptides with high levels of C^{α},C^{α}-disubstituted amino acids to promote helical conformations have been prepared. The biological activity of these peptides has been determined. Although no direct

bioactivity was observed towards *Brucella abortus*, MIC studies against representative Gram-positive and Gram-negative bacteria support the theory that increased hydrophobicity in peptide composition increases cytolytic activity. This hydrophobicity-dependent cytolytic character is also observed in mammalian non-infected peritoneal macrophages from BALB/c mice.

Studies of selective bioactivity *in vitro* against peritoneal macrophages infected with an intracellular pathogen, *Brucella abortus*-GFP, clearly show that the peptides show a selective cytolytic activity towards infected macrophages at concentrations that are non-lethal to healthy macrophages. *In vitro* activation of harvested macrophages with PMA induces peptide-promoted cell killing in a similar fashion to *Ba* infected macrophages. In contrast, PKC inhibition of PMA-induced cellular activation suppresses peptide activity completely. This suggests a cellular membrane-mediated response by infected macrophages towards the presence of a pathogen. This response may increase susceptibility of the infected cells towards peptide activity or promote peptide aggregation at the cellular membrane. Further studies to promote the understanding of cellular response towards intracellular pathogenic infections are required to fully understand the mechanism by which these peptides function. In addition, peptide activity at the cellular membrane and peptide affinity for infected versus non-infected macrophages must be determined.

4.5. REFERENCES

4.1 Araya, L.N., Elzer, P.H., Rowe, G.E., Enright, F.M., and Winter, A.J., *J. Immunol.*, **1989**, *143*, 3330-3337.

4.2 Corbel, M. J., Brinley-Morgan, W. J. *Genus Brucella*, in: *Bergey's Manual of Systematic Bacteriology, vol. 1*, N. R. Krieg, J. C. Holt, Editors. **1984**, Williams and Wilkins Co, Baltimore, MD, p. 377-388.

4.3 Young, E.J., *Clinical Manifestations of Human Brucellosis*, in *Brucellosis: Clinical and Laboratory Aspects*, E.J.C. Young, M. J., Editor. **1989**, CRC Press: Boca Raton, FL. p. 97-126.

4.4 Nicoletti, P., *Adv. Vet. Sci. Compar. Med.*, **1980**, *24*, 2469-2498.

4.5 Corbel, M. J. *Emerg. Infect. Dis.* **1997**, *3*, 213-221.

4.6 Sansom, M.S.P., *Prog. Biophys. Mol. Biol.*, **1991**, *55*, 139-236.

4.7 Reiner, N. E. *Immunol. Today* **1994**, *15*, 374-381.

4.8 Maurin, M., Raoult, D. Drugs **1996**, *52*, 45-53.

4.9 Bloom, B.R., *Tuberculosis: Pathogenesis, Protection and Control.* **1994**, Washington, DC: ASM Press.

4.10 Araya, L. N., Winter, A. J. *Infect. Immun.* **1990**, *58*, 254-256.

4.11 Dye, C., Williams, B. G. *Proc. Natl. Acad. Sci. U.S.A.*, **2000**, *97*, 8180-8185.

4.12 Murray, C. J. L., Salomon, J. A. *Proc. Natl. Acad. Sci. U.S.A.* **1998**, *95*, 13881-13886.

4.13 Mendez, P. A., Raviglione, M. C., Laszo, A., Binkin, N., Reider, H. L., Bustreo, F., Cohn, D. L., Lamgrats van Weezenbeek, C. S. B., Kim, S. J., Chaulet, P., Nunn, P. *N. Engl. J. Med* **1998**, *338*, 1641-1649.

4.14 Vemulapalli, R., He, Y., Cravero, S., Sriranganathan, N., Boyle, S. M., Schurig, G. G. *Infect. Immun.* **2000**, *68*, 3286-3289.

4.15 Smith, L. D., Ficht, T. A. *Crit. Rev. Microbiol.* **1990**, *17*, 209-230.

4.16 Roberston, G. T., Reisenauer, A., Wright, R., Jensen, R. B., Jensen, A., Shapiro, L., Roop II, R. M. *J. Bacteriol.* **2000**, *182*, 3482-3489.

4.17 Hultmark, D., Steiner, H., Rasmuson, T., Boman, H. G., *Eur. J. Biochem.* **1980**, *106*, 7-16.

4.18 Steiner, H., Hultmark, D., Engstrom, A., Bennich, H., Boman, H. G. *Nature*, **1981**, *292*, 246-248.

4.19 Boman, H. G., Faye, I., Gudmundsson, G. H., Lee, J. Y., Lidholm, D. A., *Eur. J. Biochem.* **1991**, *201*, 23-31.

4.20 Park, S., Shin, S., Kim, M., Park, D., Oh, H., Park, H. *Insect Biochem. Mol. Biol.* **1997**, *27*, 711-720.

4.21 Marchini, D., Giordani, P. C., Amons, R., Bernini, L. F., Dallai, R. *Insect Biochem. Mol. Biol.* **1993**, *23*, 591-598.

4.22 Rosetto, D., Giordano, P. C., Amons, R., Bernini, L. F., Dallai, R. *Eur. J. Biochem.* **1996**, *241*, 330-337.

4.23 Cole, A., Weis, P., Diamond, G. *J. Biol. Chem.*, **1997**, *272*, 12008-12013.

4.24 Oren, Z., Shai, Y., *Eur. J. Biochem.* **1996**, *237*, 303-310.

4.25 Shai, Y., Fox, J., Caratsch, C., Shih, Y., Edwards, C., Lazarovici, P. *FEBS Lett.* **1988**, *242*, 161-166.

4.26 Thompson, S., Tachibana, K., Nakanishi, K., Kubota, I. *Science*, **1986**, *233*, 341-343.

4.27 Bevins, C. L., Zasloff, M. *Ann. Rev. Biochem.* **1990**, *59*, 395-414.

4.28 Barra, D., Simmaco, M. *TIBTECH*, **1995**, *13*, 205-209.

4.29 Barra, D., Simmaco, M., Boman, H. *FEBS Lett.* **1998**, **430**, 130-134.

4.30 Simmaco, M., Mignogna, G., Barra, D., *Biopolymers* **1998**, *47*, 435-450.

4.31 Bals, R., Wang, X., Zasloff, M. Wilson, J. *Proc. Natl. Acd. Sci. U.S.A.* **1998**, *95*, 9541-9546.

4.32 Frohm, M., Agerberth, N., Ahangari, G., Stahle-Backdahl, M., Liden, J., Wigzell, H., Gudmundsson, G. *J. Biol. Chem.* **1997**, *272*, 15258-15263.

4.33 Andreu, D., Rivas, L. *Biopolymers, Pept. Sci.* **1998**, *47*, 415-433.

4.34 Tossi, A., Sandri, L., Giangspero, A. *Biopolymers, Pept. Sci.* **2000**, *55*, 4-30.

4.35 Hancock, R. E. W. *Expert. Opin. Inv. Drug.* **2000**, *9*, 1723-1729.

4.36 Samakovlis, C., Kylsten, P., Kimbrell, D. A., Engström, A., Hultmark, D. *EMBO J.* **1991**, *10*, 163-169.

4.37 Argiolas, A., Pisano, J. J. *J. Biol. Chem.* **1985**, *260*, 1437-1444.

4.38 Lee, I. H., Zhao, C., Cho, Y., Harwig, S. S., Copper, E. L., Lehrer, R. I. *FEBS Lett.* **1997**, *400*, 158-162.

4.39 Mor, A., Nguyen, V. H., Delfour, A., Migliore-Samour, D., Nicolas, P. *Biochemistry* **1991**, *30*, 8824-8830.

4.40 Zasloff, M., *Proc. Natl. Acad. Sci. U.S.A.* **1987**, *84*, 5449-5453.

4.41 Habermann, E. *Science* **1972**, *177*, 314-322.

4.42 Reddy, E. S. P., Bhargava, P. M. *Nature*, **1979**, *279*, 725-728.

4.43 Besalle, R., Kapitkovsky, A., Gorea, A., Shalit, I., Fridkin, M. *FEBS Lett.* **1990**, *274*, 151-155.

4.44 Juvvadi, P., Vunnum, S., Yoo, B., Merrifield, R. *J. Pept. Res.* **1999**, *53*, 244-251.

4.45 Merrifield, R., Juvvadi, P., Andreu, D., Ubach, J., Boman, A., Boman, H., *Proc. Natl. Acad. Sci. U.S.A.* **1995**, *92*, 3449-3453.

4.46 Merrifield, E., Mitchell, S., Ubach, J., Boman, H., Andreu, D., Merrifield, R. *Int. J. Pept. Protein Res.* **1995**, *46*, 214-220.

4.47 Wade, D., Boman, A., Wahlin, B., Drain, C., Andreu, D., Boman, H., Merrifield, R. *Proc. Natl. Acad. Sci. U.S.A.* **1990**, *87*, 4761-4765.

4.48 Gazit, E., Boman, A., Boman, H., Shai, Y. *Biochemistry*, **1995**, *34*, 11479-11488.

4.49 Pouny, Y., Rapaport, D., Mor, A., Nicolas, P., Shai, Y. *Biochemistry*, **1992**, *31*, 12416-12423.

4.50 Yokum, T. S., Elzer, P. H., McLaughlin, M. L. *J. Med. Chem.* **1996**, *39*, 3603-3605.

4.51 Saberwal, G. and Nagaraj, R., *Biochim. Biophys. Acta*, **1994**, *1197*, 109-131.

4.52 Prasad, B.V.V. and Balaram, P., *CRC Crit. Rev. Biochem.*, **1984**, *16*, 307-348.

4.53 Radzioch, D., Varesio L. *J Immunol.* **1980**, *140*, 1259-1263.

4.54 Bever, L. Q. *Ch. Immun. Pharm Immunotox* **1996**, *18*, 375-396.

4.55 Nishizuka Y. *Science*, **1992**, *258*, 607-614.

4.56 Newton, A.C. *J. Biol. Chem.* **1995**, *270*, 28495-28498.

4.57 Dekker LV, Parker PJ. *Trend. Biochem. Sci.* **1994**, *19*, 73-77.

4.58 Blumberg P.M., *Mol. Carcinogenesis*, **1991**, *4*, 339-344.

4.59 Toullec D. Pianetti P, Coste H, Bellevergue P, Grand-Perret T., Ajakane M, Baudet V., Boissin P, Boursier E, Loriolle F. Duhamel L, Charon D., Kirilovsky J. *J. Biol. Chem.* **1991**, *266*, 15771-15781.

4.60 Freer, E., Moreno, E., Moriyon, I., Pizzaro-Cerda, J., Weintraub, A., Gorvel, J. P. *J. Bacteriol.* **1996**, *178*, 5867-5875.

4.61 Martinez de Tejeda, G., Moriyon, I. *J. Bacteriol.* **1993**, *175*, 5273-5275.

4.62 Martinez de Tejeda, G., Pizzaro-Cerda, J., Moreno, E., Moriyon, I. *Infect. Immun.* **1995**, *63*, 3054-3061.

4.63 United States Department of Health and Human Services. *Biosafety in Microbiological and Biomedical Laboratories*. H.H.S. Publication No. (NIH) 86-23. **1993**, Washington, DC: U.S. Government Printing Office.

4.64 United States Department of Health and Human Services. *Guide for the Care and Use of Laboratory Animals*. H.H.S. Publication No. (NIH) 86-23. **1985**, Washington, DC: U.S. Government Printing Office.

CHAPTER 5
ANHYDROUS SYNTHESIS AND SPECTROSCOPIC CHARACTERISTICS OF *o*-NITROBENZENE SULFONYL-C^{α},C^{α}-DISUBSTITUTED AMINO ACID ADDUCTS

5.1 INTRODUCTION

Since the first pioneering publication by Merrifield in 1953,[5.1] solid-phase peptide synthesis (SPPS) has become the primary route by which to obtain many synthetic peptides,[5.2] and peptidomimetics.[5.3-7] The technique has since been adapted to a number of other biomolecules, such as nucleic acids[5.8,9] and oligosaccharides.[5.10] More recently, the use of solid-phase synthesis has been at the center of a chemical revolution with the development of combinatorial methods[5.11] and high throughput synthesis and screening, causing an enormous impact on several aspects of chemistry and molecular biology, especially drug-discovery. In the wake of the first solid-phase applications, several new techniques have been developed which further this exciting new aspect of synthetic chemistry. This chapter introduces new insights with which to enhance productivity and efficacy of a recently introduced coupling-protection scheme of solid phase peptide synthesis (SPPS). This scheme is intended to overcome problems associated with difficult couplings in synthetic peptides incorporating high levels of C^{α},C^{α}-disubstituted amino acids. The material covers the synthesis of *o*NBS-C^{α},C^{α}-disubstituted amino acid adducts and the UV spectroscopic characterization of the *o*NBS-cleavage product.

The process of solid phase synthesis of any compound or peptide is characterized by the covalent anchoring of a starting material, or first residue of an oligomeric material, to an insoluble polymer resin, or solid support. Common resins

include divinylbenzene cross-linked polystyrene (PS),[5.12] polyamides,[5.13] polyethylene glycol grafted covalently onto divinylbenzene cross linked polystyrene (PEG-PS),[5.14] and in some cases, natural polymers such as cellulose.[5.15] An efficient polymeric support for solid-phase synthesis must have the following characteristics:[5.16] 1) Physical stability and of the right dimensions to allow for manipulation and filtration from liquids. 2) Chemical inertness to all reagents involved in the synthesis and manipulation. 3) An ability to swell to an appreciative extent while under reaction conditions to allow permeation of solvents and reagents to the reactive sites within the resin. 4) Derivatization with functional groups to allow for the covalent attachment of an appropriate linker or first monomeric unit. In most cases, this linker unit must be cleavable under conditions which allows for the isolation of the desired product after synthesis is complete.

Solid supports for SPPS are functionalized with chemically active linkers, which are stable to the reaction conditions of the coupling process, but are labile under conditions which allow for isolation of the final product. Common linker-functionalized resins include chloromethyl polystyrene (Merrifield resin)[5.12], *p*-(carbamoylmethyl) benzyl ester (PAM resin)[5.17], 4-(2',4'-dimethoxyphenyl-aminomethyl)-phenoxymethyl) (Rink amide resin), tris(alkoxy)-benzylamide (PAL resin), 4-alkoxybenzyl alcohol (Wang resin) and 2-chlorotrityl resin.[5.15] Excess reagents and solvent can be removed by filtration from the insoluble support and subsequent reagents or residues are added in an iterative fashion. After the desired monomer units have been attached to the linker the product is chemically cleaved from the resin and isolated by filtration. Cleavage conditions are dictated by which linker is

used. The advantage of solid phase synthesis lies in the ease of separation of the product from excess reagents, which minimizes loss of material during intermediate product purification.

The key to successful solid phase synthesis lies in the protection scheme that is used to assure reaction only at the desired position(s). Any monomeric unit (X) that is utilized in solid-phase synthesis can be expressed with the empirical formula *n*-X-*e*, where *n* is the nucleophilic portion of the residue and *e* is the electrophilic portion. The first monomeric unit is coupled to the resin at either the nucleophilic or the electrophilic site. However, the portion of the molecule that is not covalently bound to the resin must be protected to avoid subsequent polymerization of excess monomers in solution. Thus, if the electrophilic portion of the first residue is coupled to the resin, the nucleophilic portion must be protected, and vice versa. The protecting group must be stable to the reaction conditions under which the couplings are executed. After coupling is performed, the protecting group is removed to expose a new reactive site and synthesis continues.

If several nucleophilic and/or electrophilic groups are present in a monomeric unit, they must be orthogonally protected with groups that vary in reactivity. This allows for deprotection of the portion of the molecule to which further reaction is desired to take place in subsequent couplings, while preventing reaction at side-chain functional groups. SPPS is almost exclusively performed in the C→N direction, with the amino group being the nucleophilic portion and the C-terminus the electrophilic portion (Figure 5.1). Common protecting groups and the conditions under which they are cleaved are listed in Table 5.1.

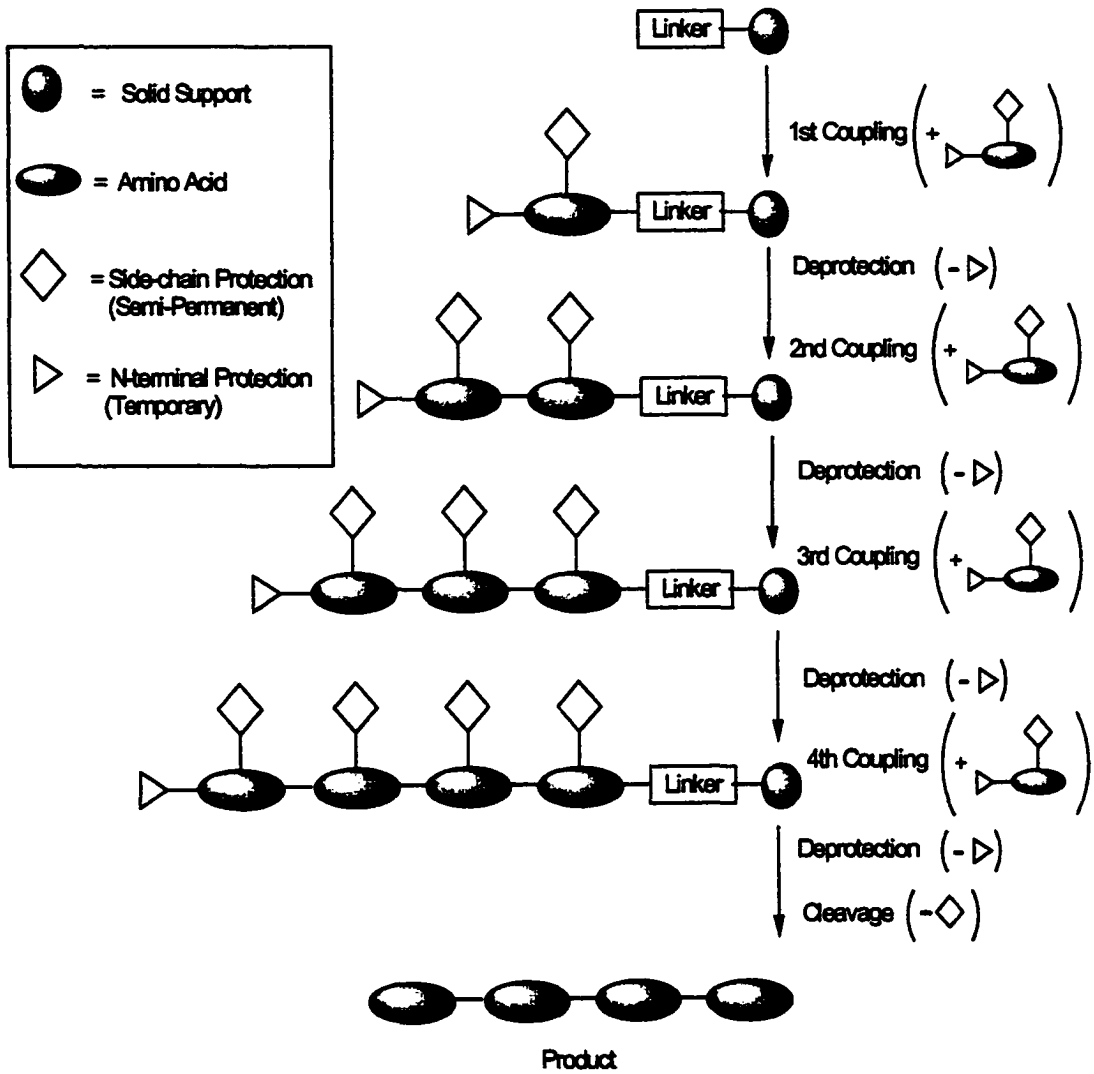

Figure 5.1. General scheme for solid-phase peptide synthesis.[5.2]

Table 5.1. Common linkers used in SPPS.

Protecting Group	Structure	Cleavage Method	Reference
N^{α}-Protecting Groups			
Fluorenylmethoxy-carbonyl (Fmoc)	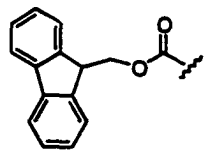	Base-catalyzed (20% Piperidine in DMF)	5.19
Allyloxycarbonyl (Alloc)	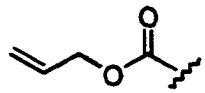	Hydrogenolysis (Pd/C; ethanol)	5.20
2-(4-nitrophenylsulfonyl) ethoxycarbonyl (Nsc)	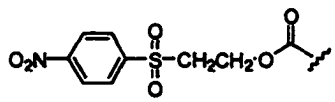	Base catalyzed (20% piperidine in DMF	5.21
Benzothiazole-2-sulfonyl (Bts)	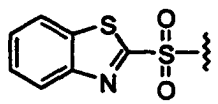	Zn-Acetic Acid Al-Hg/THF/H_2O $Na_2S_2O_4$	5.22
5-Methyl-1,3,4-thiadiazole-2-sulfonyl (Ths)	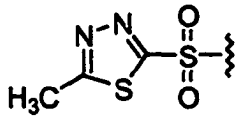	Zn-Acetic Acid Al-Hg/THF/H_2O	5.22
Side-Chain Protecting Groups			
Benzyloxycarbonyl (Z)	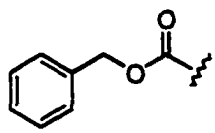	Catalytic Hydrogenation Acidolysis	5.18
t-Butyl	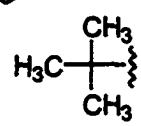	Acidolysis (TFA)	5.24,25
Dimethoxytrityl (Dmt)	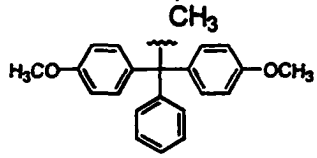	Acidolysis (Weak Acid)	5.26
t-Butyloxycarbonyl (Boc)	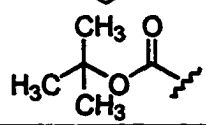	Acidolysis (TFA/DCM)	5.1,27

One of the difficulties associated with solid-phase peptide chemistry is prevention of reaction on functionalized side chains of amino acids such as lysine, glutamic acid and cysteine. In order to prevent these reactions from taking place, side-chain protecting groups must be applied. These groups must be stable to the coupling conditions, stable under conditions that cleave the active terminus for continued growth, but labile under conditions which cleave the product from the resin, allowing for isolation of the fully deprotected product. Thus, the *N*-terminal and side-chain protecting groups must be orthogonal to each other in a solid-phase coupling scheme. Several coupling schemes have been developed which match linker, *N*-terminal protection and side-chain protection in an orthogonal manner. Some of the most commonly used include the Boc-benzyl strategy[5.1,28] (Figure 5.2), the Fmoc-Boc strategy[5.19,29] (Figure 5.3).

One aspect of solid phase synthesis that has seen tremendous development is in the field of coupling reagents. Traditionally, peptide coupling under solid phase conditions can be realized in two ways: 1) A reactive electrophilic derivative of the amino acid , such as an acid halide[5.30-36] or an N-carboxyanhydride (NCA)[5.37] can be synthesized, isolated and then allowed to react with the nucleophilic portion of the resin-bound residue. These active species are easy to synthesize and relatively stable, allowing for characterization. In addition, the simplicity of by-products released from such couplings, such as a carbon dioxide, chloride or fluoride ion, allow for simple purification after coupling has occurred. Alternately, a coupling reagent may be added to the reaction mixture, to generate a reactive electrophilic derivative *in situ*. These coupling reagents include carbodiimides[5.38-40] such as DCC, DEC, and DIPCDI, triazole

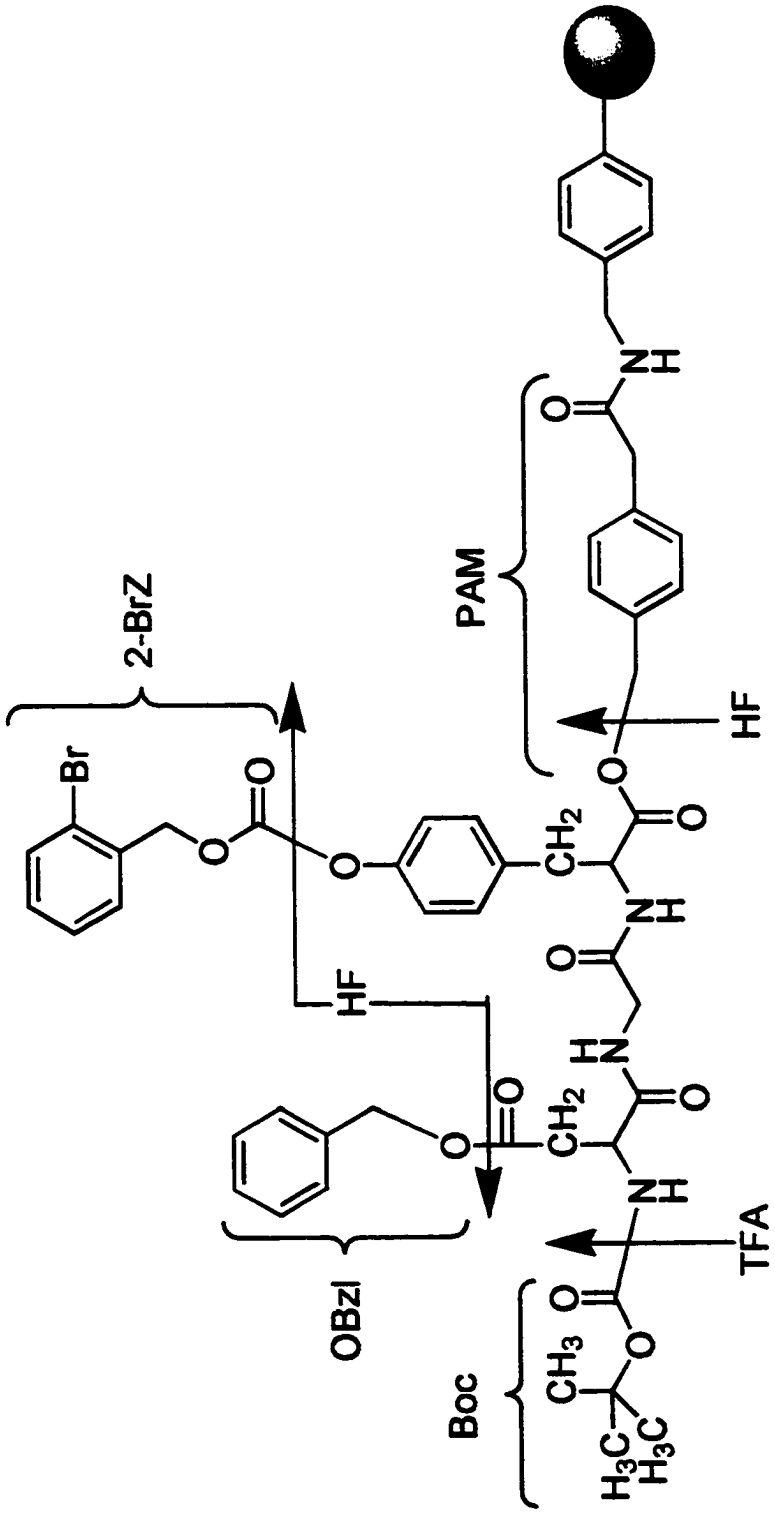

Figure 5.2. The Benzyl-/Boc-SPPS protecting group strategy.[5.2]

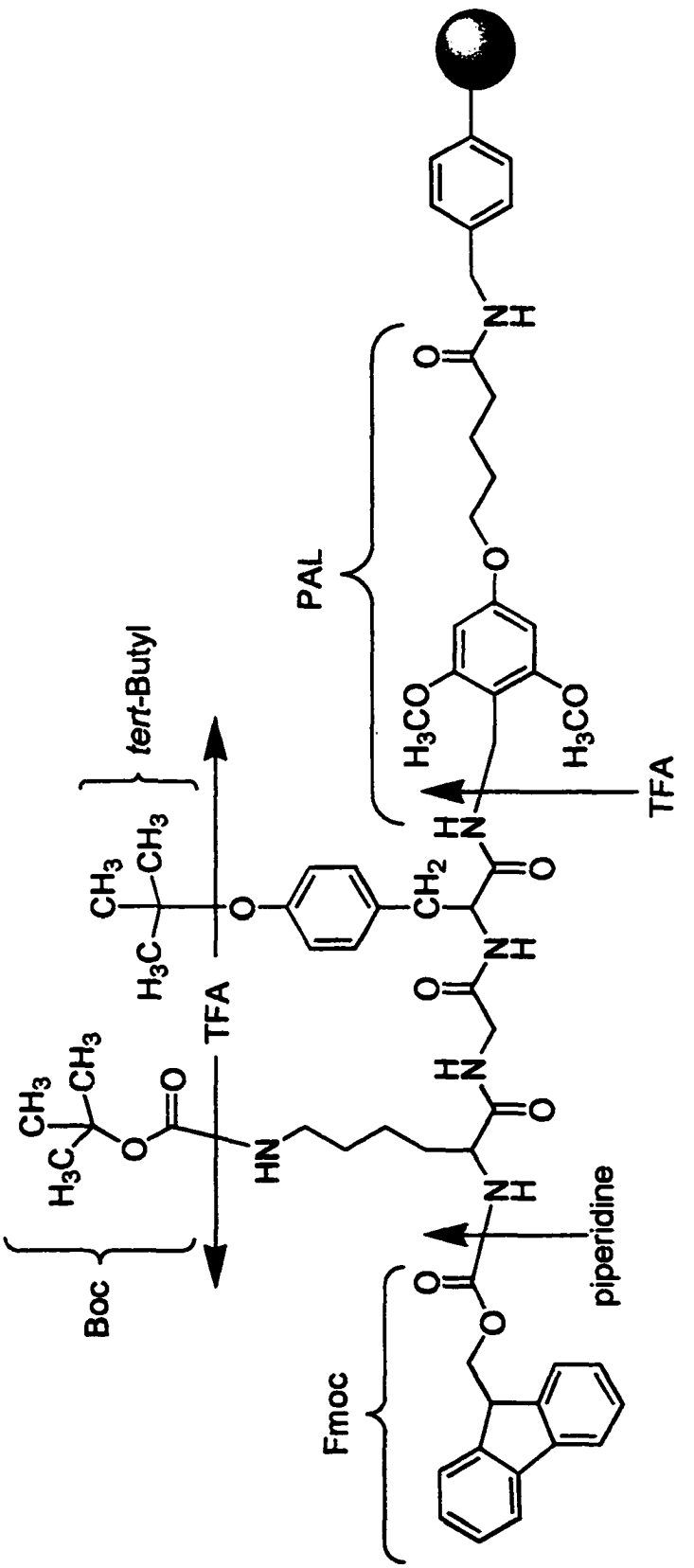

Figure 5.3. The Fmoc-/Boc-SPPS protecting group strategy.[5.2]

Table 5.2. Common coupling reagents used in SPPS.

Coupling Reagent	Structure	Reference
DCC *N,N'*-Dicyclohexyl-carbodiimide	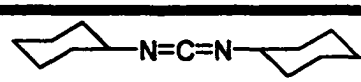	5.38-40
DEC *N,N'*-Diethyl-carbodiimide	$H_3CH_2C-N=C=N-CH_2CH_3$	5.38-40
DIPCDI *N,N'*-Diisopropyl-carbodiimide	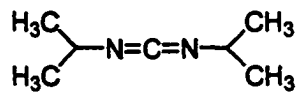	5.38-40
HOBt 1-Hydroxybenzotriazole	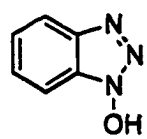	5.41
HOAt 7-Aza-1-hydroxybenzo-triazole	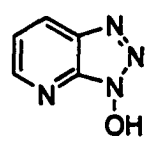	5.42-44
HBTU *N*-[(1-*H*-Benzotriazol-1-yl)-(dimethylamino)methylene]-*N*-methylmethanaminium hexafluorophosphate N-oxide	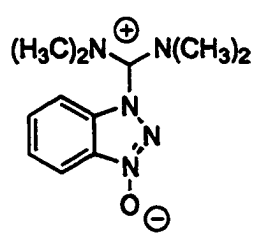	5.45
HATU *N*-[(1-*H*-7-Azabenzotriazol-1-yl)-(dimethylamino)-methylene]-*N*-methylmethanaminium hexafluorophosphate	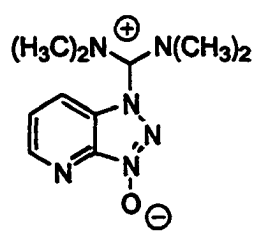	5.43,46

derivatives, such as HOBt[5.41] and HOAt[5.42-44] and tertiary ammonium salts of triazole N-oxides, such as HBTU[5.45] and HATU[5.43,46] (Table 5.2), in addition to several others.[5.39] The advantage of these types of coupling is the relative ease of handling of non-activated species which are introduced into the reaction along with the coupling reagent. In addition, *in situ* activation allows for the preparation of highly activated species that are often not isolable.

C^{α},C^{α}-Disubstituted amino acids, such as Aib (2-aminoisobutyric acid), Ac_6c (1-amino-1-cyclohexylcarboxylic acid), and Api (4-aminopiperidine-4-carboxylic acid) (Figure 5.4), are becoming recognized tools for the selective control of peptide secondary structure[5.47-51] and for accentuating physiological properties of resulting peptides (refer to chapters 2,3 and 4). Recently, these derivatives have been shown to generate highly helical segments with peptides as short as 10 residues in length.[5.52] In particular, close proximity of these residues cause dramatic increases in the helical propensity of resulting peptides, and stabilization of the peptides towards enzymatic degradation under physiological conditions.[5.53] C^{α},C^{α}-Disubstituted amino acids ($\alpha\alpha$AAs) are of current interest in the development of novel amphipathic peptides with high levels of helicity for study as *in vivo* selective weapons against macrophages infected with intracellular pathogens (See Chapter 4).[5.53]

As with *N*-alkylated amino acids, C^{α},C^{α}-disubstituted amino acids offer a significant challenge in their ability to couple under solid phase peptide synthesis conditions. Their inherent difficulty in coupling stems primarily from the steric repulsion that arises between the residue which is being coupled and the residue which is already on the resin.

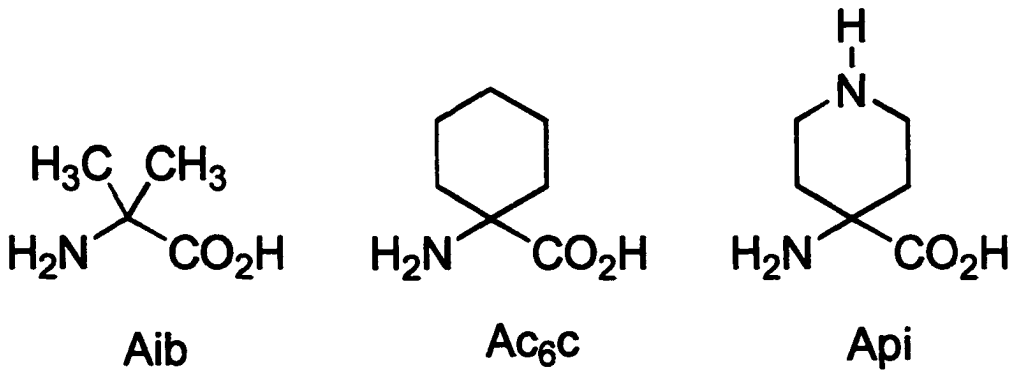

Figure 5.4. Examples of C^{α},C^{α}-disubstituted amino acids: 2-aminoisobutyric acid (Aib), 1-amino-1-cyclohexanecarboxylic acid (Ac_6c), and 4-amino-4-piperidine-carboxylic acid (Api).

A number of methods for the solid phase coupling of C^{α},C^{α}-disubstituted amino acids have been presented over the years, the most efficient and cost effective being the Fmoc-protected amino acid fluorides, developed during the early 1990s by Carpino and coworkers.[5,31,33,34] For the purposes of proteinogenic amino acids and some less hindered C^{α},C^{α}-disubstituted amino acids, this technique provides a fast, cheap and efficient method towards peptide synthesis. However, we have found that on-resin couplings involving multiple C^{α},C^{α}-disubstituted amino acids, in high proximity, result in low yields and require reaction times on the order of several days. These difficulties are particularly accentuated with the continuous coupling of several residues of very bulky amino acids, such as Ac_6c and Api. These couplings require large molar excesses of amino acid and high temperature conditions to achieve acceptable coupling yields. Thus, difficult couplings of this nature become very time-consuming and expensive, consuming large quantities of excess reagent and solvents.

In an attempt to develop a new, faster method for couplings of these difficult amino acids, our attention has turned to the higher reactivity of amino acid chlorides, which have been shown to have very high reaction rates in solution phase couplings.[5.30,32,35] In addition to being of higher reactivity, amino acid chlorides are considerably less expensive to synthesize in comparison to their corresponding acid fluorides and can be prepared by a number of simple reagents such as thionyl chloride, oxalyl chloride and phosphorous trichloride. Recently, Falb and coworkers described the effective *in situ* generation of proteinogenic Fmoc amino acid chlorides using bis(trichloromethyl)-carbonate.[5.30] However, pre-formed C^{α},C^{α}-disubstituted amino acid chlorides generally do not perform as well in solid phase peptide synthesis. Oxazalone formation, by intramolecular cyclization of the acid chloride functionality with N-urethanyl-type moieties like the Fmoc protecting group (Figure 5.5), compete with coupling.[5.32]

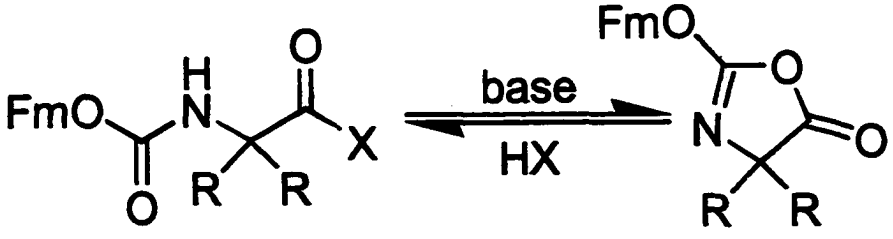

Figure 5.5. Base promoted oxazalone formation of N^{α}-fluorenylmethoxycarbonylated C^{α},C^{α}-disubstituted amino acid halides.

$C^{\alpha}C^{\alpha}$-Disubstituted amino acid fluorides have been found to react faster than corresponding amino acid chlorides under solid phase conditions due to their lower rate of oxazalone formation.[5.35] To take advantage of the increased reactivity of the amino acid chlorides, we face the task of incorporating a different protecting group incapable of intramolecular cyclization. The protecting group must have chemical properties that allow it to be orthogonal to the Boc side-chain protection scheme used in Api and lysine residues. In addition, it must have a quantifiable cleavage chromophore, which allows for the monitoring of coupling rates and yields by resin tests. The fluorenyl-piperidine adduct produced as a result of base promoted Fmoc deprotection has a characteristic UV absorbance at 300 nm and a molar absorbtivity (ε_{300}) of 7800 $M^{-1}cm^{-1}$, which allows for quantitative monitoring of the couplings by sample resin testing. Other SPPS monitoring procedures include on-resin ninhydrin testing,[5.54] and on-resin infra-red spectroscopy.[5.55-58] Because of the difficult, and highly varied, coupling conditions associated with C^{α},C^{α}-disubstituted amino acids, couplings can take anywhere from a few minutes to several days. It is thus imperative that a coupling strategy includes facile, quantitative monitoring of coupling efficiency.

Arylsulfonyl-groups were introduced as protecting groups for solution phase peptide synthesis as early as the 1950s.[5.59] Specific use of the *o*- and *p*-nitrobenzenesulfonyl (*o*NBS) derivatives was first described by Fukuyama in 1994 for the purposes of *N*-alkylation.[5.60,61] The *p*-nitrobenzenesulfonyl group has also been described by Sabirov and coworkers as a suitable side chain protecting group for the indole moiety of tryptophan.[5.62] However, Miller first incorporated this group into solid phase synthesis context, *albeit* for use in site specific *N*-alkylation.[5.63,64] Recently, Reichwein and Liskamp reported successful *N*-alkylation of amino acid esters or resin

bound amino acids, in which the Fmoc protecting group had been removed and replaced by the *o*NBS group while on resin.[5.65] In addition to being orthogonal to both acid and base labile groups, *o*NBS-groups introduce high levels of crystallinity to the amino acid residues. This has allowed for easy isolation and purification of synthesized adducts, as well as crystallographic description.[5.66] Other arylsulfonyl protecting groups include the benzothiazole-2-sulfonyl group (Bts) and the 5-methyl-1,3,4-thiadiazole-2-sulfonyl group (Ths).[5.22]

The sulfonyl oxygens of the *o*NBS group are less nucleophilic than the carbonyl group of a urethanyl type protecting group, such as Fmoc, Alloc or Boc. Thus, intramolecular cyclization is not of concern in the preparation and application of *o*NBS-amino acid chlorides or other activated ester functional groups, such as those of HATU and/or DIC. This phenomenon may in turn result in lower racemization of *o*NBS protected proteinogenic amino acids, since oxazalone formation is the key intermediate in facilitating this side reaction. The protecting group differs from the recently introduced and very popular 2-(4-nitrophenylsulfonyl)ethoxycarbonyl (Nsc) in that cleavage is performed by an *ipso*-nucleophilic aromatic substitution. The Nsc group is cleaved by base-catalyzed elimination.[5.67] This, and the fact that the N^{α}-Nsc connection is achieved through a urethanyl bond, capable of oxazalone formation, make the Nsc group chemically related to the Fmoc group. Other arylsulfonyl protecting groups, such as Bts and Ths are generally removed by Zn-acetic acid hydrolysis. Thus, they are generally considered to be chemically unrelated to the *o*NBS group. The *o*NBS group is stable to acidic and basic conditions (when N-alkylated). Thus, a feasible solid-phase protection scheme, with *o*NBS orthogonal to Boc and Z groups, can be visualized (Figure 5.6).

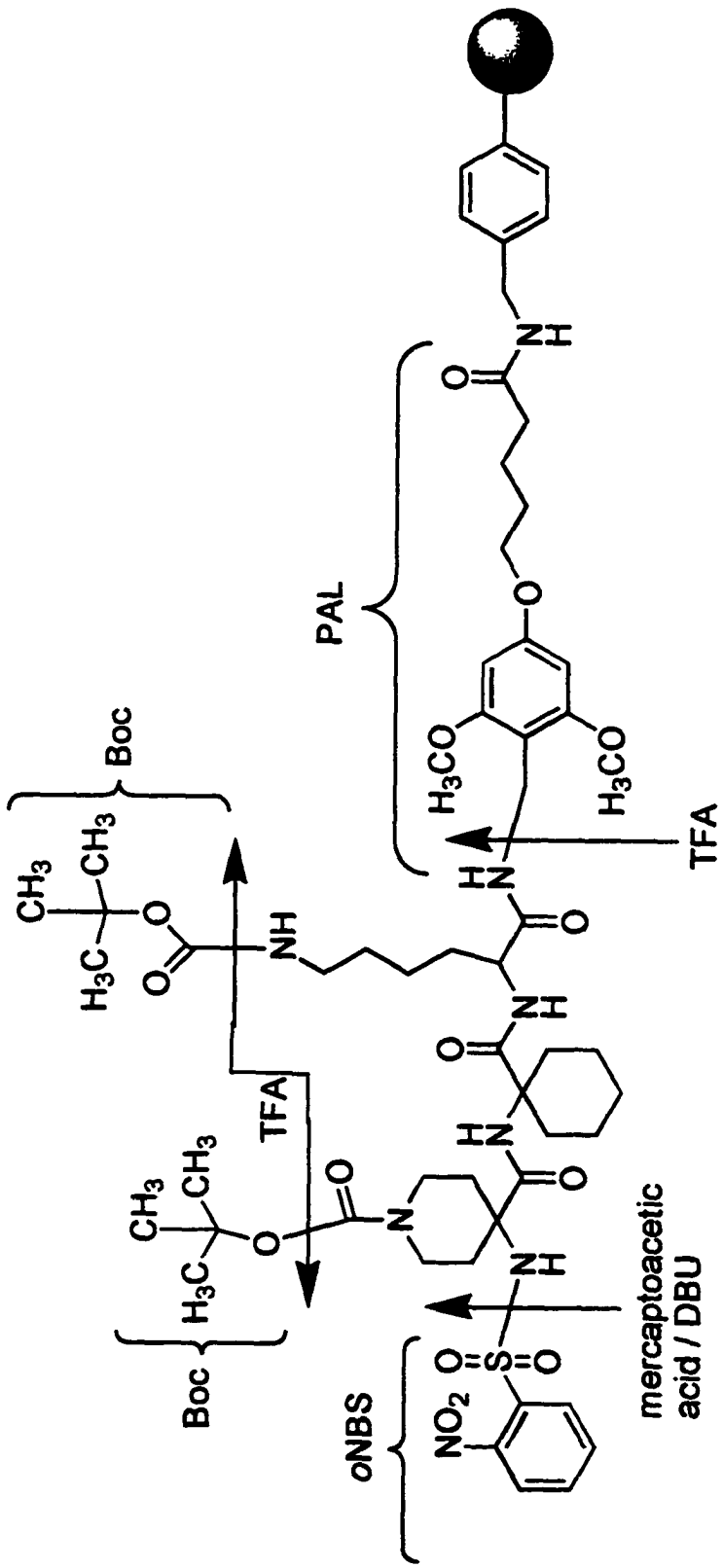

Figure 5.6. Solid-phase protection scheme for oNBS-protected C^{α},C^{α}-disubstituted and proteinogenic amino acids on PAL-PEG-PS resin.

This chapter discusses the development of a spectroscopic standard by which the *o*NBS group can be monitored during solid-phase synthesis. Anhydrous synthesis conditions of *o*NBS-amino acid adducts are described, as well as the UV activity of the *o*NBS-cleavage adduct. This information will help develop the use of the *o*NBS group as a successful N^{α}-protecting group for difficult couplings under solid-phase peptide conditions.

5.2 RESULTS AND DISCUSSION

Standard conditions to generate *o*NBS adducts of proteinogenic amino acids under aqueous conditions were reported by Milne and Peng in 1957.[5.59] This process involves dissolving the free amino acids in aqueous base, such as sodium hydroxide, followed by treatment with the corresponding arylsulfonyl chlorides. However, this method is ineffective in generating *o*NBS-C^{α},C^{α}-disubstituted amino acid adducts due to the low solubility of these compounds under aqueous conditions. This is especially true in the case of the very hydrophobic residue Ac_6c. A similar difficulty is faced when attempting to introduce the Fmoc-group to C^{α},C^{α}-disubstituted amino acids via an aqueous approach using Fmoc-succinimide. This problem is overcome by the use of a non-aqueous procedure using Fmoc-Cl. This procedure seemed logical to extend towards the generation of *o*NBS-adducts as well. Thus, we present an effective way to generate *o*NBS adducts of C^{α},C^{α}-disubstituted amino acids under anhydrous conditions based on the procedure set forth by Bolin.[5.58] This technique has also been extended to proteinogenic amino acids, such as lysine(Z). Theoretically, it could be extended to a variety of amino acids. In the procedure, chlorotrimethylsilane is used to facilitate solubilization of the diisopropyl-ethylammonium salts of the C^{α},C^{α}-disubstituted amino

acids in DCM. This is followed by the slow addition of 2-nitrobenzenesulfonyl chloride. The silylated amino acids react very quickly and efficiently. Using this procedure, the amino acids are successfully protected in high yield and without need for further purification after crystallization (Figure 5.7). The high crystallinity of the *o*NBS adducts allows for easy purification and analysis.

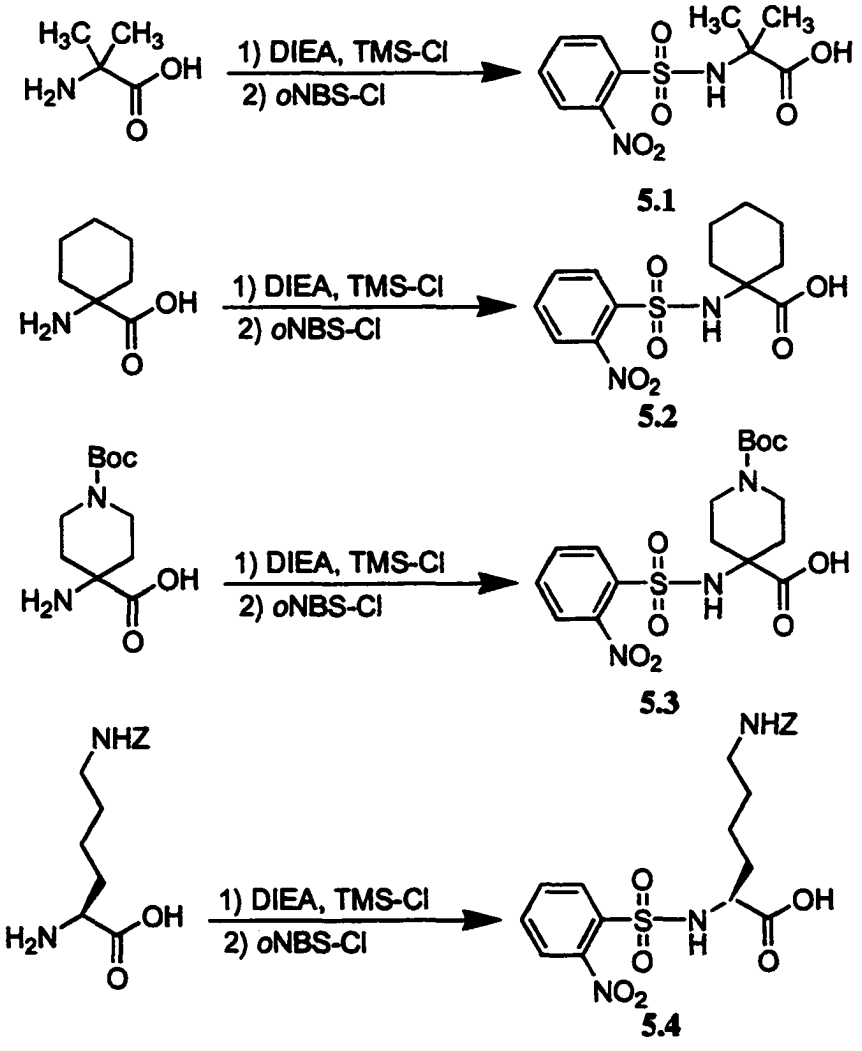

Figure 5.7. Synthesis of *o*NBS adducts of Aib, Ac_5c, Api(Boc) and Lys(Z) to yield *o*NBS-amino acid adducts **5.1**, **5.2**, **5.3** and **5.4**.

Several reagents have been proposed as suitable cleavage agents for the removal of the *o*NBS-group, such as mercaptoethanol / potassium *tert*-butyloxide, thiophenol / potassium carbonate and *n*-propylamine in DCM. Cleavage of the *o*NBS group by all of these methods is reported as an ipso-attack of the mercaptoacetic acid sulfide followed by sulfur dioxide elimination and subsequent deprotection through a nucleophilic aromatic substitution mechanism (Figure 5.8).[5.60,61] Cleavage with mercaptoacetic acid offers the advantage of using a relatively non-noxious reagent, and the cleavage adduct which is generated (**8**) by this reagent has spectroscopic advantages which allow for *in situ* monitoring of the progress of the reaction. The cleavage product, 2-nitrophenylcarboxymethylthioether (**5.5**), can be readily synthesized by nucleophilic aromatic substitution using the DBU salt of mercaptoacetic acid with o-chloronitrobenzene (Figure 5.9).

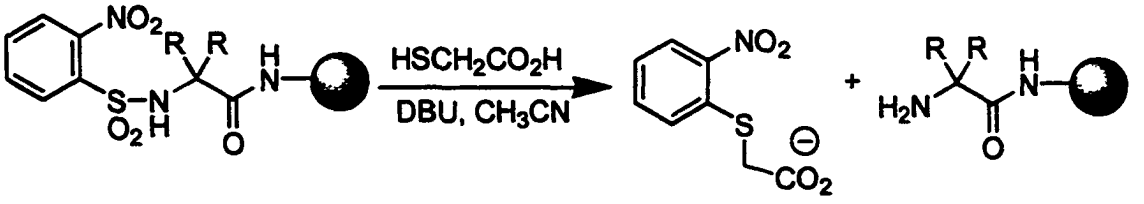

5.5

Figure 5.8. On-resin nucleophilic displacement of the *o*NBS-group by the mercaptoacetic acid anion yielding the 2-(2-nitrothiophenyl)acetate anion (**5.5**) as a cleavage product.

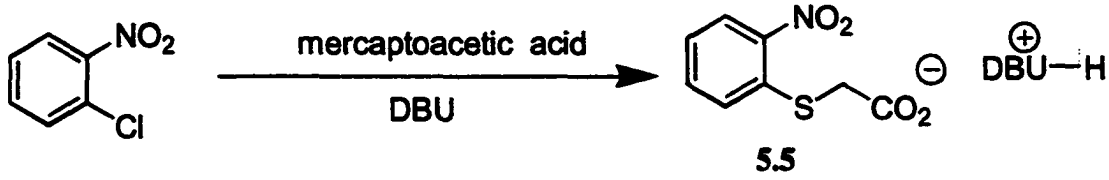

5.5

Figure 5.9. Nucleophilic aromatic substitution of *o*-nitrochlorobenzene by the mercaptoacetic acid anion to yield the cleavage adduct **5.5**.

One of the key advantages of traditional Fmoc procedures in solid phase peptide synthesis is the ability to actively monitor coupling rates and efficiency by spectrometric analysis. The piperidine-fulvene adduct which result from the deprotection of Fmoc groups can be analyzed by removing a small portion of resin from the reaction and cleaving the Fmoc-groups which are covalently linked to the solid support. This cleavage adduct has a molar absorptivity of 7800 $M^{-1}cm^{-1}$ at 300 nm in DMF/MeOH which can be quantitated on a very small scale (4-8mg resin; ~20μM) by UV-spectroscopy. By comparing the level of Fmoc-protected termini on the resin with the established substitution level of the resin used, one can determine the degree of coupling. Applying *o*NBS-amino acid chlorides as successful activated reagents in SPPS requires the adaptation of such a procedure for the quantitative analysis of coupling efficiency.

Repetitive scans from 700-200 nm of the deprotection adduct **5.5** at various concentrations shows a consistent absorption maximum at 390 nm (Figure 5.10). Thus, the cleavage product of *o*NBS-protected amino acids allows the couplings to be easily quantitated by spectrometric determination. To determine the exact spectroscopic nature of **5.5**, a series of dilution studies under reaction conditions were performed to

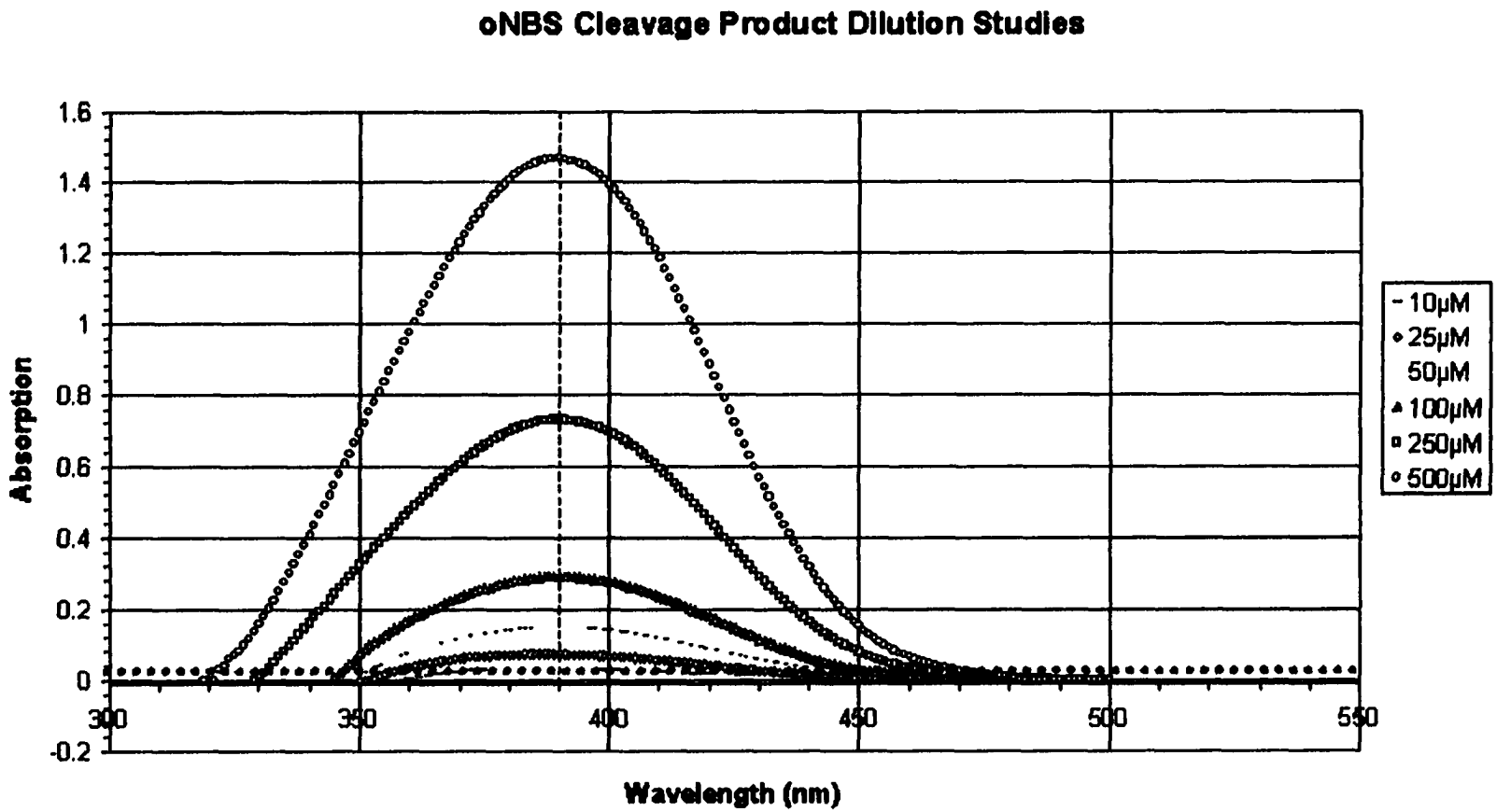

Figure 5.10. Scanning UV-Vis Spectrometry of **5.5** under reaction conditions showing consistent λ_{max} at 390 nm at various concentrations.

show a linear correlation between concentration and λ_{max} at 390nm in acetonitrile (Table 5.3). For absorbances under 2.0, Beer's Law correlation results in a molar absorptivity (ε) of 2950 $M^{-1}cm^{-1}$. At high concentrations, deviations from Beer's Law are discarded. In-solution cleavage of the *o*NBS-amino acid adducts with 0.4M mercaptoacetic acid and 0.8M DBU in acetonitrile for 20 minutes yields quantitative detection of the cleavage product, with a maximum absorbance at 390nm. According to Beer's Law, the molar absorptivity of **8** can be determined by plotting the data in Table 5.3 and extrapolating the slope for absorbance values under 2.0 as shown in Figure 5.11.

Table 5.3. Summary of dilution studies done on cleavage adduct **5.5.** [a]Absorptivities above 2.0 are discarded in averaging ε_{390} due to Beer's Law deviations at high concentrations.

Concentration (μM)	λ_{max}	A_{max} (corrected)	ε_{390}
10.0	391	0.030	3021
25.0	390	0.074	2942
50.0	390	0.149	2978
100.0	390	0.291	2949
250.0	391	0.729	2947
500.0	390	1.457	2934
1000.0	390	2.427	2425[a]
Average	390	-	2950

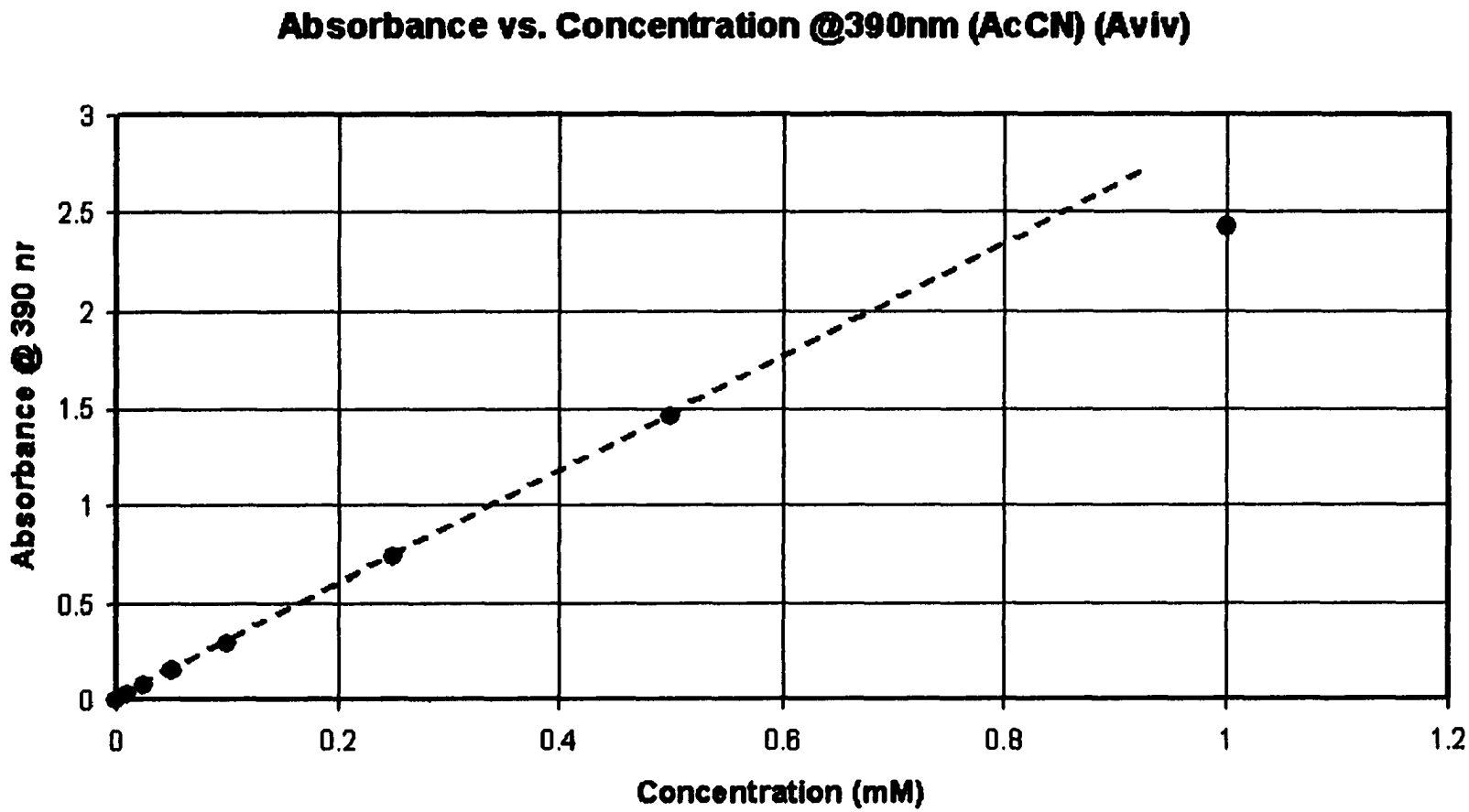

Figure 5.11. Graph showing the linear correlation of absorption versus concentration of the *o*NBS cleavage product **5.5** in 5:1 acetonitrile/water. (Slope= ε_{390} =2950). Deviation from Beer's Law linear correlation is clearly visible above A=2.0.

Thus, the progress of a potential coupling of *o*NBS-amino acid adducts on the solid phase can be monitored by a process similar to that of the Fmoc-piperidine assay. The sampled resin (5-10 mg) would be treated with 1.0mL deprotection solution for 30 minutes, washed with 6 x 1.0 mL acetonitrile and the washes combined. The cleavage sample would be analyzed for absorbance at 390 nm and percent substitution would be determined by:

$$\%\text{Substitution}=[(A_{390}x10^{6}x0.007)/(\varepsilon_{390}xW)]/L$$

, where A_{390} is the corrected absorbance at 390 nm, ε_{390} is the molar absorbtivity at 390 nm for the cleavage adduct ($2950M^{-1}cm^{-1}$), **W** is the mg of resin tested and **L** is the substitution level of the resin used (mmol/g).

To test the ability of the deprotection reagent to effectively cleave the *o*NBS group in a consistent and quantitative way, cleavage studies were performed with four *o*NBS-amino acid adducts: *o*NBS-Aib-OH **5.1**, *o*NBS-Ac_6c-OH **5.2**, *o*NBS-Api(Boc)-OH **5.3** and *o*NBS-Lys(Z)-OH **5.4**. The pure adducts are weighed out in various amounts and treated with 1.00 mL deprotection solution for 30 minutes. The resulting solutions are then diluted with 5 x 1.00 mL acetonitrile and the resulting solution tested by UV-spectroscopy at 390 nm for observed absorbance. In all cases, deprotection is efficient, quantitative, and correlates well with the theoretical predictions based on the derived molar absorbtivity of the cleavage product (Table 5.4).

Table 5.4. In-solution cleavage study of four *o*NBS-amino acid adducts.

Substrate	MW	mg	M	$A_{theo.}$	$A_{obs.}$	A_f/A_o(%)
***o*NBS-Aib-OH**	288.23	1.20	5.95e-4	1.75	1.75	100%
***o*NBS-Api(Boc)-OH**	429.42	1.71	5.55e-4	1.56	1.50	95%
***o*NBS-Ac$_6$c-OH**	328.32	1.40	6.09e-4	1.79	1.76	97.5%
***o*NBS-Lys(Z)-OH**	455.45	1.40	4.29e-4	1.29	1.32	102%

Coupling of the synthesized *o*NBS-amino acids onto PAL-PEG-PS was initially performed by the use of PyAOP/HOAt in DMF over several hours without success. The acid fluorides of the oNBS-adducts were then generated and allowed to couple in DCM / 2,4,6-collidine for 24 hours. The use of excess base in the coupling reactions of *o*NBS-protected amino acids was found to be detrimental to the reaction due to decomposition of *o*NBS protected primary amines, which was evident by the development of SO_2 gas from the resin under these conditions. This occurs by catalytic deprotonation of the sulfonamide and an intramolecular rearrangement to eliminate SO_2 via decomposition of the intermediate Mesenheimer Complex (Figure 5.12). The decomposition takes place even in the presence of excess weak, hindered bases such as 2,4,6-collidine. Although the decomposition should not directly compete with the mechanism of coupling, the resulting *o*-nitrophenylated amine, **5.6**, can not be deprotected and thus caps the peptide from further growth, in addition to preventing spectrometric analysis of coupling yield to be determined. Due to this composition, it is impossible to determine exact coupling yield. In addition, one cannot be sure as to the efficiency of the deprotection step versus the coupling efficiency.

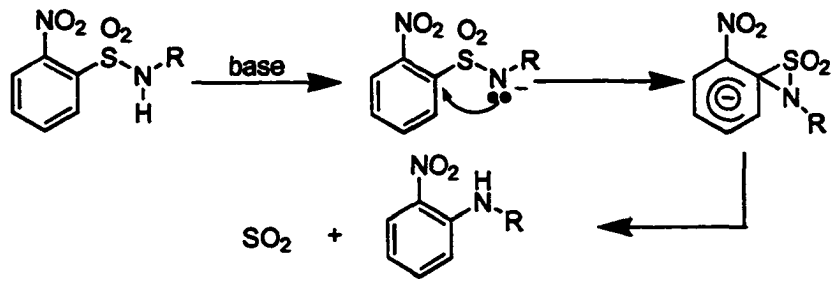

5.6

Figure 5.12. Base catalyzed rearrangement of the *o*NBS-protected N-terminus of an amino acid by sulfonamide proton extraction and subsequent intramolecular sulfur dioxide elimination, to yield N-arylated amino acid **5.6**.[5.60,61]

A number of methods were investigated for the chlorination of the *o*NBS-protected amino acids. For the chlorination of **5.1** it was found that oxalyl chloride is superior to all other chlorinating agents studied (phosgene, thionyl chloride, Bis-(trichloromethyl) carbonate (BTC)). The reaction of the free acid of *o*NBS-protected amino acids with BTC results in almost quantitative yield of the corresponding *N*-carboxyanhydride (NCA) derivative, **5.7**, by intramolecular cyclization. Cyclization results from one of two routes involving either cyclization of the initial mixed anhydride of BTC (Scheme 1; Figure 5.13), or induced nucleophilic attack of the sulfonamide on BTC followed by secondary cyclization by the free carboxylate (Scheme 2; Figure 5.13). The resulting NCA derivative, **5.7**, was verified by NMR and X-ray crystallography. Crystals were isolated in 75% yield from the corresponding *o*NBS-protected amino acid. (Figure 5.14) NCAs have been used extensively as coupling agents and have the advantages of being highly crystalline and very stable in dry conditions for extended periods of time. In addition, the coupling side product is

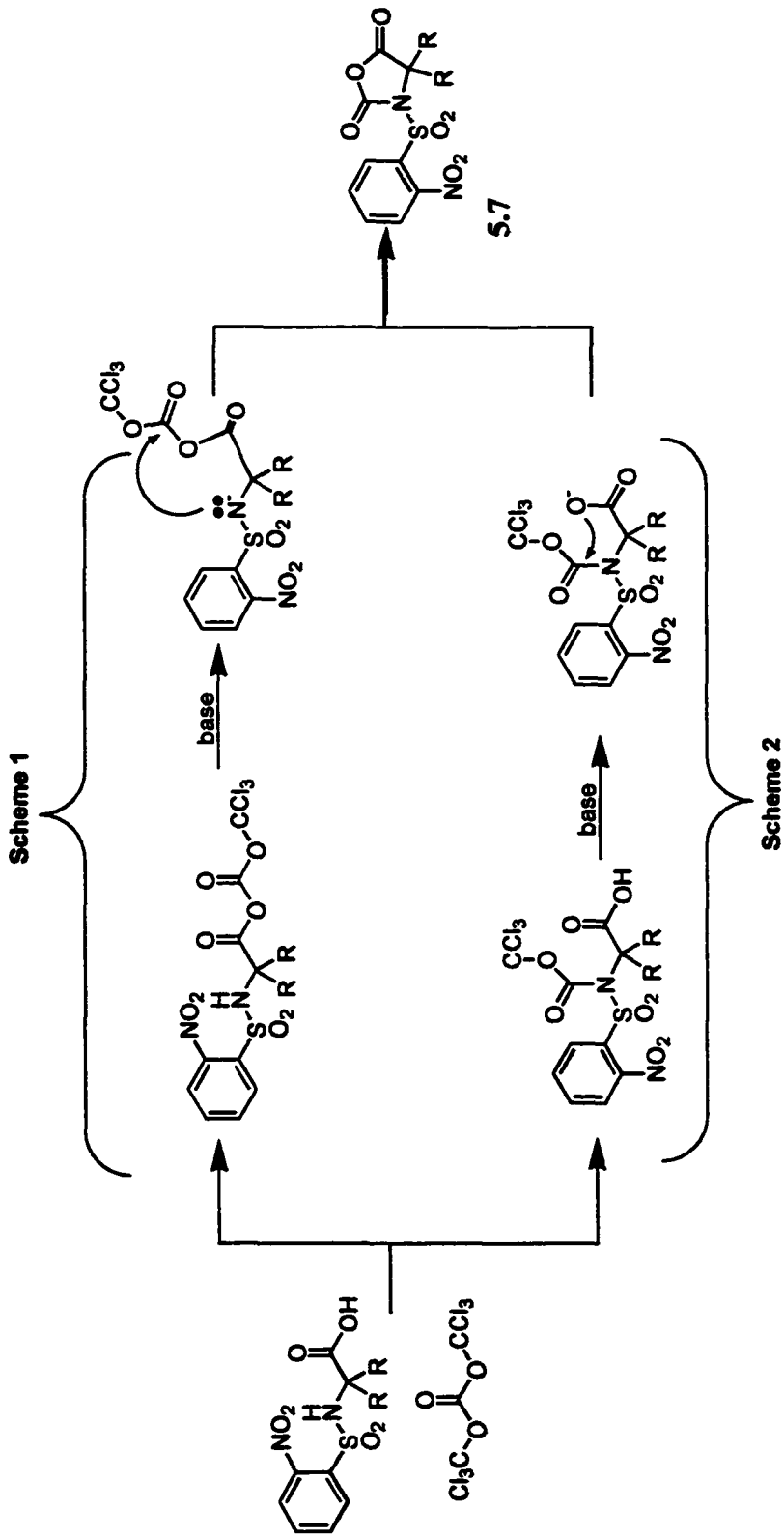

Figure 5.13. Triphosgene catalyzed intramolecular cyclization of *o*NBS-C^{α},C^{α}-disubstituted amino acid adducts to yield NCA cyclized product (**5.7**).

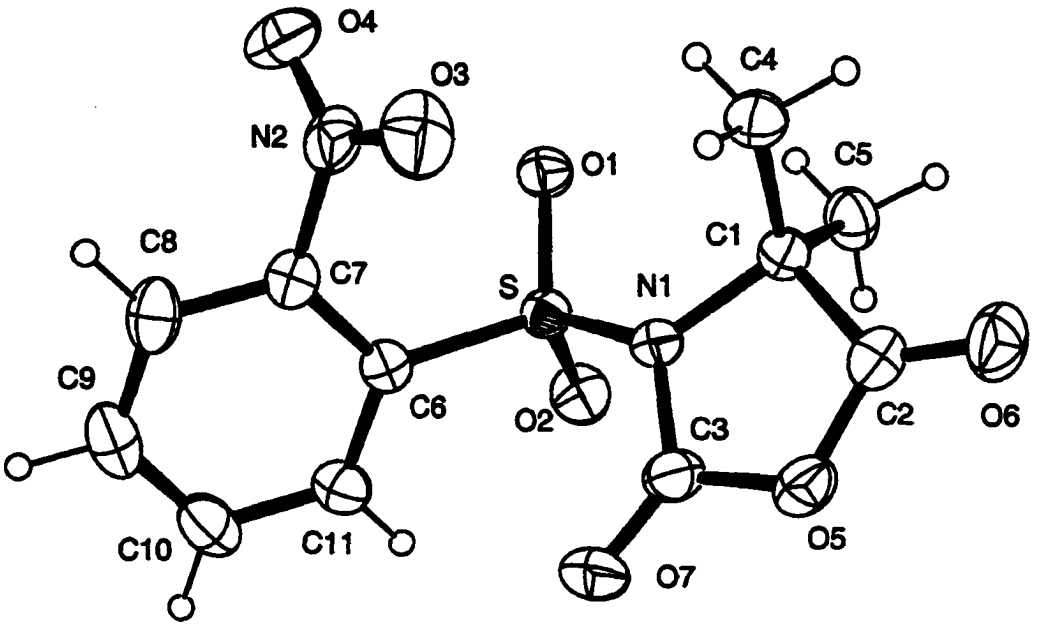

Figure 5.14. ORTEP of dimethyl-N-*o*-nitrobenzenesulfonyl N-carboxyanhydride.

carbon dioxide, causing minimal contamination during purification. Preliminary investigations of the coupling ability of **5.7** showed poor activity under solid phase synthesis conditions. However, it has not been exhaustively studied. Different coupling conditions and applications of this derivative are under current investigation and may yield desired results as a successful activated derivative of *o*NBS-Aib-OH. Further attempts to generate *o*NBS-amino acid chlorides with oxalyl chloride, $SOCl_2$, PCl_3 and PCl_5 have met with mixed results. Most problems associated with the synthesis of this derivative are due to the presence of excess base in the reaction which acts as a proton sponge to keep the α-amino group deprotonated. However, sulfonamide deprotonation may be causing severe side reactions. These synthetic problems are currently being addressed.

5.3. EXPERIMENTAL

5.3.1 *o*NBS-C^{α},C^{α}-Disubstituted Amino Acid Derivatives

5.3.1.1. N^{α}-(2-nitrophenylsulfonyl)-2-aminoisobutyric acid (5.1)

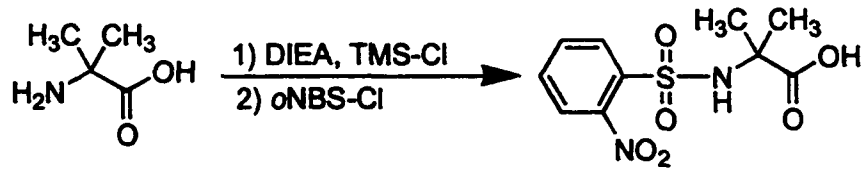

5.1

2-aminoisobutyric acid (10.0 g, 95.8 mmol) was added to a 500 mL Schlienk flask and dissolved in DCM (200 mL). Diisopropylethylamine (27.55 g; 213.0 mmol) was added and the reaction stirred for ten minutes while being flushed with argon. Chlorotrimethylsilane (21.05 g; 210.0 mmol) was added via syringe slowly and the reaction refluxed for 3 hours until all solid was in solution. After allowing the reaction to cool to room temperature, *o*-nitrobenzenesufonyl chloride (21.47 g; 194.0 mmol), dissolved in 100 mL DCM, was added dropwise from an addition funnel to the reaction mixture and the reaction stirred for 15 hours at room temperature. The DCM was removed by rotary evaporation and the resulting residue was distributed between 2.5% sodium carbonate solution (100 mL) and 100 mL diethyl ether. The aqueous layer was separated and washed with portions of diethyl ether (2 x 100 mL) . The aqueous layer was placed on a rotary evaporator to remove residual organic solvent for 10 minutes. The reaction was cooled in an ice bath and acidified to pH 2.0 with 1.0 N hydrochloric acid, then allowed to sit in a refrigerator for 1 hour. The resulting precipitate was extracted with ethyl acetate (3 x 200 mL), which was dried over Na_2SO_4 and concentrated *in vacuo* to yield 24.7 g (89%) of the crude *o*NBS-amino acid adduct. The

product was recrystallized from dichloroethane to yield 20.7 g (75%) analytically pure **5.1**. ^{1}H NMR (250 MHz, d_6-DMSO) δ 12.83 (s, 1H), 8.34 (s, 1H), 8.09-7.81 (m, 4H), 1.31 (s, 5H). ^{13}C NMR (60MHz, d_6-DMSO) 174.95, 147.10, 135.47, 133.58, 132.39, 129.34, 124.18, 58.57, 25.55. FAB-MS (glycerol) m/z 289.2 $(M+H)^+$. (For crystallographic data see Appendix I).

5.3.1.2. N^{α}-(2-nitrophenylsulfonyl)-1-amino-1-cyclohexanecarboxylic acid (5.2)

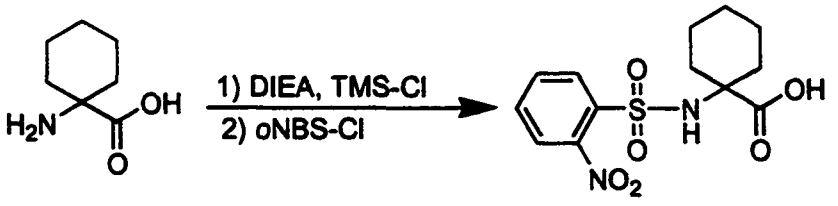

5.2

1-Aminocyclohexane-1-carboxylic acid (3.0 g; 20.95 mmol) was weighed out into a 250 mL 3-necked round bottom flask. The flask was filled with anhydrous DCM (100 mL) while flushing with argon. Diisopropylethylamine (5.95 g; 45.09 mmol) was added in one portion and the reaction allowed to stir at room temperature for 10 minutes under argon. Chlorotrimethylsilane (5.3 mL; 4.55 g; 41.90 mmol) was added via syringe and the reaction was stirred for 4 hours under argon. 2-Nitrobenzenesulfonyl chloride (4.41 g; 20.0 mmol) dissolved in 30 mL anhydrous DCM, was added dropwise from an addition funnel to the reaction while stirring in an ice bath, while flushing under a slow stream of argon. The reaction was allowed to rise to room temperature and stirred for 3 hours. The DCM was removed *in vacuo* and the crude distributed between 2.5% sodium carbonate solution (100 mL) and diethyl ether (100 mL). The aqueous layer was washed with portions of diethyl ether (2 x 100 mL), separated and residual diethyl ether removed on a rotary evaporator. The water layer was cooled in an

ice bath and acidified to pH 2.0 with 1.0 N hydrochloric acid and then allowed to sit in a refrigerator for 1 hour. The resulting precipitate was extracted with ethyl acetate (3 x 100 mL), dried over Na_2SO_4 and the solvent removed *in vacuo* to yield the crude product in 85% yield (5.5 g). The crude product was recrystallized from hot 100% ethanol to yield the analytically pure product as pale yellow crystals (4.9 g; 74%). ^1H NMR (250 MHz, d_6-DMSO) δ 12.55 (s, 1H), 8.21 (s, 1H), 8.08-7.81 (m, 4H), 1.91-1.05 (m, 10H). ^{13}C NMR (60MHz, d_6-DMSO) 175.08, 147.13, 135.04, 133.73, 132.30, 129.65, 124.18, 51.54, 32.47, 24.54, 20.88; FAB-MS (glycerol) m/z 329.2 $(M+H)^+$. (For crystallographic data see Appendix I).

5.3.1.3. N^{α}-(2-nitrophenylsulfonyl)-4-amino-1-(*tert*-butyloxycarbonyl)piperidine-4-carboxylic acid (5.3)

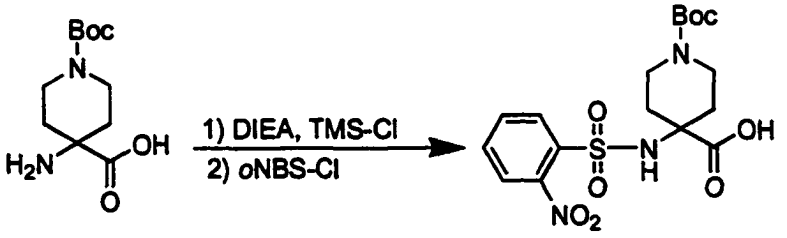

5.3

Api(Boc)-OH (4.12g;17.0mmol) was weighed out into a 250 mL 3-necked round bottom flask. The flask was filled with anhydrous DCM (100 mL) while flushing with argon. Diisopropylethylamine (5.05 g; 39.1 mmol) was added in one portion and the reaction allowed to stir at room temperature for 10 minutes under argon. Chlorotrimethylsilane (4.0 mL; 3.42 g; 31.6 mmol) was added via syringe and the reaction was stirred for 4 hours under argon. 2-Nitrobenzenesulfonyl chloride (3.39 g, 16.3mmol), dissolved in 30 mL anhydrous DCM, was added dropwise from an addition funnel to the reaction while stirring in an ice bath, while flushing under a slow stream of argon. The reaction was allowed to rise to room temperature and stirred for 3 hours.

The DCM was removed *in vacuo* and the crude distributed between 2.5% sodium carbonate solution (100 mL) and diethyl ether (100 mL). The aqueous layer was washed with portions of diethyl ether (2 x 100 mL), separated and residual diethyl ether removed on a rotary evaporator. The water layer was cooled in an ice bath and acidified to pH 2.0 with 1.0 N hydrochloric acid and then allowed to sit in a refrigerator for 1 hour. The resulting precipitate was extracted with ethyl acetate (3 x 100 mL), dried over Na_2SO_4 and the solvent removed *in vacuo* to yield the crude product in 95% yield (6.3 g). The crude product was recrystallized from hot 100% ethanol to yield the analytically pure **5.3** as pale yellow crystals (5.2 g; 79%).

^{1}H NMR (250 MHz, d_6-DMSO) δ 12.91 (s, 1H), 8.53 (s, 1H), 8.09-7.84 (m, 4H), 3.45 (m, 4H), 1.93 (m, 2H), 1.75 (m, 2H), 1.35 (s, 9H). ^{13}C NMR (60MHz, d_6-DMSO) 174.08, 153.55, 147.07, 134.53, 134.04, 132.49, 129.55, 124.35, 78.87, 59.95, 31.70, 27.99. FAB-MS (glycerol) m/z 430.2 $(M+H)^+$. (For crystallographic data see Appendix I).

5.3.1.4. N^{α}-(2-nitrophenylsulfonyl)-N^{ε}-(benzyloxycarbonyl)-L-lysine (5.4)

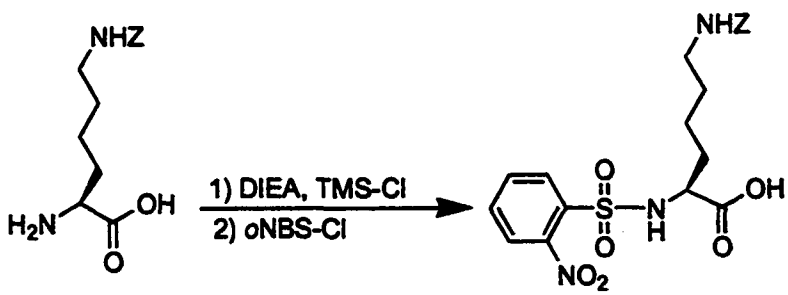

5.4

N^{ε}-(benzyloxycarbonyl)-L-lysine (3.0g; 10.7mmol) was dried for 1 hour under vacuum and suspended in 100 mL anhydrous DCM in a 250 mL three-necked round-

bottom flask fitted with an argon inlet valve, a septum and reflux condenser. Diisopropylethylamine (3.04g; 23.5mmol) was added and the reaction mixture was allowed to stir for 10 minutes at room temperature. While flushing with argon, the solution was cooled to 0 °C in an ice bath and chlorotrimethylsilane (2.33 g; 21.40 mmol) was added via syringe slowly. Extensive HCl gas production was observed. The reaction was refluxed under argon for 2 hours until the solution was homogenous. The solution was then re-cooled to 0 °C and 2-nitrobenzenesulfonyl chloride (2.26 g; 10.17 mmol), dissolved in 50 mL anhydrous DCM, was added dropwise from an addition funnel. The reaction was allowed to rise to room temperature and stirred for 2 hours. The DCM was removed *in vacuo* by rotary evaporation and the crude residue distributed between 2.5% sodium carbonate (100 mL) and diethyl ether (100 mL). The aqueous layer was washed with diethyl ether (2 x 100 mL) and placed on a rotary evaporator to remove residual organic solvent. The resulting clear aqueous solution was cooled to 0 °C and acidified to pH 2.0 with 1.0 N HCl. The solution was allowed to sit in a refrigerator for 2 hours and the resulting lightly colored precipitate was extracted with ethyl acetate (3 x 100 mL). The organic solution was dried over Na_2SO_4 and concentrated *in vacuo*, yielding the crude product in 62% yield (5.1 g). The crude was recrystallized from chloroform to yield **7** as analytically pure crystals (4.5 g; 47%). ^1H NMR (250 MHz, d_6-DMSO) δ 12.35 (s, 1H), 8.48 (d, 1H), 8.05-7.81 (m, 4H), 7.35 (m, 5H), 7.21 (t, 1H), 5.01 (s, 2H), 3.81 (m, 1H), 2.90 (m, 2H), 1.54 (m, 2H), 1.23 (m, 4H). ^{13}C NMR (60MHz, d_6-DMSO) 172.58, 155.071, 147.27, 137.30, 133.95, 133.34, 132.42, 129.84, 128.37, 127.75, 124.09, 55.13, 55.74, 31.40, 28.59, 22.38; FAB-MS (glycerol) m/z 455.2 $(M+H)^+$. (For crystallographic data see Appendix I).

5.3.2. 2-(2-nitrothiobenzene)-acetic acid (5.5)

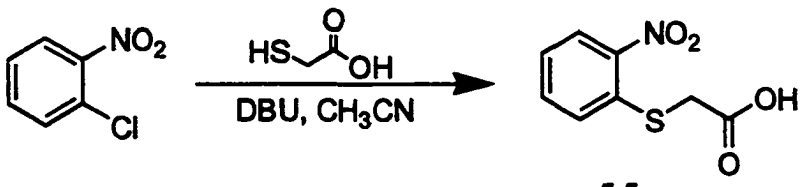

5.5

2-Chloronitrobenzene (1.0 g; 5.35mmol) was dissolved in 40 mL acetonitrile and mercaptoacetic acid (0.92 g; 9.50 mmol) was added. The reaction was cooled to 0 °C and DBU (2.85 g; 19.05 mmol) was added slowly, dropwise while stirring. The reaction was allowed to rise to room temperature over 1 hour and monitored by thin layer chromatography (1:1 DCM; Hexane) on silica. After 15 minutes, no 2-chloronitrobenzene was visible in the reaction the acetonitrile was removed *in vacuo* by rotary evaporation. The resulting crude oil was dissolved in 50 mL ethyl acetate and the organic solution was washed with 1.0 N hydrochloric acid (3 x 50 mL). The organic layer was dried over anhydrous Na_2SO_4 and the solvent removed by rotary evaporation to yield the crude product as bright yellow clumps, which has some impurity by TLC (99:1 ethyl acetate; acetic acid). Recrystallization from hot ethanol, followed by slow cooling and refrigeration yielded the analytically pure adduct **5.5** as small bright yellow crystals in good yield and with excellent purity (1.12 g; 83%). ^{1}H NMR (250 MHz, d_6-DMSO) δ 13.04 (s, 1H), 8.24 (d, 1H), 7.73 (dd, 1H), 7.59 (d, 1H), 7.42 (dd, 1H), 4.03 (s, 2H). ^{13}C NMR (60MHz, d_6-DMSO) δ 170.04, 145.39, 135.90, 134.32, 127.30, 125.95, 125.53, 34.39. FAB-MS (glycerol) m/z 213.0 $(M-H)^-$. (For crystallographic data see Appendix I).

5.3.3. *N*-(2-nitrobenzenesulfonyl)-2-aminoisobutyric acid-*N*-carboxyanhydride (5.7)

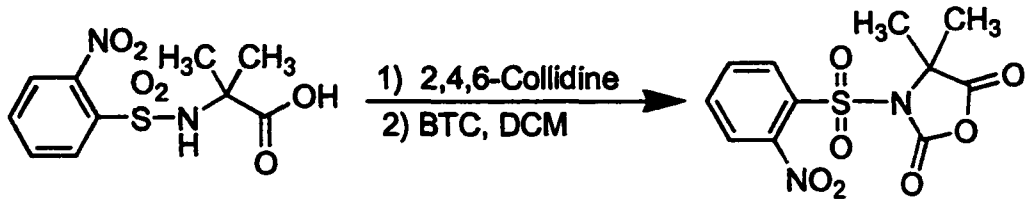

5.7

2.57g Bis-(trichloromethyl)carbonate was dissolved in anhydrous DCM (20 mL) and stirred at 0 °C. A solution of *o*NBS-Aib-OH (5.0 g, 17.35 mmol) and 2,4,6-collidine (4.2 g; 34.59 mmol), in 50 mL DCM, was slowly added and the reaction was allowed to go to room temperature. After stirring for 2 hours, 1.0 N hydrochloric acid (100 mL) was added and the reaction stirred for an additional five minutes. The organic layer was separated, washed with an additional 1.0 N hydrochloric acid (100 mL) and dried over Na_2SO_4. The solvent was removed by rotary evaporation and the crude product (5.03 g; 98%) was recrystallized from hot chloroform overnight to yield the NCA adduct as large white crystals (3.57 g; 73%). ^{1}H NMR (250 MHz, d_2-DCM) δ 8.41 (d, 1H), 7.93-7.81 (m, 3H), 1.92 (s, 5H). ^{13}C NMR (60MHz, d_2-DCM) 159.24, 148.54, 147.27, 135.99, 134.54, 132.54, 129.82, 124.97, 59.15, 24.38. FAB-MS (glycerol) m/z 315.2 $(M+H)^+$. (For crystallographic data see Appendix I).

5.3.4. Deprotection Solution

The deprotection solution (0.4 M mercaptoacetic acid; 0.8 M DBU; in acetonitrile) was prepared by diluting mercaptoacetic acid (3.58 g, 40 mmol) to 50 mL

in acetonitrile and DBU (12.18 g, 80 mmol) to 50 mL with acetonitrile. Both solutions were sealed and cooled to 5 °C. The solutions can be stored this way for several months. The DBU solution is slowly added to the thiol solution dropwise while stirring and maintaining a low temperature. After addition, the solution is stirred to ensure complete mixing, and stored in the refrigerator. Kept at 5 °C, the deprotection solution can be stored for several weeks before discoloration appears, which may cause interference in spectrometric analysis. At room-temperature, the deprotection solution becomes discolored after 2-3 days.

5.3.5. UV-Absorbance vs. Concentration Studies

Serial dilutions were made to produce the desired concentrations of 2-nitrophenyl-mercaptoacetid acid under experimental conditions (CH_3CN / Deprotection solution, 6:1). The cleavage adduct was dissolved and diluted in a 1:6 mixture of deprotection solution (0.4 M mercaptoacetic acid; 0.8 M DBU in acetonitrile) and acetonitrile. Serial dilutions were made to 1.0 mM, 500 µM, 250 µM, 125 µM, 100 µM, 50 µM, 25 µM and 10 µM. The samples were scanned on an AVIV Instruments 14DS UV-Vis-IR Scanning Spectrometer in quartz cells (path length=1 cm) from 500-250 nm. The background spectra (1:6 deprotection solution : CH_3CN), were subtracted from the sample spectra. Derivation of molar absorptivity is determined by extrapolation from Beer's Law so $\varepsilon_{390} = A_{390}/bc$ (where ε_{390} is the molar absorptivity of the cleavage product at 390nm, A_{390} is the absorbance, b is the path length (1cm) and c is the molar concentration of the dissolved cleavage adduct) for all concentrations. The observed molar absorptivities are plotted according to A vs. c, and the graph slope extrapolated to yield the average molar absorbtivity of 2950 $M^{-1}cm^{-1}$.

5.3.6. Solution Phase Cleavage Studies

In-solution deprotection studies were performed on four *o*NBS-protected amino acids: *o*NBS-Aib-OH, *o*NBS-Ac_6c-OH, *o*NBS-Api(Boc)-OH and *o*NBS-Lys(Z)-OH. All of the amino acids were weighed out and treated with 1.0 mL deprotection reagent (0.4 M mercaptoacetic acid; 0.8 M DBU in acetonitrile). The solution rapidly becomes bright yellow. The solution was agitated for 30 minutes at room temperature and then diluted with 6.0 mL acetonitrile to simulate resin cleavage conditions. The solutions are scanned from 500-300 nm using an AVIV Instruments 14DS UV-Vis-IR Spectrophotometer in a quartz cuvette with 1.0 cm path length and background corrected from a solution of 1.0 mL deprotection reagent in 6.0 mL acetonitrile in a matched quartz cuvette. The corrected absorbance at 390 nm is recorded and correlated to calculated theoretical absorbances for the corresponding concentrations.

5.3.7. Solid-Phase Cleavage Studies

Solid-phase coupling was performed with 4 equivalents of *o*NBS-Aib-OH and 4 equivalents of HATU in the presence of 2,4,6-collidine or preformed amino acid fluorides. The activated ester was preformed in CH_3CN for thirty minutes, then added to a pre-swollen suspension of PAL-PEG-PS in CH_3CN. The coupling was allowed to proceed for 24 hours with coupling tests performed every two hours. Coupling tests were performed by removing 5-10 mg of the resin, successive washing with CH_3CN and MeOH and drying the resin under high vacuum for 1 h. An exact amount of the resin was weighed out and treated with 1 mL of the deprotection solution for 30 minutes. The supernatant was then removed and the resin washed with CH_3CN (6 x 1.00 mL) to give a total volume of 7.00 mL. A 1.0 mL sample of the combined washes

was studied by scanning UV-spectroscopy from 500-300 nm and the background corrected absorbance value at 390 nm was noted. This value was entered into the substitution equation $\%Substitution=[(A_{390}x10^{6}x0.007)/(\varepsilon_{390}xW)]/L$. Couplings of several attempts never reached higher values than 32%. This may be due to poor coupling or poor compatibility of the highly polar deprotection solution with the relatively hydrophobic interior of the PEG-PS resin. Increased coupling efficiency may be reached with the use of more polar resins.

5.4. CONCLUSIONS

We have shown that the *ortho*-nitrobenzenesulfonyl group (oNBS) is a viable potential alternative to many common protecting groups, including the Fmoc-group. The *o*NBS group should allow for the use of highly activated C-terminus activating groups, such as acid chlorides and HATU adducts. The lowered nucleophilicity of the sulfonamide oxygen of *o*NBS-amino acid adducts are not prone to oxazalone formation and should greatly increase coupling yields and lower reaction times. In addition, the *o*NBS group is considerably less bulky than the Fmoc-group and should interfere less with solid-phase couplings of hindered amino acids. The deprotection of the *o*NBS group by mercaptoacetic acid in basic media is fast, effective and quantitative. In addition, the cleavage reaction yields a stable chromophore that can be detected by UV-spectroscopy for *in situ* reaction monitoring in real time. Solid-phase coupling attempts using preformed amino acid fluorides and activated esters (HATU) of the *o*NBS-adducts were inconclusive. Poor observed coupling yields may be due to poor activity of the activated amino acid derivative, or incompatibility of the deprotection solution with the PEG-PS resin. The use of different resins and varying solvents may aid in coupling efficiency. The application of this new coupling scheme could lead to the

ability to generate longer, more difficult sequences in high yields, with lower costs and decreased reaction times.

5.5. REFERENCES

5.1 Merrifield, R. B. *J. Am. Chem. Soc.* **1953**, *85*, 2149-2154.

5.2 Yokum, S. T., Barany, G. B. In *Solid-Phase Synthesis: A Practical Guide.*, Kates, S. A., Albericio, F., Eds., Marcel Dekker, Inc.: New York, **2000**, 79-102.

5.3 Gisin, B., F., Merrifield, R. B., Tosteson, D. C., *J. Am. Chem. Soc.* **1959**, *91*, 2591-2595.

5.4 Rothe, M., Dunkel, W. *J. Polym. Sci., Part B*, **1957**, *5*, 589-593.

5.5 Burgess, K., Linthicum, D. S., Shin, H. *Angew. Chem., Int. Ed. Engl.* **1995**, *34*, 907-909.

5.6 Cho, C. Y., Moran, E. J., Cherry, S. R., Stephans, J. C., Fodor, S. P. A., Adams, C. L., Sundaram, A., Jacobs, J. W., Schultz, P. G. *Science*, **1993**, *251*, 1303-1305.

5.7 Simon, R. J., Kania, R. S., Zuckermann, R. N., Huebner, V. D., Jewell, D. A., Banville, S., Ng, S., Wang, L., Rosenberg, S., Marlowe, C. K., Spellmeyer, D. C., Tan, R., Frankel, A. D., Santi, D. V., Cohen, F. E., Bartlett, P. A. *Proc. Natl. Acad. Sci. U.S.A.* **1992**, *89*, 9357-9371.

5.8 Caruthers, M. H. *Science* **1985**, *230*, 281-285.

5.9 Osborne, S. E., Ellington, A. D. *Chem. Rev.* **1997**, *97*, 349-370.

5.10 Randolph, J. T., McClure, K. F., Danishefsky, S. J. *J. Am. Chem. Soc.* **1995**, *117*, 5712-5719.

5.11 Thompson, L. A., Ellman, J. A. *Chem. Rev.* **1995**, *95*, 555-500.

5.12 Barany, G., Merrifield, R. B. In *The Peptides: Analysis, Synthesis, Biology*, Vol. 2, Gross, E., Meienhofer, J., Eds., Academic: New York, **1979**, pp 1-284, and references therein.

5.13 Atherton, E., Sheppard, R. C. *Solid Phase Peptide Synthesis: A Practical Approach*, IRC: Oxford, **1989**.

5.14 Zalipsky, S., Chang, J. L., Albericio, F., Barany, G. *React. Poly.* **1994**, *22*, 243-258.

5.15 Frank, R., Döring, R. *Tetrahedron* **1998**, *44*, 5031-5040.

5.16 Forns, P., Fields, G. B. In *Solid-Phase Synthesis: A Practical Guide.*, Kates, S. A., Albericio, F., Eds., Marcel Dekker, Inc.: New York, **2000**, pp 1-77.

5.17 Mitchell, A. R., Erickson, B. W., Ryabtsev, M. N., Hodges, R. S., Merrifield, R. B. *J. Am. Chem. Soc.* **1975**, *98*, 7357-7352.

5.18 Bergmann, M., Zervas, L. *Ber. Dtsch. Chem. Ges.*, **1932**, *55*, 1192-1201.

5.19 Carpino, L. A., Han, G. Y. *J. Org. Chem.* **1972**, *37*, 3404-3505.

5.20 Kuntz, H., Unverzagt, C. *Angew. Chem., Int. Ed. Engl.* **1988**, *23*, 435-438.

5.21 Carpino, L. A., Han, G. Y. *J. Am. Chem. Soc.* **1970**, *92*, 5748-5749.

5.22 Vedejs, E., Lin, S., Klapars, A., Wang, J. *J. Am. Chem. Soc.* **1995**, *118*, 9795-9797.

5.23 Kuntz, H., Waldmann, H. *Angew. Chem., Int. Ed. Engl.* **1984**, *23*, 71-74.

5.24 Coleman, D. *J. Chem. Soc.* **1951**, 2294-3395.

5.25 Lajoie, G., Crivici, A., Adamson, J. G. *Synthesis* **1990**, 571-572.

5.26 Matysiak, S., Böldicke, T., Tegge, W., Frank, R. *Tetrahedron Lett.* **1998**, *39*, 1733-1734.

5.27 Carpino, L. *J. Am. Chem. Soc.* **1957**, *79*, 4427-4431.

5.28 Alewood, P., Alewood, D., Miranda, L., Love, S., Meutermans, W., Wilson, D. *Methods Enzymol.* **1997**, *289*, 14-29.

5.29 Atherton, E., Fox, H., Harkiss, D., Logan, C. J., Sheppard, R. C., Williams, B. J. *J. Chem. Soc., Chem. Commun.* **1978**, 537-539.

5.30 Falb, E., Yechezkel, T., Salitra, Y., Gilon, C. *J. Peptide Res.* **1999**, *53*, 507-517.

5.31 Carpino, L. A., Sadat-Aalaee, D., Chao, H. G., DeSelms, R. H. *J. Am. Chem. Soc.* **1990**, *112*, 9551-9552.

5.32 Carpino, L. A., Chao, H. G., Beyermann, M., Bienert, M. *J. Org. Chem.* **1991**, *55*, 2535-2542.

5.33 Carpino, L. A., Mansour, E. M. E., El-Faham, A. *J. Org. Chem.* **1993**, *58*, 4152-5154.

5.34 Wenschuh, H., Beyermann, M., Krause, E., Brudel, M., Winter, R., Schümann, M., Carpino, L. A., Bienert, M. *J. Org. Chem.* **1994**, *59*, 3275-3280.

5.35 Carpino, L. A., Beyermann, M., Wenshuh, H., Bienert, M. *Acc. Chem. Res.* **1995**, *29*, 258-274.

5.36 Carpino, L. A., Ionescu, D., El-Faham, A., Henklein, P., Wenschuh, H., Bienert, M., Beyermann, M. *Tetrahedron Lett.* **1998**, *39*, 241-244.

5.37 Fuller, W. D., Cohen, M. P., Shabankareh, M., Blair, R. K., Goodman, M. *J. Am. Chem. Soc.* **1990**, *112*, 7414-7415.

5.38 Sheehan, J. C., Hess, G. P. *J. Am. Chem. Soc.* **1955**, *77*, 1057-1058.

5.39 Albericio, F., Kates, S. A. In *Solid-Phase Synthesis: A Practical Guide.*, Kates, S. A., Albericio, F., Eds., Marcel Dekker, Inc.: New York, **2000**, pp 275-330.

5.40 Williams, A., Ibrahim, I. T. *Chem. Rev.*, **1981**, *81*, 589-535.

5.41 Kõnig, W., Geiger, R. *Chem. Ber.* **1970**, *103*, 2034-2040.

5.42 Carpino, L. A., El-Faham, A. *J. Org. Chem.* **1994**, *59*, 595-598.

5.43 Carpino, L. A. *J. Am. Chem. Soc.* **1993**, *115*, 4397-4398.

5.44 Carpino, L. A., El-Faham, A. *Tetrahedron* **1999**, *55*, 5813-5830.

5.45 Dourtoglou, V., Ziegler, J. C., Gross, B. *Tetrahedron Lett.* **1978**, 1259-1272.

5.46 Carpino, L. A., El-Faham, A., Minor, C. A., Albericio, F. *J. Chem. Soc., Chem. Commun.* **1994**, 201-203.

5.47 Nagaraj, R., Shamala, N., Balaram, P. *J. Am. Chem. Soc.* **1979**, *101*, 15-20.

5.48 Toniolo, C., Crisma, M., Formaggio, F., Benedetti, E., Santini, A., Iacovino, R., Saviono, M., Di Blasio, B., Pedone, C., Kamphius, J. *Biopolymers* **1997**, *39*, 519-522.

5.49 Paul, P. K. C., Sukumar, M., Bardi, R., Piazzesi, A. M., Valle, G., Toniolo, C., Balaram, P. *J. Am. Chem. Soc.* **1985**, *108*, 5353-5370.

5.50 Toniolo, C., Benedetti, E. *Macromolecules* **1991**, *24*, 4004-4009.

5.51 Marshall, G. R., Hodgkin, E. E., Langs, D. A., Smith, G. D., Zabrocki, J., Leplawy, M. T. *Proc. Natl. Acad. Sci. U.S.A.* **1990**, *87*, 487-491.

5.52 Yokum, T. S., Gauthier, T. J., Hammer, R. P., McLaughlin, M. L. *J. Am. Chem. Soc.* **1997**, *119*, 1157-1158.

5.53 Yokum, T. S., Elzer, P. H., McLaughlin, M. L. *J. Med. Chem.* 1995, 39, 3503-3505.

5.54 Sarin, V. K., Kent, S. B. H., Tam, J. P., Merrifield, R. B. *Anal. Biochem.* **1981**, *117*, 147-157.

5.55 Yan, B., Kumaravel, G., Anjaria, H., Wu, A., Petter, R. C., Jewell, C. F., Wareing, J. R. *J. Org. Chem.* **1995**, *50*, 5735-5738.

5.56 Yan, B., Kumaravel, G. *Tetrahedron* **1995**, *53*, 843-848.

5.57 Pivonka, D. E., Simpson, T. R. *Anal. Chem.*, **1997**, *59*, 3851-3853.

5.58 Russell, K., Cole, D. C., McLaren, F. M., Pivonka, D. E. *J. Am. Chem. Soc.* **1995**, *118*, 7941-7945.

5.59 Milne, H. B., Peng, C. H. *J. Am. Chem. Soc.* **1957**, *79*, 539-544.

5.60 Fukuyama, T., Jow, C, H,, Cheung, M. *Tetrahedron Lett.* **1995**, *35*, 5373-5374.

5.61 Fukuyama, T., Cheung, M., Jow, C. H., Hidai, Y., Kan, T. *Tetrahedron Lett.* **1997**, *38*, 5831-5834.

5.62 Sabirov, A. N., Samukov, V. V., Pozdnyakov, P. I., Kim, H. J., Presented at the 15th American Peptide Symposium, Minneapolis, **1999**.

5.63 Miller, S. C., Scanlan, T. S. *J. Am. Chem. Soc.* **1997**, *119*, 2301-2302.

5.64 Miller, S. C., Scanlan, T. S. *J. Am. Chem. Soc.* **1998**, *120*, 2590-2591.

5.65 Reichwein, J. F., Liskamp, R. M. J. *Tetrahedron Lett.*, **1998**, *39*, 1243-1245.

5.66 Hammarström, L. G. J., Giraldes, J., McLaughlin, M. L., Billodeaux, D. R., Fronczek, F. R. *Acta. Cryst.* **2000**, in print.

5.67 Balse, P. M., Kim, H. J., Han, G., Hruby, V. J. *J. Peptide Res.*, **2000**, *55*, 70-79.

5.68 Bolin, D. R., Sytwu, I. –I., Humiec, F., Meienhofer, J., *Int. J. Pept. Protein Res.*, **1989**, *33*, 353-359.

CHAPTER 6
SUMMARY, FUTURE STUDIES AND INSIGHTS

6.1. DISCUSSION

There is still much to be learned about the synthesis, structure, and bioactivity of linear, helical, amphipathic peptides. This dissertation addresses some of the hurdles that must be overcome if the development of this field is to continue. The design and synthesis of short, amphipathic helical peptides incorporating high levels of C^{α},C^{α}-disubstituted amino acids is a difficult task. Development of new methods with which to synthesize these difficult targets with greater efficiency and purity is crucial for the successful continued study of the bioactivity of these compounds. New amino acids need to be synthesized and their helix promoting ability and their ability as structure stabilizing elements need to be assessed. Foremost, the mechanism by which antimicrobial peptides function must be further studied. Insights into these and other areas of peptide synthesis, characterization and biological screening will allow linear, helical peptides to be at the forefront of biomedical studies in the next few years. As bacterial resistance becomes a growing problem, newer and "smarter" drugs are required to battle increasing pathogenic activity. Antimicrobial peptides are one of the best candidates to take on this task.

Chapter 2 of this dissertation presents the synthesis of orthogonally protected polyfunctional C^{α},C^{α}-disubstituted amino acids (Fmoc-Api(Boc)-OH, Fmoc-Bglu(tBu)$_2$-OH, Fmoc-Basp(tBu)$_2$-OH and Fmoc-Bap(Boc)$_2$-OH). C^{α},C^{α}-Disubstituted amino acids have provided peptide chemists with powerful tools for secondary structure promotion.[6.1-5] Api has found a niche as the preferred source of cationic C^{α},C^{α}-disubstituted amino acids for the synthesis of peptides of this family.[6.6-8] It allows high

levels of ionizable residues to be incorporated into short peptides containing up to 80% C^{α},C^{α}-disubstituted amino acids, yet still retain a preferred helical sense, allowing secondary structure studies to be performed.[6.9] Api complements the family of alicyclic C^{α},C^{α}-disubstituted amino acids, all of which have been found to be strongly helix promoting.[6.10-13] The synthesis of Api is characterized by the selective hydrolysis of a di-Boced hydantoin, which can be easily purified under aqueous/organic alkaline conditions to yield the N^{γ}-protected amino acid in good yield. N^{α}-Fmoc-protection is then realized to give the orthogonally protected amino acid.[6.14]

Ethyl nitroacetate (ENA) is a common precursor to a number of organic targets.[6.15] It has provided us with an exciting starting material for the synthesis of orthogonally protected, polyfunctional C^{α},C^{α}-disubstituted amino acids. The mild conditions under which ENA can be alkylated, allows for tremendous versatility in the choice of electrophilic alkylating agents. Mild base-catalyzed alkylation of ENA allows for the preparation of a number of tetrafunctional precursors, suitable for conversion towards orthogonally protected polyfunctionalized C^{α},C^{α}-disubstituted amino acids.[6.16]

The synthesis of Fmoc-Bglu(tBu)$_2$-OH, an orthogonally protected tetrafunctional C^{α},C^{α}-disubstituted amino acid analog of glutamic acid, and Fmoc-Bap(Boc)$_2$-OH, an orthogonally protected tetrafunctional C^{α},C^{α}-disubstituted amino acid analog of lysine, are based on base catalyzed nucleophilic alkylation of the ethyl nitroacetate (ENA) anion. This electrophilic addition has been highly accelerated by utilizing a tetraalkyl ammonium halide to function as a highly dissociated counter-ion during alkylation.[6.16] The nucleophilic addition of the ethyl nitroacetate anion has been extended to several alkyl halide acceptors and Michael acceptors. As a result of the

base-catalyzed cyclization of ethyl-2,2-bis(*t*-butylcarboxyethyl) glycine during the α-amino ester hydrolysis, the synthesis was refocused on the corresponding Bis-aspartic acid derivative Fmoc-Basp(tBu)$_2$-OH. The shorter side-chain length allows for hydrolysis without competition from cyclization reactions. Subsequent N$^{\alpha}$-protection of this amino acid is currently underway.

Regioselective reduction of ethyl 2,2-bis(3-cyanoethyl)-2-nitro acetate towards the synthesis of Bap(Boc)$_2$-OH has proven very difficult. Thus, several alternative synthetic pathways have been envisioned for the successful synthesis of Bap-like analogs. These schemes are illustrated in Figure 6.1 and Figure 6.2. The synthetic scheme in Figure 6.1 takes advantage of the already optimized dialkylation of ethyl nitroacetate with *t*-butyl acrylate. Acid catalyzed *t*-butyl ester cleavage may allow for the preparation of a Boc-protected diamino derivative through a modified Curtius rearrangement. Subsequent nitro reduction and ethyl ester hydrolysis should allow for the preparation of Fmoc-Bae(Boc)$_2$-OH (Bae=Bis(amino ethyl)).

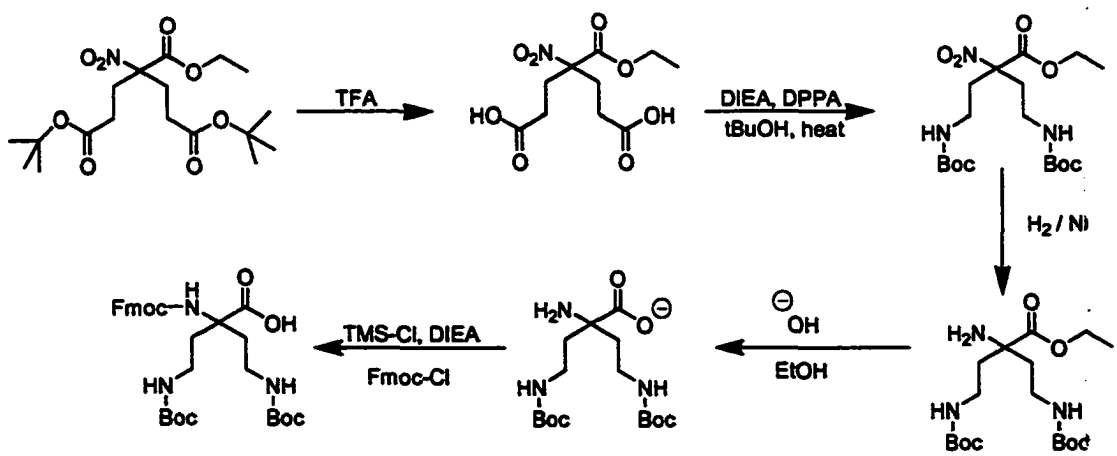

Figure 6.1. Curtius rearrangement approach towards the synthesis of Fmoc-Bae(Boc)$_2$-OH.

The second synthetic scheme (Figure 6.2) is based on the ring opening ability of N-alkylated aziridines. The high nucleophilicity of the ethyl nitroacetate anion may allow for a one-step conversion to the side-chain protected α-nitro ester. Subsequent nitro reduction, hydrolysis and N^{α}-protection may provide a very rapid and efficient route to Fmoc-Bae(Boc)$_2$-OH. The development of these exciting new amino acids towards functional SPPS monomers will allow for the preparation of new peptides with which to further study amino acid induced secondary structure promotion.

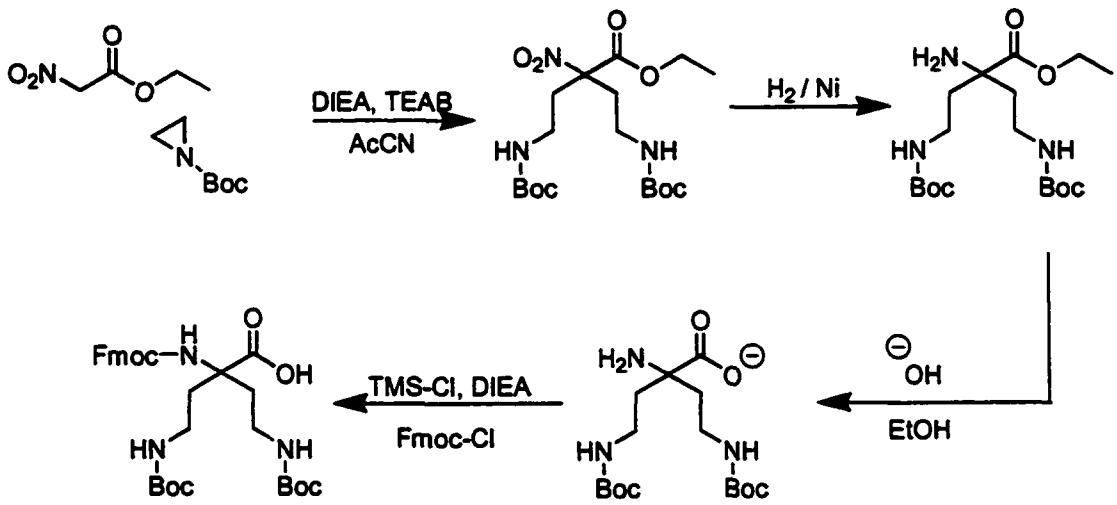

Figure 6.2. Aziridine ring-opening approach towards the synthesis of Fmoc-Bae(Boc)$_2$-OH.

Several key secondary structure questions can be addressed utilizing these new amino acids. It has recently been shown that helical secondary structures can be induced and stabilized by amphipathic control.[6.9] Studies have also determined that higher bis(*n*-alkyl) C^{α},C^{α}-disubstituted amino acids strongly favor extended conformations.[6.3,4] Incorporation of bifunctional amino acids, such as Bap or Bae into a

short peptide increases the amphipathic character of the peptide by introducing higher levels of cationic functional groups. According to amphipathic stabilization of secondary structures, this should increase the peptides ability to form helical conformations under micellar-type environments. However, these amino acids structurally resemble the bis(*n*-alkyl) C^{α},C^{α}-disubstituted amino acids which are known to preferentially adopt an extended conformation. Table 6.1 shows proposed variations of peptides that could be synthesized to determine the secondary structure promoting ability of these amino acids.

Table 6.1. Suggested helical peptides incorporating Bap.

Peptide	Sequence	Helix Design
Pi-10^{B}	H-Aib-Aib-**Bap**-*Lys*-Aib-Aib-**Bap**-*Lys*-Aib-Aib-NH_2	α
Ipi-10^{B}	H-**Bap**-Aib-Aib-*Lys*-Aib-Aib-*Lys*-Aib-Aib-**Bap**-NH_2	3_{10}
Ach-10α^{B}	H-Ac_6c-Aib-*Lys*-**Bap**-Aib-Ac_6c-**Bap**-*Lys*-Ac_6c-Aib-NH_2	α
Ach-10^{B}	H-**Bap**-Aib-Ac_6c-*Lys*-Ac_6c-Aib-*Lys*-Aib-Ac_6c-**Bap**-NH_2	3_{10}
Bap-6	H-Ac_6c-Ac_6c-**Bap**-*Lys*-Ac_6c-Ac_6c-NH_2	α
Bap-8	H-Ac_6c-Ac_6c-*Lys*-Ac_6c-Ac_6c-**Bap**-Ac_6c-Ac_6c-NH_2	3_{10}

Salt-bridge stabilization of secondary structure is also well documented. The presence of tetrafunctional amino acids, such as Bglu and Bap should provide several interesting opportunity to study highly salt-bride stabilized secondary structures as is illustrated in Figure 6.3. These peptides complement the family of peptides presented

in Chapter 3 of this dissertation and would greatly increase our understanding of the factors that promote and stabilize secondary structures in peptides. In addition to determining structures by electronic circular dichroism spectroscopy, vibrational circular dichroism spectroscopy (VCD) (10) and NMR will be utilized to gain better understanding of helical conformations.[6.18-20]

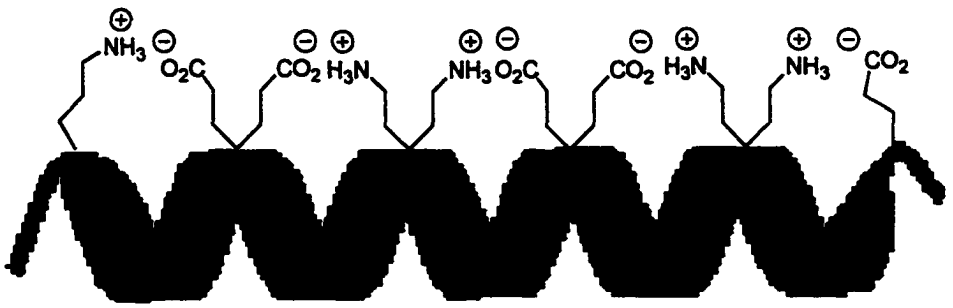

Figure 6.3. Highly stabilized salt-bridge peptide incorporating Bap and Bglu.

Chapter 4 of this dissertation addresses the bioactivity of the presented peptides as selective cytolytic agents towards macrophages infected with intracellular pathogens. Due to exponential growth in the use of classical antibiotic therapy, bacterial resistance towards antibiotics is becoming an ever-growing problem. This problem is exacerbated in the case of intracellular pathogens since they reside within the cellular environment of the very immune system which is used to target it, and infection is not associated with a significant extracellular component of the pathogen. Because of this resistance

problem, several new approaches towards antimicrobial defense have been explored within the past twenty years. One of the most promising routes toward developing a new weapon to battle bacterial agents have been the growing interest in linear amphipathic peptides as antimicrobial agents. Amphipathic peptides are highly ubiquitous in nature and make up an important part of the natural defenses of several species in the animal kingdom. The peptides are characterized by the presence of a definable cationic amphipathic helical structure and are usually relatively short (<40 residues), thus suggesting that considerable biological activity can be exhibited by relatively short sequences.[6.21] These peptides have been found to be active against a wide array of pathogens, including gram-positive and gram-negative bacteria, protozoa, and fungi.[6.22] Although currently not prevalent as therapeutic agents, some peptides are currently under review for use as drugs.

Although no direct bioactivity was observed towards *Brucella abortus*, MIC studies against representative Gram-positive and Gram-negative bacteria support the theory that increased hydrophobicity in peptide composition increases cytolytic activity. This hydrophobicity-dependent cytolytic character is also observed in mammalian non-infected peritoneal macrophages from BALB/c mice. Thus, Pi-10 and Ipi-10, which contain Aib as their hydrophobic residues, show the lowest cytolytic activity. In contrast, Cyh-10 and Ich-10, in which the Aib residues have been substituted with much more hydrophobic Ac_6c, show the highest levels of cytotoxicity. ACh-10 and ACh-10α, which contain a mixture of Aib and Ac_6c residues, show cytolytic activities roughly in between those of Pi-10 and Cyh-10. These peptides may be the best suited for further study as *in vivo* therapeutics.

Studies of the selective bioactivity *in vitro* against peritoneal macrophages infected with an intracellular pathogen, *Brucella abortus*-GFP, clearly show that the peptides show a selective cytolytic activity towards infected macrophages at concentrations that are non-lethal to healthy macrophages. An additional interesting feature to note is the higher selectivity of α-helical peptides versus 3_{10}-helical peptides. This suggests a strongly structure-dependent mechanism of cell lysis and activity. *In vitro* activation of harvested macrophages with PMA induces peptide-promoted cell killing in a similar fashion to *Ba* infected macrophages. In contrast, PKC inhibition of PMA-induced cellular activation suppresses peptide activity completely. This suggests a cellular membrane-mediated response by infected macrophages towards the presence of a pathogen. This response may increase susceptibility of the infected cells towards peptide activity or promote peptide aggregation at the cellular membrane. Further studies to promote the understanding of cellular response towards intracellular pathogenic infections are required to fully understand the mechanism by which these peptides function. These studies include fluorescently labeling peptides to observe peptide distribution in infected versus non-infected macrophages, and PKC inhibitor treatment of *Ba*-infected macrophages. In addition, peptide activity at the cellular membrane and peptide affinity for infected versus non-infected macrophages must be determined. We plan to further test the presented peptides through *in vivo* studies to determine cytotoxicity and efficacy in combination with classical antibiotic therapy. These studies are planned to be extended towards the search for potent therapeutic approaches to treat bacterial infections of greater current interest, such as *Mycobacterium tuberculosis*.

Chapter 5 of this dissertation addresses the role of C^{α},C^{α}-disubstituted amino acids, such as Aib (2-aminoisobutyric acid), Ac_6c (1-amino-1-cyclohexylcarboxylic acid), and Api (4-aminopiperidine-4-carboxylic acid), in solid phase peptide synthesis. C^{α},C^{α}-Disubstituted amino acids have become recognized tools for the selective control of peptide secondary structure[6,10-13] and for accentuating physiological properties of resulting peptides (see chapters 2,3 and 4). Recently, these derivatives have been shown to generate highly helical segments with peptides as short as 10 residues in length.[6,9] In particular, close proximity of these residues causes dramatic increases in the helical propensity of resulting peptides, as well as stabilizes these peptides towards enzymatic degradation under physiological conditions.[6,6] These amino acids are of current interest in the development of novel amphipathic peptides with high helicity for study as *in vivo* selective weapons against macrophages infected with intracellular pathogens (See Chapter 4). As with *N*-alkylated amino acids, C^{α},C^{α}-disubstituted amino acids offer a significant challenge in their ability to couple under solid phase peptide synthesis conditions. Couplings generally require large excesses of reagent and extended coupling-times. This, in turn, makes peptides rich in C^{α},C^{α}-disubstituted amino acids very expensive to synthesize. The inherent difficulty in coupling of several residues of C^{α},C^{α}-disubstituted amino acids in a row stems primarily from the steric repulsion that arises between the residue that is being coupled and the residue that is already on the resin.

In an attempt to develop a new, faster method for couplings of these difficult amino acids, our attention has turned to the higher reactivity of amino acid chlorides, which have been shown to have very high reaction rates in solution phase couplings.[6,23-25] In addition to being of higher reactivity, amino acid chlorides are considerably less

expensive to synthesize in comparison to their corresponding acid fluorides and can be prepared by a number of simple reagents such as thionyl chloride, oxalyl chloride and phosphorous trichloride. However, pre-formed amino acid chlorides generally do not perform as well in solid phase peptide synthesis due to competing oxazolone formation.[6.24]

The sulfonyl oxygens of the *o*-nitrobenzenesulfonyl (*o*NBS) group are considerably less nucleophilic than the corresponding carbonyl group of a urethanyl type protecting group. Thus, the problem of intramolecular cyclization is not of concern in the preparation and application of *o*NBS-amino acid chlorides or other activated ester functional groups. This phenomenon may in turn result in lower racemization of *o*NBS protected proteinogenic amino acids, since oxazalone formation is the key intermediate in facilitating this process.

Chapter 5 of this dissertation introduces a new scheme for solid-phase peptide synthesis based on the *o*NBS group as the N^{α}-protecting group. The group has been shown to be easily introduced into a number of C^{α},C^{α}-disubstituted amino acids,[6.26] is stable as an amino acid adduct and is readily cleaved to form a UV-active chromophore which is quantitatively characterizable during the coupling reaction is in progress.

The *o*NBS group should allow for the use of highly activated C-terminus activating groups, such as acid chlorides and HATU adducts. The lowered nucleophilicity of the sulfonamide oxygen of *o*NBS-amino acid adducts are not prone to oxazalone formation and should greatly increase coupling yields and lower reaction times. The deprotection of the *o*NBS group by mercaptoacetic acid is fast, effective and quantitative. This coupling scheme should lead to the ability to generate longer, difficult sequences in high yields, with lower costs and decreased reaction times.

6.2. REFERENCES

6.1 Nagaraj, R., Shamala, N., Balaram, P. *J. Am. Chem. Soc.* **1979**, *101*, 15-20.

6.2 Toniolo, C., Crisma, M., Formaggio, F., Benedetti, E., Santini, A., Iacovino, R., Saviono, M., Di Blasio, B., Pedone, C., Kamphius, J. *Biopolymers* **1997**, *39*, 519-522.

6.3 Paul, P. K. C., Sukumar, M., Bardi, R., Piazzesi, A. M., Valle, G., Toniolo, C., Balaram, P. *J. Am. Chem. Soc.* **1986**, *108*, 6363-6370.

6.4 Toniolo, C., Benedetti, E. *Macromolecules* **1991**, *24*, 4004-4009.

6.5 Marshall, G. R., Hodgkin, E. E., Langs, D. A., Smith, G. D., Zabrocki, J., Leplawy, M. T. *Proc. Natl. Acad. Sci. U.S.A.* **1990**, *87*, 487-491.

6.6 Yokum, T. S., Elzer, P. H., McLaughlin, M. L. *J. Med. Chem.* **1996**, *39*, 3603-3605.

6.7 Yokum, T.S., Gauthier, T. J., Hammer, R. P., McLaughlin, M. L. *J. Am. Chem. Soc.* **1997**, *119*, 1167-1168.

6.8 Wysong, C. L., Yokum, T. S., Morales, G. A., Gundry, R. L. McLaughlin, M. L., Hammer, R. P. *J. Org. Chem.* **1996**, *61*, 7650-7651.

6.9 Hammarstrom, L. G. J., Gauthier, T. J., Yokum, T. S., Hammer, R. P., McLauglin, M. L. *J. Peptide Res.* **2001**, submitted for publication.

6.10 Paul, P. K. C., Sukumar, M., Bardi, R., Piazzesi, A. M., Valle, G., Toniolo, C., Balaram, P. *J. Am. Chem. Soc.* **1986**, *108*, 6363-6370.

6.11 Toniolo, C., Benedetti, E. *Macromolecules* **1991**, *24*, 4004-4009.

6.12 Benedetti, E., DiBlasio, B., Iacovino, R., Menchise, V., Saviao, M., Pedone, C., Bonora, G. M., Ettorre, A., Graci, L., Formaggio, F., Crisma, M., Valle, G., Toniolo, C. *J. Chem. Soc., Perkin Trans. 2.* **1997**, 2023-2032.

6.13 Toniolo, C., Crisma, M., Formaggio, F., Benedetti, E., Santini, A., Iacovino, R., Saviano, M., Di Blasio, B., Pedone, C., Kamphius, J. *Biopolymers* **1996**, *40*, 519-522.

6.14 Hammarström, L. G. J., McLaughlin, M. L. *Org. Syn.* **2001**, submitted for publication.

6.15 Shipchandler, M. T. *Synthesis*, **1979**, *9*, 666-686.

6.16 Fu, Y,, Hammarström, L. G. J., Miller, T. J., McLaughlin, M. L., Hammer, R. P. **2001** (manuscript in preparation).

6.17 Keiderling, T. A., Silva, Ragd. P., Yoder, G., Dukor, R. K. *Bioorg. Med. Chem.* **1999**, *7*, 133-141.

6.18 Iqbal, M. & Balaram, P. *Biopolymers* **1982**, *21*, 1427-33.

6.19 Gratias, R., Konat, R., Kessler, H., Crisma, M., Valle, G., Polese, A., Formaggio, F., Toniolo, C., Broxterman, Q. B. & Kamphuis, J. *J. Am. Chem. Soc.* **1998**, *120*, 4763-4770.

6.20 Long, H. W. & Tycko, R. *J. Am. Chem. Soc.* **1998**, *120*, 7039-7048.

6.21 Andreu, D., Rivas, L. *Biopolymers, Pept. Sci.* **1998**, *47*, 415-433.

6.22 Tossi, A., Sandri, L., Giangspero, A. *Biopolymers, Pept. Sci.* **2000**, *55*, 4-30.

6.23 Falb, E., Yechezkel, T., Salitra, Y., Gilon, C. *J. Peptide Res.* **1999**, *53*, 507-517.

6.24 Carpino, L. A., Chao, H. G., Beyermann, M., Bienert, M. *J. Org. Chem.* **1991**, *56*, 2635-2642.

6.25 Carpino, L. A., Beyermann, M., Wenshuh, H., Bienert, M. *Acc. Chem. Res.* **1996**, *29*, 268-274.

6.26 Hammarström, L. G. J., Giraldes, J., McLaughlin, M. L., Billodeaux, D. R., Fronczek, F. R. *Acta Cryst.* **2000**, *C56*, 1484-1486.

APPENDIX. CRYSTAL STRUCTURE ANALYSIS OF *o*-NITROBENZENESULFONYL AMINO ACID DERIVATIVES

A.1. *o*NBS-Aib-OH

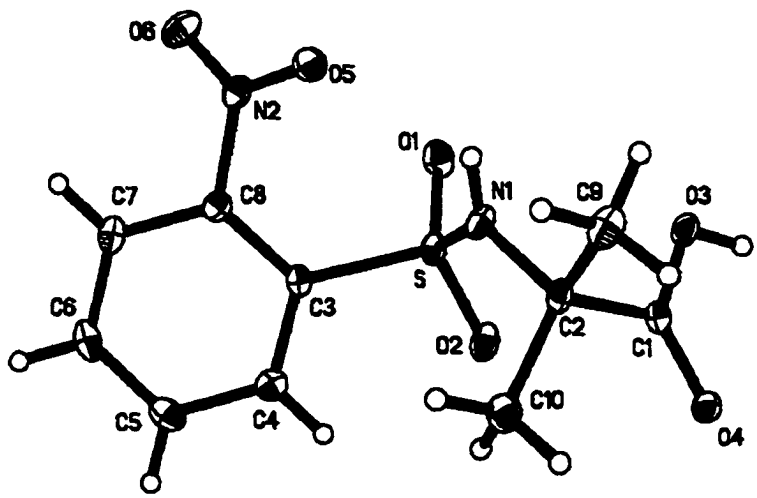

Coordinates

Atom	X	Y	Z
S	0.72056(4)	0.74709(4)	0.66517(4)
O1	0.7351(1)	0.6310(1)	0.7369(1)
O2	0.6911(1)	0.8615(1)	0.7143(1)
O3	0.9857(1)	0.8572(1)	0.9103(1)
O4	0.9402(1)	1.0585(1)	0.8421(1)
O5	0.7824(1)	0.5380(1)	0.5226(1)
O6	0.6262(1)	0.4020(1)	0.4448(1)
N1	0.8494(1)	0.7755(1)	0.6512(2)
N2	0.6668(1)	0.5099(1)	0.4677(2)
C1	0.9453(2)	0.9467(2)	0.8181(2)
C2	0.9124(2)	0.8995(2)	0.6751(2)

Coordinates (continued)

C3	0.5912(2)	0.7231(2)	0.4981(2)
C4	0.4957(2)	0.8161(2)	0.4452(2)
H4	0.505	0.891	0.496
C5	0.3871(2)	0.8002(2)	0.3197(2)
H5	0.324	0.865	0.284
C6	0.3702(2)	0.6904(2)	0.2465(2)
H6	0.296	0.680	0.161
C7	0.4617(2)	0.5946(2)	0.2986(2)
H7	0.449	0.518	0.250
C8	0.5715(2)	0.6127(2)	0.4224(2)
C9	1.0419(2)	0.8788(2)	0.6737(2)
H9A	1.093	0.816	0.742
H9B	1.090	0.958	0.694
H9C	1.026	0.849	0.584
C10	0.8295(2)	0.9953(2)	0.5664(2)
H10A	0.811	0.963	0.477
H10B	0.876	1.075	0.584
H10C	0.748	1.008	0.570
H3O	1.010(3)	0.894(3)	0.991(3)
H1N	0.887(2)	0.716(2)	0.648(3)

Bond Distances and Bond Angles

Bond	Distance	Bond Angle	
S - O1	1.434(1) Å	O1 - S - O2	120.1(1)°
S - O2	1.438(1) Å	O1 - S - N1	109.9(1)°
S - N1	1.610(1) Å	O1 - S - C3	106.3(1)°
S - C3	1.783(2) Å	O2 - S - N1	106.2(1)°
		O2 - S - C3	106.3(1)°
		N1 - S - C3	107.5(1)°
O1 - S	1.434(1) Å		
O2 - S	1.438(1) Å		
O3 - C1	1.314(2) Å	C1 - O3 - H3O	107.3(20)°
O3 - H3O	0.896(30) Å		
O4 - C1	1.224(2) Å		
O5 - N2	1.229(1) Å		
O6 - N2	1.220(2) Å		
N1 - S	1.610(1) Å	S - N1 - C2	124.1(1)°
N1 - C2	1.470(2) Å	S - N1 - H1N	115.0(10)°
N1 - H1N	0.780(18) Å	C2 - N1 - H1N	119.3(11)°
N2 - O5	1.229(1) Å	O5 - N2 - O6	124.1(1)°
N2 - O6	1.220(2) Å	O5 - N2 - C8	118.0(1)°
N2 - C8	1.469(2) Å	O6 - N2 - C8	117.8(1)°
C1 - O3	1.314(2) Å	O3 - C1 - O4	124.6(1)°
C1 - O4	1.224(2) Å	O3 - C1 - C2	113.4(1)°

Bond Distances and Bond Angles (continued)

C1 - C2	1.535(2) Å	O4 - C1 - C2	121.9(1)°
C2 - N1	1.470(2) Å	N1 - C2 - C1	110.0(1)°
C2 - C1	1.535(2) Å	N1 - C2 - C9	106.4(1)°
C2 - C9	1.533(1) Å	N1 - C2 - C10	111.9(1)°
C2 - C10	1.530(2) Å	C1 - C2 - C9	106.6(1)°
		C1 - C2 - C10	111.2(1)°
		C9 - C2 - C10	110.5(1)°
C3 - S	1.783(2) Å	S - C3 - C4	117.3(1)°
C3 - C4	1.396(2) Å	S - C3 - C8	124.6(1)°
C3 - C8	1.398(2) Å	C4 - C3 - C8	117.7(1)°
C4 - C3	1.396(2) Å	C3 - C4 - H4	119.6°
C4 - H4	0.949 Å	C3 - C4 - C5	120.8(2)°
C4 - C5	1.390(2) Å	H4 - C4 - C5	119.6°
C5 - C4	1.390(2) Å	C4 - C5 - H5	119.8°
C5 - H5	0.950 Å	C4 - C5 - C6	120.5(2)°
C5 - C6	1.382(3) Å	H5 - C5 - C6	119.8°
C6 - C5	1.382(3) Å	C5 - C6 - H6	120.0°
C6 - H6	0.950 Å	C5 - C6 - C7	120.0(2)°
C6 - C7	1.390(2) Å	H6 - C6 - C7	120.0°
C7 - C6	1.390(2) Å	C6 - C7 - H7	120.4°
C7 - H7	0.950 Å	C6 - C7 - C8	119.1(2)°
C7 - C8	1.389(2) Å	H7 - C7 - C8	120.5°

Bond Distances and Bond Angles (continued)

C8 - N2	1.469(2) Å	N2 - C8 - C3	122.1(1)°
C8 - C3	1.398(2) Å	N2 - C8 - C7	116.0(1)°
C8 - C7	1.389(2) Å	C3 - C8 - C7	121.9(1)°
C9 - C2	1.533(1) Å	C2 - C9 - H9A	109.4°
C9 - H9A	0.980 Å	C2 - C9 - H9B	109.5°
C9 - H9B	0.980 Å	C2 - C9 - H9C	109.5°
C9 - H9C	0.980 Å	H9A - C9 - H9B	109.5°
C10 - C2	1.530(2) Å	C2 - C10 - H10A	109.5°
C10 - H10A	0.980 Å	C2 - C10 - H10B	109.5°
C10 - H10B	0.980 Å	C2 - C10 - H10C	109.5°
C10 - H10C	0.980 Å	H10A - C10 - H10B	109.5°

Experimental

Crystal Data

$C_{10}H_{12}N_2O_6S$	$a = 11.665$ (3) Å	D_x=1.572 Mg m^{-3}
$M_r = 288.28$	$b = 10.614$ (2) Å	Mo K_α radiation
Monoclinic	$c = 11.121$ (4) Å	$\lambda = 0.71073$ Å
Space Group: $P2_1/c$	$\beta = 117.80$ (2)°	$T = 100$ K

Data collection

3536 independent reflections

$\theta_{max} = 30.0°$

$R(F) = 0.042$ (183 parameters)

A.2. *o*NBS-Ac$_6$c-OH

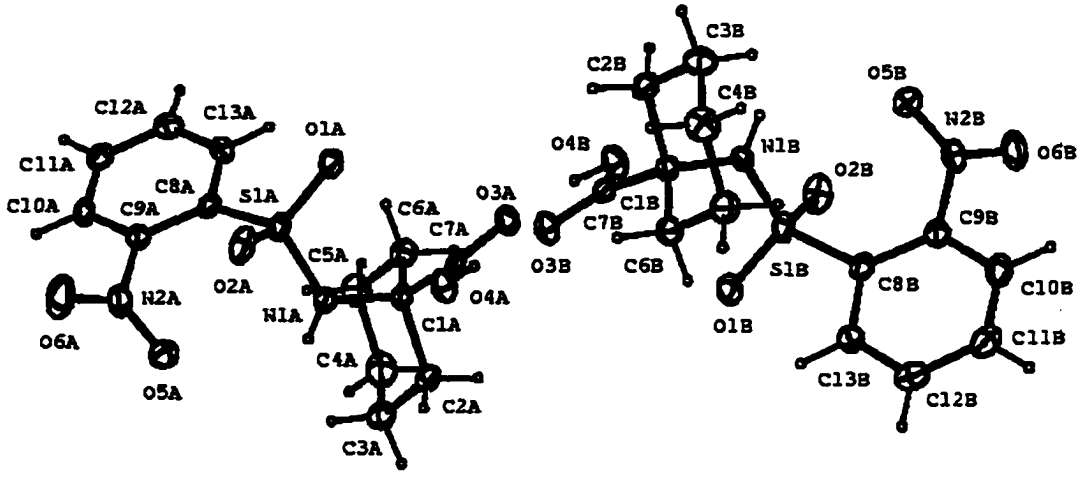

Coordinates

Atom	X	Y	Z
S1	0.09596(3)	0.97588(3)	0.32063(4)
O1	0.07698(10)	0.95375(10)	0.2103(1)
O2	0.06725(10)	0.91675(10)	0.3854(1)
O3	0.2461(1)	0.81592(10)	0.4065(1)
H3O	0.241(2)	0.760(2)	0.413(2)
O4	0.24094(10)	0.81240(9)	0.5707(1)
O5	0.14870(10)	1.1214(1)	0.1952(1)
O6	0.0177(1)	1.1534(2)	0.0649(1)
N1	0.2041(1)	0.9921(1)	0.3861(1)
H1N	0.230(2)	1.003(2)	0.345(2)
N2	0.0665(1)	1.1387(1)	0.1599(1)
C1	0.2458(1)	0.8540(1)	0.4949(2)

Coordinates (continued)

C2	0.2565(1)	0.9556(1)	0.4958(2)
C3	0.0400(1)	1.0790(1)	0.3179(2)
C4	0.0017(1)	1.0927(2)	0.3932(2)
H4	0.011	1.050	0.449
C5	-0.0502(1)	1.1680(2)	0.3893(2)
H5	-0.075	1.177	0.443
C6	-0.0664(1)	1.2302(1)	0.3079(2)
H6	-0.103	1.281	0.304
C7	-0.0290(1)	1.2184(1)	0.2318(2)
H7	-0.040	1.261	0.176
C8	0.0245(1)	1.1443(1)	0.2386(2)
C9	0.3585(1)	0.9748(1)	0.5226(2)
H9A	0.397	0.945	0.592
H9B	0.375	0.950	0.465
C10	0.2294(1)	0.9995(1)	0.5820(2)
H10A	0.164	0.989	0.563
H10B	0.264	0.971	0.654
C11	0.3792(1)	1.0750(1)	0.5333(2)
H11A	0.446	1.084	0.556
H11B	0.348	1.104	0.462
C12	0.3490(2)	1.1189(2)	0.6155(2)
H12A	0.358	1.184	0.615

Coordinates (continued)

H12B	0.387	1.096	0.689
C13	0.2488(2)	1.0999(1)	0.5899(2)
H13A	0.210	1.129	0.520
H13B	0.233	1.126	0.647
S1'	0.39312(3)	0.48665(3)	0.68607(4)
O1'	0.3976(1)	0.49706(10)	0.7938(1)
O2'	0.42115(10)	0.55820(10)	0.6352(1)
O3'	0.2330(1)	0.63264(10)	0.5829(1)
H3O'	0.231(2)	0.691(2)	0.573(2)
O4'	0.23567(10)	0.64204(9)	0.4180(1)
O5'	0.34019(10)	0.3166(1)	0.7739(1)
O6'	0.4629(1)	0.2774(1)	0.9117(1)
N1'	0.2909(1)	0.4609(1)	0.6055(1)
H1N'	0.260(2)	0.433(2)	0.632(2)
N2'	0.4230(1)	0.3043(1)	0.8187(1)
C1'	0.2384(1)	0.5980(1)	0.4959(2)
C2'	0.2447(1)	0.4959(1)	0.4948(2)
C3'	0.4653(1)	0.3952(1)	0.6891(2)
C4'	0.5174(1)	0.4014(2)	0.6278(2)
H4'	0.512	0.453	0.584
C5'	0.5775(2)	0.3341(2)	0.6293(2)
H5'	0.611	0.339	0.585

Coordinates (continued)

C6'	0.5890(1)	0.2599(2)	0.6956(2)
H6'	0.630	0.214	0.697
C7'	0.5399(1)	0.2535(1)	0.7599(2)
H7'	0.549	0.204	0.807
C8'	0.4778(1)	0.3197(1)	0.7547(2)
C9'	0.1459(1)	0.4597(1)	0.4502(2)
H9'1	0.118	0.474	0.502
H9'2	0.110	0.490	0.380
C10'	0.2909(1)	0.4666(1)	0.4192(2)
H10C	0.260	0.496	0.348
H10D	0.355	0.486	0.450
C11'	0.1424(1)	0.3588(1)	0.4324(2)
H11C	0.172	0.329	0.504
H11D	0.078	0.339	0.400
C12'	0.1897(2)	0.3313(2)	0.3586(2)
H12C	0.190	0.265	0.353
H12D	0.156	0.356	0.285
C13'	0.2877(1)	0.3656(1)	0.4029(2)
H13C	0.316	0.350	0.352
H13D	0.323	0.336	0.473

Bond Distances and Bond Angles

Bond	Distance	Bond Angle	
S1 - O1	1.429(2) Å	O1 - S1 - O2	119.9(1)°
S1 - O2	1.440(1) Å	O1 - S1 - N1	109.7(1)°
S1 - N1	1.613(1) Å	O1 - S1 - C3	106.5(1)°
S1 - C3	1.778(2) Å	O2 - S1 - N1	107.1(1)°
		O2 - S1 - C3	105.5(1)°
		N1 - S1 - C3	107.5(1)°
O1 - S1	1.429(2) Å		
O2 - S1	1.440(1) Å		
O3 - H3O	0.850(30) Å	H3O - O3 - C1	107.5(16)°
O3 - C1	1.319(2) Å		
O4 - C1	1.224(2) Å		
O5 - N2	1.232(2) Å		
O6 - N2	1.221(2) Å		
N1 - S1	1.613(1) Å	S1 - N1 - H1N	112.3(16)°
N1 - H1N	0.829(21) Å	S1 - N1 - C2	123.0(1)°
N1 - C2	1.478(3) Å	H1N - N1 - C2	119.9(16)°
N2 - O5	1.232(2) Å	O5 - N2 - O6	125.3(2)°
N2 - O6	1.221(2) Å	O5 - N2 - C8	117.3(2)°
N2 - C8	1.465(2) Å	O6 - N2 - C8	117.3(1)°
C1 - O3	1.319(2) Å	O3 - C1 - O4	123.6(2)°
C1 - O4	1.224(2) Å	O3 - C1 - C2	113.4(2)°

Bond Distances and Bond Angles (continued)

C1 - C2	1.531(3) Å	O4 - C1 - C2	123.0(2)°
C2 - N1	1.478(3) Å	N1 - C2 - C1	110.1(2)°
C2 - C1	1.531(3) Å	N1 - C2 - C9	106.7(1)°
C2 - C9	1.548(2) Å	N1 - C2 - C10	112.0(1)°
C2 - C10	1.538(3) Å	C1 - C2 - C9	106.9(1)°
		C1 - C2 - C10	111.5(1)°
		C9 - C2 - C10	109.4(1)°
C3 - S1	1.778(2) Å	S1 - C3 - C4	118.5(2)°
C3 - C4	1.391(2) Å	S1 - C3 - C8	124.1(1)°
C3 - C8	1.394(3) Å	C4 - C3 - C8	117.2(2)°
C4 - C3	1.391(2) Å	C3 - C4 - H4	119.3°
C4 - H4	0.950 Å	C3 - C4 - C5	121.5(2)°
C4 - C5	1.389(3) Å	H4 - C4 - C5	119.2°
C5 - C4	1.389(3) Å	C4 - C5 - H5	120.1°
C5 - H5	0.950 Å	C4 - C5 - C6	119.9(2)°
C5 - C6	1.381(3) Å	H5 - C5 - C6	120.0°
C6 - C5	1.381(3) Å	C5 - C6 - H6	120.1°
C6 - H6	0.951 Å	C5 - C6 - C7	119.9(2)°
C6 - C7	1.386(2) Å	H6 - C6 - C7	120.1°
C7 - C6	1.386(2) Å	C6 - C7 - H7	120.3°
C7 - H7	0.950 Å	C6 - C7 - C8	119.4(2)°
C7 - C8	1.382(2) Å	H7 - C7 - C8	120.3°

Bond Distances and Bond Angles (continued)

C8 - N2	1.465(2) Å	N2 - C8 - C3	121.3(1)°
C8 - C3	1.394(3) Å	N2 - C8 - C7	116.7(2)°
C8 - C7	1.382(2) Å	C3 - C8 - C7	122.1(1)°
C9 - C2	1.548(2) Å	C2 - C9 - H9A	109.3°
C9 - H9A	0.990 Å	C2 - C9 - H9B	109.2°
C9 - H9B	0.989 Å	C2 - C9 - C11	111.8(1)°
C9 - C11	1.532(3) Å	H9A - C9 - H9B	108.0°
		H9A - C9 - C11	109.2°
		H9B - C9 - C11	109.3°
C10 - C2	1.538(3) Å	C2 - C10 - H10A	109.4°
C10 - H10A	0.989 Å	C2 - C10 - H10B	109.5°
C10 - H10B	0.990 Å	C2 - C10 - C13	111.2(1)°
C10 - C13	1.531(3) Å	H10A - C10 - H10B	108.0°
		H10A - C10 - C13	109.4°
		H10B - C10 - C13	109.4°
C11 - C9	1.532(3) Å	C9 - C11 - H11A	109.2°
C11 - H11A	0.989 Å	C9 - C11 - H11B	109.2°
C11 - H11B	0.990 Å	C9 - C11 - C12	111.9(2)°
C11 - C12	1.521(3) Å	H11A - C11 - H11B	107.9°
		H11A - C11 - C12	109.2°
		H11B - C11 - C12	109.3°
C12 - C11	1.521(3) Å	C11 - C12 - H12A	109.4°

Bond Distances and Bond Angles (continued)

C12 - H12A	0.990 Å	C11 - C12 - H12B	109.4°
C12 - H12B	0.990 Å	C11 - C12 - C13	111.4(2)°
C12 - C13	1.524(2) Å	H12A - C12 - H12B	108.0°
		H12A - C12 - C13	109.4°
		H12B - C12 - C13	109.3°
C13 - C10	1.531(3) Å	C10 - C13 - C12	111.4(2)°
C13 - C12	1.524(2) Å	C10 - C13 - H13A	109.4°
C13 - H13A	0.990 Å	C10 - C13 - H13B	109.4°
C13 - H13B	0.990 Å	C12 - C13 - H13A	109.3°
C12 - C13 - H13B	109.3°	H13A - C13 - H13B	108.0°
S1' - O1'	1.429(2) Å	O1' - S1' - O2'	120.1(1)°
S1' - O2'	1.436(1) Å	O1' - S1' - N1'	109.6(1)°
S1' - N1'	1.604(1) Å	O1' - S1' - C3'	106.9(1)°
S1' - C3'	1.781(2) Å	O2' - S1' - N1'	106.6(1)°
		O2' - S1' - C3'	105.3(1)°
		N1' - S1' - C3'	107.8(1)°
O1' - S1'	1.429(2) Å		
O2' - S1'	1.436(1) Å		
O3' - H3O'	0.883(30) Å	H3O' - O3' - C1'	105.6(16)°
O3' - C1'	1.314(2) Å		
O4' - C1'	1.223(2) Å		
O5' - N2'	1.228(2) Å		

Bond Distances and Bond Angles (continued)

O6' - N2'	1.222(2) Å		
N1' - S1'	1.604(1) Å	S1' - N1' - H1N'	117.0(16)°
N1' - H1N'	0.828(22) Å	S1' - N1' - C2'	124.2(1)°
N1' - C2'	1.468(2) Å	H1N' - N1' - C2'	118.0(16)°
N2' - O5'	1.228(2) Å	O5' - N2' - O6'	124.7(1)°
N2' - O6'	1.222(2) Å	O5' - N2' - C8'	117.9(2)°
N2' - C8'	1.471(2) Å	O6' - N2' - C8'	117.4(1)°
C1' - O3'	1.314(2) Å	O3' - C1' - O4'	123.7(2)°
C1' - O4'	1.223(2) Å	O3' - C1' - C2'	115.5(2)°
C1' - C2'	1.532(3) Å	O4' - C1' - C2'	120.7(2)°
C2' - N1'	1.468(2) Å	N1' - C2' - C1'	110.8(2)°
C2' - C1'	1.532(3) Å	N1' - C2' - C9'	106.9(1)°
C2' - C9'	1.546(2) Å	N1' - C2' - C10'	112.7(1)°
C2' - C10'	1.540(2) Å	C1' - C2' - C9'	107.1(1)°
		C1' - C2' - C10'	110.0(1)°
		C9' - C2' - C10'	109.2(1)°
C3' - S1'	1.781(2) Å	S1' - C3' - C4'	118.1(2)°
C3' - C4'	1.389(2) Å	S1' - C3' - C8'	124.5(1)°
C3' - C8'	1.398(3) Å	C4' - C3' - C8'	117.3(2)°
C4' - C3'	1.389(2) Å	C3' - C4' - H4'	119.4°
C4' - H4'	0.951 Å	C3' - C4' - C5'	121.2(2)°
C4' - C5'	1.387(3) Å	H4' - C4' - C5'	119.4°

Bond Distances and Bond Angles (continued)

C5' - C4'	1.387(3) Å	C4' - C5' - H5'	119.9°
C5' - H5'	0.949 Å	C4' - C5' - C6'	120.3(2)°
C5' - C6'	1.390(3) Å	H5' - C5' - C6'	119.9°
C6' - C5'	1.390(3) Å	C5' - C6' - H6'	120.2°
C6' - H6'	0.950 Å	C5' - C6' - C7'	119.6(2)°
C6' - C7'	1.384(2) Å	H6' - C6' - C7'	120.2°
C7' - C6'	1.384(2) Å	C6' - C7' - H7'	120.3°
C7' - H7'	0.949 Å	C6' - C7' - C8'	119.4(2)°
C7' - C8'	1.384(2) Å	H7' - C7' - C8'	120.3°
C8' - N2'	1.471(2) Å	N2' - C8' - C3'	121.7(1)°
C8' - C3'	1.398(3) Å	N2' - C8' - C7'	116.1(2)°
C8' - C7'	1.384(2) Å	C3' - C8' - C7'	122.1(1)°
C9' - C2'	1.546(2) Å	C2' - C9' - H9'1	109.2°
C9' - H9'1	0.990 Å	C2' - C9' - H9'2	109.2°
C9' - H9'2	0.990 Å	C2' - C9' - C11'	112.0(1)°
C9' - C11'	1.528(3) Å	H9'1 - C9' - H9'2	107.9°
		H9'1 - C9' - C11'	109.2°
		H9'2 - C9' - C11'	109.2°
C10' - C2'	1.540(2) Å	C2' - C10' - H10C	109.2°
C10' - H10C	0.990 Å	C2' - C10' - H10D	109.1°
C10' - H10D	0.990 Å	C2' - C10' - C13'	112.4(1)°
C10' - C13'	1.527(3) Å	H10C - C10' - H10D	107.8°

Bond Distances and Bond Angles (continued)

		H10C - C10' - C13'	109.1°
		H10D - C10' - C13'	109.1°
C11' - C9'	1.528(3) Å	C9' - C11' - H11C	109.2°
C11' - H11C	0.991 Å	C9' - C11' - H11D	109.2°
C11' - H11D	0.990 Å	C9' - C11' - C12'	111.9(2)°
C11' - C12'	1.525(3) Å	H11C - C11' - H11D	107.9°
		H11C - C11' - C12'	109.2°
		H11D - C11' - C12'	109.3°
C12' - C11'	1.525(3) Å	C11' - C12' - H12C	109.5°
C12' - H12C	0.990 Å	C11' - C12' - H12D	109.5°
C12' - H12D	0.990 Å	C11' - C12' - C13'	110.7(2)°
C12' - C13'	1.524(2) Å	H12C - C12' - H12D	108.1°
H12C - C12' - C13'	109.5°	H12D - C12' - C13'	109.5°
C13' - C10'	1.527(3) Å	C10' - C13' - C12'	111.1(1)°
C13' - C12'	1.524(2) Å	C10' - C13' - H13C	109.4°
C13' - H13C	0.990 Å	C10' - C13' - H13D	109.4°
C13' - H13D	0.990 Å	C12' - C13' - H13C	109.4°
		C12' - C13' - H13D	109.4°
		H13C - C13' - H13D	108.1°

Experimental

Crystal data

$C_{13}H_{16}N_2O_6S$	$a = 15.9780\ (12)$ Å	$Dx = 1.479$ Mg m^{-3}
$M_r = 328.34$	$b = 14.9840\ (11)$ Å	Mo K_α radiation
Monoclinic	$c = 13.4360\ (10)$ Å	$\lambda = 0.71073$ Å
Space Group: $P2_1/c$	$\beta = 113.568\ (6)°$	$T = 100$ K

Data Collection

7815 independent reflections

$R[F^2>2\sigma(F^2)] = 0.043$

$\theta_{max} = 29.0°$

A.3. *o*NBS-Api(Boc)-OH

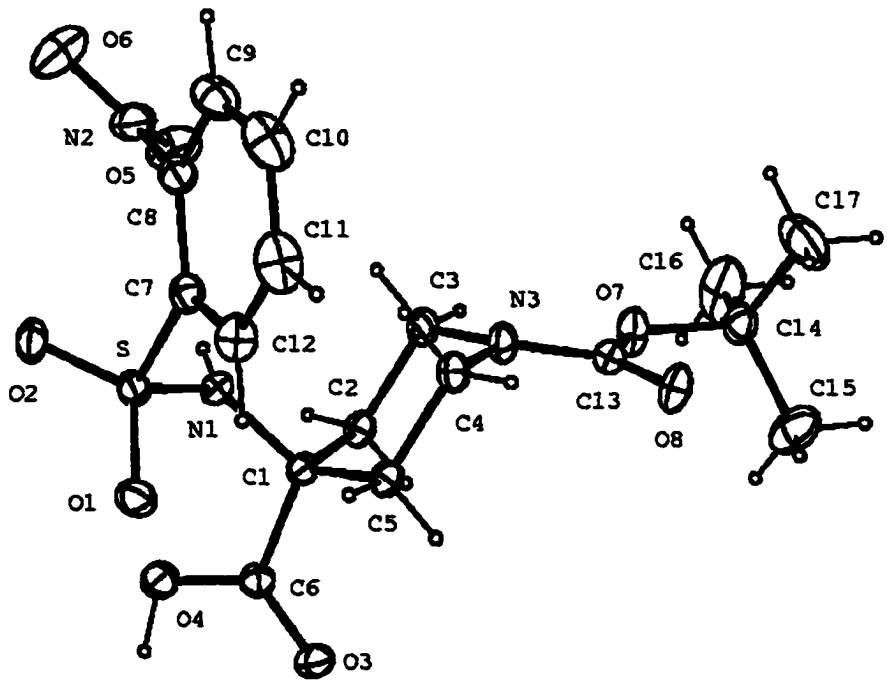

Coordinates

Atom	X	Y	Z
S	0.40527(8)	0.15956(2)	0.93612(5)
O1	0.5100(2)	0.13887(5)	1.04800(10)
O2	0.2038(2)	0.17126(5)	0.9391(2)
O3	0.6663(2)	0.02447(5)	0.9209(2)
O4	0.3601(2)	0.04815(5)	0.9285(2)
O5	0.2524(3)	0.20772(6)	0.6689(2)
O6	0.1454(3)	0.26927(7)	0.7482(3)
O7	0.8907(2)	0.08623(6)	0.41070(10)
O8	1.1248(2)	0.11205(5)	0.5641(2)

Coordinates (continued)

N1	0.4260(2)	0.12758(5)	0.8108(2)
N2	0.2692(3)	0.23997(6)	0.7425(2)
N3	0.8018(2)	0.12037(6)	0.5896(2)
C1	0.5716(3)	0.09143(6)	0.8013(2)
C2	0.5404(3)	0.07291(7)	0.6596(2)
C3	0.5994(3)	0.10653(8)	0.5574(2)
C4	0.8353(3)	0.14132(7)	0.7190(2)
C5	0.7825(3)	0.10889(7)	0.8263(2)
C6	0.5367(3)	0.05204(7)	0.8925(2)
C7	0.5302(3)	0.21103(7)	0.9088(2)
C8	0.4530(3)	0.24542(7)	0.8264(2)
C9	0.5494(4)	0.28608(8)	0.8136(3)
C10	0.7278(4)	0.29226(9)	0.8827(3)
C11	0.8077(4)	0.25951(9)	0.9655(3)
C12	0.7087(4)	0.21879(8)	0.9802(2)
C13	0.9540(3)	0.10617(7)	0.5241(2)
C14	1.0210(3)	0.07312(8)	0.3102(2)
C15	1.1620(5)	0.03750(10)	0.3628(3)
C16	0.8829(5)	0.05520(10)	0.2018(3)
C17	1.1285(6)	0.11400(10)	0.2665(3)
H1N	0.340(3)	0.1287(6)	0.756(2)
H4O	0.358(4)	0.0218(9)	0.980(3)

Coordinates (continued)

H2a	0.4060	0.0658	0.6409
H2b	0.6162	0.0462	0.6537
H3a	0.5869	0.0928	0.4725
H3b	0.5169	0.1323	0.5572
H4a	0.7571	0.1678	0.7215
H4b	0.9693	0.1493	0.7342
H5a	0.8693	0.0838	0.8288
H5b	0.7959	0.1241	0.9089
H9	0.4930	0.3093	0.7580
H10	0.7969	0.3197	0.8729
H11	0.9310	0.2644	1.0133
H12	0.7636	0.1963	1.0391
H15a	1.2450	0.0295	0.2965
H15b	1.2384	0.0490	0.4379
H15c	1.0919	0.0116	0.3874
H16a	0.9539	0.0456	0.1305
H16b	0.8133	0.0303	0.2335
H16c	0.7934	0.0783	0.1721
H17a	1.2126	0.1053	0.2015
H17b	1.0372	0.1357	0.2302
H17c	1.2035	0.1267	0.3403

Bond Distances and Bond Angles

Bond	Distance	Bond Angle	
S - O1	1.429(1) Å	O1 - S - O2	120.6(1)°
S - O2	1.430(1) Å	O1 - S - N1	107.8(1)°
S - N1	1.602(2) Å	O1 - S - C7	105.8(1)°
S - C7	1.781(2) Å	O2 - S - N1	108.2(1)°
		O2 - S - C7	106.1(1)°
		N1 - S - C7	107.7(1)°
O1 - S	1.429(1) Å		
O2 - S	1.430(1) Å		
O3 - C6	1.223(2) Å		
O4 - C6	1.303(2) Å	C6 - O4 - H4O	106.8(15)°
O4 - H4O	0.939(28) Å		
O5 - N2	1.211(3) Å		
O6 - N2	1.219(3) Å		
O7 - C13	1.333(2) Å	C13 - O7 - C14	123.0(1)°
O7 - C14	1.467(2) Å		
O8 - C13	1.221(2) Å		
N1 - S	1.602(2) Å	S - N1 - C1	126.0(1)°
N1 - C1	1.473(2) Å	S - N1 - H1N	115.5(14)°
N1 - H1N	0.777(20) Å	C1 - N1 - H1N	117.6(14)°
N2 - O5	1.211(3) Å	O5 - N2 - O6	124.0(2)°
N2 - O6	1.219(3) Å	O5 - N2 - C8	118.4(2)°

Bond Distances and Bond Angles (continued)

N2 - C8	1.470(3) Å	O6 - N2 - C8	117.6(2)°
N3 - C3	1.460(2) Å	C3 - N3 - C4	113.3(2)°
N3 - C4	1.453(3) Å	C3 - N3 - C13	124.4(2)°
N3 - C13	1.354(2) Å	C4 - N3 - C13	120.5(1)°
C1 - N1	1.473(2) Å	N1 - C1 - C2	106.2(2)°
C1 - C2	1.537(3) Å	N1 - C1 - C5	112.4(1)°
C1 - C5	1.539(3) Å	N1 - C1 - C6	111.9(2)°
C1 - C6	1.520(3) Å	C2 - C1 - C5	109.1(2)°
		C2 - C1 - C6	106.3(2)°
		C5 - C1 - C6	110.6(2)°
C2 - C1	1.537(3) Å	C1 - C2 - C3	112.5(2)°
C2 - C3	1.517(3) Å	C1 - C2 - H2a	108.7°
C2 - H2a	0.950 Å	C1 - C2 - H2b	108.8°
C2 - H2b	0.951 Å	C3 - C2 - H2a	108.7°
		C3 - C2 - H2b	108.7°
		H2a - C2 - H2b	109.4°
C3 - N3	1.460(2) Å	N3 - C3 - C2	109.6(2)°
C3 - C2	1.517(3) Å	N3 - C3 - H3a	109.4°
C3 - H3a	0.950 Å	N3 - C3 - H3b	109.4°
C3 - H3b	0.950 Å	C2 - C3 - H3a	109.4°
		C2 - C3 - H3b	109.4°
		H3a - C3 - H3b	109.5°

Bond Distances and Bond Angles (continued)

C4 - N3	1.453(3) Å	N3 - C4 - C5	110.5(2)°
C4 - C5	1.519(3) Å	N3 - C4 - H4a	109.2°
C4 - H4a	0.951 Å	N3 - C4 - H4b	109.2°
C4 - H4b	0.950 Å	C5 - C4 - H4a	109.3°
		C5 - C4 - H4b	109.2°
		H4a - C4 - H4b	109.5°
C5 - C1	1.539(3) Å	C1 - C5 - C4	111.9(2)°
C5 - C4	1.519(3) Å	C1 - C5 - H5a	108.8°
C5 - H5a	0.951 Å	C1 - C5 - H5b	108.8°
C5 - H5b	0.949 Å	C4 - C5 - H5a	108.9°
		C4 - C5 - H5b	108.9°
		H5a - C5 - H5b	109.5°
C6 - O3	1.223(2) Å	O3 - C6 - O4	123.5(2)°
C6 - O4	1.303(2) Å	O3 - C6 - C1	120.3(2)°
C6 - C1	1.520(3) Å	O4 - C6 - C1	116.0(2)°
C7 - S	1.781(2) Å	S - C7 - C8	123.6(1)°
C7 - C8	1.392(3) Å	S - C7 - C12	118.4(2)°
C7 - C12	1.389(3) Å	C8 - C7 - C12	117.8(2)°
C8 - N2	1.470(3) Å	N2 - C8 - C7	122.1(2)°
C8 - C7	1.392(3) Å	N2 - C8 - C9	115.8(2)°
C8 - C9	1.384(3) Å	C7 - C8 - C9	122.0(2)°
C9 - C8	1.384(3) Å	C8 - C9 - C10	118.8(2)°

Bond Distances and Bond Angles (continued)

C9 - C10	1.371(4) Å	C8 - C9 - H9	120.6°
C9 - H9	0.950 Å	C10 - C9 - H9	120.6°
C10 - C9	1.371(4) Å	C9 - C10 - C11	121.0(2)°
C10 - C11	1.366(4) Å	C9 - C10 - H10	119.6°
C10 - H10	0.950 Å	C11 - C10 - H10	119.5°
C11 - C10	1.366(4) Å	C10 - C11 - C12	120.2(2)°
C11 - C12	1.397(4) Å	C10 - C11 - H11	120.0°
C11 - H11	0.951 Å	C12 - C11 - H11	119.8°
C12 - C7	1.389(3) Å	C7 - C12 - C11	120.2(2)°
C12 - C11	1.397(4) Å	C7 - C12 - H12	119.9°
C12 - H12	0.950 Å	C11 - C12 - H12	120.0°
C13 - O7	1.333(2) Å	O7 - C13 - O8	125.7(2)°
C13 - O8	1.221(2) Å	O7 - C13 - N3	110.7(2)°
C13 - N3	1.354(2) Å	O8 - C13 - N3	123.6(2)°
C14 - O7	1.467(2) Å	O7 - C14 - C15	110.7(2)°
C14 - C15	1.498(4) Å	O7 - C14 - C16	102.7(2)°
C14 - C16	1.488(4) Å	O7 - C14 - C17	109.8(2)°
C14 - C17	1.503(4) Å	C15 - C14 - C16	111.4(2)°
		C15 - C14 - C17	110.6(2)°
		C16 - C14 - C17	111.5(2)°
C15 - C14	1.498(4) Å	C14 - C15 - H15a	109.4°
C15 - H15a	0.949 Å	C14 - C15 - H15b	109.3°

Bond Distances and Bond Angles (continued)

C15 - H15b	0.951 Å	C14 - C15 - H15c	109.5°
C15 - H15c	0.950 Å	H15a - C15 - H15b	109.5°
		H15a - C15 - H15c	109.6°
C16 - C14	1.488(4) Å	C14 - C16 - H16a	109.5°
C16 - H16a	0.951 Å	C14 - C16 - H16b	109.5°
C16 - H16b	0.949 Å	C14 - C16 - H16c	109.5°
C16 - H16c	0.951 Å	H16a - C16 - H16b	109.5°
		H16a - C16 - H16c	109.5°
C17 - C14	1.503(4) Å	C14 - C17 - H17a	109.4°
C17 - H17a	0.950 Å	C14 - C17 - H17b	109.4°
C17 - H17b	0.949 Å	C14 - C17 - H17c	109.4°
C17 - H17c	0.950 Å	H17a - C17 - H17b	109.6°
		H17a - C17 - H17c	109.5°

Crystal data

$C_{17}H_{23}N_3O_8S$	$a = 6.8729$ (2) Å	$Dx = 1.386$ Mg m^{-3}
$M_r = 429.45$	$b = 29.564$ (2) Å	Cu-K_α radiation
Monoclinic	$c = 10.1549$ (7) Å	$\lambda = 1.54184$ Å
Space Group: $P2_1/c$	$\beta = 94.946$ (4)°	$T = 294$ K

Data Collection

4239 independent reflections

$R = 0.044$	$\theta_{max} = 75.0°$

A.4. *o*NBS-Lys(Z)-OH

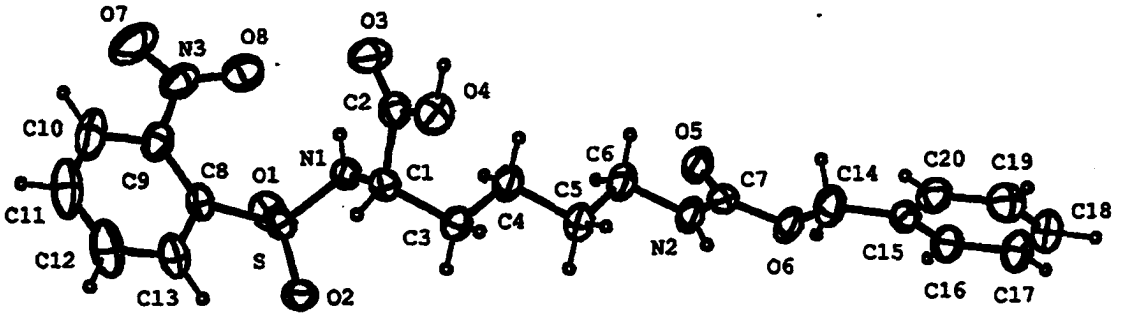

Coordinates

Atom	X	Y	Z
S	0.44587(7)	0.67712(2)	0.46520(10)
O1	0.4531(2)	0.68197(6)	0.7285(4)
O2	0.5378(2)	0.68989(6)	0.3148(4)
O3	0.2694(2)	0.58453(7)	0.2571(5)
O4	0.3539(2)	0.57244(6)	-0.1043(5)
O5	0.8200(2)	0.47620(6)	0.8214(5)
O6	0.9475(2)	0.45421(6)	0.5450(4)
O7	0.1068(2)	0.68812(9)	0.8071(6)
O8	0.2359(2)	0.64832(7)	0.7029(5)
N1	0.4293(2)	0.63241(6)	0.4098(4)
N2	0.8168(2)	0.49479(7)	0.4197(5)
N3	0.1852(2)	0.67845(8)	0.6774(6)
C1	0.4419(3)	0.61719(8)	0.1570(5)
C2	0.3451(3)	0.58965(8)	0.1150(7)
C3	0.5575(3)	0.59816(8)	0.1208(6)

Coordinates (continued)

C4	0.5763(3)	0.56441(9)	0.2916(7)
C5	0.6926(3)	0.54563(9)	0.2592(6)
C6	0.7085(3)	0.51490(9)	0.4496(8)
C7	0.8582(2)	0.47533(8)	0.6128(7)
C8	0.3251(3)	0.70409(8)	0.3652(6)
C9	0.2178(3)	0.70464(9)	0.4745(7)
C10	0.1358(3)	0.72990(10)	0.3948(9)
C11	0.1598(4)	0.75480(10)	0.2063(9)
C12	0.2634(4)	0.75470(10)	0.0963(8)
C13	0.3464(3)	0.72966(9)	0.1770(7)
C14	0.9931(3)	0.42960(10)	0.7356(7)
C15	1.0614(3)	0.39888(8)	0.6157(6)
C16	1.1617(3)	0.38783(9)	0.7161(7)
C17	1.2246(3)	0.35840(10)	0.6177(7)
C18	1.1872(3)	0.33990(10)	0.4125(8)
C19	1.0859(3)	0.35010(10)	0.3057(7)
C20	1.0236(3)	0.37970(10)	0.4082(7)
H4OH	0.300(3)	0.5537(9)	-0.097(6)
H1N	0.378(3)	0.6235(8)	0.472(6)
H2N	0.850(3)	0.496(1)	0.273(5)
H1	0.4392	0.6373	0.0384
H3a	0.6148	0.6167	0.1511

Coordinates (continued)

H3b	0.5629	0.5894	-0.0454
H4a	0.5197	0.5457	0.2594
H4b	0.5697	0.5731	0.4577
H5a	0.7500	0.5645	0.2781
H5b	0.6975	0.5346	0.0987
H6a	0.7063	0.5263	0.6093
H6b	0.6487	0.4968	0.4347
H10	0.0632	0.7301	0.4703
H11	0.1035	0.7723	0.1513
H12	0.2788	0.7718	-0.0361
H13	0.4190	0.7301	0.1014
H14a	0.9329	0.4185	0.8274
H14b	1.0398	0.4442	0.8435
H16	1.1892	0.4009	0.8584
H17	1.2939	0.3510	0.6931
H18	1.2313	0.3199	0.3421
H19	1.0590	0.3369	0.1634
H20	0.9537	0.3870	0.3345

Bond Distances and Bond Angles

Bond	Distance	Bond Angle	
S - O1	1.435(2) Å	O1 - S - O2	118.8(1)°
S - O2	1.427(2) Å	O1 - S - N1	107.9(1)°
S - N1	1.598(2) Å	O1 - S - C8	106.5(1)°
S - C8	1.791(3) Å	O2 - S - N1	106.9(1)°
		O2 - S - C8	105.7(1)°
		N1 - S - C8	110.9(1)°
O1 - S	1.435(2) Å		
O2 - S	1.427(2) Å		
O3 - C2	1.192(4) Å		
O4 - C2	1.332(4) Å	C2 - O4 - H4OH	103.2(21)°
O4 - H4OH	0.913(33) Å		
O5 - C7	1.214(4) Å		
O6 - C7	1.337(3) Å	C7 - O6 - C14	115.2(3)°
O6 - C14	1.444(4) Å		
O7 - N3	1.209(4) Å		
O8 - N3	1.216(4) Å		
N1 - S	1.598(2) Å	S - N1 - C1	120.8(2)°
N1 - C1	1.473(3) Å	S - N1 - H1N	114.4(22)°
N1 - H1N	0.759(34) Å	C1 - N1 - H1N	110.1(24)°
N2 - C6	1.467(4) Å	C6 - N2 - C7	118.4(3)°
N2 - C7	1.337(4) Å	C6 - N2 - H2N	117.5(22)°

Bond Distances and Bond Angles (continued)

N2 - H2N	0.885(29) Å	C7 - N2 - H2N	124.1(22)°
N3 - O7	1.209(4) Å	O7 - N3 - O8	123.5(3)°
N3 - O8	1.216(4) Å	O7 - N3 - C9	117.2(3)°
N3 - C9	1.477(5) Å	O8 - N3 - C9	119.3(3)°
C1 - N1	1.473(3) Å	N1 - C1 - C2	107.0(3)°
C1 - C2	1.509(5) Å	N1 - C1 - C3	111.4(2)°
C1 - C3	1.530(5) Å	N1 - C1 - H1	110.9°
C1 - H1	0.950 Å	C2 - C1 - C3	112.4(2)°
		C2 - C1 - H1	110.0°
		C3 - C1 - H1	105.3°
C2 - O3	1.192(4) Å	O3 - C2 - O4	124.4(3)°
C2 - O4	1.332(4) Å	O3 - C2 - C1	124.5(3)°
C2 - C1	1.509(5) Å	O4 - C2 - C1	111.1(3)°
C3 - C1	1.530(5) Å	C1 - C3 - C4	113.0(3)°
C3 - C4	1.511(5) Å	C1 - C3 - H3a	108.6°
C3 - H3a	0.950 Å	C1 - C3 - H3b	108.6°
C3 - H3b	0.951 Å	C4 - C3 - H3a	108.6°
		C4 - C3 - H3b	108.5°
		H3a - C3 - H3b	109.5°
C4 - C3	1.511(5) Å	C3 - C4 - C5	113.2(3)°
C4 - C5	1.531(5) Å	C3 - C4 - H4a	108.6°
C4 - H4a	0.950 Å	C3 - C4 - H4b	108.5°

Bond Distances and Bond Angles (continued)

C4 - H4b	0.950 Å	C5 - C4 - H4a	108.5°
		C5 - C4 - H4b	108.5°
		H4a - C4 - H4b	109.5°
C5 - C4	1.531(5) Å	C4 - C5 - C6	109.8(3)°
C5 - C6	1.496(5) Å	C4 - C5 - H5a	109.4°
C5 - H5a	0.950 Å	C4 - C5 - H5b	109.4°
C5 - H5b	0.950 Å	C6 - C5 - H5a	109.4°
		C6 - C5 - H5b	109.3°
		H5a - C5 - H5b	109.5°
C6 - N2	1.467(4) Å	N2 - C6 - C5	112.0(3)°
C6 - C5	1.496(5) Å	N2 - C6 - H6a	108.9°
C6 - H6a	0.950 Å	N2 - C6 - H6b	108.8°
C6 - H6b	0.950 Å	C5 - C6 - H6a	108.8°
		C5 - C6 - H6b	108.9°
		H6a - C6 - H6b	109.5°
C7 - O5	1.214(4) Å	O5 - C7 - O6	124.1(3)°
C7 - O6	1.337(3) Å	O5 - C7 - N2	125.2(3)°
C7 - N2	1.337(4) Å	O6 - C7 - N2	110.7(3)°
C8 - S	1.791(3) Å	S - C8 - C9	127.0(2)°
C8 - C9	1.398(5) Å	S - C8 - C13	114.7(3)°
C8 - C13	1.375(5) Å	C9 - C8 - C13	118.0(3)°
C9 - N3	1.477(5) Å	N3 - C9 - C8	122.8(3)°

Bond Distances and Bond Angles (continued)

C9 - C8	1.398(5) Å	N3 - C9 - C10	116.3(3)°
C9 - C10	1.377(5) Å	C8 - C9 - C10	120.9(3)°
C10 - C9	1.377(5) Å	C9 - C10 - C11	119.5(4)°
C10 - C11	1.367(6) Å	C9 - C10 - H10	120.3°
C10 - H10	0.949 Å	C11 - C10 - H10	120.2°
C11 - C10	1.367(6) Å	C10 - C11 - C12	120.7(4)°
C11 - C12	1.360(7) Å	C10 - C11 - H11	119.7°
C11 - H11	0.950 Å	C12 - C11 - H11	119.6°
C12 - C11	1.360(7) Å	C11 - C12 - C13	120.1(4)°
C12 - C13	1.383(5) Å	C11 - C12 - H12	120.0°
C12 - H12	0.948 Å	C13 - C12 - H12	119.9°
C13 - C8	1.375(5) Å	C8 - C13 - C12	120.8(3)°
C13 - C12	1.383(5) Å	C8 - C13 - H13	119.6°
C13 - H13	0.950 Å	C12 - C13 - H13	119.6°
C14 - O6	1.444(4) Å	O6 - C14 - C15	108.6(3)°
C14 - C15	1.488(5) Å	O6 - C14 - H14a	109.6°
C14 - H14a	0.949 Å	O6 - C14 - H14b	109.7°
C14 - H14b	0.950 Å	C15 - C14 - H14a	109.9°
C15 - C14	1.488(5) Å	C14 - C15 - C16	120.2(3)°
C15 - C20	1.379(5) Å	C16 - C15 - C20	118.0(3)°
C16 - C15	1.358(5) Å	C15 - C16 - C17	121.9(3)°

Bond Distances and Bond Angles (continued)

C16 - C17	1.373(5) Å	C15 - C16 - H16	119.0°
C16 - H16	0.951 Å	C17 - C16 - H16	119.1°
C17 - C16	1.373(5) Å	C16 - C17 - C18	119.7(3)°
C17 - C18	1.356(5) Å	C16 - C17 - H17	120.2°
C17 - H17	0.950 Å	C18 - C17 - H17	120.2°
C18 - C17	1.356(5) Å	C17 - C18 - C19	120.2(3)°
C18 - C19	1.375(5) Å	C17 - C18 - H18	119.8°
C18 - H18	0.949 Å	C19 - C18 - H18	119.9°
C19 - C18	1.375(5) Å	C18 - C19 - C20	119.2(3)°
C19 - C20	1.382(5) Å	C18 - C19 - H19	120.4°
C19 - H19	0.951 Å	C20 - C19 - H19	120.5°
C20 - C19	1.382(5) Å	C15 - C20 - H20	119.5°
C20 - H20	0.951 Å	C19 - C20 - H20	119.6°

Crystal data

$C_{20}H_{23}N_3O_8S$	$a = 11.8092\ (13)$ Å	$D_x = 1.391$ Mg m^{-3}
$M_r = 465.49$	$b = 34.832\ (4)$ Å	Cu-K_α radiation
Orthorhombic	$c = 5.4033\ (6)$ Å	$\lambda = 1.54184$ Å
Space Group: $P2_12_12$	$V = 2222.6\ (7)$ Å	$T = 296$ K

Data Collection

2680 independent reflections

$R = 0.039$	$\theta_{max} = 75.0°$

A.5. *o*NBS-Aib-NCA

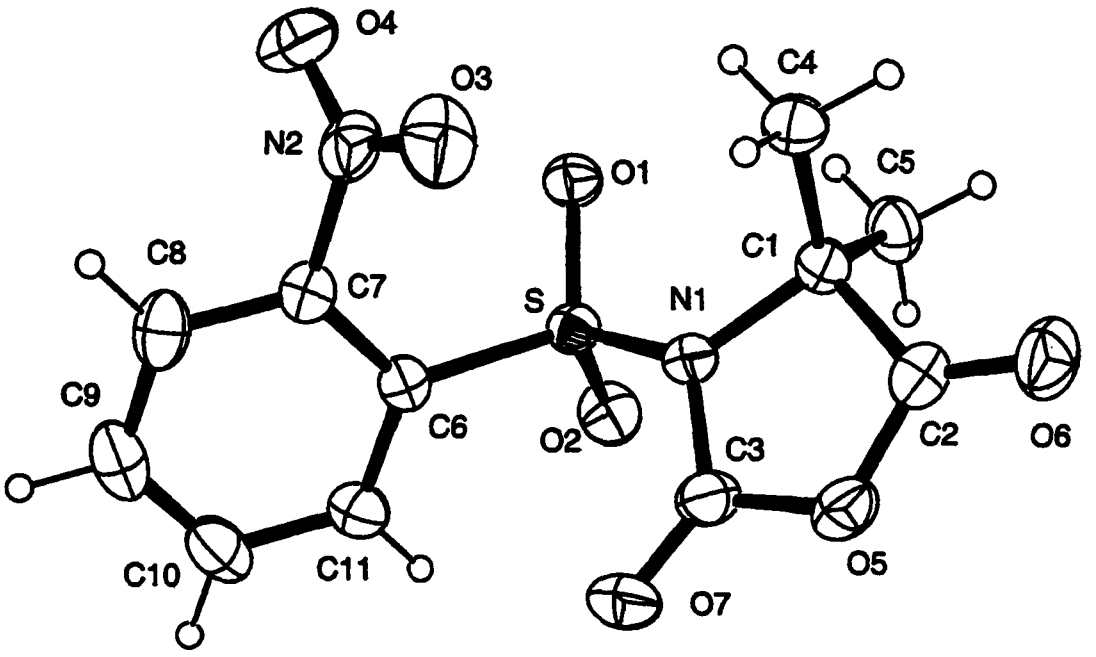

Coordinates

Atom	X	Y	Z
S	0.38287(3)	1.00000	0.22477(3)
O1	0.26310(10)	1.0866(2)	0.14078(9)
O2	0.55330(10)	1.0747(2)	0.25570(10)
O3	0.0169(2)	0.7683(3)	0.1517(2)
O4	0.0698(2)	0.7896(3)	-0.02220(10)
O5	0.2661(2)	0.9594(2)	0.52552(9)
O6	0.0771(2)	1.1794(3)	0.55930(10)
O7	0.4541(2)	0.7813(2)	0.44240(10)
N1	0.27750(10)	0.9938(2)	0.34001(9)

Coordinates (continued)

N2	0.1103(2)	0.7518(3)	0.07750(10)
C1	0.1524(2)	1.1395(2)	0.36710(10)
C2	0.1565(2)	1.1025(3)	0.49300(10)
C3	0.3461(2)	0.9003(3)	0.43430(10)
C4	-0.0350(2)	1.1062(3)	0.3096(2)
C5	0.2160(2)	1.3324(3)	0.3487(2)
C6	0.4124(2)	0.7722(2)	0.18340(10)
C7	0.2888(2)	0.6795(2)	0.10970(10)
C8	0.3284(2)	0.5143(3)	0.06310(10)
C9	0.4936(3)	0.4408(3)	0.0912(2)
C10	0.6181(2)	0.5306(3)	0.1647(2)
C11	0.5782(2)	0.6967(3)	0.2101(2)
H4a	-0.0689	0.9843	0.3234
H4b	-0.1137	1.1884	0.3393
H4c	-0.0386	1.1251	0.2304
H5a	0.3324	1.3467	0.3857
H5b	0.2152	1.3540	0.2699
H5c	0.1401	1.4172	0.3788
H8	0.2429	0.4522	0.0124
H9	0.5222	0.3272	0.0596
H10	0.7313	0.4781	0.1841
H11	0.6648	0.7594	0.2597

Bond Distances and Bond Angles

Bond	Distance	Bond Angle	
S - O1	1.421(1) Å	O1 - S - O2	120.2(1)°
S - O2	1.420(1) Å	O1 - S - N1	104.8(0)°
S - N1	1.674(1) Å	O1 - S - C6	108.7(1)°
S - C6	1.763(1) Å	O2 - S - N1	108.4(1)°
		O2 - S - C6	107.0(1)°
		N1 - S - C6	107.1(1)°
O1 - S	1.421(1) Å		
O2 - S	1.420(1) Å		
O3 - N2	1.208(2) Å		
O4 - N2	1.222(2) Å		
O5 - C2	1.369(2) Å	C2 - O5 - C3	109.4(1)°
O5 - C3	1.379(2) Å		
O6 - C2	1.194(2) Å		
O7 - C3	1.197(2) Å		
N1 - S	1.674(1) Å	S - N1 - C1	122.8(1)°
N1 - C1	1.495(2) Å	S - N1 - C3	120.8(1)°
N1 - C3	1.365(2) Å	C1 - N1 - C3	111.9(1)°
N2 - O3	1.208(2) Å	O3 - N2 - O4	125.8(2)°
N2 - O4	1.222(2) Å	O3 - N2 - C7	117.2(1)°
N2 - C7	1.471(2) Å	O4 - N2 - C7	116.9(1)°
C1 - N1	1.495(2) Å	N1 - C1 - C2	98.5(1)°

Bond Distances and Bond Angles (continued)

C1 - C2	1.520(2) Å	N1 - C1 - C4	112.2(1)°
C1 - C4	1.531(2) Å	N1 - C1 - C5	114.2(1)°
C1 - C5	1.520(3) Å	C2 - C1 - C4	108.6(1)°
		C2 - C1 - C5	109.8(1)°
		C4 - C1 - C5	112.5(1)°
C2 - O5	1.369(2) Å	O5 - C2 - O6	121.2(1)°
C2 - O6	1.194(2) Å	O5 - C2 - C1	110.8(1)°
C2 - C1	1.520(2) Å	O6 - C2 - C1	128.1(2)°
C3 - O5	1.379(2) Å	O5 - C3 - O7	122.2(1)°
C3 - O7	1.197(2) Å	O5 - C3 - N1	109.1(1)°
C3 - N1	1.365(2) Å	O7 - C3 - N1	128.7(1)°
C4 - C1	1.531(2) Å	C1 - C4 - H4a	109.4°
C4 - H4a	0.950 Å	C1 - C4 - H4b	109.5°
C4 - H4b	0.950 Å	C1 - C4 - H4c	109.5°
C4 - H4c	0.950 Å	H4a - C4 - H4b	109.5°
		H4a - C4 - H4c	109.5°
		H4b - C4 - H4c	109.5°
C5 - C1	1.520(3) Å	C1 - C5 - H5a	109.5°
C5 - H5a	0.950 Å	C1 - C5 - H5b	109.5°
C5 - H5b	0.951 Å	C1 - C5 - H5c	109.5°
C5 - H5c	0.950 Å	H5a - C5 - H5b	109.4°
		H5a - C5 - H5c	109.5°

Bond Distances and Bond Angles (continued)

		H5b - C5 - H5c	109.4°
C6 - S	1.763(1) Å	S - C6 - C7	122.7(1)°
C6 - C7	1.387(2) Å	S - C6 - C11	117.3(1)°
C6 - C11	1.385(2) Å	C7 - C6 - C11	119.0(1)°
C7 - N2	1.471(2) Å	N2 - C7 - C6	121.9(1)°
C7 - C6	1.387(2) Å	N2 - C7 - C8	116.9(1)°
C7 - C8	1.381(2) Å	C6 - C7 - C8	121.2(1)°
C8 - C7	1.381(2) Å	C7 - C8 - C9	119.0(2)°
C8 - C9	1.377(3) Å	C7 - C8 - H8	120.5°
C8 - H8	0.950 Å	C9 - C8 - H8	120.5°
C9 - C8	1.377(3) Å	C8 - C9 - C10	120.6(2)°
C9 - C10	1.380(3) Å	C8 - C9 - H9	119.7°
C9 - H9	0.950 Å	C10 - C9 - H9	119.7°
C10 - C9	1.380(3) Å	C9 - C10 - C11	120.0(2)°
C10 - C11	1.381(3) Å	C9 - C10 - H10	120.0°
C10 - H10	0.950 Å	C11 - C10 - H10	120.0°
C11 - C6	1.385(2) Å	C6 - C11 - C10	120.1(2)°
C11 - C10	1.381(3) Å	C6 - C11 - H11	119.9°
C11 - H11	0.951 Å	C10 - C11 - H11	119.9°

Crystal data

$C_{11}H_{10}N_2O_7S$	$a = 7.6466$ (5) Å	$D_x = 1.58$ Mg m^{-3}
$M_r = 314.28$	$b = 7.3302$ (3) Å	Cu-K_α radiation
Monoclinic	$c = 11.9056$ (5) Å	$\lambda = 1.54184$ Å
Space Group: $P2_1$	$\beta = 96.966$ (4) °	$T = 298$ K

Data Collection

2703 independent reflections

$R = 0.028$	$\theta_{max} = 75.0°$

VITA

Lars Gustav Johan Hammarström was born on October 28th, 1973, in Sandviken, Sweden. After graduating from Canadian Academy International High School in Kobe, Japan, in 1992, he attended The University of Tampa, Tampa, Florida, as a Presidential Scholarship recipient. He earned his bachelor of science degree in 1996, majoring in biochemistry and graduating *Cum Laude* with Honors as the 1996 University of Tampa Outstanding Chemistry Graduate. In the fall of 1996, he began his graduate studies at Louisiana State University under the guidance of Professor Mark L. McLaughlin. He will receive the degree of Doctor of Philosophy, concentrating on peptide and organic chemistry in the spring of 2001. Lars plans to accept a position at Roche BioScience in Palo Alto, California, in the summer of 2001, as a post-doctoral fellow.

DOCTORAL EXAMINATION AND DISSERTATION REPORT

Candidate: Lars Gustav Johan Hammarstrom

Major Field: Chemistry

Title of Dissertation: Synthetic Peptides: Design, Structure and Biological Function

Approved:

Major Professor and Chairman

Dean of the Graduate School

EXAMINING COMMITTEE:

Date of Examination:

March 22, 2001